UNIVERSITÉ DE GENÈVE

Archive ouverte UNIGE
https://archive-ouverte.unige.ch

Thèse 2010

Open Access

This version of the publication is provided by the author(s) and made available in accordance with the copyright holder(s).

The interplay between endosomal sorting of the epidermal growth factor receptor and signaling

Brankatschk, Ben

How to cite

BRANKATSCHK, Ben. The interplay between endosomal sorting of the epidermal growth factor receptor and signaling. Doctoral Thesis, 2010. doi: 10.13097/archive-ouverte/unige:14275

This publication URL: https://archive-ouverte.unige.ch/unige:14275
Publication DOI: 10.13097/archive-ouverte/unige:14275

© This document is protected by copyright. Please refer to copyright holder(s) for terms of use.

UNIVERSITÉ DE GENÈVE FACULTÉ DES SCIENCES

Section de chimie et biochimie
Département de biochimie Professeur Jean Gruenberg

The Interplay Between Endosomal Sorting of the Epidermal Growth Factor Receptor and Signaling

THÈSE

présentée à la Faculté des sciences de l´Université de Genève
pour obtenir le grade de Docteur ès sciences, mention biochimie

par

Ben BRANKATSCHK

de
Bautzen (Allemagne)

Thèse N° 4265

GENÈVE
Atelier ReproMail
2010

UNIVERSITÉ
DE GENÈVE

FACULTÉ DES SCIENCES

Doctorat ès sciences
Mention biochimie

Thèse de *Monsieur Ben BRANKATSCHK*

intitulée :

" The Interplay between Endosomal Sorting of the Epidermal Growth Factor Receptor and Signaling "

La Faculté des sciences, sur le préavis de Messieurs J. GRUENBERG, professeur ordinaire et directeur de thèse (Département de biochimie), M. GONZALEZ-GAITAN, professeur ordinaire (Département de biochimie), P. COSSON, professeur ordinaire (Faculté de médecine, Département de physiologie cellulaire et métabolisme) et M. ROSSNER, professeur assistant (Abteilung Entwicklungsbiologie, Biologische Fakultät, Georg-August Universität und Max Planck Institut für Experimentelle Medizin, Göttingen, Deutschland), autorise l'impression de la présente thèse, sans exprimer d'opinion sur les propositions qui y sont énoncées.

Genève, le 3 décembre 2010

Thèse - 4265 -

Le Doyen, Jean-Marc TRISCONE

N.B. - La thèse doit porter la déclaration précédente et remplir les conditions énumérées dans les "Informations relatives aux thèses de doctorat à l'Université de Genève".

Acknowledgements

Jean, I am deeply grateful for your guidance during my PhD in your lab. Already the first time when I visited Geneva I was very impressed about you taking so much of your time to discuss, get to know to each other, and to show me around. This good feeling never vanished, and I wish to express my gratitude for your ability to always find the time for helpful troubleshooting or fundamental discussions. Many ideas originated from those spontaneous debates that led me through my research and taught me plenty about cell biology. Thank you also for your patience, for creating a truly pleasant and productive atmosphere in the lab, and for constant support, allowing me to pursue my scientific interests in great depth. Merci!

Best of thanks to everybody in the lab! It is quite outstanding to be working within such a relaxed, cheerful and cooperative crew. Vero, Pierre, Zeina, Etienne, Cameron, Stefania, Fabrizio, Thomas, Karine, Katarina, Alejandra, Christin, Cansel, Shem, you rock! I am also much obliged to Brigitte, Marie-Claire, and Marie-Helene, for taking care of business, making the lab run smooth and our work more efficient.

Special thanks to my good friend and collaborator Sven the Wichert. For ten years now, we have been experiencing a lot together, and it was both a challenge and a pleasure to do the microarray project with you. I have also learned a great deal about how to extract and illustrate information from large amounts of data, and I hope we will carry on in combining friendship and work. Danke. Many thanks to Moritz Rossner from the Max Planck Institute of Experimental Medicine in Göttingen for supporting this project in the course of a very interesting collaboration – to be continued.

I am indebted to Olivier Schaad for the tremendous help in the handling and analysis of the microarray and NanoString data. Cheers to the Genomics Platform team, particularly to Mylène Docquier, Didier Chollet, and Patrick Descombes, for aiding two rather large-scale NanoString measurements in the summer heat of Geneva.

I would also like to thank Christoph Bauer, Jérôme Bosset, and Michal Parkan from the Imaging Platform, for assistance with microscopy, image analysis, and computer issues, and for always being good for a joke!

Sincere thanks to Pierre Cosson, Marcos González-Gaitán, and Moritz Rossner, for agreeing to be in my thesis defense committee and for reading through this piece of work.

At this point, I must express my deepest and warmest gratitude to my family and to friends who became family. Iris, Šćěpan, Jürgen, Mat, Bož, a Marke, mejće dźak! Basti und Sven, ich bin froh dass ich in euch Freunde für´s Leben gefunden habe. Chris, verdammt schade dass du nicht mehr bei uns bist, in Gedanken wirst du es immer sein. Teemu, dude, what would Geneva have been like without you? Thanks for everything! Best of thanks also to Henry, Tom, Alba, Andrea, Fabiana, Carole, Shem, Gordon, Leo, and many others, for enjoying ourselves together, frequent visits to good old Ferbi included, and for painting the city red on many an occasion. Your friendship is invaluable.

Wutrobity a wosebity runks hišće raz na starych přećelow z Łužicy. Mat, Bož, Marke, Merč, Flaki, Micha, boroggnbezacunka, a wjele druhich, bjez was bych zawěsće žno dawno wobłudnił. Rjesće nutř a dale tak!

Najwutrobniši dźak słuša mojej swójbje, bjez kotrejež mój studij njeby móžny był. Nano, mać a Jürgen, sym móhł stajnje na wašu podpěru ličić, a to je mi njesměrnje wjele hódne. Dźakuju za wšitko!

Ben

Table of contents

Summaries III

1. English summary of the thesis III

2. Résumé de la thèse en français V

Introduction 1

1. The ERBB family of receptor tyrosine kinases and their ligands 1

1.1. Members of the ERBB family of receptor tyrosine kinases 1

1.2. The structure of ERBB ligand-binding domains 3

1.3. Members of the EGF family of ligands 4

1.4. Structure and processing of EGF family ligands 5

1.5. Ligand binding and ERBB receptor activation 6

1.6. Intracellular activation of the EGFR kinase domain 8

1.7. Regulatory sequences in the ERBB intracellular regions 10

2. The network of ERBB signaling 11

2.1. Phosphosites in the cytoplasmic tail of ERBBs as docking platforms 12

2.2. The initiation of signaling networks downstream of ERBBs 14

2.3. The RAF-MEK-ERK mitogen-activated protein kinase cascade 17

2.4. The architecture of transcriptional responses induced by ERBB ligands 19

2.5. Biological outcomes of differential signaling in the ERBB system 21

2.5.1. Biological responses of different EGF family ligands 21

2.5.2. Signaling specificity of distinct ligand-induced heterodimers 22

2.6. Intracellular modulation of ERBB signaling 24

2.6.1. Negative feedback regulators of the ERBB-mediated signaling cascade 25

2.6.2. Coordination of the ERK MAPK cascade by scaffold proteins 33

3. Receptor trafficking in the endosomal system 40

3.1. Overview of the endosomal system 40

3.1.1. Determinants of organelle identity in the endosomal system 41

3.1.2. Pathways of entry into cells 43

3.1.3. Recycling from early endosomes as the first sorting station 44

3.1.4. Cargo sorting to late endosomes as the second sorting station 45

3.1.5. The role of cholesterol and LBPA in late endosomal dynamics 51

3.1.6. Cargo delivery to lysosomes as the terminal degradative compartment 54

3.2. The EGFR as a model to study the interplay of trafficking and signaling 55

3.2.1. Internalization routes of the EGFR 56

3.2.2. EGFR sorting at early endosomes 59

3.2.3. EGFR sorting at late endosomes and delivery to lysosomes 63

3.2.4. The interplay between EGFR trafficking and signaling 64

4. Project outline 70

Results 71

1. Establishing a live-cell signaling assay to measure ELK1-driven transcription 71
2. EGFR signaling in cells depleted of ESCRTs or ESCRT-associated proteins 72
3. EGFR degradation and signaling under different EGF stimulation conditions 78
4. EGF signaling upon interference with EGFR internalization and ubiquitination 80
5. Outlook: specific effects of HRS and TSG101 depletion, and late EGFR activity 84

Discussion 86

Materials and Methods 96

1. Reagents, antibodies, siRNAs, and constructs 96
2. Cell culture, transfection, EGF stimulation, and harvest of cells 97
3. Live-cell signaling assay and quantitative real-time RT-PCR 98
4. Sample preparation for microarray analysis 98
5. mRNA measurements using the NanoString technology 99
6. Software used for data analysis 100

Bibliography 101

Appendix 140

1. List of abbreviations 140
2. Target sequences of ON-TARGETplus SMARTpool siRNAs from Dharmacon 145
3. Target sequences of NanoString probes 146
4. Microarray analysis – EGF response genes 150
5. Microarray analysis – knockdown effects 154
6. Manuscript “The phosphoinositide-binding protein SNX16 controls the formation of tubulo-cisternal membrane domains in late endosomes” (158) - 1 -

Summaries

1. English summary of the thesis

The epidermal growth factor (EGF)-induced removal of the EGF receptor (EGFR) from the plasma membrane and its endocytic downregulation is a major negative feedback mechanism controlling the intensity and duration of receptor signaling. Different mechanisms of ligand-accelerated endocytosis, rapid ubiquitination of activated EGFR, and sorting of the receptor into multivesicular bodies for lysosomal degradation, are the underlying principles of EGFR downregulation. The physical degradation of the EGFR is thought to protect cells from excessive stimulation. In addition, sequestering the receptor into intralumenal vesicles of endosomes, thereby uncoupling the intracellular tyrosine kinase domain from its downstream effectors, is proposed to contribute to signal attenuation. On the other hand, endosomal EGFR can be active and is able to compensate for signaling initiated at the plasma membrane. How the pool of active endosomal receptor is regulated, and to what extend it contributes to the biological response, has not been investigated conclusively to date.

In this study, we aimed to dissect the precise contribution of endocytic sorting events to the EGF response. Consequences of perturbations in EGFR sorting, particularly upon interfering with clathrin- and dynamin-dependent endocytosis, after knockdown of CBL ubiquitin ligases, and of depletion of endosomal sorting complex required for transport (ESCRT) subunits, were investigated in detail. The activation status of signaling components was determined, and a reporter assay was set up to measure EGF-dependent transcriptional activation in living cells. The induction of endogenous target genes downstream of the EGFR-MAPK (mitogen-activated protein kinase) cascade was quantified by real-time RT-PCR, microarray analysis, and by utilizing the recently developed NanoString technology.

We observed that increased levels of phosphorylated EGFR and downstream kinases, for example upon depletion of the ESCRT subunits HRS, TSG101, and VPS4A, are not necessarily indicative of increased transcription. Hence, monitoring the activation status of the MAPK cascade does not seem to allow general conclusions about signaling outputs.

The overall architecture of the EGF-induced transcriptional response, determined by genome-wide analysis using microarrays, was not significantly affected under any ESCRT knockdown condition, although specific effects on NF-kappa-B and cytokine signaling were observed. No general shift or delay in gene expression was obvious upon interfering with ESCRT function, despite of effects on EGFR degradation and activity. The wave-like organization of the response to EGF, namely the coordinated and temporally restricted expression of functionally related clusters of genes, is defined by the interplay between forward-driving and negative feedback mechanisms. This balance, leading to the definition of an activation interval, may provide significant robustness to the system. Presumably because

of this inherent property, increased activation of the EGFR and MAPKs in cells depleted of ESCRT proteins does not lead to global changes in the EGF-induced program, in contrast to the dogma of ESCRT function in attenuating EGFR signaling from endosomes.

To identify the “point of commitment” from where the receptor is still able to affect gene expression, we interfered with receptor trafficking events further upstream of ESCRTs. Impairing clathrin- and dynamin-dependent internalization as well as CBL-mediated ubiquitination of the EGFR increased EGF-driven transcriptional activation in our reporter assay and led to upregulation of many endogenous target genes measured by NanoString. Strikingly, the pattern and strength of effects was reminiscent of the impact of EGFR overexpression. Increased transcriptional activity was therefore specifically due to defects in receptor sorting upstream of ESCRTs. However, the overall organization of the EGF response was not affected even under those conditions, demonstrating again the robustness of the system in HeLa cells. Only stimulation with the phorbol ester PMA increased both the strength and duration of the response globally, providing the proof-of-principle that a general change in the expression of EGF-responsive genes can be achieved.

Overexpressed EGF receptors are internalized significantly slower due to the limited capacity of (clathrin-dependent) rapid internalization. Depletion of clathrin and dynamin interferes with this rapid internalization mechanism, and abrogation of EGFR ubiquitination leads to increased recycling of ligand-stimulated receptor. The effects on EGF signaling observed in HRS-depleted cells, rather weak but compared to the other ESCRT knockdowns still the most significant, may also be explained in part by increased EGFR recycling. Taken together, our observations argue that conditions increasing the number of active receptors at the plasma membrane have the strongest impact on downstream transcriptional activation. More precisely, continuous ubiquitination *via* CBL, and to a lesser extend recruitment of the ubiquitinated receptor by HRS for ESCRT-mediated downregulation, seem to define the point after which EGFR sorting events do not influence signaling to the nucleus anymore.

Interfering simultaneously with TSG101 and ALIX, a regulator of lysobisphosphatidic acid (LBPA)-mediated sorting, did not lead to a strong increase in EGF-driven transcription. This demonstrates that one pathway of intralumenal vesicle formation can not compensate for the other, and that both pathways together do not regulate intracellular EGFR signaling.

In conclusion, only conditions interfering with EGFR internalization or ubiquitination lead to upregulation of many EGF response genes, comparable to receptor overexpression, and EGFR ubiquitination seems to define the crucial point of signal termination. Secondly, the EGF-induced transcriptional program appears extremely stable. We speculate that the underlying principles may be general to ensure biological robustness, and that flexibility and specificity arise from combinatorial effects of several active signaling cascades *in vivo*. However, late requirement for EGFR kinase activity hints to the existence of an EGFR pool which is not regulated by any of the investigated mechanisms of receptor downregulation.

2. Résumé de la thèse en français

Lorsqu'il est ajouté à des cellules, le facteur de croissance épidermique (*epidermal growth factor*, EGF) provoque l'endocytose de son récepteur (EGFR), induisant alors une diminution du nombre de molécules de récepteur à la membrane plasmique. Ce mécanisme de rétroaction négative joue un rôle essentiel dans le contrôle de l'intensité et de la durée de la signalisation par l'EGF. Les principes fondamentaux de cette régulation négative impliquent différents mécanismes d'endocytose accélérée par le ligand, l'ubiquitination rapide du récepteur activé, et le tri des récepteurs dans les corps multivésiculaires impliqués dans le transport vers les lysosomes pour la dégradation. La destruction physique de l'EGFR est censée protéger les cellules contre une stimulation excessive. En outre, il est admis que la séquestration de l'EGFR dans des vésicules intraluminales de l'endosome découple le domaine tyrosine kinase du récepteur de ses effecteurs en aval, contribuant ainsi à l'atténuation du signal. D'autre part, l'EGFR dans l'endosome peut aussi être actif et est en mesure de compenser la signalisation initiée à la membrane plasmique. Par contre, on ne sait pas à ce jour de façon concluante ce qui contrôle l'activité du récepteur endosomal, ni dans quelle mesure ce pool de récepteur contribue à la réponse biologique.

Dans cette étude, nous avons cherché à déterminer quelle est la contribution précise de chaque événement de tri dans l'endocytose à la réponse de l'EGFR. J'ai étudié dans le détail les conséquences des perturbations dans le tri de l'EGFR, en interférant en particulier avec l'endocytose dépendante de la clathrine et de la dynamine, avec l'ubiquitination par les *ubiquitin ligases* CBL, et avec le tri endosomal par les complexes ESCRTs (endosomal sorting complex required for transport). L'état d'activation des composants de signalisation a été déterminé, et un test a été mis en place pour mesurer l'activation transcriptionnelle dépendante de l'EGF dans les cellules vivantes. L'induction de gènes cible endogènes en aval de la cascade des MAPK (mitogen-activated protein kinases) a été quantifiée en temps réel grâce à la RT-PCR, l'analyse de type *microarray* , et la technologie NanoString récemment développée.

Nous avons observé que le niveau élevé de phophorylation de l'EGFR et des kinases, par exemple après déplétion des sous-unités ESCRT HRS, TSG101, et de VPS4A avec des siRNAs, n'est pas nécessairement indicatif d'une transcription accrue. Par conséquent, la mesure de l'état d'activation de la cascade MAPK ne semble pas permettre de tirer des conclusions générales sur la signalisation.

L'architecture globale de la réponse transcriptionnelle de l'EGF, déterminée par l'analyse du génome entier par *microarrays*, n'a pas été significativement affectée par la déplétion de sous-unités ESCRT, bien que des effets spécifiques ont été observés sur NF-kappa-B et la signalisation de cytokines. Je n'ai observé aucun décalage ou retard dans l'expression des gènes, en dépit des effets sur la dégradation et l'activité de EGFR. L'organisation ondulatoire

de la réponse à l'EGF, à savoir l'expression bien ordonnée et limitée dans le temps de groupes de gènes aux fonctions semblables, est définie par l'interaction entre les mécanismes de rétroaction positifs et négatifs. Cet équilibre, conduisant à la définition d'un intervalle d'activation, peut fournir une grande robustesse au système. Probablement à cause de cette propriété intrinsèque, l'augmentation de l'activation de l'EGFR et des MAPK après déplétion de sous-unités ESCRT ne conduit pas à des changements globaux dans le programme transcriptionnel de l'EGF. Ceci est contraire au dogme que la fonction des ESCRTs est d'atténuer la signalisation de l'EGFR à partir des endosomes.

Pour identifier le moment critique à partir duquel le récepteur est toujours en mesure d'influer sur l'expression des gènes, j'ai perturbé le trafic des récepteurs en amont des ESCRTs, lors de l'endocytose. L'inhibition de l'endocytose par la déplétion de la clathrine ou l'inhibition de l'ubiquitination par CBL a augmenté de manière significative l'activation transcriptionnelle de l'EGF dans notre système-test ainsi que de plusieurs gènes cible endogènes mesurée par NanoString. Étonnamment, le type et l'intensité des effets sont comparables à ceux observés après surexpression de l'EGFR. En d'autres termes, l'augmentation de l'activité transcriptionnelle résulte de défauts dans le tri du récepteur en amont de ESCRTs. Toutefois, l'organisation générale de la réponse de l'EGF n'a pas été affectée, même dans ces conditions, démontrant une nouvelle fois la robustesse du système. Seule la stimulation causée par l'ester de phorbol PMA a permis d'augmenter à la fois la force et la durée de la réponse de manière globale, démontrant qu'un changement général dans l'expression des gènes sensibles à l'EGF est possible.

Après surexpression, l'EGFR est internalisé sensiblement plus lentement en raison de la capacité limitée de l'endocytose dépendante de la clathrine. La déplétion en clathrine et dynamine interfère avec ce mécanisme d'internalisation rapide – alors que l'abrogation de l'ubiquitination conduit à l'augmentation du recyclage de l'EGFR. La déplétion en HRS, cette dernière liant directement le récepteur ubiquitiné, cause des effets plus faibles que ceux observés après déplétion de la clathrine ou de la dynamine, mais néanmoins plus importants que ceux dus à la déplétion des ESCRTs. Ceci peut aussi s'expliquer par une augmentation du recyclage de l'EGFR. Globalement, mes observations indiquent que l'augmentation du nombre de récepteurs actifs à la membrane plasmique a un impact majeur sur l'activation de la transcription en aval. Plus précisément, l'ubiquitination continue par CBL et dans une moindre mesure le recrutement du récepteur ubiquitiné par HRS semblent définir le point de contrôle (*checkpoint*) à partir duquel le tri du récepteur n'a plus d'influence sur la signalisation vers le noyau.

En interférant simultanément avec les fonctions de TSG101 et ALIX, impliqué dans le tri via l'acide lysobisphosphatidic (LBPA), je n'ai pas observé une forte augmentation de la transcription par l'EGF. Ceci suggère qu'une voie de formation des vésicules intraluminales ne peut pas être compensée par une voie alternative.

En conclusion, seules des conditions qui permettent d'inhiber l'internalisation de l'EGFR ou l'ubiquitination conduisent à une augmentation de l'expresssion de nombreux gènes, et l'ubiquitination de l'EGFR semble déterminer le point de non-retour dans la terminaison du signal. En second lieu, le programme de transcription induit par l'EGF apparaît extrêmement stable. Nous pensons que les principes sous-jacents peuvent être de nature générale pour assurer la robustesse biologique, et que souplesse et spécificité découlent des effets combinatoires de plusieurs cascades de signalisation actives in vivo. Toutefois, le fait qu'une activité kinase retardée semble être nécessaire pour la réponse à l'EGF suggère de plus l'existence d'un pool d'EGFR qui ne serait pas sous le contrôle d'un mécanisme connu.

Introduction

1. The ERBB family of receptor tyrosine kinases and their ligands

The epidermal growth factor (EGF) and the EGF receptor (EGFR) are the founding members of the EGF family of ligands and the ERBB family of receptor tyrosine kinases (RTKs), respectively. EGF was discovered almost 40 years ago in mice (Cohen, 1962), and was named after further characterization in 1965 (Cohen, 1965). The human EGF was discovered 10 years later (Cohen and Carpenter, 1975; Starkey et al., 1975). For the discovery of the epidermal and nerve growth factors, Stanley Cohen and Rita Levi-Montalcini were awarded the Nobel Prize in Physiology and Medicine in 1986.

By using labeled EGF, it became clear that the growth factor binds a receptor at the cell surface, after which the EGF•receptor complex is internalized *via* small membrane vesicles and eventually degraded in lysosomes (Carpenter and Cohen, 1976; Haigler et al., 1978). The observation that EGF stimulates protein phosphorylation in a cell-free system containing membranes, led to the notion that the receptor has kinase activity (Carpenter et al., 1978). It was the first cell-surface receptor to be linked directly to cancer (Blomberg et al., 1980; de Larco and Todaro, 1978; Ullrich et al., 1984). Finally, the EGFR was identified as the first RTK and purified in 1980 (Cohen et al., 1980; Ushiro and Cohen, 1980). It was also the first RTK gene to be cloned and sequenced in 1984 (Ullrich et al., 1984).

The EGFR remains the most investigated RTK, and serves as a model receptor both in the field of signal transduction and membrane trafficking. Indeed, many of the key concepts and mechanisms of internalization and endosomal trafficking have been established by studying the EGFR. Moreover, it is also one of the most popular models used to reveal the crosstalk between endocytosis and signaling.

1.1. Members of the ERBB family of receptor tyrosine kinases

The ERBB family of receptors, named after the homology to the avian retroviral oncogene v-erb-B (erythroblastoma viral oncogene, encoding a truncated form of EGFR) (Ullrich et al., 1984), consists of four structurally related RTKs in mammals: EGFR (also termed ERBB1 or HER1 for human EGF receptor), ERBB2/HER2/neu (in rodents), ERBB3/HER3, and ERBB4/HER4. They share a similar molecular architecture with all 58 known human RTKs, reviewed in (Lemmon and Schlessinger, 2010). The modular single-chain proteins contain ligand-binding domains in the extracellular region, a single transmembrane helix, and a cytoplasmic part that includes the protein tyrosine kinase domain plus additional carboxy- (C-) terminal and juxtamembrane regulatory sequences, as depicted in Fig. 1 (Burgess et al., 2003).

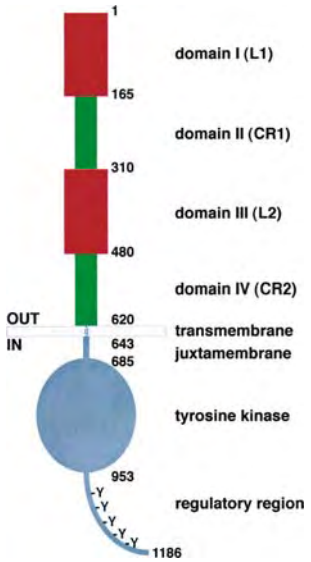

Fig. 1: Domain organization of ERBB receptors.
ERBBs are type I transmembrane glycoproteins with a single transmembrane helix. Domain II and IV are the ligand-binding domains in the extracellular region. The cytoplasmic part includes the tyrosine kinase domain as well as juxtamembrane and C-terminal regulatory sequences, particularly the tyrosine residues which are autophosphorylated upon receptor activation and serve as docking sites to initiate downstream signaling events. The residue numbers for domain boundaries are for the EGFR without the signal peptide (Burgess et al., 2003).

Binding of an EGF family ligand (see 1.3., Fig. 4) induces the formation of ERBB homo- and heterodimers (actually heterotetramers including bound ligands) and activation of the intrinsic kinase domain, resulting in receptor autophosphorylation on specific tyrosine residues within the cytoplasmic tail. These phosphorylated residues serve as docking sites for downstream signaling proteins containing SRC (viral sarcoma oncogene homolog) homology 2 (SH2) or phosphotyrosine binding (PTB) domains, initiating and modulating complex signaling cascades as illustrated in Fig. 2 (Yarden and Sliwkowski, 2001).

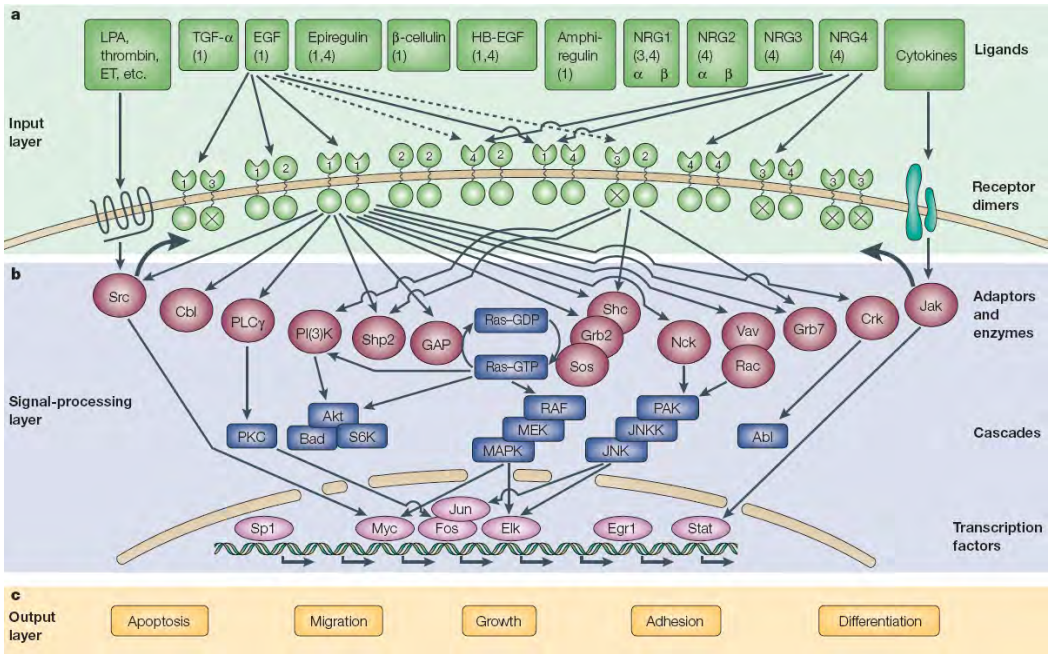

Fig. 2: The ERBB signaling network.
A) Ligands and potentially ten dimeric receptor combinations comprise the input layer. Numbers in each ligand block indicate the respective high-affinity ERBB receptors. For simplicity, specificities of receptor binding are shown only for EGF and NRG4. ERBB2 binds no ligand, and ERBB3 is catalytically inactive; both were not found to form homodimers. Transactivation by GPCRs and cytokine receptors is shown by wide arrows. **B)** Signaling to the adaptor-enzyme layer is shown only for two receptor dimers: the EGFR/ERBB1 homodimer, and the strongly mitogenic ERBB2-ERBB3 heterodimer. Only some of pathways and transcription factors of this layer are shown. **C)** The biological output is defined by the transcriptional response initiated downstream of MAPK cascades, but the mechanisms of specificity are not fully understood (Yarden and Sliwkowski, 2001).

The expression and localization of both the ligands and the receptors is highly regulated, and the same holds true for many downstream components of the signal transduction mechanism. The transcriptional response and the final physiological outcome (proliferation, migration *vs.* differentiation, adhesion; tumorigenesis *vs.* apoptosis) upon activation of the ERBB signaling network is thus determined by several layers of complexity: 1) multiple ligands and possible ERBB receptor combinations; 2) a multitude of affected pathways and their crosstalk with other signaling events in the same cell (the cellular context, or even cell type specificity); 3) the spatial and temporal regulation of potentially all signaling components. The signaling cascades initiated by ERBB receptors are therefore not linear and unidirectional, but can be regarded as four-dimensional networks.

1.2. The structure of ERBB ligand-binding domains

The extracellular region of ERBBs is heavily glycosylated. In the case of EGFR, 9 out of 11 potential glycosylation sites are utilized (Zhen et al., 2003), with reported functions in receptor translocation, maturation, and dimerization (Fernandes et al., 2001). The ligand-binding region consists of four distinct protein domains of two different types. There are two homologous large (L) domains (members of the leucine-rich repeat family), and two cysteine-rich (CR) domains, which occur in the order L1 - CR1 - L2 - CR2 (Ward et al., 1995). An alternative nomenclature of those domains is simply I - II - III - IV (Fig. 1 and 3), which will be used thereafter.

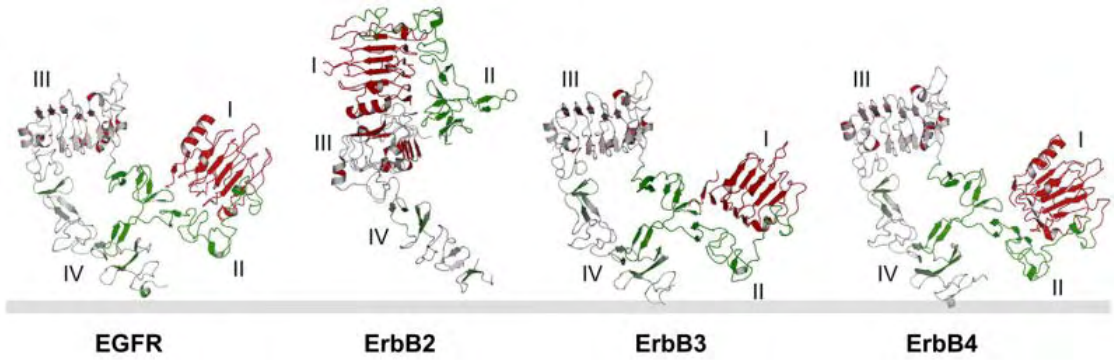

Fig. 3: Structures of the human ERBB receptor extracellular regions without bound ligand.
Ligand-binding domains of the EGFR, ERBB3 and ERBB4 all adopt the tethered conformation in the absence of ligand, whereas ERBB2 adopts an extended conformation that resembles the ligand-activated, dimerization-competent EGFR in the dimer shown in Fig. 6 (Lemmon, 2009).

Between 2002 and 2005, major advances in understanding how the ERBB receptors are regulated by their growth factor ligands have come from crystallographic studies, reviewed in (Burgess et al., 2003; Lemmon, 2009). The X-ray crystal structures of all four human ERBB receptor extracellular regions without bound ligand are shown in Fig. 3. Additional structures of a large part of the EGFR extracellular domain in ligand-induced dimers or heterotetramers (Garrett et al., 2002; Ogiso et al., 2002) laid the foundation for a satisfying model of ligand-

induced ERBB receptor dimerization and activation, which will be discussed in more detail below (see 1.5., Fig. 6). Briefly, the combined information gained from recent structural studies has yielded several surprises: a dramatic conformational transition was shown to occur upon ligand binding; an unprecedented, entirely receptor-mediated mode of dimerization was identified; and an unexpected apparently "pre-activated" state was defined for the ERBB2 monomer (Fig. 3). Hence, these advances also explain differences between ERBB family members, since ERBB2 is an orphan receptor without known ligand that nonetheless has robust tyrosine kinase activity. On the other hand, the notion that ERBB receptors also form heterodimers helped to clarify the role of ERBB3, which binds neuregulin (NRG) ligands (see below) but lacks tyrosine kinase activity (Guy et al., 1994).

1.3. Members of the EGF family of ligands

The EGF family peptide growth factors, encoded by several distinct genes and by alternatively spliced transcripts, serve as agonists for ERBB family receptors. In *Caenorhabditis elegans*, a single EGF-like ligand known as LIN-3 (and one receptor called LET-23) can be found; *Drosophila melanogaster* expresses four ligands named Spitz, Gurken, Vein, and Keren, plus the ligand-sequestering protein Argos (and one receptor, Egfr) (Klein et al., 2004; Shilo, 2003). Mammalian family members include EGF, transforming growth factor-alpha (TGFA), amphiregulin (AREG/AR), betacellulin (BTC), heparin-binding EGF-like growth factor (HBEGF), epiregulin (EREG/EPR), epigen (EPGN/EPG), and the neuregulins (NRGs). These ligands exhibit differences in receptor affinity and display exquisite receptor binding specificity, summarized in Fig. 4 (Wilson et al., 2009). Other factors contribute to ligand specificity, including distinctions in the timing and tissue specificity of ligand expression, and differences in post-translational cleavage and processing (see below). Accessory molecules and co-receptors such as heparan sulfate proteoglycans may contribute to ligand specificity by sequestering local high concentrations of these growth factors or by controlling their bioavailability.

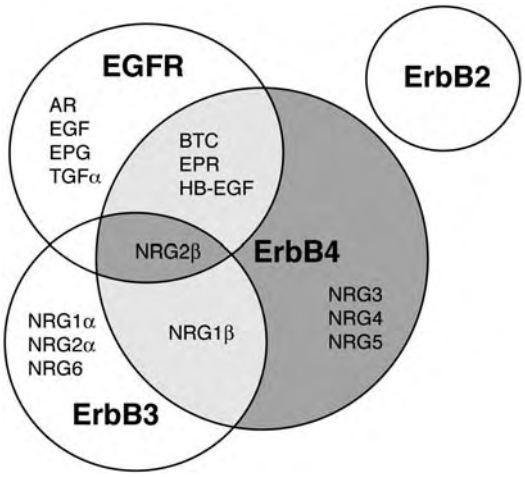

Fig. 4: EGF family ligands bind and activate multiple ERBB receptors. A Venn diagram illustrating the interactions of the four ERBB receptors with EGF family members. EGFR and ERBB4 are able to bind eight distinct ligands, whereas ERBB3 is activated by neuregulins only. NRG2-beta binds all receptors except for ERBB2 which is "pre-activated" without bound ligand (Fig. 3). Other ligands are more selective, but together with different receptor heterodimer combinations, a complex pattern of possible interactions is eminent (Wilson et al., 2009).

The EGF family ligands exhibit a complex pattern of interactions with the four ERBB family receptors. For example, EGFR can bind eight different EGF family members and NRG2-beta binds EGFR, ERBB3, and ERBB4 (Fig. 4). Given that the four ERBB receptors display distinct patterns of coupling to signaling effectors (Fig. 8), differences in the intrinsic properties of EGF-like ligands can lead to distinct biological outcomes of receptor stimulation (chapter 2.5.). The ten potential receptor dimers depicted in Fig. 2 add to the complexity of the input layer of the ERBB signaling network (Yarden and Sliwkowski, 2001). However, it should be noted that the ligand-lacking ERBB2 and the kinase-dead ERBB3 do not seem to significantly form homodimers under physiological conditions, reducing the number of different receptor combinations from ten to eight (Tzahar et al., 1996).

1.4. Structure and processing of EGF family ligands

Each of the mature peptide growth factors is characterized by a consensus sequence consisting of six spatially conserved cysteine residues, contained within a sequence of 35 to 40 amino acids (CX_7 CX_{4-5} CX_{10-13} $CXCX_8$ C) (Dreux et al., 2006). Cysteins within the EGF motif have the potential to form three intra-molecular disulfide bond pairings between C1-C3, C2-C4 and C5-C6 to produce three loops that are essential for high-affinity binding to the receptor (Harris et al., 2003). HBEGF and AREG also contain an N-terminal heparin-binding domain rich in basic amino acids (Thompson et al., 1994; Thorne and Plowman, 1994).

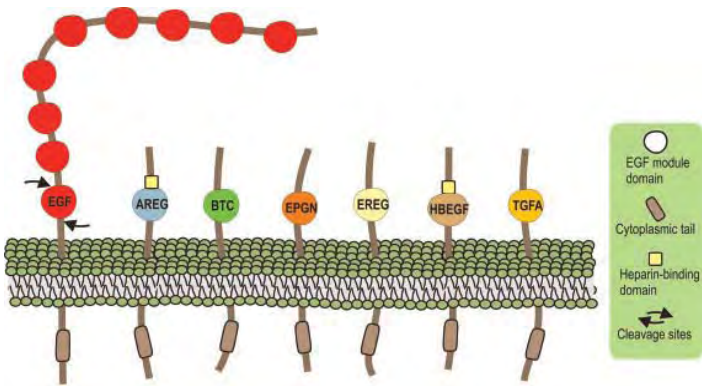

Fig. 5: Structure of EGFR ligand precursors. Schematic representation of the membrane-anchored precursors of seven mammalian EGFR ligands. EGF motifs, heparin-binding domains of AREG and HBEGF, and cytosolic tails are indicated. ProEGF is composed of 1200 residues and contains nine EGF-like repeats, of which only the first gives rise to the soluble ligand. Arrows indicate sites of cleavage by metallo-proteinases. The size of other precursors is between 150-160 amino acids, and mature ligands contain up to 90 residues (Schneider and Wolf, 2009).

Members of the EGF family are derived from type I transmembrane glycoprotein precursors (Fig. 5), consisting of an extracellular region containing the growth factor sequence (originally with the signal peptide and a pro-region), a transmembrane domain and a cytoplasmic tail. To release soluble, biologically active growth factors, the ligand precursors can be cleaved by members of the family of “a disintegrin and metalloproteinase” (ADAM), intregral membrane proteins with extracellular metalloproteinase and integrin-binding sites. ADAMs are involved in ectodomain shedding of various growth factors and receptors, cytokines, and cell adhesion molecules, reviewed by (Edwards et al., 2008; Reiss and Saftig, 2009). ADAM10 emerged as the main sheddase of EGF and BTC, and ADAM17 (TACE,

TNF-alpha converting enzyme) as the major convertase of EREG, TGFA, AREG, and HBEGF in mouse embryonic cells lacking candidate-releasing enzymes (Sahin et al., 2004). ADAM9, 12, 15, and 19 can also participate in ligand processing (Reiss and Saftig, 2009), indicating a certain degree of redundancy. HBEGF is also capable of being cleaved by matrix metalloproteinases (MMPs), notably MMP3 and MMP7 (Suzuki et al., 1997; Yu et al., 2002). By a not well defined mechanism, G protein-coupled receptors (GPCRs) can activate EGF family precursor-processing enzymes, thereby transactivating the corresponding ERBB receptors (Bhola and Grandis, 2008; Ohtsu et al., 2006).

Most precursors for ERBB ligands have between 150 and 250 amino acids, the mature growth factors range from about 45 to 90 residues (Dreux et al., 2006). Mature EGF is a 53 amino acid peptide; the transmembrane precursor ProEGF, however, has the remarkable size of EFGR itself (about 1200 residues). It contains nine EGF-like motifs in its extracellular domain (Fig. 5). Cleavage occurs between the first and second motifs, and the EGF subunit closest to the plasma membrane is released as the mature growth factor (Harris et al., 2003); the fate of the other eight EGF domains seems unknown.

Some ERBB ligand precursors including HBEGF, TGFA, AREG, and BTC are capable of receptor activation even when they are tethered to the plasma membrane, suggesting their capability of functioning as juxtacrine factors (Anklesaria et al., 1990; Singh and Harris, 2005). In the case of HBEGF, the biological outcome of juxtacrine activation was shown to be different than stimulation *via* an autocrine or paracrine mode (Iwamoto et al., 1999; Pan et al., 2002; Singh et al., 2004). One distinctive feature of juxtacrine factors in general is that they are “non-diffusable”, transmitting the signal not further than to neighboring cells and thus restricting the response locally.

1.5. Ligand binding and ERBB receptor activation

More than two decades ago, the model of intermolecular allosteric activation of the EGFR by a ligand-induced dimerization mechanism was proposed (Yarden and Schlessinger, 1985, 1987a, b). Despite extensive investigation, how ligand engagement induced EGFR dimerization remained elusive for 15 years thereafter.

Early studies of RTKs and cytokine receptors suggested a conceptually straightforward mechanism for ligand-induced dimerization. The paradigm of receptor dimerization mediated by bivalent ligand binding was established by studying the human growth hormone (GH1) and its receptor GHR, where one ligand crosslinks two extracellular receptor regions to form a 1:2 complex (Cunningham et al., 1991; de Vos et al., 1992). Bivalent, usually dimeric ligand species at the receptor-receptor interface directly mediating dimerization were also seen for example for the vascular endothelial growth factor (VEGF) and its receptor FLT1, the nerve

growth factor (NGF) and its receptor NTRK1/TRKA, the ephrin•EPHB2 complex, and for the stem cell factor (SCF) bound to KIT (summarized in (Burgess et al., 2003; Lemmon and Schlessinger, 2010)). The previously suggested hypothesis that EGF family ligands mediating ERBB dimerization by binding simultaneously to two receptor molecules and crosslinking them into a dimer (Gullick, 1994; Tzahar et al., 1997), followed largely from these examples suggesting that multivalence is the key for ligand-mediated receptor oligomerization.

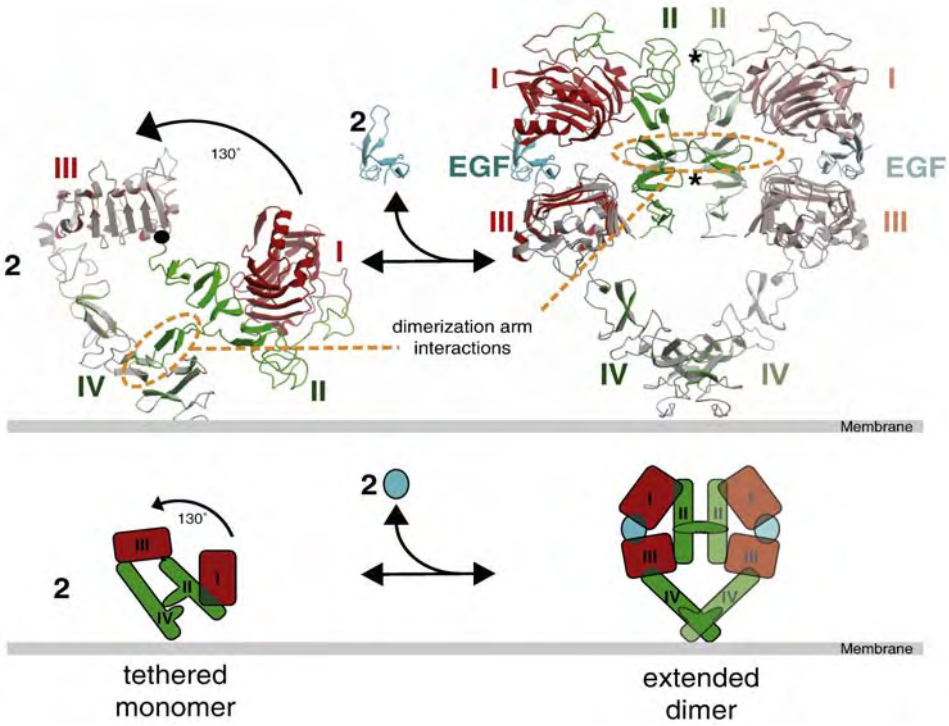

Fig. 6: Model for EGF-induced dimerization of the EGFR extracellular region.
The top panel shows ribbon representations of sEGFR structures with- and without bound EGF. The left-hand structure shows the domain II/IV tether (ringed with orange oval) that occludes the dimerization arm. EGF binding to this structure induces a conformational change that can be modeled approximately by a 130° rotation of the domain I/II fragment. This change causes EGFR to adopt the extended conformation, in which the dimerization arm is exposed to drive dimerization as shown in the right-hand panel. Dimerization arm contacts at the dimer interface are ringed with an orange oval. The lower panel shows a cartoon representation of this dimerization reaction (Lemmon, 2009).

Already in 1997, the observation that dimerization of sEGFR (secreted, truncated extracellular domain of the receptor) requires the participation of two molecules of monomeric EGF (in a 2:2 dimer / heterotetramer, *via* a stable intermediate 1:1 EGF-sEGFR complex), suggested differences to the paradigm established for receptor dimerization by GH1 (Lemmon et al., 1997). The requirement for two monomeric EGF ligands provides also a context for understanding the ability of different EGF-like ligands to induce heterodimerization of ERBBs. Contrary to most expectations, crystal structures of ligand-bound sEGFR showed that dimerization is entirely receptor mediated (Garrett et al., 2002; Ogiso et al., 2002). The structures confirmed that two individual ligand molecules are present. However, the two bound TGFA (Garrett et al., 2002) or EGF (Ogiso et al., 2002) molecules could hardly be further from the dimer interface (Fig. 6 and 7, right). Although the ligand is bivalent like those

discussed above, in this case it contacts two distinct sites within a single receptor molecule (on domains I and III) rather than crosslinking two separate receptors. The ligand binding promotes substantial conformational changes in the extracellular region of EGFR, ERBB3 and ERBB4, which unmask a dimerization arm in domain II. Deletions or mutations in this region completely prevent ligand-induced receptor activation (Garrett et al., 2002; Ogiso et al., 2002). Before ligand binds, the dimerization arm is completely buried by intramolecular interactions with domain IV, stabilizing a tethered, autoinhibited conformation (Bouyain et al., 2005; Cho and Leahy, 2002; Ferguson et al., 2003). Ligand binding “extends” the receptor conformation and breaks the tether, allowing the dimerization arm of domain II to interact with a second ligand-bound receptor molecule (Fig. 6). The membrane-proximal domain IV is also thought to make contacts across the dimer interface after its exposure upon ligand binding, which may orient the dimers in the configuration required for maximal activation (Burgess et al., 2003).

By marked contrast with other family members, monomeric ERBB2 extracellular regions display an extended conformation (Fig. 3), explaining its inability to bind ligand (Cho et al., 2003; Garrett et al., 2003). The receptor is thus constitutively poised to interact with other ERBB receptors by virtue of its exposed dimerization arm. Hence, the crystal structures shed light on the unique ability of ERBB2 to transform cells by simple overexpression (Di Fiore et al., 1987), and facilitate molecular treatment strategies for certain types of cancer involving *ERBB2* gene amplification or overexpression (Hynes and Lane, 2005; Slamon et al., 1987; Slamon et al., 1989).

A significant volume of literature discusses evidence for the existence of EGFR dimers at the cell surface in the absence of EGF, reviewed by (Lemmon, 2009). Whether these pre-formed dimers are physiologically relevant for the mechanism of receptor activation, is still a question of debate. However, defining the nature of the dimers presumed to be in equilibrium with monomers is a central challenge in understanding receptor regulation.

1.6. Intracellular activation of the EGFR kinase domain

Crystallographic studies on the intracellular kinase domain of ERBBs led again to breakthroughs in our understanding of the mechanism controlling ERBB receptor activation. Monomeric and dimeric structures of the EGFR kinase became available between 2002 and 2006, the atomic structure of the ERBB4 kinase was solved in 2008 (Qiu et al., 2008), recently reviewed in (Bose and Zhang, 2009).

For most ligand•RTK complexes, ligand-mediated receptor dimerization is thought to position the two cytoplasmic kinase domains for efficient *trans*-phosphorylation of tyrosine residues in the kinase activation loop, the juxtamembrane region, and elsewhere in the cytoplasmic part. These phosphorylation events, particularly in the activation loop and

juxtamembrane region, stabilize the catalytically competent state of RTKs (reviewed in (Hubbard, 2004; Huse and Kuriyan, 2002)). Phosphorylation sites also serve to recruit downstream signaling proteins containing SH2 or PTB domains. In contrast with most RTKs, however, almost all of the EGFR sites for tyrosine autophosphorylation reside in the long flexible C-terminal region (see Fig. 8 below). Moreover, despite containing a conserved tyrosine residue in the activation loop (Tyr845; residue numbers used here are based on the mature EGFR protein, which can be converted to the plus signaling peptide numbering by adding 24), phosphorylation of this site is not required for activation of the EGFR kinase (Gotoh et al., 1992).

At this point, crystal structures provided crucial and elegant explanations to these riddles. A structure of the soluble monomeric EGFR kinase domain showed the kinase to be in an active state (Stamos et al., 2002), with the principal regulatory elements – the activation loop in the C-terminal kinase lobe (C-lobe) and alpha-helix C in the amino- (N-) terminal kinase lobe (N-lobe) – properly positioned for catalysis. This is consistent with the observation that phosphorylation of the activation loop is not necessary for kinase activity, but it raised the question of why the EGFR kinase is not constitutively active. Further studies, by increasing the local concentration of the protein (or by mutating a critical leucine (L834R) in the activation loop), suggested that the kinase domain is intrinsically autoinhibited, and an intermolecular interaction promotes its activation (Zhang et al., 2006). In fact, a previous crystal structure of the EGFR kinase with an inhibitor bound provided the first indication of this autoinhibited state (Wood et al., 2004), but it was unclear whether the inhibitor induced this conformation.

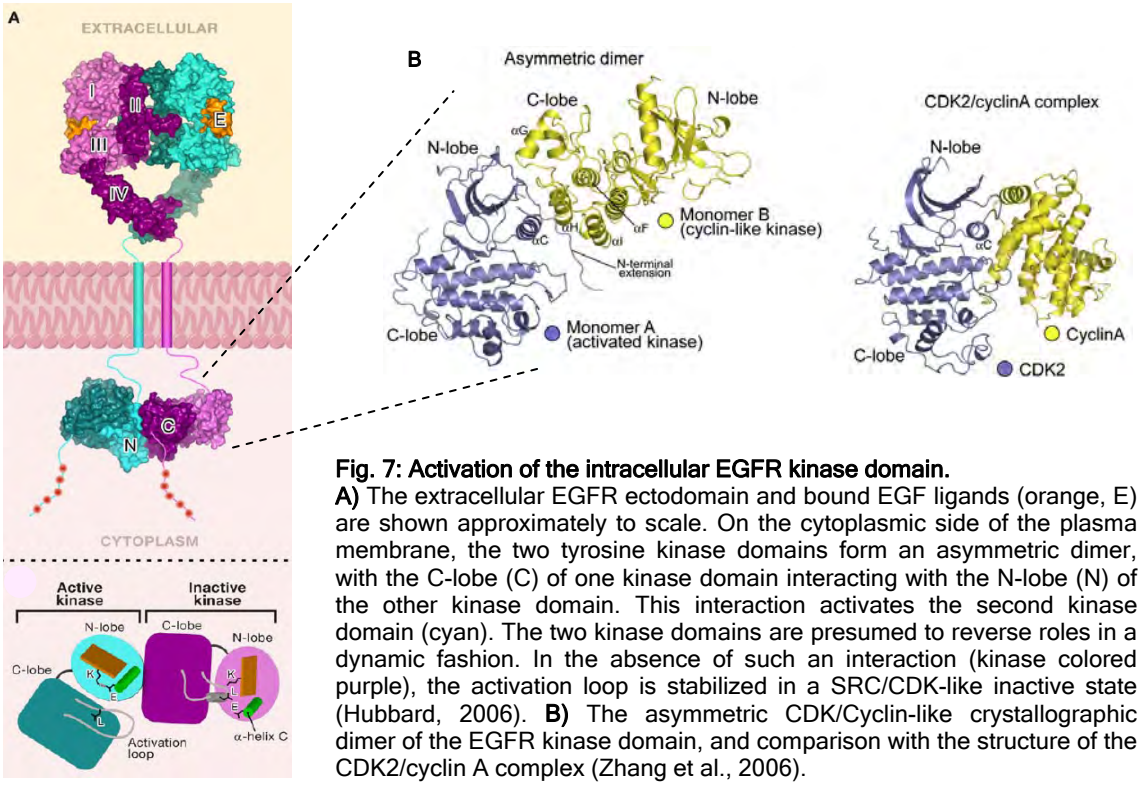

Fig. 7: Activation of the intracellular EGFR kinase domain.
A) The extracellular EGFR ectodomain and bound EGF ligands (orange, E) are shown approximately to scale. On the cytoplasmic side of the plasma membrane, the two tyrosine kinase domains form an asymmetric dimer, with the C-lobe (C) of one kinase domain interacting with the N-lobe (N) of the other kinase domain. This interaction activates the second kinase domain (cyan). The two kinase domains are presumed to reverse roles in a dynamic fashion. In the absence of such an interaction (kinase colored purple), the activation loop is stabilized in a SRC/CDK-like inactive state (Hubbard, 2006). **B)** The asymmetric CDK/Cyclin-like crystallographic dimer of the EGFR kinase domain, and comparison with the structure of the CDK2/cyclin A complex (Zhang et al., 2006).

To summarize the findings of (Zhang et al., 2006): ligand-induced, receptor-mediated dimerization leads intracellularly to the formation of an asymmetric dimer of two kinase domains, where the C-lobe of one kinase domain interacts with and activates the N-lobe of the other allosterically (for details, see Fig. 7). More precisely, these contacts induce conformational changes in the N-lobe of the receiver kinase that disrupt *cis*-autoinhibitory interactions seen in the monomer. As a result, the receiver kinase can adopt the characteristic active configuration without phosphorylation of its activation loop. In the absence of ligand, the activation loop is stabilized in a SRC/CDK-like inactive state (reviewed in (Huse and Kuriyan, 2002; Bose and Zhang, 2009)). In addition, the authors provide evolutionary evidence to support this mechanism: not only is this interaction highly reminiscent of the activation of CDK2 by binding of cyclin A (Fig. 7 B), but all four kinase domains of the ERBB family share conserved C-lobe residues in the dimerization interface, that is, all four members are potential activators. Indeed, a recent structural study shows that the ERBB4 kinase domain also forms an asymmetric dimer essentially identical to that of EGFR (Qiu et al., 2008). In the case of the catalytically inactive ERBB3, the conserved C-lobe interface allows the NRG receptor to activate its heterodimerization partner, explaining the functional role and mode of action of this unusual ERBB family member.

1.7. Regulatory sequences in the ERBB intracellular regions

Recent studies show that the intracellular juxtamembrane (JM) region of the EGFR plays a key part in promoting the allosteric mechanism of its activation, instead of serving the autoinhibitory role described for JM regions of several other RTKs. It is indispensable for allosteric EGFR kinase activation and productive interactions within a dimer (Thiel and Carpenter, 2007). Interestingly, the EGFR JM region harbors protein kinase C (PKC) and mitogen-activated protein kinase (MAPK) phosphorylation sites that modulate receptor activity and fate (Hunter et al., 1984; Lin et al., 1986; Northwood et al., 1991). Mechanistically, part of the JM region of the receiver kinase “cradles” the C-lobe of the activator kinase in the dimer (Jura et al., 2009; Red Brewer et al., 2009). This interaction promotes dimerization and allosteric activation. The remainder of the receiver’s JM region may interact with its counterpart in the activator to further stabilize the asymmetric dimer. Dimerization of the transmembrane domains also has a direct role in the EGFR activation process (Bennasroune et al., 2004; Bocharov et al., 2008; Mendrola et al., 2002). These data are consistent with a mechanism in which the extracellular domains block the intrinsic ability of the transmembrane and cytoplasmic domains to dimerize, with ligand binding releasing this block.

Interestingly, the Kuriyan lab also identified a structure of a potential inactive dimer for the EGFR kinase domain, in which C-terminal sequences mask docking sites for JM dimerization

(Jura et al., 2009; Zhang et al., 2006). This supports an autoinhibitory role for the EGFR C terminus, as suggested previously (Walton et al., 1990). In addition, studies of intact EGFR argue that the JM region allosterically controls ligand binding by the receptor (Macdonald-Obermann and Pike, 2009), suggesting inside-out signaling in the EGFR system.

Like many RTKs, ERBBs become rapidly ubiquitinated after receptor activation by the ubiquitin ligase CBL (casitas B-lineage lymphoma proto-oncogene) (Levkowitz et al., 1999; Levkowitz et al., 1998). This modification of the cytosolic tail promotes receptor degradation, creating an important negative feedback mechanism. The degradative sorting of EGFR and other family members in the endosomal system, and the crosstalk between intracellular receptor trafficking and signaling, will be the topics of chapter 3.

Probably the most complex aspect of ERBB receptor activation and subsequent signal transmission concerns the numerous tyrosine, but also serine and threonine phosphorylation sites in the cytoplasmic tail. The dynamically and differentially phosphorylated C terminus of ERBBs serves as docking platform for a variety of signaling molecules, which in turn can interact with multiple downstream effectors, branching into the network of ERBB receptor signaling. The link between RTK autophosphorylation and the initiation of signaling networks, as well as differences between individual ERBB family members in this respect, will be discussed below.

2. The network of ERBB signaling

Studying the mechanism of signal propagation by ERBBs from the extracellular space across the plasma membrane into the cytosol revealed several unique features of this RTK family: 1) ligands induce receptor dimerization not by crosslinking of receptor monomers, but by releasing an autoinhibited confirmation of the ligand-binding domains – dimerization is entirely receptor-mediated; 2) the monomeric kinase domain of ERBBs is constitutively in an active conformation, but intrinsically autoinhibited – not receptor *trans*-phosphorylation in the activation loop, but ligand-induced intermolecular interactions within an asymmetric dimer promote receptor activation; 3) both the transmembrane and juxtamembrane regions participate proactively in the dimerization and activation mechanism, in contrast to their passive or autoinhibitory role observed for several other RTKs.

The main determinant of signaling specificity and potency is the vast array of phosphotyrosine-binding proteins (*e.g.* more than 100 EGFR-interacting proteins reported) that differentially associate with the tail of each ERBB molecule after engagement into heterotetrameric complexes (see examples in Fig. 2). Which sites are autophosphorylated,

and hence which signaling proteins are engaged, is determined by the identity of both ligand and receptor (Citri and Yarden, 2006; Hynes et al., 2001; Yarden and Sliwkowski, 2001).

The first response to ERBB autophosphorylation is the recruitment and activation of a host of downstream signaling molecules containing SH2 or PTB domains, specifically binding to phosphotyrosines (Schlessinger and Lemmon, 2003). Typically, these signaling adaptors and enzymes are multidomain proteins, able to integrate more than one stimulus-dependent modification by coincidence detection (Lemmon and Schlessinger, 2010; Seet et al., 2006). Thus, multivalency appears to be a key solution, with several domains in a single protein cooperating with one another to drive formation of a signaling complex or network node.

2.1. Phosphosites in the cytoplasmic tail of ERBBs as docking platforms

Fig. 8 summarizes sites of ERBB tyrosine phosphorylation, as well as signaling effectors predicted or shown to bind to these sites of phosphorylation (Wilson et al., 2009). Large-scale “precision proteomics” based on mass spectrometry now enables the system-wide characterization of signaling events at the level of posttranslational modifications, namely phosphorylation, and resulting protein-protein interactions (Choudhary and Mann, 2010). Altogether, 20 different tyrosine residues have been shown to be phosphorylated in the EGFR and up to 27 in ERBB4 (Schulze et al., 2005), not only by autophosphorylation, but also by recruitment of the kinases SRC and JAK2 (Olayioye et al., 1999; Yamauchi et al., 1997). In this proteomics-based approach, EGFR is the family member with most interaction partners and the highest percentage of tyrosines with more than one binding partner (Fig. 8 and 9). However, in another study using protein microarrays, EGFR and ERBB2 become markedly promiscuous and ERBB2 can be the receptor with most binding partners due to lowered affinity thresholds (Jones et al., 2006). ERBB3 is characterized by a many binding sites for phosphatidylinositol-3-kinase (PI3K; more precisely for the regulatory subunit p85 alpha), while EGFR and ERBB2 have no direct binding site for PI3K subunits. ERBB4 and EGFR have a variety of tyrosines that bind the adaptor GRB2 (and SHC), and both recruit the transcription factor STAT5 (Schulze et al., 2005). The overall pattern of interaction partners of EGFR and ERBB4 suggests similar roles during signaling through their respective ligands.

In contrast to the modification of tyrosines responsible for signal propagation, phosphorylation of serines and threonines is rather connected to negative feedback mechanisms, for example the downregulation of receptor kinase activity (Countaway et al., 1990). Most of the autophosphorylated tyrosine sites were activated immediately within seconds after receptor stimulation (Dengjel et al., 2007), with maximum levels between one to five minutes, while serine and threonine sites showed slower dynamics, comprehensively studied by (Olsen et al., 2006) (in fact, this report provided the first dynamic view of a global signaling network in mammalian cells). Surprisingly, the observation by (Dengjel et al., 2007)

that the abundances of corresponding nonphosphorylated peptides did not change substantially (despite high EGF concentrations used) suggests that only a small subset of receptor molecules are involved in signal transduction at this early stage.

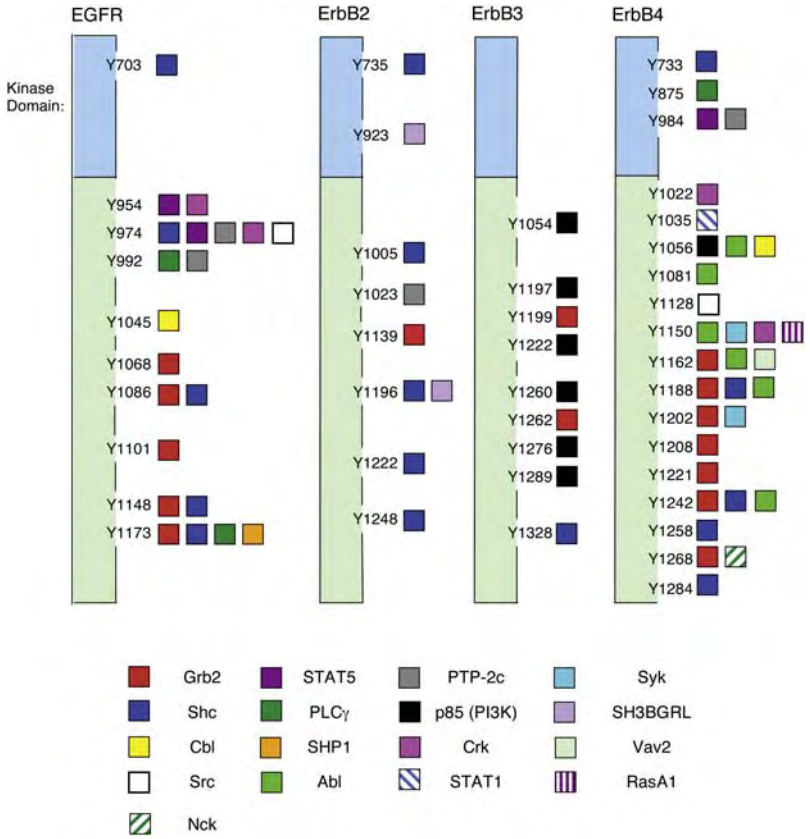

Fig. 8: ERBB tyrosine phosphosites in the C-terminal region as docking sites for downstream signaling effectors. Ligand stimulation of ERBB receptor tyrosine phosphorylation creates docking sites for numerous signaling effectors. Putative sites of EGFR, ERBB2, ERBB3, and ERBB4 tyrosine phosphorylation are denoted, as well as signaling effectors predicted or shown to bind to these sites of phosphorylation (Wilson et al., 2009).

A few words of caution should be brought forward at this point. Detailed analysis of activation profiles from different cell types (HeLa, HMEC, A431) showed that in each cell line different interacting proteins with varying dynamics are recruited to the activated EGFR (Morandell et al., 2008). This will lead to differential initiation of distinct signaling networks for certain cell lines or tissues. In addition, single residues display remarkable differences in their activation levels ranging from estimated 2.5 to 40% at their maximum of stimulation (Wu et al., 2006), indicating unequal limitation of docking sites. In this respect, the relative concentration of receptors and their downstream binding partners is crucial. The amount of endogenous EGFR, for example, differs substantially between cell lines (Morandell et al., 2008), which will also influence the availability of docking sites, competition and binding specificity of downstream signaling components. Studies on cells with different expression levels of ERBB2 showed that its increasing expression is associated with enhanced proliferation and migration upon stimulation with either EGF or HRG (heregulin, Type I NRG1) (Kumar et al., 2007; Wolf-Yadlin et al., 2006), with strong implications for ERBB2-

positive tumor development, but also in respect to different growth factor stimuli and receptor heterodimers. Finally, rather low reproducibility of data (due to technical differences or restrains) in large scale proteomics analyses further hampers the approach to understand initiation and propagation of ERBB signaling on a systems level.

However, integration and modeling of global phosphorylation data from methodologically different contexts and cell types, as well as considering spatiotemporal modification and localization of signaling components, are the current challenges in deciphering signal transduction networks (Choudhary and Mann, 2010; Linding et al., 2007). To this end, systems biology approaches integrating data from proteomic studies, gene expression analyses, and imaging-based phenotypic screens, could be the key to understand the regulation and function of signaling networks holistically.

2.2. The initiation of signaling networks downstream of ERBBs

Different classes of proteins bind to the phosphorylated C-terminal tail of ERBB receptors, for example adaptor and scaffold proteins (GRB2, SHC), kinases (SRC, PI3K), phosphatases (SHP1/2), lipases (PLCG1, PLD2), transcription factors (STAT3/5), GTPase-activating proteins (RASA1 or (RAS)GAP, RACGAP1, IQGAP1), guanine nucleotide exchange factors for RAS proteins (SOS1/2), E3 ubiquitin-protein ligases (all three CBLs), and endocytic adaptor or scaffolding proteins (AP2 subunits, epsin 1, EPS15, CAV1). In total, more than 100 interacting proteins for the EGFR and more than 200 EGF-related substrates are described in the literature (Morandell et al., 2008). Here, the focus will be on a few components of major pathways in the signaling network, shown in Fig. 9 (and Fig. 2).

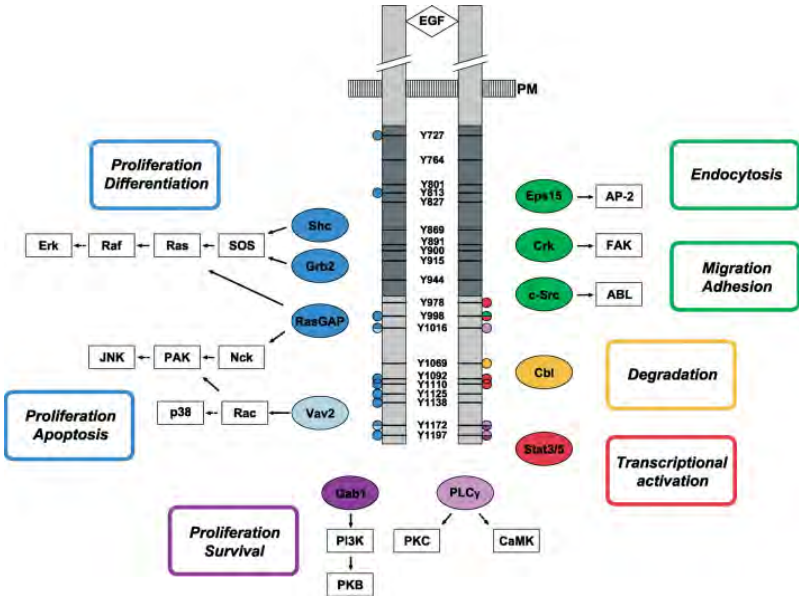

Fig. 9: EGFR downstream signaling effectors and major pathways in the EGFR signaling network.
Tyrosine phosphorylation sites on the EGFR homodimer are indicated by black bars, and known binding sites are labeled with colored circles; corresponding colors indicate direct interaction partners. The receptor kinase domain is shown in dark gray. Residue numbering is with the signal peptide (+ 24) (Morandell et al., 2008).

Phospholipase C gamma 1 (**PLCG1**), initiating pathways important for proliferation and survival *via* PKC and CAMK1, illustrates vividly the multivalency of receptor-proximal interactions. Two SH2 domains, two PH domains (one split into two parts), one C2 domain, and one SH3 domain all participate in multivalent signal-dependent targeting of PLCG1 to its site of action at the membrane (Fig. 10 B). The SH2 domains bind phosphotyrosines in the receptor; the PH domains bind phosphoinositides at the plasma membrane, including the PI3K product phosphatidylinositol 3,4,5-triphosphate (PI(3,4,5)P_3); the C2 domain also binds membrane components; and the SH3 domain binds CBL (Lemmon and Schlessinger, 2010). PLCG1 thus integrates multiple signals through a combination of recognition modules, permitting coincidence detection (Pawson, 2007).

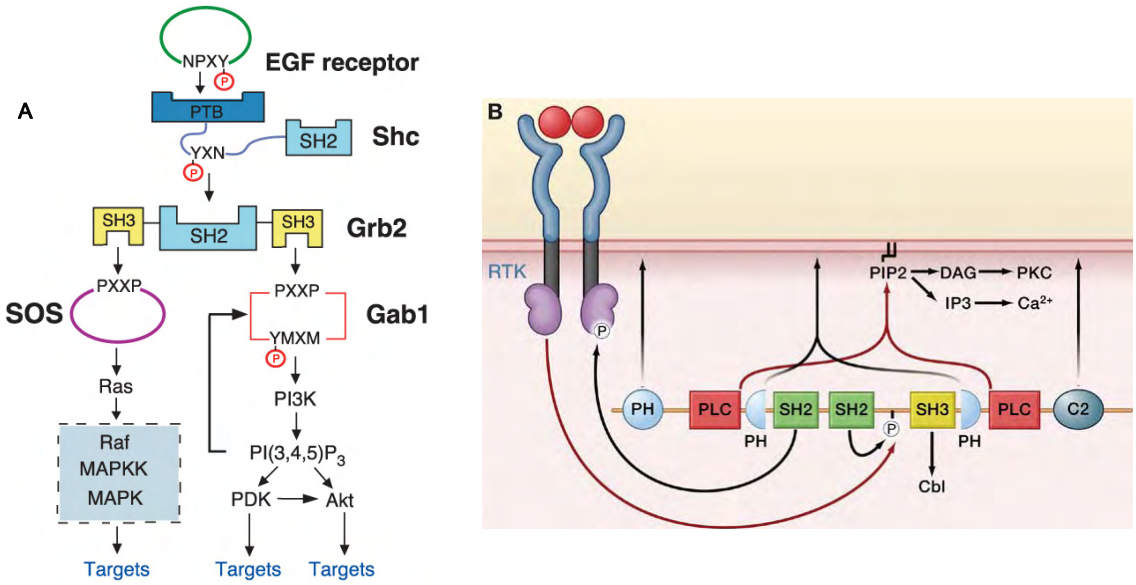

Fig. 10: Cooperativity of PTB domains in adaptors downstream of EGFR, initiating MAPK and PI3K signaling.
A) The PTB domain of SHC binds to an NPXpY motif in activated EGFR, resulting in tyrosine phosphorylation of SHC on at least two canonical binding sites for the SH2 domain of the adaptor protein GRB2. GRB2 can recruit the guanine nucleotide-releasing factor SOS and the docking protein GAB1. GRB2-mediated membrane recruitment of SOS results in activation of the RAS-MAPK cascade. Recruitment of GAB1 leads to tyrosine phosphorylation of the docking protein on multiple sites, including a canonical binding site for the SH2 domains of the p85 regulatory subunit of PI3K, resulting in stimulation of PI3K and activation of the antiapoptotic AKT signaling pathway. Binding of the PH domains of PDK and AKT to PI(3,4,5)P_3 leads to membrane translocation, followed by stimulation of the protein kinase activities of PDK and AKT. In addition, PI(3,4,5)P_3 binds to the PH domain of GAB1, which results in a positive-feedback mechanism mediated by membrane translocation of the docking protein (Schlessinger and Lemmon, 2003). **B)** An extreme example of multivalency in adaptor or scaffold proteins proximal of RTKs is the cooperation of multiple domains in PLCG, integrating many signals at the plasma membrane. The N-terminal SH2 domain is responsible for complex formation with activated RTKs. The C2 and PH domains cooperate with the SH2 domain to target PLCG to the plasma membrane. One or both of the PH domains may also specifically recognize products of RTK-activated PI3K. RTK-mediated tyrosine phosphorylation of PLCG leads to intramolecular binding of the C-terminal SH2 domain to a phosphotyrosine. This stimulates enzymatic activity of PLCG, leading to hydrolysis of PI(4,5)P_2 (PIP2) and consequently to the formation of Ins(1,4,5)P_3 (IP3) and diacylglycerol (DAG) (Lemmon and Schlessinger, 2010).

The scaffolding adaptor protein **GAB1** (GRB2-associated binder 1) is the primary mediator of EGF-stimulated activation of the PI3K-AKT/PKB cell survival pathway (Mattoon et al., 2004), as the autophosphorylation sites on EGFR do not include canonical PI3K interaction sites (in contrast to ERBB3 and 4, Fig. 8). All GAB proteins contain binding sites for the SH2 domain of the p85 subunit of PI3Ks (which recruits p110 proteins, the class I

PI3Ks), as well as an N-terminal PH domain, proline-rich motifs and multiple phosphorylation sites (Gu and Neel, 2003). Most GAB – receptor interactions are mediated indirectly *via* binding of proline-rich domains to GBR2 (Holgado-Madruga et al., 1996) (Fig. 10 A), but it can be phosphorylated (Lehr et al., 1999) and recruited by the EGFR directly (Rodrigues et al., 2000). The PH domain of GAB1 was shown to bind specifically to PI(3,4,5)P_3 (yet another example of domain cooperativeness), which is required for activation of GAB1-mediated EGFR signaling. Hence, class I PI3Ks function both as a downstream effectors and upstream regulators of EGFR-GAB1 signaling, a feedback loop negatively controlled by the lipid phosphatases PTEN. The complex events further downstream of PI3Ks, particularly the anti-apoptotic PKB/AKT signaling network, are excellently reviewed in (Scheid and Woodgett, 2001; Vanhaesebroeck et al., 2010). By recruiting the tyrosine phosphatases SHP2 (PTPN11), GAB1 also regulates RAS-MAPK activation (Gu and Neel, 2003).

The prototypic signaling adaptor **GRB2** (growth factor receptor-bound protein 2) has a single SH2 domain that binds several phosphosites of all ERBBs (Fig. 8), and two flanking SH3 domains that engage for example the RAS guanine nucleotide exchange factor **SOS** (son of sevenless homolog) (Bowtell et al., 1992; Chardin et al., 1993; Rozakis-Adcock et al., 1993) and the above mentioned GABs. GRB2 can therefore couple ERBBs to both the RAS-MAPK cascades and PI3K pathways involved in growth, proliferation and differentiation. In Fig. 10 A, indirect binding of GRB2 to the EGFR *via* the scaffold protein **SHC** (SRC homology 2 domain containing) is shown (Schlessinger and Lemmon, 2003). The receptor-associated (SHC-)GRB2-SOS complex is thus brought close to its membrane-bound target RAS, which is then activated by SOS (Buday and Downward, 1993; Gale et al., 1993; Li et al., 1993).

Cellular homologues of the *ra*t *s*arcoma retrovirus-encoded ***RAS*** genes where identified almost 30 years ago (Chang et al., 1982; DeFeo et al., 1981), and named *HRAS* and *KRAS* (Harvey / Kirsten rat sarcoma viral oncogene homolog). By 1983, the third member of the mammalian family of *RAS*-related genes, *NRAS* (neuroblastoma RAS viral oncogene homolog), had been cloned (Hall et al., 1983; Shimizu et al., 1983). The exciting history of research in the RAS field is reviewed in (Karnoub and Weinberg, 2008), involving conceptual milestones concerning tumor development and RTK downstream signaling. The discovery of the molecular mechanism of RAS activation in the 1990s is also one of the most striking examples of cross-discipline and cross-species work of many teams simultaneously. The first indication that RAS activity is vital for signaling by extracellular mitogens came from the observation that EGF increased the guanine nucleotide-binding by HRAS (Kamata and Feramisco, 1984). The connection of RAS with MAPK signaling was discovered in the early 1990s (Leevers and Marshall, 1992; Wood et al., 1992). The first identified mammalian RAS effector was RAF1 (v-raf-1 murine leukemia viral oncogene homolog 1), the Ser/Thr kinase upstream of MEK and ERK (Moodie et al., 1993; Vojtek et al., 1993; Zhang et al., 1993).

RAS-mediated signaling networks and biological outcomes are summarized in Fig. 11. As for GRB2, activated RAS can stimulate both the PI3K-AKT/PKB pathway (downstream of most active ERBB dimers) and the ERK1/2 MAPK cascade. The latter became the prototype of a number of other plasma membrane to nucleus signal transduction pathways, and is an invariable target of all ERBB ligands.

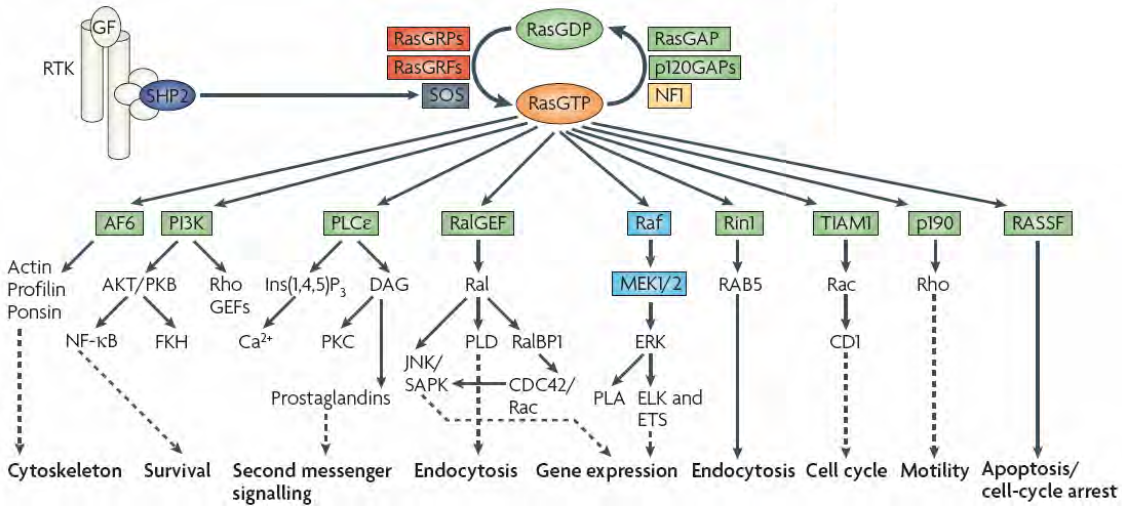

Fig. 11: RAS signaling networks.
Ras proteins function as nucleotide-driven switches that relay extracellular cues to cytoplasmic signaling cascades. The binding of GTP to Ras proteins locks them in their active states, which enables high affinity interactions with downstream targets. Subsequently, a slow intrinsic GTPase activity cleaves off the phosphate, leading to RAS functional inactivation and thus termination of signaling. This on-off cycle is tightly controlled by GTPase-activating proteins (GAPs) and guanine-nucleotide exchange factors (GEFs). Activated RAS engages effector molecules that initiate several signal-transduction cascades. Outputs shown represent the main thrusts of the indicated pathways, for example activation of the ERK MAPK cascade *via* RAF (Karnoub and Weinberg, 2008).

2.3. The RAF-MEK-ERK mitogen-activated protein kinase cascade

Sequential activation of kinases within the MAPK cascades is a common, evolutionary conserved mechanism of signal transduction. Four cascades have been identified in the last 20 years, which are named according to the terminal Ser/Thr MAPKs. These are ERK1/2 (extracellular signal-regulated kinase 1/2), JNKs (c-JUN N-terminal kinases), p38 kinases, and ERK5 (Roberts and Der, 2007; Shaul and Seger, 2007). Each of these cascades consists of a core module of three tiers of protein kinases termed MAPK kinase kinase (MAPKKK), MAPK kinase (MAPKK), and MAPK (up to five tiers in certain cell lines or stimulation conditions). The transmission of the signal is mediated by sequential phosphorylation and activation of the components in the subsequent tiers. These cascades cooperate *via* crosstalk and integrate various extracellular signals, thus controlling a large number of distinct and even opposing cellular processes such as proliferation, differentiation, survival, development, stress response, and apoptosis. Specificity of each cascade is regulated through the existence of several distinct components in each tier, the strength and duration of the signals, and subcellular localization of components (Shaul and Seger, 2007;

Yao and Seger, 2009), leading to partially differential activation of transcription factors. About 70 genes, which are each translated to several alternatively spliced isoforms, encode the entire MAPK system (Keshet and Seger, 2010; Rubinfeld and Seger, 2005).

The ERK1/2 cascade is the best characterized MAPK pathway. The primary MAPKKK components are the three different **RAFs**, RAF1/CRAF, ARAF and BRAF, whose founding member was cloned in 1983 (Rapp et al., 1983). They are key downstream effectors of the above mentioned RAS family of small GTPases, the most frequently mutated oncogenes in human cancers. Although RAFs have functions that are independent of their ability to signal to the ERK1/2 cascade (McCubrey et al., 2007; Wellbrock et al., 2004), to date, the only validated physiologically relevant substrates remain the two MAPKKs **MEK1/2** (for MAPK/ERK kinase 1/2 (Crews et al., 1992; Zheng and Guan, 1993); the official symbols are MAP2K1/2). The transcriptional response to RAF activation was shown to be almost completely dependent on MEK1/2 activity (Schulze et al., 2004). MEK1/2 then phosphorylate and activate the ERK1/2 MAPKs (Boulton et al., 1991; Boulton et al., 1990; Ray and Sturgill, 1987).

Activated **ERKs** regulate the activities of an ever growing roster of substrates that where estimated to comprise over 160 proteins in 2006 (Yoon and Seger, 2006). The majority of ERK substrates are nuclear proteins, and nuclear translocation of ERKs is necessary to regulate various transcription factors such as members of the ETS oncogene family (Brunet et al., 1999) and AP-1 transcription factors, ultimately leading to changes in gene expression (see below). The ETS (E-twenty six) family, derived from the avian erythroblastosis virus E26 carrying the *v-ets* oncogene (Leprince et al., 1983; Nunn et al., 1983), is comprised of 29 members in humans, for example ELKs and ELFs (Sharrocks, 2001). The heterodimeric AP-1 (activator protein 1) transcription factors are composed of proteins belonging to the FOS, JUN, ATF and JDP families (Hess et al., 2004; Shaulian and Karin, 2002), whose founding members have been identified by their homology to viral oncogenes as well (Bohmann et al., 1987; Van Beveren et al., 1983).

Transcription factors can also be phosphorylated by ERK1/2 in the cytosol and then shuttle to the nucleus. Cytosolic ERK targets are often part of feedback loops regulating the MAPK cascade itself: the EGFR, PLCG1, GABs, SOS, SHC, RAFs, MEK1/2, and several MAPK phosphatases are phosphorylated by ERK1/2 (to name a few examples mentioned above). Next to transcription factors, kinases, phosphatases, RTKs and their associated signaling proteins, ERK targets include cytoskeletal components, regulators of apoptosis, and a variety of other signaling-related molecules (Yoon and Seger, 2006). Beside the activation by phosphorylation, ERK1/2 can activate their targets by direct binding, thereby extending the repertoire of downstream targets of the ERK cascade.

2.4. The architecture of transcriptional responses induced by ERBB ligands

Microarray-based studies to elucidate the global transcriptional response of cells to growth factors were pioneered by experiments using human fibroblasts stimulated with serum (Iyer et al., 1999; Winkles, 1998), even before the human genome was sequenced (Lander et al., 2001; Venter et al., 2001). Genes which could be clustered into groups on the basis of their temporal expression patterns were found to correlate often with similarity of protein function, especially for immediate-early transcription factors and other proteins involved in the regulation of signal transduction, cell cycle progression, and inflammation. A rather indirect approach to study RTK/EGFR downstream gene expression utilized inducible RAF1 constructs to activate the MEK-ERK cascade (Schulze et al., 2001; Schulze et al., 2004). Interestingly, at least one half of the transcription induced by RAF activation required EGFR function, and an autocrine feed-forward loop *via* the induction of EGF-like growth factors such as HBEGF, TGFA, and AREG was identified.

The first comprehensive kinetic profile of the transcriptional response (of HeLa and MCF10A cells) to EGF (and serum) was published by Yosef Yarden' s group in 2007 (Amit et al., 2007a). On a time scale of up to eight hours, more than 450 genes were induced by EGF to at least twice the baseline level, in clearly defined waves of transcription. The initial wave, peaking at 20 - 40 min, consisted of a small number of "forward-driving", previously characterized immediate early genes (IEGs), such as AP-1 (*JUN, FOS*; see above) and EGR family (*EGR1/3*, early growth response) transcription factors. A large number of genes induced at later time points (referred to as delayed early genes, DEGs), however, were implicated in negative transcriptional regulation. Examples include *FOSL1/2, JUNB, JUND, ATF3* (all of which can interfere with AP-1 function), *NAB2* (inhibiting EGR1), and other novel transcriptional repressors (*MAFF, KLFs*) and regulators of mRNA stability (*ZFP36*). The authors propose that the recruitment of these negative regulators into existing transcriptional complexes permits the transient activation followed by rapid attenuation of the initial burst of transcription, explaining the observed waves of EGF-induced gene expression.

In addition, a coordinated induction of multiple MAPK phosphatases (MKPs, a subgroup of dual-specificity phosphatases, DUSPs) was observed, as part of a pathway-specific negative feedback loop interfering with MAPK activity (Fig. 12 and chapter 2.6.). Other intriguing examples are LRIG1, several SOCS proteins (Kario et al., 2005), and MIG6 (mitogen-induced gene 6) or ERRFI1 (ERBB receptor feedback inhibitor 1, also abbreviated RALT), which interfere with the signaling cascade at the very upstream part, the ERBB receptors themselves (chapter 2.6.). Surprisingly, the peak of *MIG6* transcription occurred (60 to) 120 min after EGF stimulation, thus it is probably active only at times when the EGFR is being sorted into endosomes and degraded in lysosomes (chapter 3). The authors

therefore assume that MIG6 and other late-induced negative feedback regulators maintain a refractory period that decouples the cells from repetitive stimulation.

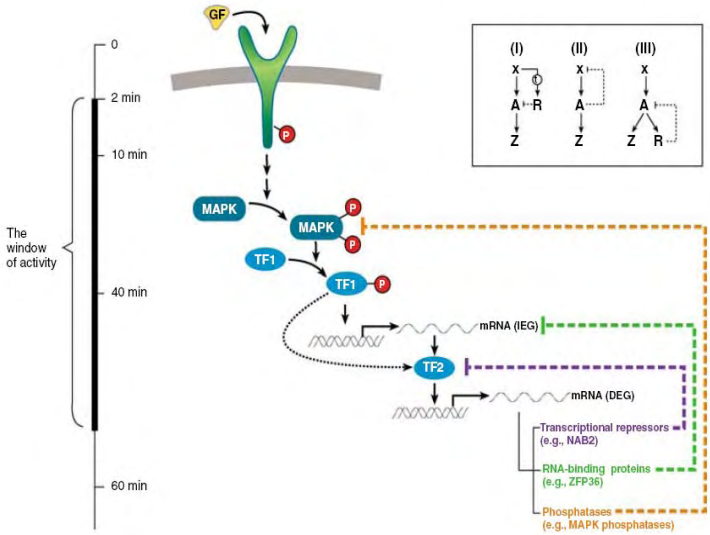

Fig. 12: Feedback circuits define the window of RTK activity.
The timeline (left) indicates the window of signaling activity downstream of RTKs. MAPK activation and translocation to the nucleus enables direct phosphorylation of transcription factors (TF1), which activate transcription of IEGs (e.g. the AP-1 components JUN and FOS). IEGs regulate a second wave of transcription. The DEGs encode a broad range of proteins, including negative regulators. The signaling arm is regulated at the tier of MAPKs by the group of DUSPs (orange line), whereas transcription is regulated by the induction of transcriptional repressors (violet line) and RNA-binding proteins (green line). Collectively, these feedback loops shut the window of RTK signaling (Amit et al., 2007b).

In summary, the induction of negative regulators serves to attenuate the same pathway that induced their expression, leading to the definition of an activation interval. Comparison of EGF-induced transcription profiles from HeLa *vs.* MCF10A cells, as well as EGF *vs.* serum stimulation, showed that the identities of the active components vary between systems, but the overall signaling architecture including the balance between forward-driving actions and feedback attenuation mechanisms is conserved across cell types and stimuli (Amit et al., 2007a). In this respect, pathologies like cancer and various viruses can be viewed as hijackers of biological robustness (Amit et al., 2007b).

A small number of other studies describe global transcriptional profiles upon stimulation with ERBB ligands, mostly in comparison with other growth factors in the effort to explain differences in cell fate determination. By comparing HRG- (heregulin, type I NRG1) with EGF-induced gene expression, it was proposed that at the early stage of transcription, the cellular program is controlled by means of quantitative magnitude or duration of stimulation, not specificity (Nagashima et al., 2007) (see below). In another study, genes upregulated in human epithelial cells treated with EGF, VEGF, or IL1A were compared (Schweighofer et al., 2009). A number of differentially *vs.* commonly regulated genes was identified, and IEGs in the EGF response from previous reports were confirmed in a different cell culture model. As a last example, gene expression in desmoid cells stimulated with EGF or TGFA was analyzed by microarrays (Trang et al., 2010). A transcriptional redundancy between 55-65% was observed for different time points, and approximately 150 genes were co-stimulated, suggesting both overlapping and specific functions of the two EGFR ligands.

2.5. Biological outcomes of differential signaling in the ERBB system

One of the major challenges for cell signaling studies is to understand how different stimuli determine unique responses and distinct cell fate decisions, despite signal propagation through shared core pathways such as the ERK MAPK cascade. Crosstalk with other signaling cascades – the cellular context in general - as well as the spatiotemporal organization of pathway components (chapter 2.6.) are crucial elements for signaling specificity. Here, examples of how different ERBB ligand•receptor combinations can elicit varying biological outcomes will be discussed.

2.5.1. Biological responses of different EGF family ligands

In a variety of cell culture systems and tumors, different EGF family ligands that bind the same receptor can promote divergent biological responses, reviewed in (Wilson et al., 2009). The EGFR ligands TGFA and AREG stimulate equivalent levels of DNA synthesis in MDCK cells, but AREG also stimulates a morphologic change whereas TGFA does not (Chung et al., 2005). In MCF10A human mammary epithelial cells, AREG stimulates greater motility and invasiveness than does EGF, probably *via* an AREG autocrine loop (Willmarth and Ethier, 2006), and by differentially affecting the fate of stimulated EGFR (see below and chapter 3.2.2.). The expression of specific ERBBs and their ligands in certain tumors is differentially associated with prognosis (Normanno et al., 2001; Normanno et al., 2005; Normanno et al., 2006). Presence of EGF in breast tumor samples is associated with a rather favorable prognosis, whereas high expression of TGFA, HBEGF, and NRG2 is related to more aggressive tumors (Revillion et al., 2008). A number of other studies indicate that TGFA and AREG couple EGFR signaling to tumor cell aggressiveness and chemoresistance, while EGF fails to do so (Wilson et al., 2009).

Generally, the duration of ERBB and MAPK signaling seems a key component of ligand signaling specificity and cell fate determination (Marshall, 1995; Murphy et al., 2004; Murphy et al., 2002; Santos et al., 2007). It has been postulated that EGF family ligands differentially stimulate receptor phosphorylation on distinct sets of tyrosine residues, thereby coupling ERBBs to specific signaling effectors (see Fig. 8 and 9, chapters 2.1. and 2.2). For example, the strong mitogenicity of epigen was attributed to evasion of receptor-ligand depletion due to inefficient receptor phosphorylation and ubiquitination, as compared to EGF (Kochupurakkal et al., 2005). EGF stimulates abundant EGFR phosphorylation at Tyr1045 (a binding site for the E3 ubiquitin ligase CBL; chapter 3), whereas AREG does so to a much lesser extend (Gilmore et al., 2008; Stern et al., 2008). Thus, AREG and EGF differentially regulate the turnover of stimulated EGFR, leading to differences in the duration of ligand-induced EGFR signaling (accounting for the inability of EGF to stimulate motility and invasiveness in cells

that do respond to AREG). In a comprehensive study utilizing six different EGFR ligands, it was shown that HBEGF, BTC, and EGF target the receptor predominantly for degradation *via* persistent EGFR phosphorylation and ubiquitination, whereas stimulation with AREG, EREG, and TGFA leads to recycling back to the plasma membrane (Roepstorff et al., 2009).

It has been hypothesized that differences in the conformation of the liganded extracellular domain may account for the distinct patterns of ERBB receptor tyrosine phosphorylation and downstream signaling (Wilson et al., 2009). Subtly different conformations of dimeric extracellular regions could alter the interaction between the two intracellular domains in the asymmetric dimer (see chapters 1.5. and 1.6.), in turn influencing which tyrosine residues in the cytoplasmic tails are most efficiently phosphorylated. Studies using constitutively active ERBB2 and ERBB4 mutants reveal that artificially manipulating the structural relationship between two receptor monomers within a dimer can result in divergent receptor signaling and coupling to downstream events (Burke and Stern, 1998; Pitfield et al., 2006). In addition, evidence for ligand-specific receptor conformations can be seen in a comparison of the EGFR extracellular region bound to EGF or TGFA (Garrett et al., 2002; Harte and Gentry, 1995; Ogiso et al., 2002). However, it should be pointed out that no crystal structure of ERBB heterodimers has been determined, thus it is difficult to evaluate the impact of different receptor conformations for downstream signaling. Finally, competition between multiple EGF family ligands in a given tissue is likely to influence the physiological signaling outcome.

Effects of disrupting the function of EGF ligands in mice are rather mild (Schneider and Wolf, 2009; Wilson et al., 2009), except for knockout of neuregulins (see below). Relatively benign phenotypes have been observed in the knockouts of EGF and AREG (Luetteke et al., 1999), and TGFA-deficient mice had only eye abnormalities and derangement of hair follicles (Mann et al., 1993). Even in the triple knockout of EGF, TGFA, and AREG, the animals were rather healthy and fertile, despite of defects in gastrointestinal development, growth retardation (Troyer et al., 2001), and in mammary gland development (Luetteke et al., 1999). This indicates overlapping or compensatory functions among the EGF ligands, in contrast to above mentioned observations from cell culture systems regarding ligand specificity.

2.5.2. Signaling specificity of distinct ligand-induced heterodimers

The basic functional unit of ERBB signaling is a receptor dimer, to which each partner contributes unique features. Therefore, in addition to intrinsic properties of the EGF family ligands, signaling specificity at the input level can be appointed to distinct ligand-induced heterodimers, which are more potent signal transducers than receptor homodimers in general (Pinkas-Kramarski et al., 1996).

As mentioned in chapter 2.1., ERBB4 shares many interaction partners as well as ligands with the EGFR, suggesting similar functions of these two receptors. Both receptors bind at

least four different ligands commonly (Fig. 4), and recruit for example GRB2, SHC, STAT5, and SRC (Schulze et al., 2005) (Fig. 8). However, ERBB4 seems more selective than other ERBBs regarding interaction partners (Kaushansky et al., 2008), and the receptor is endocytosis-impaired in contrast to EGFR (Baulida et al., 1996). The question of ERBB4 association with CBL and its ubiquitination is controversial, because for example (Levkowitz et al., 1996) states that only EGFR interacts with CBL while other studies found that ERBB4, too, can recruit CBL (Jansen et al., 2009; Kaushansky et al., 2008; Laederich et al., 2004). In addition, ubiquitination of a cleaved intracellular domain of ERBB4 by another E3 ubiquitin ligase, NEDD4, was reported recently (Zeng et al., 2009) (see chapter 3.2.2.).

ERBB2 can be viewed as a non-autonomous amplifier: without the requirement for an ERBB2 ligand, the receptor is constantly primed for interactions with other ligand-bound receptors of the family (Fig. 3 and chapter 1.5.). The property of ERBB2 to function as the preferred heterodimerization partner (Graus-Porta et al., 1997; Tzahar et al., 1996) is thus inherent in its structure. ERBB2-containing heterodimers undergo slow endocytosis (Baulida et al., 1996; Sorkin et al., 1993), and are frequently recycled back to the plasma membrane (Lenferink et al., 1998; Worthylake et al., 1999). These features translate to potent mitogenic signals, owing to prolonged engagement of multiple signaling pathways. The kinase-defective and therefore also non-autonomous ERBB3 can recruit PI3K subunits directly *via* six different phosphotyrosines (Fig. 8). ERBB3 does not seem to contain binding sites for CBL and is thus poorly degraded upon stimulation (Waterman et al., 1999). So, paradoxically, the ERBB2-ERBB3 pair of the two non-autonomous receptors seems the most potent signaling module in the ERBB receptor family in terms of cell growth and transformation (Citri et al., 2003; Pinkas-Kramarski et al., 1996; Wallasch et al., 1995).

Taken together, a given ERBB receptor has distinct signaling properties depending on differential phosphorylation by its dimerization partner (Graus-Porta et al., 1997; Olayioye et al., 1999; Olayioye et al., 1998), and the heterodimers can acquire novel signaling properties that are not the sum of the activity of individual receptor monomers (Hynes et al., 2001). The importance of heterodimer formation was also demonstrated for **mouse models** in which ERBBs have been individually knocked out. For example, in ERBB2 null mice NRG1-induced ERBB4 homodimers can not replace the function of the ERBB2-ERBB4 heterodimer (Lee et al., 1995). NRG1-deficient mice die very early during embryonic development, due to aberrant cardiac and neural development (Crone and Lee, 2002; Meyer and Birchmeier, 1995). NRGs and their receptors (ERBB2 and ERBB4, Fig. 4) are involved in the interaction between nerves and their target cells, for example muscle, glia and Schwann cells (Burden and Yarden, 1997). Indeed, ERBB2- (Lee et al., 1995) and ERBB4- (Gassmann et al., 1995) mutant mice share the same embryonic lethal phenotype as NRG1 knockouts, demonstrating NRG1 signaling *via* the ERBB2-ERBB4 heterodimer in heart development. ERBB3 knockout mice die slightly later during embryogenesis due to cardiac defects (Britsch et al., 1998;

Riethmacher et al., 1997), indicating that NRG1 and ERBB2 are reused at this developmental stage, now in the context of ERBB3 (Citri and Yarden, 2006; Erickson et al., 1997). This suggests rather specific functions for neuregulin-binding ERBB receptor heterodimers in the (sympathetic) nervous system, particularly in heart development. Knockout of the EGFR demonstrated its more general role during epithelial cell development in several organs, and affected mice die at various developmental stages, depending on the genetic background (Miettinen et al., 1995; Sibilia and Wagner, 1995; Threadgill et al., 1995). In addition, mutant mice that survive after birth develop strain-independent progressive neurodegeneration (Sibilia et al., 1998). Aberrant proliferation, migration or differentiation of specific epithelial cells during morphogenesis underlie these broad effects of EGFR knockout. Notably, ERBB2-deficient mice share various features with mice lacking other ERBBs, but no phenotype unique to ERBB2 has emerged. This observation is consistent with its non-autonomous function within heterodimers as positive regulator of ERBB signaling.

2.6. Intracellular modulation of ERBB signaling

Positive and negative feedback loops tightly regulate ERBB signaling at virtually every step of the cascade. Suppressive mechanisms at the input level include: 1) inhibition of RTK activity by stoichiometric binding (*e.g.* ERRFI1/MIG6/RALT) or by dephosphorylation (*e.g.* PTPN1/PTP1B, PTPN2, and PTPRE); 2) removal of active receptors from the cell surface, their ubiquitination *via* CBLs and degradation (endocytic ERBB trafficking and the link to signaling will be discussed separately); and 3) ligand sequestration for example by Argos in *Drosophila* (Klein et al., 2004; Schweitzer et al., 1995). Positive feedback loops at the input layer include the induction of ligand and receptor expression upon pathway activation leading to autocrine stimulation, a hallmark of transformed or malignant cells (Sporn and Todaro, 1980). Feed-forward mechanisms in the signal processing layer are intrinsic to the MAPK cascade, since the signal can be amplified by enzymatic activation in each tier. Negative regulators downstream of ERBBs are for example SPRED (Sprouty-related, EVH1 domain containing) and possibly SPRY (Sprouty) proteins, the ERK1/2 MAPKs themselves (phosphorylate and negatively regulate pathway components at multiple steps, *e.g.* the EGFR, adaptors and scaffolds, RAF and MEK; see chapter 2.3.), and diverse MKPs/DUSPs regulating the MAPK cascade. The activity of forward-driving transcription factors defining the signaling output is limited by an inducible set of transcriptional repressors and RNA-binding proteins discussed in chapter 2.4. The transcriptional induction of factors involved in negative feedback by the very pathway that is eventually inhibited is a common motif ensuring signal desensitization. The expression of MIG6, LRIG1 and several SOCSs (regulating EGFR degradation), Argos, SPRYs and SPREDs, multiple MKPs/DUSPs, and transcriptional repressors, for instance, can be induced by EGF.

Spatiotemporal localization of pathway components regulates signal transduction at all layers. Degradation *vs.* recycling of ERBBs presumably contributes to the magnitude and duration of MAPK activation (see 2.5.). Internalized, endosomal receptors can be active and associate with downstream signaling proteins, but to which extend these complexes participate directly in signal propagation is still a matter of debate (chapter 3.2.4.). A number of scaffold proteins, such as KSR1, IQGAPs, paxillin, SEF, beta-arrestins, MP1 and MORG1, are able to orchestrate the cytosolic MEK-ERK cascade at various intracellular locations (the plasma membrane and cytoskeleton, focal adhesions, the Golgi apparatus, early and late endosomes, respectively). As mentioned in chapter 2.3., the nuclear-cytoplasmic shuttling of MEK1/2 (Jaaro et al., 1997), ERK1/2 (Chen et al., 1992; Zehorai et al., 2010), and of many MAPK-activated transcription factors, is regulated by stimuli in a time-dependent manner. Finally, all ERBBs have also been reported to translocate in the nucleus (Marti et al., 1991; Wang and Hung, 2009), acting as transactivators of transcription (for example complexed with STATs) and as protein kinases with various reported nuclear substrates.

Here, the focus will be on ligand-induced negative feedback regulators of the receptors and downstream components of the cascade, as well as on MAPK scaffold proteins, providing both robustness and specificity of ERBB signaling.

2.6.1. Negative feedback regulators of the ERBB-mediated signaling cascade

One of the first direct negative feedback regulators of ERBB activity to be discovered in mammals was **MIG6** (mitogen-induced gene 6, or RALT for receptor-associated late transducer; the official symbol is ERRFI1 for ERBB receptor feedback inhibitor 1). Its expression can be induced by a number of stimuli such as serum (Wick et al., 1995) and a range of growth factors like EGF (Zhang and Vande Woude, 2007). The activation of the ERK MAPK cascade is necessary and sufficient to drive MIG6 expression (Fiorini et al., 2002). However, it specifically interacts with and regulates all members of the ERBB family (Anastasi et al., 2003; Fiorentino et al., 2000; Hackel et al., 2001). MIG6 directly suppresses the catalytic activity of ERBBs (Anastasi et al., 2007; Zhang et al., 2007a) by binding to the C lobe of the EGFR kinase domain in the CDK/SRC-like inactive conformation, blocking the formation of the asymmetric dimer interface (chapter 1.6.; Fig. 7). Interestingly, the segment responsible for binding only to the kinase active state is highly homologous to the corresponding region in ACK1 (CDC42-associated tyrosine kinase 1), involved in the regulation of ligand-induced EGFR degradation (Shen et al., 2007). Recently it was shown that MIG6 also mediates EGFR internalization, thereby integrating suppression of kinase activity with receptor endocytosis and degradation (Frosi et al., 2010). Additional reported functions of MIG6 (reviewed in (Zhang and Vande Woude, 2007)), sequestering for example

GTP-bound CDC42 (cell division cycle 42) and the NFKB inhibitor NFKBIA/IKBA (nuclear factor of kappa light polypeptide gene enhancer in B-cells inhibitor, alpha), support its importance as a tumor suppressor gene (Ferby et al., 2006; Zhang et al., 2007b).

Several protein tyrosine phosphatases (**PTPs**) negatively regulate ERBB activity. **PTP1B**/PTPN1 has been shown to dephosphorylate the EGFR (Flint et al., 1997; Liu and Chernoff, 1997) at contact sites between endosomes and the endoplasmic reticulum (Eden et al., 2010; Haj et al., 2002). However, relatively mild effects of PTP1B knockout concerning EGFR downstream signaling suggested that other pathways or phosphatases can compensate for PTP1B deficiency (Haj et al., 2003).

Both the EGFR and the scaffold protein SHC1 are substrates of **PTPN2**/TCPTP (T-cell protein tyrosine phosphatase) (Tiganis et al., 1998). Overexpression of this phosphatase seems to affect the PI3K-PKB/AKT-JNK signaling branch downstream of the EGFR more efficiently than the ERK MAPK cascade, thereby selectively regulating distinct pathways originating from the same receptor (Tiganis et al., 1999). The tumorigenicity of glioblastoma cells expressing a mutant EGFR, on the other hand, is suppressed by PTPN2 *via* inhibition of ERK2 activation (Klingler-Hoffmann et al., 2001).

Downstream of the EGFR, **PTPRE** (PTP-epsilon) was shown to inhibit ERK1/2 both in phosphorylation status and activity (Toledano-Katchalski et al., 2003; Wabakken et al., 2002). Its slow induction upon mitogenic stimulation, for instance with serum or EGF (Elson and Leder, 1995), suggests a function of this phosphatase in terminating prolonged, rather than acute, activation of ERK in the cytosol, or in maintaining a refractory period to avoid premature re-stimulation. PTPRE was also found to associate with the adaptor protein GRB2 (Toledano-Katchalski and Elson, 1999), and it binds and dephosphorylates the scaffold protein SHC, reducing the recruitment of GRB2 and concomitant activation of the ERK MAPK cascade (Kraut-Cohen et al., 2008).

Two **SHPs** (SRC homology phosphotyrosine phosphatases) are capable of binding to the EGFR and other ERBBs directly, or *via* adaptor proteins (see chapter 2.2.). SHP1/PTPN6 was shown to bind and dephosphorylate the EGFR, interfering with EGF-dependent MAPK stimulation (Keilhack et al., 1998). Both direct as well as indirect association with the EGFR *via* GAB1 was reported, indicating that GAB1 is another physiological substrate of SHP1 (Agazie and Hayman, 2003). SHP2/PTPN11 binds a conserved phosphotyrosine on both the EGFR and ERBB2 (Schulze et al., 2005). As for SHP1, it can also be recruited by the adaptor GAB1, necessary for EGF-induced ERK2 activation (Cunnick et al., 2000), and it can interact with GRB2 under certain stimulation conditions (Tauchi et al., 1994). Another recently identified phosphatase for both the EGFR and ERBB2 is PTPN9, regulating for example STAT3/5 signaling downstream of ERBBs (Yuan et al., 2010).

The putative tyrosine phosphatase **HD-PTP**/PTPN23 (His-domain / type N23 protein tyrosine phosphatase) has been shown to affect EGFR degradation (Doyotte et al., 2008) and signaling (Miura et al., 2008). It is an essential gene during mouse embryonic development, expressed early but maintained in adult tissues, especially in epithelial cells of many organs (Gingras et al., 2009a). It was also reported to regulate endothelial migration *via* its interaction with FAK (focal adhesion kinase) and SRC (Castiglioni et al., 2007; Mariotti et al., 2009a). *HD-PTP* is a candidate tumor suppressor gene (Toyooka et al., 2000), and its protein function has been found to contribute to motility of carcinoma cells upon stimulation with EGF (Mariotti et al., 2009b). The rat homolog Ptpn23/Ptp-Td14 is able to suppress Hras-mediated transformation (Cao et al., 1998), and human HD-PTP reduces colony growth formation independently of its phosphatase activity status (Gingras et al., 2009b). Low catalytic activity of HD-PTP was observed in one study (Mariotti et al., 2009a), whereas other reports show that it is basically catalytically inert (Barr et al., 2009), and back mutation of a key residue located in the phosphatase domain restored the HD-PTP tyrosine phosphatase activity (Gingras et al., 2009b). Some functions of HD-PTP such as cargo (EGFR) sorting during multivesicular body morphogenesis are dependent on its similarity to ALIX. BRO1 domain-dependent interaction with CHMP4B and PRD (proline-rich domain) -mediated interactions with ALG-2/PDCD6 and TSG101 have been demonstrated both for ALIX and HD-PTP (Doyotte et al., 2008; Ichioka et al., 2007). In addition, the BRO1 domains of all proteins containing this motif (ALIX, HD-PTP, BROX/C1orf58, and rhophilin) are able to bind the HIV Gag protein and to stimulate the production of virus-like particles (Popov et al., 2009). The machinery of endosomal cargo sorting and membrane invagination away from the cytosol, hijacked for example by HIV during viral budding, and the role of ALIX in these processes will be discussed in chapter 3.1.

In summary, a large number of PTPs, some of which are transcriptionally induced upon stimulation, can bind either directly or indirectly to ERBBs and regulate their activity. Certainly, not all of these interactions will take place in the same cell, but they suggest a degree of redundancy to ensure proper desensitization of the input signal. Transcriptional induction of phosphatases and partially overlapping functions seem reminiscent of MAPK cascade regulation by MKPs/DUSPs (see below).

Sprouty proteins (**SPRYs**) are evolutionary conserved inducible feedback regulators of RTK signaling. Their mode of action is multifaceted, modulating multiple events downstream of growth factor receptors, and subject to complex regulation. The first member of the SPRY protein family was discovered in *Drosophila melanogaster* as an antagonist of FGF, the fibroblast growth factor (Hacohen et al., 1998). This function, as well as the induction of SPRY expression by FGF, was confirmed for vertebrate SPRYs (Minowada et al., 1999). At

the same time, it was shown that Sprouty is an inducible inhibitor of EGF-mediated RAS signaling in flies (Casci et al., 1999; Kramer et al., 1999; Reich et al., 1999).

Mammalian genomes encode four SPRYs (Mason et al., 2006), and together with mammalian Sprouty-related proteins with an EVH1 domain (SPREDs, see below) they contain a conserved cysteine-rich domain at their C-terminus important for membrane targeting of the proteins (Casci et al., 1999; Lim et al., 2002). In addition, SPRYs share a short N-terminal region containing multiple conserved phosphosites that mediate their interaction with signaling molecules (Edwin et al., 2009).

The general site of action of SPRYs and SPREDs is downstream of the RTK and upstream of MEK-ERK, but the precise point at which RTK signaling is intercepted seems to vary depending on the biological context (Kim and Bar-Sagi, 2004). In different systems, Sprouty can act either upstream of RAS or at the level of RAS or RAF activation. SPRY-interacting proteins include the adaptors GRB2 and GAB1, two RAFs, the phosphatases SHP2, PTPN1/PTP1B and PP2A/PPP2R4 subunits, two CBLs and the CBL-interacting endocytic adaptor protein CIN85, reviewed in (Edwin et al., 2009; Mason et al., 2006).

Although insect Sprouty proteins have been initially considered to be general inhibitors of RTK signaling, more recent work in cell culture systems has challenged this paradigm. Mammalian SPRYs are antagonists of FGF-, VEGF-, and PDGF- (platelet derived growth factor) mediated MAPK signaling, but their function in EGF downstream signaling is a matter of intense debate. For example, EGF-induced proliferation of endothelial cells was inhibited by SPRY1/2 overexpression, but activation of ERK1/2 was not affected (Impagnatiello et al., 2001). In a number of cell types, EGF-induced ERK activation is insensitive to overexpressed SPRYs (Sasaki et al., 2003; Sasaki et al., 2001), or even potentiated. The agonistic effect of SPRYs is strictly dependent on their association with CBL (Wong et al., 2001), which is believed to sequester the ubiquitin ligase, abrogating EGFR ubiquitination and endocytosis and thus augmenting EGF-induced ERK signaling (Wong et al., 2002). This model was further expanded by a report proposing that the C terminus of SPRY2 (containing the cysteine-rich domain) represses EGF-induced ERK MAPK activation, whereas the N terminus (and the full-length protein) containing the CBL interaction motif enhances EGF signaling (Egan et al., 2002). The authors state that at least SPRY2 could function both as a negative and positive regulator of EGFR-mediated MAP kinase signaling in a domain-dependent fashion. A dual function of this kind could provide a mechanism for achieving a proper balance between the activation and repression of EGFR signaling. The inhibitory effect of SPRY2 on EGFR downregulation was later shown to depend on the concomitant binding to CBL and CIN85 (Haglund et al., 2005). SPRY4, which lacks CIN85-binding sites, did not inhibit EGFR downregulation, providing a molecular explanation for functional differences between Sprouty isoforms. SPRY isoform-specific functions can also arise from differential binding of adaptor proteins, for example SPRY1 interaction with GRB2 and

SPRY4 binding to SOS1 (Ozaki et al., 2005). Experiments utilizing knockdown (KD) strategies instead of overexpression confirmed the rather forward-driving role of SPRY2 in EGF-mediated signaling. Slightly decreased activation of ERK in response to EGF was observed upon SPRY2 KD (Rubin et al., 2005), and in another study silencing of SPRY2 decreased serum- or EGF-elicited activation of AKT and ERK1/2 and reduced the levels of EGF receptor (Edwin and Patel, 2008). In summary, SPRYs differentially regulate RTK signaling at multiple downstream events, in an isoform- and cell type-specific manner, and much remains to be investigated in order to elucidate the precise function of each Sprouty protein. Notably, it remains unclear to date why SPRY2 can upregulate EGF signaling but downregulates FGF signaling, as in both systems CBL mediates receptor degradation, and SPRY2 forms a phosphorylation-dependent complex with the ubiquitin ligase (Mason et al., 2004). In addition, binding to CBL promotes ubiquitination and proteolytic degradation of SPRY2, both in the case of EGF and FGF stimulation (Hall et al., 2003). EGF- *vs.* FGF-specific phosphorylation of SPRY2 in regions not involved in CBL binding might provide answers to this mystery (Rubin et al., 2005).

SPRED proteins seem more consistently associated with negative regulation of growth factor-induced ERK activation (Bundschu et al., 2007). In the first report describing SPRED1/2, constitutive association with RAS was demonstrated (Wakioka et al., 2001). Overexpression of SPRED1/2 did not prevent activation of RAS or membrane translocation of RAF, but inhibited the phosphorylation and activation of RAF, possibly by sequestering the inactive MAPKKK in a SPRED-RAS-RAF complex. All three SPREDs are able to suppress ERK activation by several mitogens including EGF, FGF, VEGF, NGF, SCF, and serum (Kato et al., 2003; Wakioka et al., 2001). Thus, SPREDs do not seem to recapitulate the growth factor selectivity of mammalian SPRYs. Both SPRY and SPRED steady-state levels are regulated by growth factor-dependent phosphorylation and CBL-mediated ubiquitination (Lock et al., 2006), but nothing seems to be known about the transcriptional regulation or induction of SPRED expression. In contrast to SPRYs, the inhibitory function of SPRED proteins appears to be restricted to the RAS-to-ERK pathway induced by various RTKs and cytokine receptors (King et al., 2005; Nonami et al., 2004).

Shortly following the identification of Sprouty as an inducible inhibitor of FGF signaling, the transmembrane protein **Kekkon-1** was shown to inhibit the activity of the *Drosophila* Egfr during oogenesis (Freeman, 2000; Ghiglione et al., 1999). The protein is expressed in response to the Egfr ligand Gurken and interferes with Egfr signaling as a negative feedback regulator. Kekkon-1 was shown to be capable of physically interacting with each of the mammalian ERBBs, inhibiting growth factor binding, receptor autophosphorylation and Erk1/2 activation in response to ligand (Ghiglione et al., 2003). The Kekkon proteins of insects have no clear orthologs in mammals, but share a common domain organization with

the three mammalian **LRIGs** (leucine-rich repeats and immunoglobulin-like domain) (Guo et al., 2004; Nilsson et al., 2001). Similar to Kekkon-1, LRIG1 is transcriptionally induced upon EGF stimulation, and interacts directly with all members of the ERBB family (Gur et al., 2004; Laederich et al., 2004). The recognition involves the ectodomains of LRIG1 and the receptors, without the requirement for ligand stimulation. In contrast to the mechanism of ERBB inhibition by Kekkon-1, LRIG1 directly binds CBL *via* the juxtamembrane region, shortening the receptor half-life, in the case of EGFR and ERBB4 due to enhanced ubiquitination and subsequent degradation (Gur et al., 2004; Laederich et al., 2004). However, in a few cases, CBL- and ubiquitin-independent downregulation of the EGFR *via* LRIG1 have been reported. The oncogenic mutant EGFRvIII, resulting from deletion of exons 2 to 7 (out of 28 in humans) encoding domain I and II of the extracellular region, is constitutively active and may (Han et al., 2006) or may not (Davies et al., 2006) be poorly ubiquitinated due to compromised interaction with CBL. LRIG1 retains its ability to interact with this EGFR mutant, and ectopic expression as well as silencing of LRIG1 affect EGFRvIII (and wilt-type EGFR) turnover and tumorigenicity in a CBL-independent manner (Stutz et al., 2008). Similarly, it has been shown that LRIG1 interacts with and downregulates MET (the met proto-oncogene, or hepatocyte growth factor receptor) in a ligand- and CBL-independent way (Shattuck et al., 2007). And finally, a soluble recombinant ectodomain of LRIG1 could suppress both basal and ligand-induced EGFR activity as well as cell proliferation by itself, without physical downregulation of the receptor (Goldoni et al., 2007). Hence, LRIG1 is considered a tumor suppressor in the majority of the situations where it downregulates tumor-promoting RTKs (Hedman and Henriksson, 2007).

Suppressors of cytokine signaling (**SOCS**) proteins were originally identified as target genes of cytokine stimulation that function to suppress Janus kinase (JAK)/signal transducer and activator of transcription (STAT) signaling in an autocrine loop (Endo et al., 1997; Naka et al., 1997; Starr et al., 1997; Yoshimura et al., 1995). The eight mammalian SOCS family members (CIS(H) for cytokine inducible SH2-containing protein, and SOCS1-7) are encoded by immediate early genes acting in a feedback loop to inhibit cytokine signaling, but several SOCS can also be induced by other growth factors (Adams et al., 1998). They are characterized by an N-terminal region of varying length, a central SH2 domain, and a highly conserved C-terminal motif known as the SOCS box (Hilton et al., 1998), reviewed in (Alexander, 2002; Piessevaux et al., 2008). In addition to regulating JAK/STAT activity, SOCS proteins have been shown to suppress RTK signaling pathways, and can be phosphorylated in response to a number of growth factors such as EGF and PDGF (Cacalano et al., 2001). The EGFR can activate STATs in certain conditions, but because in many cancer cell lines this could not be detected, an EGFR-associated inhibitory factor was proposed to block EGF-mediated STAT activation (Iwamoto et al., 1998). Subsequently,

SOCS1 and SOCS3 were found to interact with the EGFR C-terminal tail, inhibiting STAT activation presumably by inducing ubiquitin-dependent EGFR degradation (Xia et al., 2002). In the first characterization of a SOCS protein in *Drosophila*, genetic interactions implied that SOCS36E (homologous to the mammalian SOCS5) can suppress activities of the JAK/STAT and EGFR signaling pathways in the imaginal wing disc in a CBL-dependent manner (Callus and Mathey-Prevot, 2002). Later it was shown that the *Drosophila* genome contains three SOCS homologues (most similar to mammalian SOCS5-7), which differentially regulate JAK and EGFR signaling pathways (Rawlings et al., 2004). Microarrays (fully published by Yosef Yarden´s group in 2007, see chapter 2.4.) and quantitative real-time RT-PCR analysis revealed upregulation of SOCS2-5 upon stimulation of HeLa cells with EGF (Kario et al., 2005). SOCS5- (and SOCS4-) overexpressing cells showed enhanced degradation of the EGFR, ERBB2 and ERBB4 in a ligand- and CBL-independent way. However, SOCS5 directly interacted with the EGFR *via* its SH2 domain, and forms an Elongin B/C-Cullin-SOCS (ECS) complex at the receptor interface recruiting the E3 ubiquitin ligase RBX1/ROC1 (Kamura et al., 2001; Kamura et al., 1998). Consequently, EGFR ubiquitination was enhanced in SOCS5-expressing cells. Furthermore, EGFR was translocated to intracellular vesicles and EGF-induced STAT3 signaling was attenuated (Kario et al., 2005). These findings were confirmed in another study, showing also that SOCS5 inhibited EGF-driven proliferative responses (Nicholson et al., 2005). Recently, the crystal structure of the SOCS4-ElonginB/C complex was solved, providing the molecular basis for EGFR degradation by SOCS4 and SOCS5 but not by other SOCS proteins, and further explaining the inhibition of STAT3 signaling by direct competition for their common binding site (Bullock et al., 2007).

Deactivation of MAPKs plays a key role in determining the magnitude and duration, hence the physiological outcome of RTK signaling. About 16 mammalian dual-specificity phosphatases (**DUSPs**) that show activity at least *in vitro* towards MAPKs have been identified to date (Boutros et al., 2008; Jeffrey et al., 2007). The unique feature characterizing DUSPs is their ability to dephosphorylate tyrosine and serine/threonine residues within one substrate. The DUSPs that regulate MAPK activity are divided into the subgroups of “typical” MAPK phosphatases (**MKPs**) and “atypical” DUSPs that share some characteristics of the MKPs but are phylogenetically quite distinct from classical PTPs and MKPs (Patterson et al., 2009). Based on their gene structure, sequence similarity, substrate specificity and subcellular organization, MKPs are further grouped into three subfamilies (Tarrega and Pulido, 2009). DUSP1/MKP1, DUSP2/PAC1, DUSP4/MKP2, and DUSP5/HVH3, comprising the first subfamily, consist of four highly conserved exons, localize to the nucleus and are induced by growth factors or stress. All members of subfamily I are able to inactivate ERKs, with DUSP4 and DUSP5 being particularly selective for ERK MAPKs. Subfamily II MKPs (DUSP6/MKP3/PYST1, DUSP7/MKPX/PYST2, and DUSP9/MKP4/PYST3) are encoded by

three exons, localize mainly in the cytoplasm and preferentially recognize ERKs *in vitro*, especially DUSP6. Subfamily III consists of DUSP8/HVH5, DUSP10/MKP5, and DUSP16/MKP7, preferentially inactivating JNK and/or p38 MAPKs. However, assessing the precise substrate specificity of DUSPs has proven difficult, often because *in vitro* assays do not always reflect the physiological situation *in vivo*. In addition, data from different research groups are partially conflicting, especially in the case of the "atypical" DUSPs (Patterson et al., 2009). Efficacies may differ between MKPs for a certain MAPK, and it is possible that multiple phosphatases work together to inactivate MAPKs.

The MKPs themselves are subject to tight regulation at multiple levels. Many MKPs are early response genes such as the first identified DUSP1/MKP1 (Alessi et al., 1993; Keyse and Emslie, 1992; Sun et al., 1993). Especially members of the MKP subfamily I are inducible negative feedback regulators and display low expression in resting or unstressed cells (Brondello et al., 1997; Keyse, 2000; Ward et al., 1994). DUSP6/MKP3 of subfamily II is also inducible by growth factors *via* ERK1/2 and the transcription factor ETS2 (Ekerot et al., 2008; Smith et al., 2006). All members of subfamily III are induced by oxidative stress *via* JNK and the AP-1 transcription factors JUN and ATF2 (Teng et al., 2007) (see also chapter 2.3.). DUSP10/MKP5 expression can be greatly increased upon activation of Toll-like receptors in innate and adaptive immune responses (Zhang et al., 2004). In some cancers, expression of MKPs is epigenetically regulated by methylation or chromatin modification; one example is the loss of DUSP6 expression in pancreatic cancer (Xu et al., 2005).

The catalytic activity of certain DUSPs can be enhanced upon binding to their MAPK substrates. Particularly all subgroup II MKPs are stimulated by direct binding to ERK2, independent of its kinase activity (Camps et al., 1998; Dowd et al., 1998). Similarly, the nuclear DUSP1/MKP1 is activated by binding to p38 (Hutter et al., 2000), and DUSP4/MKP2 by interaction with ERK1/2 and JNK1 (Chen et al., 2001). This direct coupling of MKP activation to MAPK inactivation, together with the control of MKP expression *via* MAPK signaling, enables these two key enzyme families to keep each other in check. In addition, post-translational modifications can stabilize and activate MKPs. For instance, DUSP1/MKP1 can be phosphorylated directly by its substrates ERK1/2, leading to increased stimulation and prolonged half-life of the MKP *via* reduced ubiquitination and proteasomal degradation (Brondello et al., 1999). Recently, acetylation of DUSP1/MKP1 was shown to enhance its interaction with p38, leading to increased phosphatase activity under certain conditions (Cao et al., 2008).

In addition to the dephosphorylation activity, MKPs can control the subcellular localization of MAPKs, namely their nuclear-cytoplasmic shuttling. The cytosolic DUSP16/MKP7 contains both a nuclear localization and export signal, and is able to transport JNK and p38 MAPKs from the nucleus into the cytosol (Masuda et al., 2001). Similarly, the cytosolic DUSP6/MKP3 containing a nuclear export signal causes the retention of ERK2 in the cytosol (Karlsson et

al., 2004). Thus, signaling can be terminated by MKPs *via* inactivation and sequestration of MAPKs both in the cytosol and in the nucleus (Volmat et al., 2001).

2.6.2. Coordination of the ERK MAPK cascade by scaffold proteins

Some scaffold proteins can sequester and negatively regulate MAPKs as well, but their main function is to create multienzyme complexes that bring together components of a single kinase cascade at a specific subcellular location. These complexes can insulate the module from activation by irrelevant stimuli, favor rapid signal transmission through the cascade, modify signaling thresholds, duration and intensity, and the crosstalk with other signaling pathways. Scaffold proteins can also provide increased stability to some signaling components, and cause distinct functions of a given cascade by recruiting different substrates (Kholodenko, 2006; Kolch, 2005; Shaul and Seger, 2007; Yao and Seger, 2009). However, despite of the key function of scaffold proteins in the spatiotemporal control of MAPK cascades, only a fraction of some cascade components can be found in certain intracellular compartments, compared to the massive shuttling of MAPKKs and MAPKs between the cytosol and the nucleus.

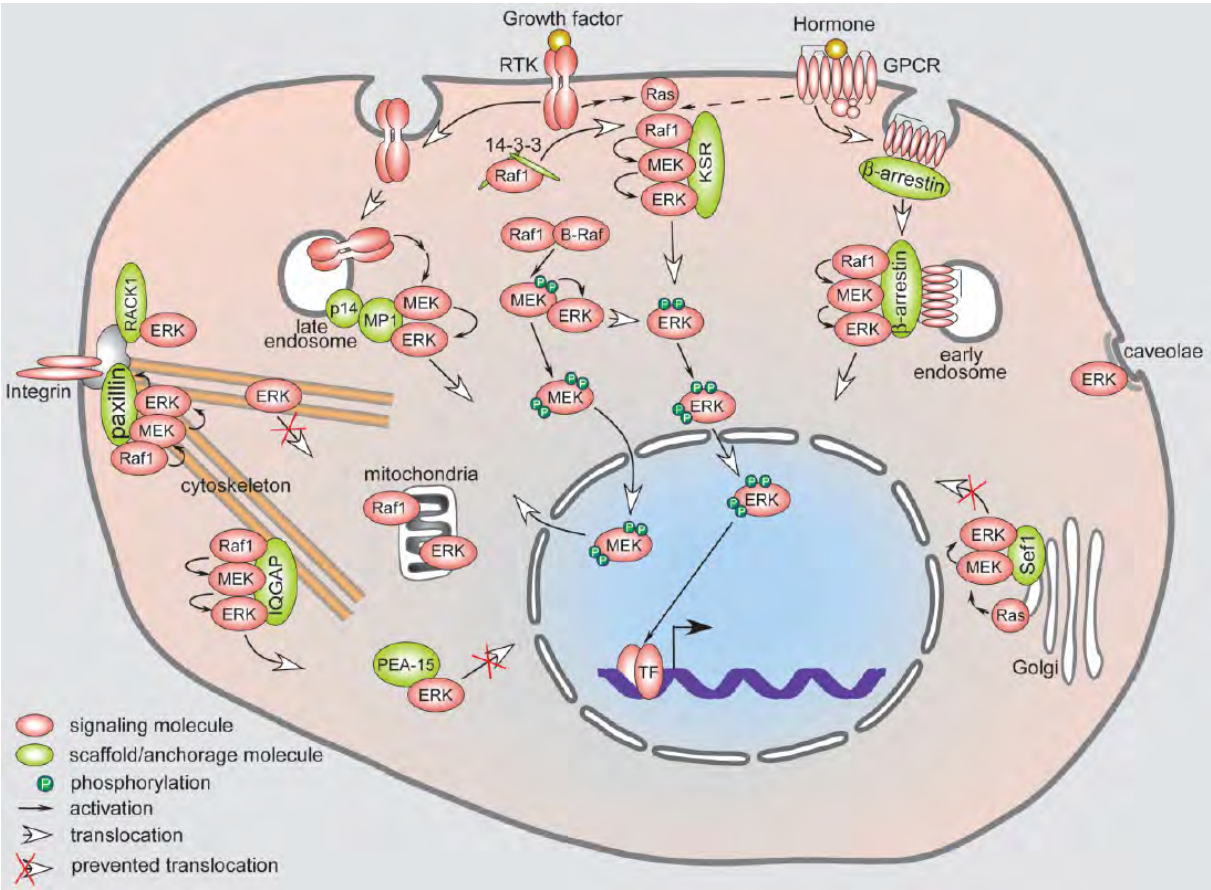

Fig. 13. Intracellular localizations of different components of the ERK cascade mediated by scaffold proteins. Scaffold and adaptor proteins are depicted in green, and components of signaling cascades in red; for more details, see text (Yao and Seger, 2009).

The first identified MAPK scaffold protein was **Ste5p** in *Saccharomyces cerevisiae* (Choi et al., 1994; Kranz et al., 1994; Printen and Sprague, 1994), and the importance of yeast scaffold proteins was demonstrated by their ability to regulate distinct processes *via* interacting with different signaling components (Schwartz and Madhani, 2004). In the last 15 years, scaffold proteins were also implicated in the regulation of signaling cascades in mammals, but most of them have very limited or no sequence similarity to the yeast proteins. Mammalian scaffold proteins regulating the ERK MAPK cascade are summarized in Fig. 13. They include KSR1, IQGAPs, paxillin, SEF, beta-arrestins, MP1 and MORG1.

KSR1 (kinase suppressor of RAS 1) was originally identified in genetic screens as a Raf-related kinase required for Ras signaling in *Drosophila melanogaster* and *Caenorhabditis elegans* (Kornfeld et al., 1995; Sundaram and Han, 1995; Therrien et al., 1995). It is still not clear whether it can be active, but mutations in key residues essential for catalytic activity suggest otherwise, and the bulk of evidence supports a kinase-independent function of KSR1 as a scaffold protein interacting with all kinase members of the ERK cascade (Michaud et al., 1997; Therrien et al., 1996; Yu et al., 1998). Similar to RAF1, KSR1 is localized in the cytosol in resting cells, mediated *via* its interaction with 14-3-3 proteins and IMP (impedes mitogenic signal propagation, official symbol BRAP). Mitogens induce the release of sequestration by 14-3-3 proteins (Muller et al., 2001) *via* the phosphatase PP2A (Ory et al., 2003), and the proteasomal degradation of IMP *via* auto-polyubiquitination (Matheny et al., 2004). The KSR1 scaffold then translocates to the plasma membrane and allows for MEK phosphorylation by RAS-activated RAF1, initiating the MAPK cascade. MEK1/2 association is constitutive, but RAF1 and ERK1/2 bind KSR1 in a stimulus-dependent manner (Cacace et al., 1999; Morrison, 2001). However, even under conditions of KSR1 expression optimal for signaling, less than 5% of endogenous RAF1, MEK or ERK coprecipitated with KSR1 (Kortum and Lewis, 2004), implying that KSR1 might affect only a subset of ERK cascade signaling functions. This and other studies (Cacace et al., 1999) also show that increased overexpression of a MAPK scaffold protein actually leads to inhibition of signaling. Thus, relative stoichiometric ratios of the scaffold and its targets determine whether the signal is enhanced or inhibited, and any scaffold has an optimal concentration for signaling, as proposed by mathematical modeling approaches (Levchenko et al., 2000).

The IQ motif containing GTPase activating protein (**IQGAP1**) was identified as a protein with multiple IQ domains, mediating interactions with calmodulin and related proteins, and a region similar to Ras GTPase activating proteins (but without GAP activity) (Weissbach et al., 1994). It was found to be an effector and regulator of the Rho family GTPases CDC42 and RAC1, modulating the actin cytoskeleton and promoting cell motility (Hart et al., 1996; McCallum et al., 1996). The many binding partners of IQGAP1 include other cytoskeleton-

associated proteins (actin, vimentin), proteins mediating cell adhesion (beta-catenin, cadherins) and receptors (EGFR, VEGFR2), to name a few. Thus, IQGAPs have functions in Ca^{2+}/calmodulin signaling, cytoskeletal architecture, cell–cell adhesion, as well as beta-catenin- and receptor-mediated signal transduction, reviewed in (Briggs and Sacks, 2003; Brown and Sacks, 2006). Recently, IQGAP1 was identified as a scaffold in the ERK signaling cascade, since it directly interacts with MEK1/2 and ERK1/2 (Roy et al., 2004, 2005). Both KD and overexpression of IQGAP1 impair EGF-stimulated activation of the cascade, a characteristic property of scaffold proteins due to the importance of their relative stoichiometry to the kinases (see above). Whereas binding of ERK seems EGF-independent, recruitment of MEK1 is enhanced and MEK2 binding to IQGAP1 is reduced upon EGF treatment. This raises the possibility that IQGAP1 preferentially activates MEK1, and different functions of MEK1 (proliferation) and MEK2 (differentiation) have been suggested (Ussar and Voss, 2004). MAPKs are regulators of cytoskeletal dynamics, and IQGAP1 may assemble the ERK module at sites of actin polymerization, thus linking MAPK signaling to the cytoskeleton (Pullikuth and Catling, 2007). Indeed, EGF stimulation can promote the formation of a CDC42-IQGAP complex (Erickson et al., 1997). Activated CDC42 was found to colocalize with IQGAP and F-actin *in vivo*, and actin, IQGAP and CDC42 were co-immunoprecipitated in an ATP- and GTP-dependent way. Taken together, these data suggest that IQGAP1 links the EGFR and actin dynamics through the regulation of Rho GTPases (possibly by promoting CDC42- and/or RAC1-dependent regulation of the ERK cascade), and therefore has a role in EGF-induced cellular migration. On the other hand, a significant fraction of ERK1/2 molecules is tethered to cytoskeletal elements such as actin, vimentin and tubulin (in fact, ERK1 was originally characterized as microtubule-associated protein 2 kinase (Ray and Sturgill, 1987)), and some studies suggest that this interaction with cytoskeletal elements prevents nuclear translocation of ERKs (Smith et al., 2004; Yao and Seger, 2009). It is conceivable that IQGAP could fulfill a similar function, thereby restricting the activity of an ERK pool towards cytosolic substrates in a certain location, another common function of scaffold proteins.

Having first been identified as a phosphoprotein from cells transformed with Rous sarcoma virus expressing the tyrosine kinase SRC (Glenney and Zokas, 1989), **paxillin** was demonstrated to be one of the first focal adhesion proteins (Turner et al., 1990). Paxillin regulates cell spreading and migration through its central role as a multiadaptor MAPK scaffold in focal adhesion assembly (Deakin and Turner, 2008; Turner, 2000). It is constitutively associated with MEK, and recruits RAF1 and ERK in response to HGF (hepatocyte growth factor) (Ishibe et al., 2003). Initially, paxillin-bound ERK is inactive, presumably to ensure that ERK activation occurs specifically at newly forming focal adhesions. Like most scaffold proteins, paxillin is phosphorylated by bound kinases, which

promotes association with FAK (focal adhesion kinase, official symbol PTK2) and further downstream the activation of RAC (Ishibe et al., 2004). FAK induces the local disassembly of focal adhesions, and the GTPase RAC initiates migration *via* cytoskeletal reorganization at the leading edge (Pullikuth and Catling, 2007). Thus, paxillin regulates the turnover of focal adhesions during migration by serving as a platform for a localized switch between ERK and FAK signaling pathways. Another recently identified scaffold protein at focal adhesions is **RACK1** (receptor of activated protein kinase C 1, official symbol GNB2L1), anchoring not only PKC, but also RAF, MEK and ERK to the sites of cell-matrix adhesion (Vomastek et al., 2007). RACK1 only facilitates ERK activation induced by integrin *via* FAK, and not by growth factors.

The transmembrane protein **SEF** (similar expression to *FGF* genes, official symbol IL17RD) was identified as an inducible negative feedback regulator of FGF signaling *via* the ERK cascade in zebrafish (Furthauer et al., 2002; Tsang et al., 2002). SEF interacts with FGF receptors, interferes with the phosphorylation of their substrates and with MEK-mediated ERK activation, although the precise mechanisms remained elusive (Tsang and Dawid, 2004). Soon thereafter, human SEF was found to bind MEK upon stimulation with FGF, EGF, or serum, and to capture active MEK-ERK complexes at the Golgi apparatus and ruffling plasma membrane regions (Torii et al., 2004). Ectopically expressed SEF did not alter the phosphorylation of the kinases, but prevented dissociation of the MEK-ERK complex, nuclear translocation of ERK, and ELK1-driven reporter gene expression, restricting MAPK signaling to cytosolic substrates. Conversely, KD of SEF increased nuclear translocation of ERK upon EGF treatment, and increased the expression of EGFR/ERK downstream target genes such as *FOS*, *EGR1* and *JUNB* (see chapter 2.4.). These data demonstrate that human SEF is a MAPK scaffold protein being able to inhibit downstream activation of nuclear transcription factors, thereby spatially regulating ERK signaling by targeting a population of active ERK to cytoplasmic locations. Interestingly, a part of RAS is also localized to and activated at the Golgi in response to EGF (Chiu et al., 2002; Choy et al., 1999). Golgi anchoring of the ERK MAPK module *via* SEF, allowing activation by Golgi-localized RAS, could therefore account for specific cellular responses by a mechanism involving PLCG, Ca^{2+}, and RASGRP1 (RAS guanyl releasing protein 1), distinct from the canonical RTK signal transduction pathway (Bivona et al., 2003).

The paradigmatic function of **beta-arrestins** (ARRB1-4) is to desensitize GPCRs (or seven membrane spanning receptors, 7MSRs) by sterically blocking their interaction with heterotrimeric G proteins (Luttrell, 2008). Beta-arrestins also play a central role in mediating the clathrin-dependent internalization of GPCRs by linking them to elements of the endocytotic machinery, such as the E3 ubiquitin ligase MDM2, clathrin and the clathrin

adaptor AP2 (Lefkowitz and Whalen, 2004). Non-GPCRs regulated by beta-arrestins are for example receptors for TGFB (transforming growth factor, beta), the IGF1R (insulin-like growth factor 1 receptor), and a number of chemokine receptors, reviewed in (Defea, 2008; Shenoy and Lefkowitz, 2005). Thus, beta-arrestins regulate many G protein-independent events, in addition to crosstalk of GPCR signaling with other pathways such as the transactivation of ERBBs (Bhola and Grandis, 2008; Ohtsu et al., 2006). Novel functions of beta-arrestins are being continuously revealed. The discovery that beta-arrestin 1 can recruit and activate the non-receptor tyrosine kinase SRC provided the first evidence that beta-arrestins are not only involved in turning off GPCR signaling, but have additional roles in turning on signaling to the ERK cascade (Luttrell et al., 1999). SRC recruitment to GPCRs *via* beta-arrestins could also provide another link between GPCR and EGFR/ERBB signaling (Pierce et al., 2001), next to the induction of EGF family precursor-processing enzymes by GPCRs mentioned in chapter 1.4.

Ten years ago, the scaffolding function of beta-arrestins for MAPKs at endosomal membranes began to emerge. Similar to the mammalian MAPK scaffold **JIP1** (JNK-interacting protein 1, official symbol MAPK8IP1) (Whitmarsh et al., 1998), beta-arrestin 2 was found to recruit the MAPK JNK3 and its upstream activators MAPKK4 and the MAPKKK ASK1 (McDonald et al., 2000). Ectopic expression of beta-arrestin 2 caused cytosolic retention of JNK3, its enhanced phosphorylation upon stimulation of the angiotensin II type 1A GPCR (AGTR1), and translocation of the active beta-arrestin-JNK MAPK module to endosomal vesicles (nuclear JNK3 was not active). Beta-arrestin- and dynamin-mediated endocytosis of GPCRs was shown to be essential for downstream ERK activation (Daaka et al., 1998), and a large endosomal complex containing not only the GPCR PAR2 (protease-activated receptor 2, official symbol F2RL1) and beta-arrestin but also RAF1 and activated ERK1/2 was identified (DeFea et al., 2000). Again, beta-arrestin overexpression caused cytosolic retention of ERKs, their decreased nuclear translocation and reduced proliferation. Another multiprotein complex containing the AGTR1, beta-arrestin 2, RAF1, MEK1 and ERK1 was subsequently shown to assemble on early endosomes upon angiotensin stimulation (Luttrell et al., 2001), enhancing cytosolic ERK activity but inhibiting ERK-mediated transcription (Tohgo et al., 2002). GPCRs that only bind transiently to beta-arrestin 2 generate less activated ERK but permit stronger nuclear signaling (Tohgo et al., 2003; Wei et al., 2003). In conclusion, the interplay between GPCRs, beta-arrestins and MAPK cascade components mediates the strength, kinetics, localization, and physiological consequences of the signal transduction process.

MEK1 partner 1 (**MP1**, official symbol MAPKSP1 for MAPK scaffold protein 1) was identified in a yeast two-hybrid screen for non-enzymatic interactors of MEK1 (Schaeffer et al., 1998). Specific binding of MEK1 and ERK1 *in vivo* (and to a lesser extend MEK2 and

ERK2 *in vitro*) demonstrated that MP1 is a scaffold for the ERK cascade. Overexpression up to a certain extend increased the binding of ERK1 to MEK1, facilitated the activation of both MEK1 (by BRAF *in vitro*) and ERK1, and enhanced the expression of a reporter gene driven by the transcription factor ELK1 downstream of ERK. However, at high concentrations of MP1 a decrease in MEK1-ERK1 binding was observed, indicating the formation of probably less active binary MP1-MEK1 and MP1-ERK1 complexes. These findings again highlight the importance of the relative stoichiometric ratios, or the balance between the components, in determining the effect of scaffold proteins, as mentioned already for KSR1 and IQGAP1.

In another two-hybrid screen with a novel, late endosome-associated protein of 14 kDa as a bait (**p14**, official symbol ROBLD3 for roadblock domain containing 3), MP1 was identified as an interaction partner (Wunderlich et al., 2001). A protein complex containing p14, MP1, MEK and ERK could be reconstituted *in vitro*. Moreover, the artificial mislocalization of p14 to the plasma membrane *via* a CAAX motif of RAS proteins (Hancock et al., 1991) co-mislocalized MP1 from late endosomes to the plasma membrane, demonstrating that p14 recruits the MP1-MAPK complex to the late endosomal compartment. Similarly, p14 KD redistributed MP1 from late endosomes to the cytosol (and the nucleus), and prevented localization of active ERK1/2 at late endosomes after 10 min of EGF stimulation (Teis et al., 2002). Overexpression of both p14 and MP1 had an additive effect on ERK1/2 activation and ELK1-driven transcription, which was abolished when the complex was targeted to the plasma membrane. These results, together with the observation that p14 or MP1 downregulation inhibits EGF-induced signal transduction, indicate that targeting of MEK and ERK to late endosomes *via* the scaffold protein MP1 and its adaptor p14 is required for sustained activity of the ERK cascade. Association of MP1 with MEK and ERK seems constitutive (Schaeffer et al., 1998), but activation of the ERK pathway causes the dissociation of the MP1-ERK interaction (Sharma et al., 2005) and nuclear signaling, in contrast to other scaffold proteins (*e.g.* IQGAP1, SEF, beta-arrestins). On the other hand, inhibitory effects of the p14•MP1 complex on ERK phosphorylation of the transcription factor ETS1 have also been reported (Brahma and Dalby, 2007). Gel filtration experiments showed that MP1 is part of a large oligomeric complex that may involve other proteins besides MEK1 and ERK1. Indeed, MP1 was also found to associate with active PAK1 (p21 protein (CDC42/RAC)-activated kinase 1). Together with p14, MP1 regulates MEK1 and ERK activation by PAK1, transiently suppressing Rho GTPase pathways necessary for the turnover of adhesion structures and cell spreading (Pullikuth et al., 2005). Interestingly, this study furthermore shows that PDGF-mediated activation of MEK1 was independent of MP1 function, whereas previous data involving p14/MP1 in EGF-dependent signaling were confirmed. Thus, MP1 seems able to direct the ERK module to specific upstream regulators and downstream targets in a context-dependent manner, insulating functionally distinct pathways with common components.

Conditional gene disruption of p14 in mice revealed the importance of the p14-MP1-MAPK complex in early embryonic development (Teis et al., 2006). Apparently, p14 is not only required for endosomal ERK activation during epidermal development and cell proliferation, but also for late endosomal positioning as well as EGFR transport and degradation. Cells derived from patients with a novel primary immunodeficiency syndrome, caused by loss of p14 expression, show a perturbed distribution of late endosomes and lysosome-related organelles, interfering with the function of immune cells (Bohn et al., 2007). These studies suggest a more general role of p14 in endosomal biogenesis and function, but whether and how p14/MP1 directly control endosomal EGFR trafficking, and whether active EGFR participates in late endosomal signaling *via* the p14/MP1 recruited MAPK module, remains elusive.

Recently, a novel lipid raft adaptor termed **p18** (C11orf59) was isolated from detergent-resistant membranes of EGF-stimulated cells (Nada et al., 2009). Late endosomal localization of p18 was presumably mediated by its putative myristoylation and palmitoylation sites, known to function as lipid raft signals (Zacharias et al., 2002). The protein was shown to interact directly with p14 and MP1, anchoring the complex to late endosomes (see Fig. 21, chapter 3.2.4.). Loss of p18 function causes relocalization of p14 and MP1 to the cytosol, and a partial reduction in the activity of MEK and ERK. $p18^{-/-}$ cells display defects in endosome dynamics and distribution, and p18 knockout is embryonic lethal, supporting a rather general role for the p18-p14-MP1 scaffold module in late endosomal organization. Another different function of the p18-p14-MP1 complex is the recruitment of Rag GTPases to late endosomes, which in turn interact with and activate the multicomponent kinase MTORC1 (mammalian target of rapamycin complex 1, official symbol MTOR) in response to amino acids (Laplante and Sabatini, 2009; Sancak et al., 2010). Thus, specific localization of active MTORC1 at late endosomes *via* p18-p14-MP1 promotes growth in response to nutrients and growth factors, revealing yet another specific scaffolding function of the late endosomal MP1.

At last, **MORG1** (MAPK organizer 1, official symbol WDR83) was shown to interact with MP1, RAF1, BRAF, MEK1/2 and ERK1/2 in a cooperative manner (Vomastek et al., 2004). Other typical scaffold properties of MORG1 are enhancement of ERK activity at low concentrations and inhibition at higher levels of MORG1 expression, and interference with MAPK signaling upon MORG1 depletion. Interestingly, MORG1 facilitates ERK1 activation in an agonist-specific manner. Lysophosphatidic acid (LPA, known to stimulate the high affinity GPCRs LPAR1-6), the phorbol ester PMA (phorbol 12-myristate 13-acetate, able to stimulate the ERK cascade *via* PKC), and serum stimulations were enhanced by moderate MORG1 overexpression, whereas EGF- and PDGF-induced ERK1 activity was unaffected. As for other scaffolding proteins, MORG1 thus controls a subset of ERK-dependent signaling pathways, probably linking specific upstream activators to distinct biological responses. Together, the two scaffolds MP1 and MORG1 seem to anchor larger MAPK cascade

modules, which are built from nested scaffolds, at specific subcellular localizations, providing both stability and signaling flexibility through combinatorial effects.

In summary, anchoring common components of the ERK MAPK cascade *via* scaffold proteins to defined intracellular locations allows for efficiency, regulation of signal strength and duration, and specificity of the response to various stimuli. One central question remains the direct contribution of endocytosed receptors to the signal propagation from intracellular organelles, which will be addressed for the EGFR in chapter 3 after describing receptor trafficking in the endosomal system.

3. Receptor trafficking in the endosomal system

3.1. Overview of the endosomal system

More than one hundred years ago, Elie Metchnikoff first recognized that material taken up by endocytosis was degraded after encountering an acidic internal environment. As early as 1866, he made his first observation of intracellular uptake of nutrients by specialized cells. In the 1880s, he discovered that certain white blood cells engulf and digest bacteria, and together with his observations of nutrient uptake, these findings formed the basis for his concept of phagocytosis. Metchnikoff and Paul Ehrlich were jointly awarded the 1908 Nobel Prize in Physiology and Medicine in recognition of their work on immunity (Kaufmann, 2008). During the last 30 years, the basic organization of the endocytic pathway was elucidated, particularly by studying ligand-induced receptor internalization and trafficking, with the EGFR as a principal model system (chapter 1).

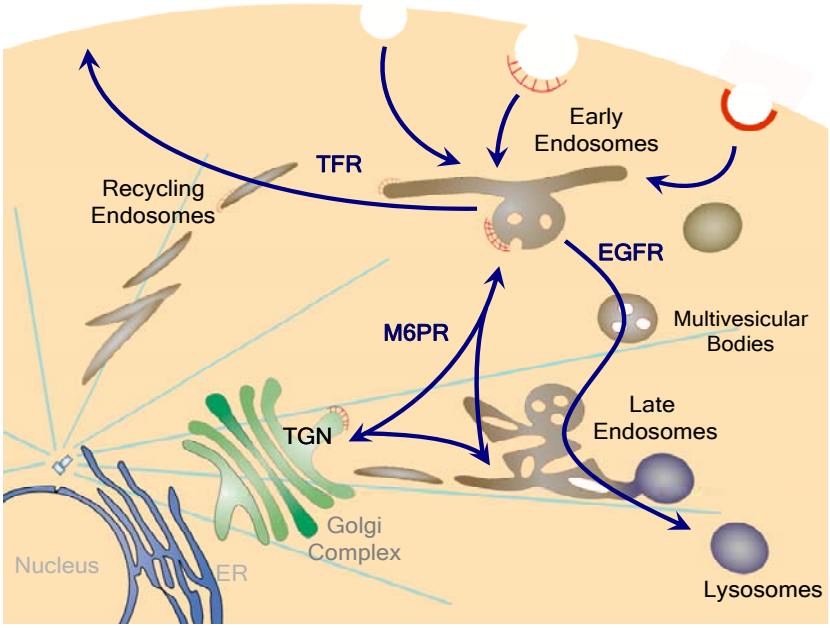

Fig. 14: The endosomal system and its major trafficking pathways.

The endosomal system is composed of morphologically, molecularly and functionally distinct compartments: early endosomes (EEs), recycling endosomes (REs), multivesicular bodies (MVBs), late endosomes (LEs), and lysosomes (Gruenberg, 2001; Perret et al., 2005). Endocytic organelles are constantly exchanging lipids, luminal content and transmembrane proteins with each other, the plasma membrane, or other organelles like the Golgi complex, *via* vesiculotubular transport or maturation (Fig. 14). These transport processes must be highly regulated in order to ensure proper delivery of cargo to its correct destination (alternatively, to be secreted or degraded), and to maintain the particular composition and function of the organelles throughout this continuous flux of material.

3.1.1. Determinants of organelle identity in the endosomal system

Organelle identity is defined by the active GTPases and specific lipid species that they display, which are in turn regulated by their guanine nucleotide exchange factors (GEFs) and GTPase-activating proteins (GAPs), and by enzymes that synthesize or degrade the relevant lipids, respectively (Behnia and Munro, 2005). Rab GTPases (Ras-related in brain (Touchot et al., 1987)) and their effectors are membrane (domain) organizers which determine transport specificity and organelle identity in the endosomal system (Miaczynska and Zerial, 2002; Zerial and McBride, 2001). For instance, EEs are characterized by the presence of RAB5, REs contain RAB4 and RAB11, and RAB7 and RAB9 associate with membranes of MVBs and LEs; RAB6 is present at the *trans*-Golgi network (TGN; Fig. 15). The precise mechanism of how RABs associate with specific membranes is not fully understood, but it clearly involves targeting of prenylated RABs by particular GDFs (GDP dissociation inhibitor (GDI) displacement factors), GEFs and GAPs, which often display restricted localizations (Behnia and Munro, 2005). By means of positive feedback loops involving local amplification of active RABs *via* recruiting RAB regulators and effector proteins (such as the class 3 PI3K VPS34 and PI(3)P-binding proteins in the case of RAB5), functional RAB domains are believed to form on particular membranes. The cooperativity and self-organization properties of the involved components is therefore crucial to establish organelle identity (Zerial and McBride, 2001). A much considered observation is the RAB5-to-RAB7 conversion as a mechanism of cargo progression from early to late endosomes (Rink et al., 2005). Interaction of a RAB7 GEF with RAB5 was shown to be necessary for the replacement of RAB5 with RAB7, indicating that RAB domains are very dynamic structures that can even change their identity by recruiting a RAB(5) effector which is in turn a RAB(7) regulator. Whether the concepts of RAB domains and RAB conversion are generalizable for the many RAB-regulated processes, remains to be determined.

Phosphoinositides define lipid territories in the endosomal system, such as PI(4,5)P_2 (phosphatidylinositol 4,5-bisphosphate) in the plasma membrane, PI(3)P

(phosphatidylinositol 3-phosphate) in membranes of EEs and LEs, and PI(3,5)P_2 (phosphatidylinositol 3,5-bisphosphate) in LEs; PI4P (phosphatidylinositol 4-phosphate) is found at the TGN (Fig. 15). Several of the kinases and phosphatases metabolizing specific phosphoinositides are recruited and/or activated by Rab and Arf GTPases (Stenmark, 2009). Other lipids than phosphoinositides defining specialized domains in the endocytic system are for example cholesterol- and sphingolipid-rich "rafts" in the plasma membrane and endosomal compartments, and the exclusively late endosomal lysobisphosphatidic acid (LBPA, see below) (Gruenberg, 2003). In general, however, it should be taken into account that boundaries between different organelles can be blurred at the molecular level, since regulatory key proteins are often found in more than one compartment, and different membrane domains might coexist in the same type of endosome.

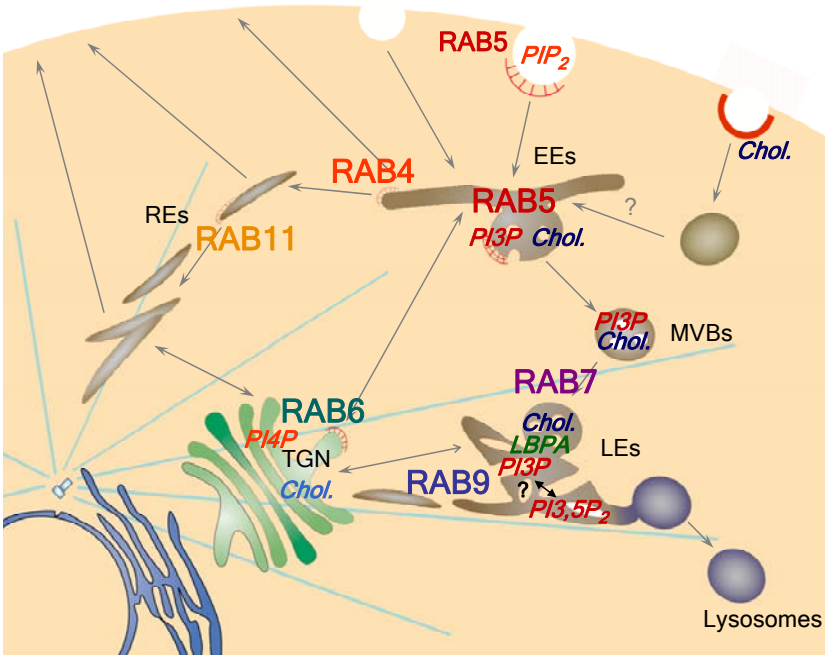

Fig. 15: Rab GTPase and lipid domains in the endosomal system.

Having discussed the distinct localization of Rab GTPases and of certain lipid species as major sources of compartment variety and specificity in the endosomal system, a brief description of the major **endocytic transport routes** is appropriate. Endocytosis comprises several mechanisms by which cells internalize plasma-resident proteins and lipids, as well as exogenous material such as nutrients and receptor ligands, into transport vesicles derived from the plasma membrane (Conner and Schmid, 2003; Mellman, 1996). The controlled entry into the cell has crucial roles for instance in the turnover of membrane proteins and lipids, intercellular communication and signal transduction, uptake of nutrients and cellular homeostasis, maintenance of cell polarity, neurotransmission, and antigen presentation in immune responses. Paradoxically, many pathogens hijack these pathways to enter cells for replication and evasion of the immune system (Gruenberg and van der Goot, 2006).

3.1.2. Pathways of entry into cells

The multiple portals of entry into mammalian cells are summarized in Fig. 16. Endocytosis can be divided into phagocytosis, the uptake of solid large particles or "cell eating", and pinocytosis, the internalization of fluid and solute cargo or "cell drinking" *via* smaller vesicles (Silverstein et al., 1977). Pinocytic events are further distinguished into macropinocytosis, clathrin-mediated endocytosis (CME), and several types of clathrin-independent endocytosis (CIE, sometimes referred to as non-clathrin-mediated endocytosis, NCE), reviewed in (Doherty and McMahon, 2009). Clathrin is a major coat protein involved in the formation of newly forming vesicles, surrounding clathrin-coated vesicles as a polyhedral lattice (Edeling et al., 2006; Traub, 2009). Clathrin-independent endocytosis is often sensitive to cholesterol depletion, and can be further subdivided into routes depending or not depending on the GTPase dynamin involved in the scission of newly formed vesicles (Mayor and Pagano, 2007). Examples of CIE are caveolin-mediated, CLIC/GEEC-type (clathrin-independent carrier/glycosylphosphatidylinositol-anchored protein-enriched early endosomal compartment), flotillin-dependent, ARF6 (ADP ribosylation factor 6) -dependent, RHOA (RAS homolog A) -regulated, and other more specialized types of endocytosis (Fig. 16). The EGFR can be internalized both by clathrin-dependent and -independent pathways, which will be discussed in more detail in chapter 3.2.1.

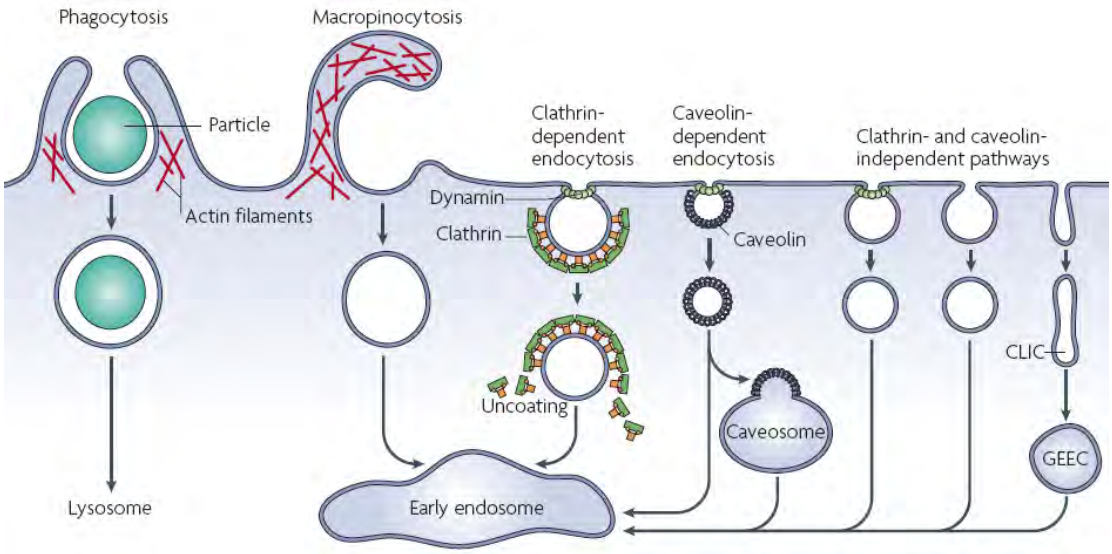

Fig. 16: Multiple portals of entry into the mammalian cell.
Large particles can be taken up by phagocytosis, whereas fluid uptake occurs by macropinocytosis. Both processes appear to be triggered by and are dependent on actin-mediated remodeling of the plasma membrane at a large scale. Compared with the other endocytic pathways, the size of the vesicles formed by phagocytosis and macropinocytosis is much larger. Numerous cargoes can be endocytosed by mechanisms that are independent of the coat protein clathrin and the fission GTPase dynamin. Most internalized cargoes are delivered to the early endosome *via* vesicular (clathrin- or caveolin-coated vesicles) or tubular intermediates (known as clathrin- and dynamin-independent carriers (CLICs) that are derived from the plasma membrane. Some pathways may first traffic to intermediate compartments, such as the glycosyl phosphatidylinositol-anchored protein enriched early endosomal compartments (GEEC), en route to the early endosome (Mayor and Pagano, 2007).

3.1.3. Recycling from early endosomes as the first sorting station

Whatever the internalization route, most endocytosed cargo is delivered to EEs as the first intracellular sorting station. [However, pre-early endosomal sorting events have been proposed to already begin during formation of clathrin-coated pits which may contain different cargo (Lakadamyali et al., 2006).] Housekeeping receptors such as the transferrin receptor (TFR or TFRC) and the low density lipoprotein receptor (LDLR) are uncoupled from their ligands (iron in the case of TFR; transferrin stays bound to its receptor) due to the mildly acidic pH in EEs, and recycle back to the plasma membrane for reutilization. Especially with increasing appreciation of CIE pathways, numerous endocytic recycling systems have been discovered in recent years, reviewed in (Grant and Donaldson, 2009; Maxfield and McGraw, 2004). Generally, a rapid recycling route directly from EEs involving RAB4, is distinguished from a so-called slow recycling route *via* the tubular endocytic recycling compartment (ERC), defined molecularly by the presence of RAB11. Other GTPases such as ARF6, RAB8, RAB10, RAB22A, RAB35, and CDC42, together with their regulators and effectors, participate in partially different recycling routes at EEs and the ERC (Grant and Donaldson, 2009). Regarding cargo selectivity, the prevailing model of geometry-based iterative sorting states that EEs extend narrow-diameter tubules that become the ERC (Fig. 17), whereas their main body is responsible for other functions of EEs (Maxfield and McGraw, 2004). The surface area-to-volume ratio of tubular structures is greater than that of the vesicular portion of EEs, therefore the pinched-off tubules preferentially contain membrane lipids and transmembrane proteins to be recycled. Thus, in the absence of a positive sorting signal for other destinations, most internalized receptors would be delivered back to the cell surface, together with the bulk of the membrane. Indeed, for the prototypic recycling cargoes TFR and LDLR, recycling seems to be the default pathway and no specific sorting signals have been found to date. The situation in epithelial cells might be different, in which transcytosed and recycling receptors transit through common REs before being sorted to opposite plasma membrane domains, but the precise mechanisms remain elusive, perhaps involving cholesterol-/lipid “raft”-mediated sorting (Perret et al., 2005).

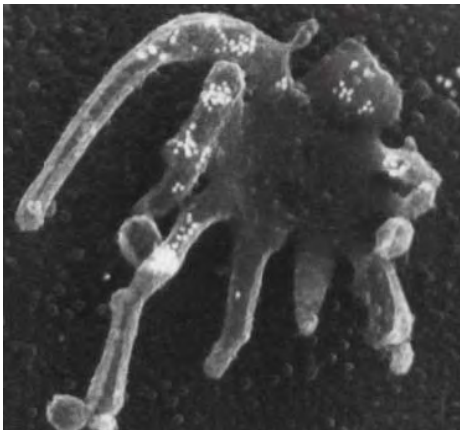

Fig. 17: The early endosome as the first endosomal sorting station - morphology and geometry-based recycling
The figure shows an early endosome containing low-density lipoprotein-gold particles endocytosed for 5 minutes (gold particles are visualized as white spots, as contrast was reversed). After internalization, cells were homogenized, crude fractions prepared and deposited on mica plates. Samples were analysed by freeze-etch electron microscopy (Gruenberg, 2001) (courtesy of John Heuser, Washington University, Missouri, USA).

3.1.4. Cargo sorting to late endosomes as the second sorting station

In contrast to the presumably geometry-based selection of material to be recycled, **targeting signals** for delivery to LEs and lysosomes have been identified (Bonifacino and Traub, 2003; Braulke and Bonifacino, 2009). The majority of luminal, soluble acid hydrolases are modified with mannose 6-phosphate (M6P) moieties, allowing their recognition by M6P receptors (M6PRs) which in turn have several lysosome targeting signals. Dileucine-based motifs such as the minimal DXXLL (where X is any amino acid) and [DE]XXXL[LI], or the tyrosine-based YXXØ motif (where Ø is a bulky hydrophobic residue), interact with clathrin adaptors. M6PRs recruit the monomeric GGAs (golgi-associated, gamma adaptin ear containing, ARF binding proteins) (Bonifacino, 2004) and the heterotetrameric adaptor protein 1 (AP1) at the TGN. These signal-adaptor interactions capture M6PRs and their cargo hydrolases into clathrin-coated vesicles. After fusion with endosomes, the acidic pH induces the release of bound acid hydrolases into the endosomal lumen, from which they are transported with the fluid phase to lysosomes. The M6PRs return to the TGN from late endosomes *via* RAB9 and its effector TIP47 (tail-interacting protein of 47 kDa, official symbol PLIN3 for perilipin 3) or a second pathway from an earlier endocytic compartment *via* the retromer multiprotein complex (Attar and Cullen, 2010; Bonifacino and Hurley, 2008). The route from the TGN to early or late endosomes without reaching the cell surface is referred to as the direct pathway. The indirect pathway involves constitutive transport from the TGN to the plasma membrane, followed by internalization into EEs and eventually delivery to LEs and lysosomes. Canonical YXXØ or [DE]XXXL[LI] motifs can mediate the interaction with all four clathrin adapter protein complexes (AP1-4) (Edeling et al., 2006), thus mediating both rapid internalization and lysosomal delivery. Since KD of the plasma membrane-localized AP2 and clathrin have by far the most dramatic effect on the surface expression and lysosomal transport for example of LAMPs (lysosomal-associated membrane proteins), the indirect route is likely more important for the correct targeting of lysosomal membrane proteins.

In the 1990s, pioneering work in yeast identified **ubiquitin** as a signal for **degradative sorting** of plasma membrane receptors, one of the first non-proteasomal functions discovered for ubiquitin. The ABC transporter Ste6p and the GPCR Ste2p were found to be modified by ubiquitin, in the case of the GPCR induced by ligand, which was necessary both for internalization and vacuolar degradation (Hicke and Riezman, 1996; Kolling and Hollenberg, 1994). Around the same time, ligand-induced, kinase-dependent ubiquitination of the PDGFR (Mori et al., 1992) and the EGFR (Galcheva-Gargova et al., 1995) was demonstrated and proposed to play a role in efficient degradation of the ligand•receptor complex. However, the situation in mammalian cells seems more complex than in yeast, since not only the receptors,

but also endocytic adaptors and other regulators are often ubiquitinated in response to stimuli. Mutational studies for example on the GHR, GPCRs, the MET receptor, FGFR, and the EGFR (discussed in more detail in chapter 3.2.1.), indicate that in mammalian cells receptor ubiquitination is not essential for internalization but for subsequent downregulation, possibly due to the existence of alternative entry routes (Acconcia et al., 2009; Raiborg et al., 2003). Ubiquitination is mediated by members of the **CBL** family of proteins (Schmidt and Dikic, 2005). The first member, v-cbl, was cloned from an oncogenic murine retrovirus causing Casitas B-lineage lymphoma, hence the name (Langdon et al., 1989). Cloning of the mouse *c-Cbl* gene revealed that v-Cbl is a truncated form of its cellular homolog, and overexpression of the full length protein did not promote tumorigenesis (Blake et al., 1991). So far, three mammalian family members, CBL or C-CBL, CBLB and CBLC/CBL-3, have been characterized. CBL and CBLB proteins consist of an N-terminal tyrosine kinase-binding (TKB) domain, a RING finger motif, a proline-rich region, and a C-terminal ubiquitin-associated (UBA) domain that overlaps with a leucine zipper (LZ) motif; CBLC lacks the C-terminal UBA/LZ domain (Thien and Langdon, 2001). The CBL interactome is comprised of more than 150 proteins that are regulated by CBL proteins, representing a cross section though the signal transduction proteome (Schmidt and Dikic, 2005). The best-studied example of how CBL proteins affect receptor trafficking is the sorting process of the EGFR (chapter 3.2.1.), initially described using the *Caenorhabditis elegans* EGFR orthologue LET-23 as a model (Langdon, 1995).

Members of the recently characterized family of ART proteins (arrestin-related trafficking adaptors) act upstream of the E3 ubiquitin ligase Rsp5p, the only member of the Nedd4 family of ubiquitin E3 ligases present in yeast (Belgareh-Touze et al., 2008). Sequence analysis revealed a total of nine ART family members in yeast (Lin et al., 2008). In addition to similarity to arrestins, the ARTs each contain multiple PY motifs which recruit the Rsp5p ubiquitin ligase. As a result, ubiquitinated cargoes are internalized and targeted to the vacuole for degradation (Lin et al., 2008; Nikko et al., 2008). The work performed in the labs of Scott Emr and Hugh Pelman provides the link between the ubiquitin ligase and its upstream substrates, perhaps within a cargo-specific quality-control pathway, and underscores the importance of endocytic scaffolding adaptor proteins (Mittal and McMahon, 2009). In mammalian systems, ARTs have not been characterized yet, but adaptor or scaffold proteins such as beta-arrestins and CIN85 acting upstream of or in parallel with ubiquitin ligases fulfill important functions in cargo recognition and receptor downregulation (Dikic, 2002; Havrylov et al., 2010; Lefkowitz and Whalen, 2004; Schmidt and Dikic, 2005; Szymkiewicz et al., 2004).

Ubiquitinated cargo is efficiently sorted away from recycling molecules within EEs into MVBs for further transport towards LEs and lysosomes, where the proteins and lipids of internal membranes are eventually degraded (Gruenberg, 2001; Gruenberg and Stenmark,

2004; Katzmann et al., 2002). The molecular machinery which sorts ubiquitinated receptors into the internal membranes of MVBs is also mediating the membrane invagination process itself, thereby ultimately linking sorting with invagination. The endosomal sorting complexes required for transport (**ESCRTs**) catalyze this membrane remodeling process with an unusual topology, budding of intra-lumenal vesicles (ILVs) away from the cytosol (Hurley, 2008; Hurley and Hanson, 2010; Raiborg and Stenmark, 2009; Williams and Urbe, 2007).

In yeast, the biogenesis of the vacuole (corresponding to the late endosome/lysosome of mammalian cells) is regulated by vacuolar protein sorting (**VPS**) **genes**, of which a subset known as class E genes are directly involved in MVB biogenesis (Raymond et al., 1992). Deletion of any of those genes causes the formation of abnormal multicisternal endosomes lacking ILVs, referred to as the class E compartment. Many of the class E VPS genes encode for core subunits of the four ESCRTs, or accessory proteins involved in the regulation of membrane scission and ESCRT disassembly (Hurley and Hanson, 2010). The most important ESCRT-associated proteins are the AAA+ ATPase Vps4p and the multifunctional Bro1p (named for its ability to confer *BCK1*-like resistance to osmotic shock (Nickas and Yaffe, 1996); known in mammals as ALIX/AIP1, ALG-2 interacting protein X/1, official symbol PDCD6IP for programmed cell death 6 interacting protein). In the following, only human symbols will be used.

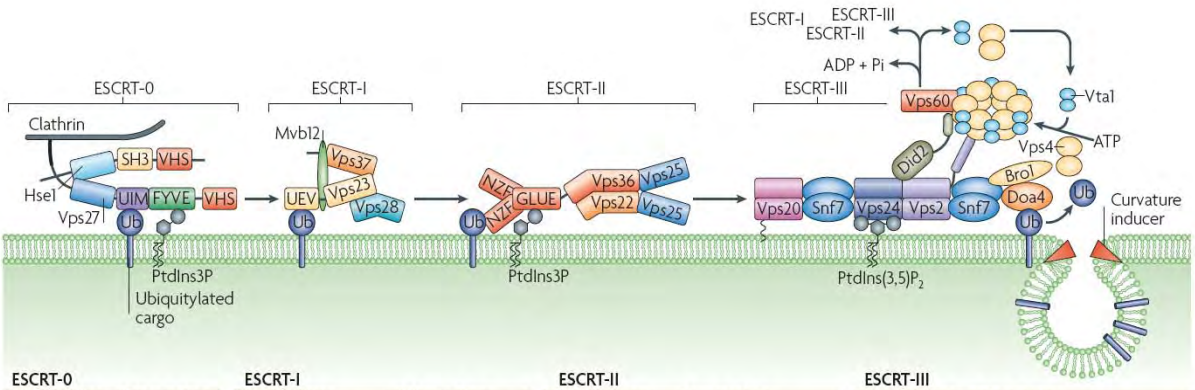

Fig. 18: The ESCRT machinery mediating cargo sorting and membrane invagination in endosomal trafficking. The four ESCRTs are recruited to endosomes by their interactions with membranes, clathrin, ubiquitin (Ub) and with each other. Features of both yeast and mammalian pathways are included. Lipid recognition of either PI(3)P by the FYVE domain of HRS (ESCRT-0) or the GLUE domain of VPS36 (ESCRT-II), and perhaps PI(3,5)P_2 by VPS24 (ESCRT-III) might contribute to the early or late endosomal localization of the components. All of the ESCRTs except ESCRT-III recognize and bind the ubiquitinated cargo, either through a ubiquitin-interacting motif (UIM) (ESCRT-0), a ubiquitin E2 variant (UEV) domain (ESCRT-I) or the GLUE domain of VPS36 (ESCRT-II). ESCRT-III orchestrates the last steps in the pathway in which ubiquitin is removed by a deubiquitinase, and the complexes are disassembled by the AAA+ ATPase VPS4. The bottom panels list ESCRT subunits and accessory proteins from yeast and their mammalian homologues (Williams and Urbe, 2007).

Fig. 18 summarizes the mechanism of ESCRT-dependent cargo sorting and membrane invagination, as well as interactions within the machinery. The **ESCRT-0** is composed of a constitutive heterodimer between **HRS** (hepatocyte growth factor-regulated tyrosine kinase substrate, official symbol HGS) and STAM1/2 (signal transducing adaptor molecule 1/2), and can associate with the endocytic adaptor EPS15 (epidermal growth factor receptor pathway substrate 15) (Bache et al., 2003b). STAM1/2 can interact with deubiquitinases (DUBs), which might regulate the ESCRT machinery and/or the sorting signal of the cargo itself (Komander et al., 2009; McCullough et al., 2006; Row et al., 2007). Both HRS and STAM contain one ubiquitin-interacting motif (UIM; in the case of HRS a so-called double-sided UIM (Hirano et al., 2006a)), but the low-affinity interactions with monoubiquitinated proteins are not the driving force for membrane targeting. Instead, the FYVE domain of HRS binds the endosomal phosphoinositide PI(3)P (Raiborg et al., 2001b). The C-terminal clathrin box motif of HRS recruits clathrin to EEs (Raiborg et al., 2001a), which in turn concentrates HRS and ubiquitinated cargo into the bilayered clathrin coats on endosomes (Raiborg et al., 2002; Raiborg et al., 2006; Sachse et al., 2002). The C terminus also contains a PSAP (more general: P(S/T)XP) motif that interacts with the ESCRT-I subunit **TSG101** (tumor susceptibility gene 101) (Bache et al., 2003a; Pornillos et al., 2003). Thus, HRS-STAM cluster dense complexes on PI(3)P-containing EEs that coordinate many interactions with membranes, cargo and coat proteins, facilitate multiple ubiquitination and deubiquitination reactions, and mediate the initial recruitment of ESCRT-I to endosomes. Importantly, PI(3)P signaling does not regulate bulk transport in the endosomal system, but specifically regulates HRS-dependent receptor sorting, demonstrating that transport and sorting can be uncoupled (Petiot et al., 2003; Pons et al., 2008).

ESCRT-I subunits other than TSG101 are VPS28, VPS37A-D, and MVB12A/B, forming a 1:1:1:1 heterotetramer (Audhya et al., 2007). TSG101 binds monoubiquitinated cargo through its ubiquitin E2 variant (UEV) domain (Katzmann et al., 2001; Sundquist et al., 2004). As is the case for HRS, TSG101 becomes ubiquitinated itself via the association with the E3 ubiquitin ligase TAL (Tsg101-associated ligase, official symbol LRSAM1) (Amit et al., 2004). TAL activity negatively affects EGFR degradation, suggesting that it may enable dissociation of TSG101 from endosomal membranes into the cytosol. Cytosolic TSG101 exists in an oligomeric complex with other components of ESCRT-I, VPS28 and VPS37. The recently characterized yeast protein Mvb12p (MVB sorting factor of 12 kDa) has been proposed to stabilize ESCRT-I in an oligomeric, inactive state in the cytosol to ensure the ordered recruitment and assembly of ESCRT-I and -II on endosomal membranes (Chu et al., 2006), and to modulate cargo recognition capabilities of ESCRT-I (Curtiss et al., 2007; Oestreich et al., 2007b). A related protein termed MVB-12 has been identified in *Caenorhabditis elegans*, and two mammalian relatives, MVB12A and B, have been found (Audhya et al., 2007; Morita et al., 2007a).

Once on the membrane, Tsg101 recruits **ESCRT-II** by binding to EAP45/VPS36 and EAP30/VPS22 (Langelier et al., 2006; von Schwedler et al., 2003). ESCRT-II acts as a molecular hub, connecting the upstream cargo-binding components with the downstream membrane remodeling machinery. The EAP45 (ELL-associated protein of 45 kDa) subunit contains a GLUE (gram-like ubiquitin-binding in EAP45) domain that has a structure reminiscent to the pleckstrin homology (PH) domain, and binds both 3-phosphoinositides and ubiquitin moieties (Alam et al., 2006; Hirano et al., 2006b; Slagsvold et al., 2005). Finally, the physical interaction between the ESCRT-II subunit EAP20/VPS25 and the myristoylated ESCRT-III subunit CHMP6/VPS20 activates the latter and triggers recruitment of ESCRT-III to endosomal membranes (Im et al., 2009; von Schwedler et al., 2003; Yorikawa et al., 2005).

In contrast to the upstream ESCRTs, structurally related CHMP subunits (charged MVB proteins, also named chromatin modifying proteins) of **ESCRT-III** are not pre-assembled, but are located in the cytosol as monomers in an autoinhibited conformation (Babst et al., 2002; Shim et al., 2007; Zamborlini et al., 2006). In addition, the ESCRT-III subunits do not contain any UIMs. In fact, it still seems unclear how ubiquitinated proteins are transferred from one complex to another. The molecular mechanism of membrane fission by ESCRT-III, however, is better characterized, mainly through studies in yeast and *in vitro* reconstructions. The ESCRT-II contains two EAP20/VPS25 molecules that generate a characteristic Y-shaped structure (Teis et al., 2010), recruiting and activating CHMP6/VPS20 (see above). Then, the sequential assembly of ESCRT-III *via* CHMP6/VPS20 results in the polymerization of two SNF7/VPS32/CHMP4 oligomers, both of which are required for cargo sequestration and vesicle formation during MVB sorting (Babst et al., 2002; Hanson et al., 2008; Teis et al., 2010). Approximately 10-20 SNF7/VPS32 molecules could form a ring-like filament that is capped by CHMP3/VPS24 (Teis et al., 2008). The capping of SNF7/VPS32 filaments recruits CHMP2/VPS2, which (together with CHMP6/VPS20) recruits the VPS4 ATPase complex (Kieffer et al., 2008; Obita et al., 2007; Stuchell-Brereton et al., 2007).

VPS4 assembles into a large circular complex, leaving a pore in the middle of the ring. VPS4 probably translocates its ESCRT-III substrates through this pore in an ATP-dependent manner (the only direct energy input in the MVB pathway), to release them from the membrane (Kieffer et al., 2008; Lata et al., 2008; Scott et al., 2005). The disassembly of ESCRT-III, capable of cleaving the neck of the bud itself, serves to recycle the components for further rounds of ILV formation (Wollert et al., 2009).

CHMP3/VPS24 recruits the deubiquitinating enzyme AMSH (associated molecule with the SH3 domain of STAM, official symbol STAMBP for STAM binding protein) (Agromayor and Martin-Serrano, 2006; McCullough et al., 2006). **DUBs** can oppose the ubiquitin-dependent sorting of receptors to lysosomes (McCullough et al., 2004), although it has also been observed that ubiquitinated cargo accumulated on endosomes upon interfering with AMSH function (Kyuuma et al., 2007). Other proposed functions of endosomal DUBs are

recycling of ubiquitin prior to cargo sorting into ILVs, and stabilization of ESCRT subunits, whereas deubiquitination of cargo is not necessary *per se* for its degradative sorting (Komander et al., 2009).

Whether recruitment of ESCRTs occurs sequentially or simultaneously, is still a matter of debate. All three human isoforms of SNF7/CHMP4 can interact with the multifunctional, BRO1 domain-containing protein **ALIX**/AIP1 (Kim et al., 2005; McCullough et al., 2008; Peck et al., 2004). But ALIX has been shown to interact also with TSG101, thus physically crosslinking ESCRT-I and ESCRT-III for example during HIV budding (Fisher et al., 2007; Lee et al., 2007b; Strack et al., 2003; von Schwedler et al., 2003). Certain viruses seem to rely on the endosomal pathway for infection in some cell types, for instance HIV (human immunodeficiency virus) (Vidricaire et al., 2004; Vidricaire and Tremblay, 2005). The best studied example is HIV budding into multivesicular structures in macrophages (Gruenberg and van der Goot, 2006; Pelchen-Matthews et al., 2003; Pelchen-Matthews et al., 2004; Raposo et al., 2002). However, these structures were shown to be connected with the extracellular space, and may thus represent a previously unknown intracellular plasma membrane domain, rather than MVBs (Deneka et al., 2007; Marsh et al., 2009). Alternatively, HIV was proposed to bud into a non-acidic endosomal compartment (Jouve et al., 2007). In lymphocytes, HIV budding from the plasma membrane, topologically similar to the invagination process at MVBs away from the cytosol, has been found to involve ESCRT subunits and accessory proteins such as TSG101, CHMP4, ALIX, and VPS4B (Booth et al., 2006; Nguyen et al., 2003; Ono and Freed, 2004) (and references above). The HIV Gag protein mimics HRS and recruits TSG101 via its P(S/T)AP motif (Pornillos et al., 2003), thereby hijacking the ESCRT machinery. In addition, viral Gag proteins can recruit ALIX directly *via* its BRO1 domain, and this boomerang-shaped domain of all four BRO1 domain-containing proteins (see paragraph about HD-PTP in chapter 2.6.1.) is sufficient to bind Gag and to facilitate virus production (Popov et al., 2009). Other functions of ESCRTs independent of MVB biogenesis are roles in cytokinesis (Carlton and Martin-Serrano, 2007; Morita et al., 2007b) and autophagy (Filimonenko et al., 2007; Lee et al., 2007a), where interfering with ALIX functions leads to stronger effects than in ILV formation. All of these pathways involve the cleavage of membrane necks with the same unconventional morphology as in MVB invagination (Hurley and Hanson, 2010).

As will be discussed further below, the EGFR itself may regulate the invagination process at MVBs, hence its own downregulation, since EGF stimulation enhances the frequency of ILVs as well as the biogenesis of multivesicular endosomes (Razi and Futter, 2006; White et al., 2006). Interestingly, only the EGF-induced formation of MVBs was sensitive to a simultaneous KD of HRS, TSG101, EAP30/VPS22, and CHMP3/VPS24, the key subunits of

all four ESCRTs (Stuffers et al., 2009). EGF-independent formation of multivesicular endosomes was unaffected by the absence of ESCRTs, arguing for the existence of an ESCRT-independent mechanism of MVB biogenesis.

Although monoubiquitination is an important sorting determinant for MVBs, non-ubiquitinated cargo can also be targeted into ILVs. The yeast protein Sna3p (McNatt et al., 2007; Oestreich et al., 2007a; Reggiori and Pelham, 2001; Watson and Bonifacino, 2007) and the mammalian LRP1 (low density lipoprotein receptor-related protein 1) were found to enter internal vesicles in a ubiquitin-independent manner. LRP1 sorting nevertheless requires the ubiquitin system, since proteasome inhibitors interfere with receptor delivery into ILVs (Melman et al., 2002; van Kerkhof et al., 2001). Degradation of the EGFR is also blocked by proteasomal inhibitors, although the receptor itself is properly ubiquitinated under these conditions (Longva et al., 2002). Presumably, negative regulators of MVB sorting can be inactivated by polyubiquitination and the proteasome, indicating a functional crosstalk between proteasomal and lysosomal degradation. Very little is known about the MVB sorting machinery recognizing non-ubiquitinated cargo. In the case of the delta opioid GPCR, GASP (G protein-coupled receptor associated sorting protein, official symbol GPRASP1) was shown to bind and direct the non-ubiquitinated receptor for degradative sorting (Whistler et al., 2002). Another study demonstrated that opioid receptors, despite their ability to undergo agonist-induced trafficking to lysosomes in the absence of covalent modification by ubiquitin, utilize some (VPS4 and HRS) but not all (TSG101) of the MVB sorting machinery (Hislop et al., 2004). Moreover, sorting of the melanosomal protein PMEL17 (official symbol SILV) into ILVs appears to be completely insensitive to functional inhibition of HRS, TSG101 and VPS4 (Theos et al., 2006), indicating the existence of an alternative, ESCRT-independent pathway of ILV sorting.

3.1.5. The role of cholesterol and LBPA in late endosomal dynamics

Lipids other than phosphoinositides have been shown to participate in various sorting events in the endosomal system. Studies investigating the trafficking of lipids carrying acyl chains of various lengths and degrees of saturation have shown that lipids partitioning rather into more fluid membranes preferentially recycle back to the plasma membrane, whereas lipids and proteins located in more rigid microdomains are predominantly transported along the degradative pathway (Mukherjee et al., 1999). Indeed, about 2/3 of endosomal **cholesterol** was found in MVBs by quantitative immuno-electron microscopy (Mobius et al., 2003), and proteins known to partition in cholesterol- and sphingolipid-rich “rafts” such as tetraspanins (Claas et al., 2001) and glycosylphosphatidylinositol-anchored proteins (GPI-APs) (Simons and Gerl, 2010; Simons and Ikonen, 1997) have been shown to follow the

same route of “rafts” in certain cell types and are often enriched in ILVs (Fivaz et al., 2002; Kobayashi et al., 2000; Sobo et al., 2007a). The fate of endosomal cholesterol is linked to the exclusively late endosomal lipid lysobisphosphatidic acid (**LBPA**; also known as bis(monoacylglyceryl)phosphate, BMP). Almost 40 years ago, LBPA was found to be enriched in “secondary lysosomes” from rat liver (Joutti et al., 1976; Wherrett and Huterer, 1972). LBPA is not easily degraded by lipases because of its unusual backbone configuration (sn-1-glycerophospho-sn-1'-glycerol) (Amidon et al., 1995; Brotherus et al., 1974), although it has been shown that phospholipase A2 (PLA2) can metabolize LBPA at the acidic ph of 5.5 typical for late endosomes/lysosomes (Ito et al., 2002). Only since the late 1990s, functional studies have begun to reveal the role of this unconventional lipid in late endosomal membrane dynamics. LBPA, enriched to about 15% of the total phospholipid amount in late endosomal fractions of BHK cells, was only found within the complex system of internal membranes of LEs (Kobayashi et al., 1998). Ingested anti-LBPA antibodies caused redistribution of M6PRs (see above) from the TGN to LEs, and led to the appearance of a late endosomal population with electron-dense, packed internal membranes, while the acidic pH was unaffected. From these data, it was proposed that LBPA regulates the organization and dynamic properties of internal membranes of LEs, as well as specific sorting processes such as M6PR trafficking through the compartment. Moreover, LBPA was identified as antigen in the antiphospholipid syndrome (Kobayashi et al., 1998; Valesini and Alessandri, 2005), underscoring the importance of LBPA-mediated endosomal sorting processes. Soon thereafter, it was demonstrated that the characteristic network of LBPA-rich membranes contained within multivesicular LEs regulates cholesterol transport (Kobayashi et al., 1999). Similar to cholesterol accumulation in fibroblasts from Niemann-Pick type C (NPC) patients, suffering from an autosomal recessive lysosomal storage disorder characterized by an intracellular accumulation of unesterified cholesterol (Karten et al., 2009), anti-LBPA antibodies caused a dramatic accumulation of cholesterol in LEs. And *vice versa*, the previously described redistribution of M6PRs to LEs upon internalization of anti-LBPA antibodies was also observed in NPC fibroblasts. Later it was shown that LEs loaded with cholesterol loose their dynamic properties and become essentially immobile, including in cells from NPC patients and cells with internalized anti-LBPA antibodies (Lebrand et al., 2002). Strikingly, LBPA was shown to induce the formation of multivesicular liposomes, depending on the same pH gradient found across late endosomal membranes, and this process was negatively controlled by the LBPA-binding protein **ALIX** (see above) *in vitro* and *in vivo* (Matsuo et al., 2004). ALIX KD reduced intracellular LBPA levels by about 50%, with profound implications for late endosomal membrane organization and dynamics. Particularly, infection of cells with the vesicular stomatitis virus (VSV), which requires acidic late endosomal compartments for fusion and nucleocapsid release into the cytoplasm, was inhibited both by ALIX KD (Matsuo et al., 2004) and anti-LBPA antibodies (Le Blanc et al.,

2005). Thus, the inverted cone-shape of LBPA might favor inward invagination required to form certain MVBs, and together with its partner ALIX, LBPA regulates dynamic fusion and fission processes between the limiting membrane and ILVs, regulating the back-fusion of ILVs containing cargo such as M6PRs, cholesterol, and pathogenic hijackers like VSV and anthrax toxin (Gruenberg, 2009; van der Goot and Gruenberg, 2006). This role of LBPA was further supported by the observation that also cholesterol accumulation leads to impaired intra-endosomal trafficking (Sobo et al., 2007b), and that cholesterol levels are tightly coupled to LBPA and ALIX functions (Chevallier et al., 2008). Intriguingly, another protein which was found to regulate VSV release from late endosomal ILV is the ESCRT-I subunit TSG101 (Luyet et al., 2008). TSG101 and ALIX control budding of ILVs into LEs not only *in vivo* (see above), but also *in vitro* (Falguieres et al., 2008). It seems more than plausible that ILV formation and back-fusion with the limiting membrane are coupled processes, in order to ensure the homeostasis of the late endosomal compartment, and proper sorting of cargo which needs to be degraded in lysosomes *vs.* cargo to be recycled from within the endosomal lumen (Falguieres et al., 2009). Hence, the late endosome can be viewed as the second major sorting station in the endosomal system (Fig. 19 B).

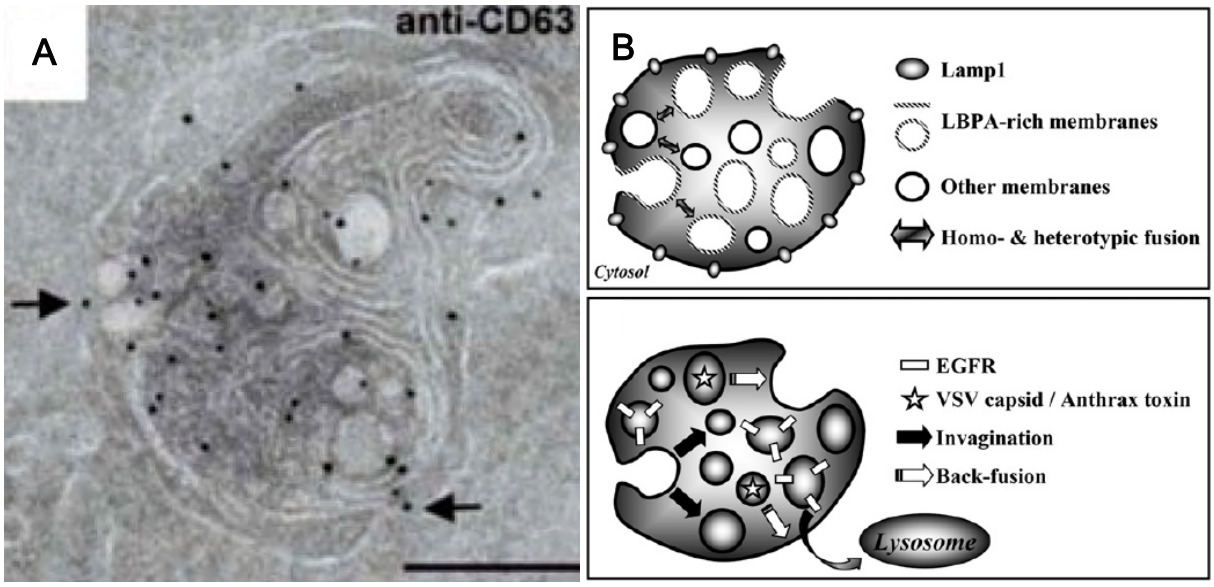

Fig. 19: The late endosome as a second major sorting station in the endosomal pathway
A) Late endosomes (LEs) are characterized by a complex system of internal membranes, both multivesicular and multilammelar appearance which can depend on the cell type. In this electron micrograph, the distribution of endogenous CD63 was analyzed by immunogold labeling of cryosections using antibodies against CD63. Arrows point at gold particles on the organelle limiting membrane (Kobayashi et al., 2002). **B)** Membrane dynamics within LEs, containing more than one type of lumenal membranes. LAMP1 is associated with the limiting membrane, while LBPA is abundant in lumenal membranes. However, biochemical and morphological evidence indicate that LEs also contain other membranes that do not contain LBPA but PI(3)P or cholesterol, that may represent vesicles containing downregulated receptors in transit to lysosomes. LBPA could appear on the limiting membrane upon back-fusion of LBPA-containing vesicles. Other possible homo- and heterotypic fusion events are indicated by double arrows. Late endosomal cargo can have different fates. The vesicular stomatitis virus capsid or the anthrax toxin lethal factor (stars) can be released into the cytoplasm by back-fusion of intralumenal vesicles with the limiting membrane (white arrows). The vesicles containing the downregulated EGFR (white rectangles) are targeted to the lysosomes for degradation. Finally, invagination from the late endosomal limiting membrane, which would lead to the formation of new vesicles, is indicated (black arrows) (Falguieres et al., 2009).

3.1.6. Cargo delivery to lysosomes as the terminal degradative compartment

In contrast to LEs with their characteristic multivesicular and/or multilamellar appearance in electron micrographs (Fig. 19 A and 20 A), lysosomes (Greek for "digestive body") are electron-dense structures containing acid hydrolases (De Duve et al., 1955; Novikoff et al., 1956). They can be distinguished from late endosomes molecularly also by the absence of M6PRs, but share for example proton-pumping vacuolar ATPases to maintain the luminal environment at a pH of around 5 (Mellman et al., 1986). Within a few years of their discovery, lysosomes were recognized as the terminal degradative compartment of the endocytic pathway (Bainton, 1981; de Duve, 2005). However, for the transfer of endocytic material to lysosomes, several mechanisms have been proposed (Fig. 20). These include maturation of LEs into lysosomes, vesicular transport from LEs to lysosomes, cycles of transient contacts followed by dissociation of those two organelles (kiss-and-run), direct fusion, and fusion-fission (an intermediate model between direct fusion and kiss-and-run, in which lysosomes re-form from hybrid organelles) (Luzio et al., 2009; Luzio et al., 2007).

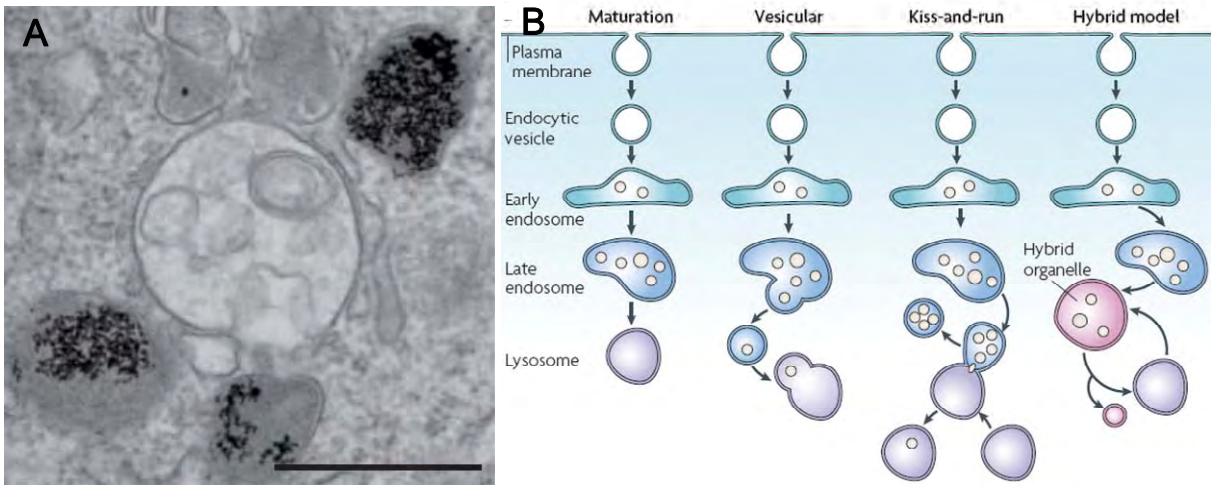

Fig. 20: Models for the delivery of cargo to lysosomes for degradation.
A) Electron microscopy of endosome-lysosome fusion. Dense-core lysosomes in normal rat kidney (NRK) cells were loaded with colloidal gold conjugated with bovine serum albumin for 4 h followed by a 24 h chase. The lysosomes (dark grey) can be compared with a less-dense late endosome in the centre of the image. **B)** Different models have been proposed to explain how cargo is trafficked from LEs to lysosomes. In the first model (maturation), LEs mature into lysosomes by the gradual addition of lysosomal components and removal of late endosomal components. In a second vesicular model, vesicles may bud from the LEs that delivers its contents to the lysosome. In the third model, LEs and lysosomes may transiently fuse (kiss), allowing for the exchange of contents between them, before departing again (run). In the final model (hybrid), endosomes and lysosomes may permanently fuse to form a hybrid organelle that contains both lysosome and late endosome components. Lysosomes are then re-formed by the selective retrieval of late endosome components (Luzio et al., 2007).

Live-cell microscopy experiments have shown that both kissing and direct fusion events contribute to the endocytic delivery to lysosomes, where kissing often preceded fusion but was not a prerequisite for it (Bright et al., 2005; Gan et al., 2009). Fusion is initiated by tethering *via* the formation of a *trans*-SNARE (soluble N-ethylmaleimide-sensitive fusion protein attachment protein receptor) complex and release of lumenal Ca^{2+}, followed by

membrane bilayer fusion (Jahn and Scheller, 2006; Mullock et al., 1998; Pryor et al., 2000). The R-SNARE (arginine-containing SNARE) protein VAMP7 (vesicle-associated membrane protein 7) is necessary for heterotypic fusion between LEs and lysosomes, whereas VAMP8 is required for homotypic fusion of LEs (Luzio et al., 2005; Pryor et al., 2004). Additional components of the molecular fusion machinery are other SNAREs (syntaxin 7-8, and VTI1B for vesicle transport through interaction with t-SNAREs homolog 1B), NSF (N-ethylmaleimide-sensitive factor), probably RAB7 and the HOPS (homotypic fusion and vacuole protein sorting) complex (Luzio et al., 2009; Luzio et al., 2007). Interestingly, the HOPS complex, an established GEF for RAB7, was also found to regulate the conversion from an RAB5- to a RAB7-positive organelle (Rink et al., 2005). Thus, a concerted action of the ESCRT, HOPS and SNARE complexes is required for cargo delivery to lysosomes for degradation.

3.2. EGFR as a model to study the interplay of RTK trafficking and signaling

The discovery of EGF and its receptor was immediately followed by the investigation of the pathways and mechanisms of EGFR endocytosis (see chapter 1). The interest in understanding EGFR endocytic trafficking has been driven by the recognition of the important role that trafficking has in the regulation of signaling processes triggered by RTKs and their ligands. The first comprehensive study of the EGFR endocytosis, in which many of the key concepts of internalization and lysosomal degradation of EGFR have been established, was published by (Carpenter and Cohen, 1976). This and other early studies by Cohen's group remain the basis of the current understanding of EGFR endocytosis. Intracellular trafficking of the EGFR is one of the most well characterized models for studying the morphology, kinetics and mechanisms of endocytic pathways, and is a prototypic model for the endocytosis of other RTKs. Studies on endocytosis of other ERBBs have been trailing the EGFR research because the natural ligands to ERBB3 and ERBB4 were discovered much later than EGF, and because the experimental tools to study these receptors and ErbB2 only began to become available during the last 10-15 years.

As will be discussed below, the process of EGFR internalization and degradation is a major negative feedback regulatory mechanism that controls the intensity and duration of receptor signaling (see also chapter 2.6.). On the other hand, the EGFR remains active in endosomes. Therefore, endocytosis and signaling may be closely linked *via* positive and negative feedbacks (chapter 3.2.4.).

The half-life of unstimulated EGFR in cultured cells expressing low or moderate levels of EGFR is in the range of 6-10 h, whereas for example in human epidermoid carcinoma A431 cells overexpressing the receptor, it could be 24 h or longer (Beguinot et al., 1984; Stoscheck

and Carpenter, 1984a, b). The turnover rate of the other ERBBs is roughly similar to that of unstimulated EGFR, depending on the cell type and sometimes also on the ERBB isoforms (Sorkin et al., 1993; Sundvall et al., 2008). The general trend is that the basal turnover rates of unstimulated ERBBs reciprocally correlate with their expression levels, presumably due to the saturability of the internalization and degradation steps of trafficking (Sorkin and Goh, 2008).

At steady-state growth conditions, the bulk of cellular ERBBs is located in the plasma membrane, besides a small endosomal pool, perhaps involving a PKA-dependent restriction in internalization (Salazar and Gonzalez, 2002). After internalization, inactive ERBB receptors are mainly recycled back to the cell surface, because the constitutive recycling rate is higher than the basic internalization rate (Austin et al., 2004; Chang et al., 1993; Herbst et al., 1994; Wiley, 2003; Wiley et al., 1991). However, that changes drastically when the receptors become activated by ligand-induced dimerization (chapters 1.5. and 1.6.).

3.2.1. Internalization routes of the EGFR

Binding of EGF to EGFR results in acceleration of receptor internalization (Wiley et al., 1991). Several lines of experimental evidence support the view that this acceleration is due to endocytosis of EGF•receptor complexes through clathrin-coated pits: 1) ligand-activated EGFR was found concentrated in coated pits and vesicles (Carpentier et al., 1982; Gorden et al., 1978; Sorkina et al., 2002), with participation of CBL as well as endocytic and signaling adaptor proteins such as EPS15 and GRB2 (Johannessen et al., 2006; Stang et al., 2004); 2) the specific rates of EGF(R) internalization are within the range measured for other receptors that are internalized by means of CME, such as TFR (Hanover et al., 1985; Hanover et al., 1984); 3) overexpression of dominant-negative mutants of proteins essential for CME, *e.g.* the DNM2 (**dynamin** 2)-K44A mutant, inhibited EGFR internalization (Damke et al., 1995); 4) depletion of **clathrin heavy chain** or dynamin, and to a lesser extend KD of the clathrin adaptor AP2 subunits, has been shown to inhibit EGFR endocytosis (Huang et al., 2004; Motley et al., 2003). These data argue that CME is the major pathway of EGFR internalization, reviewed in (Edeling et al., 2006; Traub, 2009). However, in some experimental settings, KD of AP2, epsin 1, EPS15, and EPS15R, all proteins proposed to be ubiquitin adaptors in CME (Schmidt and Dikic, 2005), did not result in specific inhibition of clathrin-dependent EGFR internalization (Motley et al., 2003; Sigismund et al., 2005). They may not be essential, perhaps because of adaptor redundancy (Huang et al., 2004), or the EGFR might utilize alternative pathways to enter the cells (see below).

Interestingly, high internalization rates of the EGFR typical for CME were observed only when EGF was used in low concentrations (around 1-2 ng/ml), whereas the rate of EGF uptake was decreased with increasing EGF concentrations (Wiley, 1988). Thus, clathrin-

dependent rapid internalization has presumably limited capacity and is overwhelmed in the presence of high concentrations of EGF•receptor complexes at the cell surface (Lund et al., 1990). In addition, it was shown that EGF uptake at high concentrations was only minimally affected by overexpression of the DNM2-K44A mutant, whereas the same mutant efficiently blocked internalization of EGF at low concentrations (Jiang and Sorkin, 2003). Moreover, KD of the clathrin heavy chain did not significantly affect EGF internalization at high concentrations (Sigismund et al., 2005). Hence, under conditions of receptor overexpression and/or high ligand concentrations, clathrin-independent internalization compensates the saturation of CME and then determines the overall rate of EGF(R) uptake into the cell. In some cell lines expressing low or moderate levels of endogenous EGFR, however, CME has the capacity to internalize EGFR stimulated with high EGF concentrations (Kazazic et al., 2006; Lund et al., 1990; Wiley, 1988).

Clathrin-independent endocytosis of EGFR was first demonstrated in early studies using A431 cells expressing very high levels of EGFR, where EGF treatment causes extensive plasma membrane ruffling and formation of pinocytic vesicles containing labeled EGF but lacking the clathrin coat (Chinkers et al., 1979; Haigler et al., 1979). Internalization of the EGFR by large macropinocytic structures morphologically distinct from conventional, clathrin-derived endosomes (that did not label for transferrin, AP2 or clathrin heavy chain) was also observed in COS cells (Yamazaki et al., 2002), and a role for GRB2 in macropinocytic internalization of the EGFR was postulated. In addition, clathrin-independent but DNM2-, PI3K- and F-actin-dependent internalization of EGFR via vesicular-tubular endocytic compartments originating from plasma membrane dorsal ruffles was observed in several cell types (Orth et al., 2006).

Endocytosis of EGF•receptor complexes *via* cholesterol-rich lipid rafts and/or caveolae was also proposed under conditions of high EGF in HeLa cells (Balbis and Posner, 2010; Sigismund et al., 2008; Sigismund et al., 2005), with implications for the fate of internalized EGFR and downstream signaling (see chapter 3.2.4. and Fig. 21). In contrast, another study in HeLa cells found no role of cholesterol-rich rafts or caveolae in EGFR endocytosis, and suggested that CME is the major internalization pathway under all EGF concentration conditions in these cells (Kazazic et al., 2006). It is possible that the localization of EGFR in cholesterol-rich domains and the contribution of these in EGFR endocytosis is cell-type-specific and may even vary in different subclones of HeLa cells.

Taken together, in addition to CME, EGF•receptor complexes can enter pinocytic vesicles and ruffle-generated endocytic compartments. In some cells, activated EGFR can be taken up by mechanisms sensitive to cholesterol-disrupting drugs (Le Roy and Wrana, 2005). All these clathrin-independent pathways are significantly slower than CME, although they may have a faster kinetics as compared to the constitutive receptor internalization. Clathrin-independent endocytosis is typically observed in experiments when high EGF concentrations are used and

a large amount of EGFR is present at the cell surface. It is possible that the contribution of these mechanisms in the endocytosis of EGFR *in vivo* is minimal (Sorkin and Goh, 2008).

Regarding the molecular machinery of EGFR endocytosis, studies during the last 20 years produced numerous observations which are difficult to reconcile with each other, probably reflecting differences in stimulation conditions and the use of cell lines with varying receptor expression levels (see above). Clearly, the autophosphorylation of tyrosines as docking sites for adaptor proteins is crucial not only to initiate downstream signaling networks (chapter 2.1.), but also to recruit endocytic machineries. However, kinase-negative EGFR mutants and EGFR inactivated by kinase inhibitors are internalized and accumulate in endosomes, albeit with lower rates than that of CME (Honegger et al., 1987; Wang et al., 2005; Wang et al., 2002; Wiley et al., 1991). These results suggest that dimerization might be the pivotal trigger for endocytosis.

Mutations of several major tyrosine phosphorylation sites in the EGFR partially reduced internalization (Chang et al., 1993; Sorkin et al., 1991b). Mutation of the major binding sites of the GRB2 adaptor protein or depletion of GRB2 strongly inhibited EGF internalization in many cell lines (Jiang et al., 2003; Sorkin and Goh, 2008), indicating that GRB2 is an adaptor necessary both for signal transduction (see chapter 2.2.) and endocytosis. One of the major GRB2-interacting proteins, the ubiquitin ligase **CBL**, is a master regulator of EGFR internalization and degradation (Levkowitz et al., 1998). But CBL has also direct binding sites on the phosphorylated EGFR cytoplasmic tail, and the relative contribution of indirect (GRB2-mediated) and direct interactions of CBL with EGFR may vary in different cell types. The general role of **ubiquitin** and CBL in degradative sorting of plasma membrane receptors has been discussed in chapter 3.1.4. Initially described in *Caenorhabditis elegans* using its single EGFR homologue LET-23 and the CBL homologue SLI-1 as a model (Jongeward et al., 1995; Langdon, 1995; Sternberg et al., 1995; Yoon et al., 1995), it was at first proposed that CBL-mediated EGFR monoubiquitination is sufficient for both internalization and degradation also in mammalian cells (Haglund et al., 2003; Joazeiro et al., 1999; Levkowitz et al., 1999; Mosesson et al., 2003). However, in CBL knockout cells or cells with a temperature-sensitive defect in ubiquitination, internalization into EEs did not require CBL function or an intact ubiquitin pathway (Duan et al., 2003). In addition, mutational studies showed that ubiquitination-deficient EGFR displayed a severe defect in its turnover rate, but was internalized at rates comparable to those of wild-type receptors (Huang et al., 2006; Pennock and Wang, 2008). Thus, ubiquitination is crucial for degradative sorting of the receptor, but dispensable for its internalization, either *via* alternative entry routes (see above and chapter 3.1.4.) or *via* ubiquitin ligase-independent functions of CBL as endocytic adaptor protein for CIN85 and endophilins (Dikic, 2002; Schmidt and Dikic, 2005; Soubeyran et al., 2002).

Interestingly, CBL stays associated with the receptor throughout the endocytic route (de Melker et al., 2001) and continues to ubiquitinate the EGFR after internalization, which requires sustained kinase activity to counteract deubiquitination (Umebayashi et al., 2008). Moreover, both CBL and CBLB cooperate in a temporal manner to ensure full receptor downregulation (Pennock and Wang, 2008). The potential ubiquitination of the other ERBBs will be briefly discussed in chapter 3.2.2., because of its implication in ERBB2-4 receptor sorting at EEs for recycling *vs.* degradation.

Importantly, the EGFR is not only regulated by proteins of the endocytic machinery, but also regulates them in turn. For example, HRS, an ESCRT-0 subunit essential for degradative sorting of the receptor (chapter 3.1.4.), undergoes EGF-induced tyrosine phosphorylation (Komada and Kitamura, 1995) *via* several kinases downstream of the receptor (Bache et al., 2002). These phosphorylation events, although affecting only a portion of the cellular HRS pool, regulate its ubiquitination by CBL and ultimately the fate of internalized EGFR (Stern et al., 2007). In a quantitative proteomics study, tyrosine phosphorylation of several proteins of the endocytic machinery upon EGF stimulation was observed, namely of CBL and the adaptor EPS15 within 5 min of stimulation, and of HRS and STAM2 at around 10-15 min after EGF addition (Blagoev et al., 2004). The differential phosphorylation profiles reflect the sequential mode of recruitment and activation of the endocytic proteins, and highlight again the intimate connection between EGFR signaling and trafficking.

3.2.2. EGFR sorting at early endosomes

A portion of internalized EGFR can recycle back from endosomes to the cell surface, varying in amount according to expression levels of the receptor (French et al., 1994). Since EGF does not significantly dissociate from the receptor at the mildly acidic pH of EEs (6.0-6.5) (Sorkin et al., 1988), an intact EGF•receptor complex is recycled (Sorkin et al., 1991a). Recycling of EGF•receptor complexes occurs either through a rapid pathway directly from EEs, or a slower second pathway involving the tubular endocytic recycling compartment (ERC; see chapter 3.1.3.). In summary of morphological studies done about 20 years ago, the model of the endosomal sorting of EGFR states that EGF•receptor complexes can be recycled in a manner similar to unoccupied EGFR and TFR unless these complexes are trapped in the intralumenal vesicles of MVBs. However, only a small part of EGF-stimulated EGFR follows recycling routes under moderate expression conditions, and the majority is efficiently segregated away from the constitutively recycling TFR (Dickson et al., 1983; Grant and Donaldson, 2009; Gruenberg and Maxfield, 1995; Maxfield and McGraw, 2004).

Different **ligands** can determine differential intracellular routing of the EGFR. Particularly, the low affinity ligand TGFA dissociates from the EGFR in EEs at higher pH values than EGF, does not induce a complete downregulation of the receptor, and leads to a faster recovery of ligand-binding ability at the cell surface (Ebner and Derynck, 1991). The release of TGFA from the receptor already in EEs leads to receptor dephosphorylation and recycling back to the plasma membrane (French et al., 1995). As mentioned in chapter 2.5.1., the strong mitogenicity of epigen (EPGN) was attributed to evasion of receptor-mediated ligand depletion due to inefficient EGFR phosphorylation and ubiquitination (Kochupurakkal et al., 2005). Similarly, stimulation of cells with AREG, compared to EGF, leads to lesser EGFR phosphorylation particularly of the CBL binding site Tyr1045, and consequently reduced association with CBL and ubiquitination (Gilmore et al., 2008; Stern et al., 2008). In addition, AREG stimulation was accompanied by the decreased degradation of the internalization inhibitor SPRY2 (chapter 2.6.1.) and the differential sorting of CBL-free EGFR away from CBL-EGFR complexes, indicating reduced internalization and increased recycling (Baldys et al., 2009). In a study comparing six different EGFR ligands, it was shown that all ligands stimulate receptor internalization, but have diverse effects on endocytic sorting. HBEGF and BTC target EGFR predominantly for lysosomal degradation *via* persistent EGFR phosphorylation and ubiquitination, whereas stimulation with TGFA and EREG leads to almost complete recycling of the receptor back to the plasma membrane (Roepstorff et al., 2009). AREG did not cause significant lysosomal degradation but led to fast as well as slow EGFR recycling, whereas EGF-stimulated receptor was targeted for both degradation and recycling. Thus, differential EGFR trafficking can be determined by ligand affinity and the sensitivity of the ligand-receptor interaction to acidic pH. Degradative sorting correlates with lasting receptor phosphorylation, CBL recruitment, and ubiquitination.

Endocytic sorting of the EGFR can also be determined by its **heterodimerization partner**, but the ubiquitination of other members of the ERBB family is controversial (chapter 2.5.2.). Initially, it was proposed that all ERBBs other than the EGFR show impaired ligand-induced rapid internalization and downregulation (Baulida et al., 1996). In another report it was shown that CBL undergoes rapid and sustained phosphorylation upon stimulation with ligands of EGFR, but activation of either ERBB3 or ERBB4 by NRG1 (or artificial stimulation of an ERBB2 chimera) did not affect tyrosine phosphorylation of CBL (Levkowitz et al., 1996), reflecting differential coupling of CBL to EGFR but not to other ERBB receptors. However, subsequently it was shown that ERBB3 and ERBB4 can be (poly)ubiquitinated by E3 ubiquitin ligases other than CBL and targeted for degradation (Acconcia et al., 2009; Bouyain and Leahy, 2007; Cao et al., 2007; Omerovic et al., 2007; Qiu and Goldberg, 2002; Zeng et al., 2009). In addition, some reports state that ERBB4 is able to recruit CBL (Jansen et al., 2009; Kaushansky et al., 2008; Laederich et al., 2004). Thus, according to the literature, ERBB2

seems to be the only family member that is not ubiquitinated. [However, a recent study claims that a putative CBL binding site of ERBB2 and ERBB4 can functionally replace the EGFR CBL binding site, suggesting that poor downregulation of ERBB2 and ERBB4 is not due to sequence variations in the putative CBL binding sites (Jansen et al., 2009).]

Chimeric ERBB2 receptors or ERBB2-containing heterodimers display slow endocytosis (Baulida et al., 1996; Sorkin et al., 1993), and are predominantly recycled back to the plasma membrane (Lenferink et al., 1998; Worthylake et al., 1999). That raises the question of how, if ERBB2 is the preferred heterodimerization partner for the other ERBBs (chapter 2.5.2.), can the other family members be targeted for degradation. One likely explanation is cell type-specific expression levels of ERBBs. EGF treatment resulted in down-regulation of ERBB2 in cells with relatively low levels of ERBB2 expression (Kornilova et al., 1992; Worthylake and Wiley, 1997). In cells with high levels of ERBB2, such as many mammary carcinoma cell lines, activation of EGFR did not affect surface expression of ERBB2 and did not accelerate its degradation (Haslekas et al., 2005; Yarden and Sliwkowski, 2001). Moreover, overexpression of ERBB2 had a dominant-negative effect on EGF-induced EGFR downregulation, either by preventing internalization or by increased recycling of the EGFR (Lenferink et al., 1998; Offterdinger and Bastiaens, 2008; Wang et al., 1999; Worthylake et al., 1999; Worthylake and Wiley, 1997).

Stimulation of ERBB3 and ERBB4 by neuregulins (Fig. 4) causes internalization and downregulation of these receptors to an extent that is significantly lower than that observed with EGFR downregulation (Baulida and Carpenter, 1997; Baulida et al., 1996; Waterman et al., 1998). Substitution of the C-terminus of EGFR by the same domain of ERBB3 results in reduced association with CBL, ubiquitination and down-regulation (Waterman et al., 1999). It was also suggested that neuregulins do not efficiently target ERBB3 to degradation due to the dissociation of ligand•receptor complexes in endosomes, as observed when EGFR is activated by TGFA (Waterman et al., 1999; Waterman et al., 1998). However, trafficking of both ERBB3 and ERBB4 can be regulated by ubiquitination (see above), and the amplitude of ligand-induced downregulation of these receptors is determined mostly by the rates of their degradation rather than the internalization rates (Sorkin and Goh, 2008).

The role of **Rab GTPases** in the regulation of endocytic trafficking of the EGFR has been reviewed comprehensively by (Ceresa, 2006). RAB5 is the best-studied Rab protein regarding EGFR trafficking. The first *RAB5* gene was cloned in 1990 (Chavrier et al., 1990), and subsequently three human RAB5 isoforms (RAB5A, B, and C) have been identified (Bucci et al., 1995). RAB5 is localized to both the plasma membrane and EEs (Chavrier et al., 1990), and several reports describe a role for RAB5 in regulating endocytic trafficking of the EGFR (Ceresa, 2006). Evidence supports a role for RAB5 regulating EGFR trafficking at the plasma membrane (Barbieri et al., 2000) and at EEs (Dinneen and Ceresa, 2004). Work from

Alexander Sorkin´s lab provides additional support that RAB5 may operate at the plasma membrane, demonstrating a 50% decrease in the amount of internalized EGFR when all three RAB5 isoforms are depleted in HeLa cells (Huang et al., 2004). Single KD of any isoform alone did not cause more than 10% reduction in EGFR endocytosis, suggesting a functional redundancy between the isoforms. Impaired internalization of the EGFR upon triple KD of RAB5 isoforms was confirmed in a recent study (Chen et al., 2009). However, depletion of RAB5A or RAB5B hampered the degradation of EGFR, whereas only KD of RAB5C had very little effect. The differential delay of EGFR degradation correlated with retarded progression of the EGFR from early to late endosomes, implying a role for specific RAB5 isoforms in early endosomal sorting of the receptor. Thus, RAB5 likely functions at both the plasma membrane (donor membrane) and the early endosome (acceptor membrane) in EGFR early endocytic trafficking. The late endosomal RAB7 seems more important than RAB5 in regulating EGFR degradation, but it was unclear until recently whether the GTPase regulates the flow of cargo into or out of LEs (see next chapter below).

The mechanism of ubiquitin- and **ESCRT**-mediated degradative sorting of cargo towards LEs and lysosomes was established in large part by using the EGFR as a model receptor, and has been discussed in detail in the chapters 3.1.4. to 3.1.6. Effects of individual ESCRT KDs on EGFR sorting and signaling will be taken into account in chapter 3.2.4.

Proteins other than ESCRT subunits have been implicated in the EGFR sorting and/or degradation. For instance, deletion of annexin A1 (ANXA1) abolishes the effect of EGF stimulation on MVB inward vesiculation mentioned in chapter 3.1.4. ANXA1 is phosphorylated at MVBs upon activation of the EGFR (Futter et al., 1993). But loss of ANXA1 has no effect on EGF degradation and causes only a small delay in EGFR degradation, indicating that ANXA1 operates downstream of HRS- and ESCRT-mediated sorting and is required solely for EGF-stimulated inward vesiculation (White et al., 2006). Depletion of annexin A2 (ANXA2) blocks EGF transport and degradation at the level of EEs, due to its general role in biogenesis of MVBs *via* regulating actin polymerization at cholesterol-containing early endosomal platforms (Gruenberg and Stenmark, 2004; Mayran et al., 2003; Morel et al., 2009). Similarly, overexpression of sorting nexin 3 (SNX3) blocked EGF transport to LEs and delayed EGFR degradation due to a general defect in early to late endosomal transport, but KD of SNX3 had only a minor effect on EGFR transport and degradation (Pons et al., 2008). Instead, depletion of SNX3 led to a severe defect in the formation of ILVs, showing (as for ANXA1) that inward vesiculation can be uncoupled from EGFR transport and degradation. Depletion of the phosphatase-defective protein HD-PTP (discussed in chapter 2.6.1.) leads to reduced transfer of the EGFR and fluid-phase markers to LEs/lysosomes, caused accumulation of ubiquitinated proteins on endosomal compartments, and disrupted the morphogenesis of MVBs (Doyotte et al., 2008). Interfering with functions of phosphoinositide-metabolizing enzymes such as the

type III PI3K VPS34 producing PI(3)P (Petiot et al., 2003), PIKFYVE generating PI(3,5)P_2 (de Lartigue et al., 2009), and the phosphatidylinositol 4-kinase alpha (PI4KA) producing PI(4)P (Minogue et al., 2006), led to defects in EGFR transport and downregulation, and so did overexpression or KD of the endosomal motor protein kinesin KIF16B (Hoepfner et al., 2005).

Thus, a number of conditions interfering with the general organization of and trafficking within the endosomal system also affect the targeting and downregulation of the EGFR, without specifically regulating receptor sorting. Many proteins specifically influencing the fate of activated EGFR are often inducible feedback regulators, as discussed in chapter 2.6.1. for MIG6/RALT, Sprouty proteins and SPREDs, LRIG1, and several SOCS proteins.

3.2.3. EGFR sorting at late endosomes and delivery to lysosomes

The late endosome can be viewed as the second major sorting station in the endocytic pathway. Through lipid-based sorting, involving particularly LBPA and cholesterol, cargo can be retrieved from the lumen of LEs *via* dynamic fusion and fission processes between ILVs and the limiting membrane, regulated by the ERSCT-associated protein ALIX and the ESCRT-I subunit TSG101 (chapter 3.1.5.). ALIX has been found to play a role in EGFR internalization at the plasma membrane, antagonizing CBL and CIN85 association with the receptor (Schmidt et al., 2004). But the role of the BRO1 domain-containing protein at later stages in the pathway is poorly defined. During *in vitro* budding of ILVs into LEs, a process regulated by TSG101, ALIX, and LBPA, the EGFR becomes protected from limited proteolysis (Falguieres et al., 2008). However, only TSG101 KD has an effect on EGFR sorting and degradation *in vivo* (Babst et al., 2000), whereas depletion of ALIX or internalization of inhibitory anti-LBPA antibodies has no impact on EGFR downregulation (Luyet et al., 2008). Presumably, once the EGFR is incorporated into ILVs via the ESCRT machinery (chapter 3.1.4.), it is not capable of being delivered back to the limiting membrane, perhaps because the EGFR-containing ILVs are different from LBPA-positive, ALIX-regulated ILVs hijacked by pathogens.

Among the Rab proteins shown to be localized to the late endosome are RAB7, RAB9, and RAB34 (Ceresa, 2006). To date, RAB9 and RAB34 have not been implicated in regulating EGFR trafficking, but instead regulate golgi-lysosomal transport (Lombardi et al., 1993; Speight and Silverman, 2005; Wang and Hong, 2002). However, evidence accumulated that **RAB7** functions in EGFR degradation. RAB7 was shown to be localized to LEs (Chavrier et al., 1990), and early characterization of RAB7 indicated a role in endocytic trafficking, acting either upstream or downstream of late endosomes (Bucci et al., 2000; Feng et al., 1995; Mukhopadhyay et al., 1997; Press et al., 1998). The Rab-interacting lysosomal protein (RILP) was subsequently identified as an effector of RAB7 on LEs, and a truncated

form of the protein inhibited the degradation of EGF and LDL, accompanied by strong morphological changes of the compartment also observed for overexpressed wild-type RILP (Cantalupo et al., 2001). Soon thereafter, it was shown that ectopic RILP expression induces the recruitment of functional dynein-dynactin motor complexes, which explained the high degree of aggregation of LE in the perinuclear region by exclusive transport of the compartment towards the minus end of microtubules (Jordens et al., 2001). Importantly, when dominant negative RAB7 was expressed, degradation of the EGF•receptor complex was slowed down and accumulated in LEs (Ceresa and Bahr, 2006). Moreover, in RAB7-depleted cells, trafficking of EGF•EGFR until MVBs/LEs was unaffected, but the complex was hardly degraded and trapped in ILVs of enlarged, densely packed LEs (Vanlandingham and Ceresa, 2009). Taken together, these data support a role for RAB7 in regulating EGFR endocytic trafficking from LEs to lysosomes, and for maintenance of the late endosomal compartment.

To finish this chapter about the degradative sorting of EGF and its receptor: already during the pioneering work 25 to 35 years ago, it was realized that the degradation of EGF and its receptor can be completely blocked by lysosomal inhibitors, setting the trend for future discoveries about EGFR downregulation after ligand stimulation (Carpenter and Cohen, 1976; Dunn et al., 1986; Stoscheck and Carpenter, 1984b).

3.2.4. The interplay between EGFR trafficking and signaling

Cell signaling and endocytic membrane trafficking have traditionally been viewed as separate processes, but it is now well appreciated that these processes are intimately and bidirectionally linked. Many excellent reviews summarize our current knowledge about the close encounter of signal transduction and endosomal trafficking (Kholodenko et al., 2010; Miaczynska et al., 2004; Scita and Di Fiore, 2010; Sorkin and Von Zastrow, 2002, 2009; von Zastrow and Sorkin, 2007). Apart from the general principle of signal attenuation by endocytic receptor downregulation, many receptors remain active and continue to signal from endosomes. These include RTKs such as the EGFR and the NGF receptor NTRK1/TRKA, GPCRs complexed to beta-arrestins (see chapter 2.6.2. and (Ritter and Hall, 2009)), receptors for TGFB, NOTCH receptors, tumor necrosis factor (TNF) receptors, and toll-like receptors. In addition, intracellular MAPK scaffolds contribute substantially to signal strength, duration, and specificity, such as beta-arrestins and the p18-p14-MP1(-MORG) complex at early and late endosomes, respectively (chapter 2.6.2.). Here, the focus will be on the regulation of EGFR signaling by endosomal sorting, and the potential contribution of the internalized, endosomal receptor itself to the signaling output. The reverse principle, that EGFR signaling regulates the intracellular fate of the receptor, has been given attention in chapter 3.2.1.

The EGFR may be the most popular model used to study the crosstalk between endocytosis and signaling. After internalization, EGF and EGFR are efficiently degraded, which results in the dramatic decrease in the half-life of the receptor (Stoscheck and Carpenter, 1984b). The process by which the number of receptors available for activation at the cell surface is decreased, is referred to as EGF-induced downregulation of EGFR, a major negative feedback mechanism controlling the intensity and duration of receptor signaling (Wells et al., 1990).

Work from Sandra Schmid' s lab indicated already some 15 years ago that EGFR signaling is differentially regulated by dynamin-dependent **internalization** (Vieira et al., 1996). Upon expression of the DNM2-K44A mutant (see chapter 3.2.1.), EGF-dependent HeLa cell proliferation was enhanced in endocytosis-defective cells, accompanied by an increase in PLCG and SHC phosphorylation (chapter 2.2.). However, early EGF-dependent signaling events were not uniformly upregulated, as observed for a decrease in EGFR, ERK1/2, and PI3K phosphorylation. Thus, normal endocytic trafficking of the EGFR was proposed to be required for full activation of downstream signaling pathways, and to contribute to signaling specificity. Why the cells displayed increased proliferation while activity of the ERK cascade and the PI3K pathway was diminished in this study, remains an open question.

As discussed in chapter 3.2.1., EGFR is able to enter mammalian cells *via* a number of different routes, for example clathrin-dependent *vs.* cholesterol-dependent but clathrin-independent pathways (Sigismund et al., 2005). The authors state that upon stimulation of HeLa cells with low EGF concentrations (1.5 ng/ml), EGFR enters almost exclusively *via* CME and is not ubiquitinated. In contrast, upon high EGF stimulation (20 ng/ml), a substantial fraction of the receptor is internalized through a clathrin-independent route which is sensitive to nystatin or filipin treatment (cholesterol-binding drugs), and EGFR becomes ubiquitinated. An ubiquitination-impaired EGFR mutant was internalized through the clathrin pathway, whereas an EGFR-ubiquitin chimera that can signal solely through its ubiquitin moiety was internalized exclusively by the non-clathrin pathway. Non-clathrin internalization of ubiquitinated EGFR depended on its interaction with ubiquitin-interacting proteins, as shown through the ablation of EPS15, EPS15R, and epsin. Later, work from the same group suggested that EGFRs internalized *via* CME at low doses of EGF are not targeted for degradation, but instead are recycled to the cell surface (Sigismund et al., 2008). By contrast, clathrin-independent (filipin-sensitive) internalization committed the receptor to degradation. CME was proposed to prolong the duration of EGFR signaling due to preferential recycling of the receptor, measured for example by increased DNA synthesis by the cells particularly at low EGF concentrations (Fig. 21). However, the data leave some important questions unanswered: despite increased DNA synthesis at low EGF doses, phospho-AKT and phospho-SHC levels were much lower compared to high EGF stimulation conditions, and ERK was also slightly less activated upon low EGF stimulation (Sigismund et al., 2008;

Sigismund et al., 2005). As mentioned above (Vieira et al., 1996), increased proliferation but diminished activity of the ERK and PI3K-AKT pathways (at low EGF in Sigismund *et al.*) is not easy to explain. Perhaps stronger stimulation of ERK and PI3K-AKT pathways by high EGF leads, under the experimental conditions used, to differentiation rather than proliferation, or *vice versa*, inappropriate activation of these pathways by DNM2-K44A overexpression, depletion of clathrin heavy chain (and AP2 subunits), or low EGF inhibits differentiation and favours proliferation. As mentioned in chapter 3.2.1., another study found only a minimal inhibitory effect of the cholesterol-removing drugs nystatin or methyl-beta-cyclodextrin on the endocytosis of EGFR at high ligand concentrations in the same HeLa cell line (and HEp2 cells in addition). Moreover, KD of clathrin heavy chain inhibited internalization of the EGFR at both low and high ligand concentrations (Kazazic et al., 2006). To explain these contradictions by differences between subclones of HeLa cells is perhaps not too satisfactory, and much remains to be investigated about EGFR internalization and its effect on downstream signaling events under different stimulation conditions, especially regarding the correlation of phospho-levels of signaling components with biological outputs.

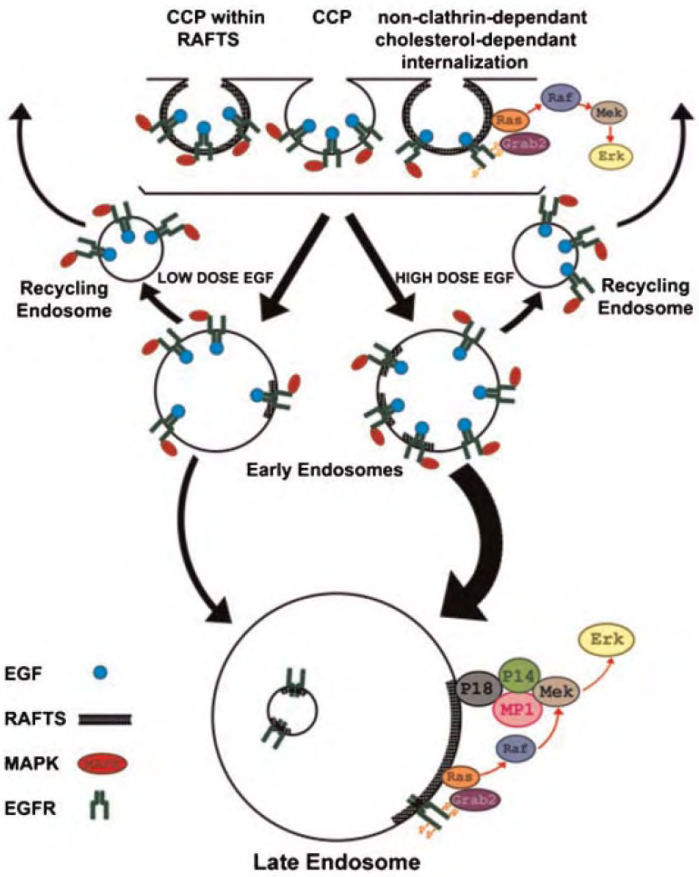

Fig. 21: Differential internalization of the EGFR and the role of cholesterol domains in EGFR signaling.
Sigismund *et al.* propose that at low doses of ligand, the EGFR is internalized *via* a clathrin-dependent, cholesterol-independent pathway. EGFR internalized through this mechanism is recycled back to the plasma membrane. However, at high doses of EGF, the internalization of the EGFR through a non-clathrin-dependent, cholesterol-dependent (filipin-sensitive) mechanism is increased, leading to trafficking of the EGFR to LEs and lysosomes for degradation. Recent work also indicates that membrane rafts in LEs constitute an important signaling platform, containing the raft adaptor p18 (anchoring the EGF-induced MAPK signaling complex to LEs; chapter 2.6.2.) and perhaps also activated EGFR (Balbis et al., 2007; Balbis and Posner, 2010).

Ubiquitin- and **ESCRT-dependent sorting** targets the EGFR for degradation and is thus responsible for switching off receptor signaling (chapters 3.1.4. and 3.2.1-2.). While the role of **CBL** and ubiquitin in receptor downregulation is extensively investigated, surprisingly very few studies aimed directly to identify the role of the ubiquitin ligase in EGFR signaling, by applying transcriptional reporter assays or inspecting the activation status of the EGFR and downstream components of the signaling cascade. A recent study shows slightly increased phosphorylation of ERK1/2 in an EGF stimulation time course upon CBL KD, which is more pronounced in cells stimulated with another EGFR ligand, AREG (Baldys et al., 2009). However, the multifunctionality of CBL as an ubiquitin ligase for many signaling proteins and as an adaptor with more than 150 known interacting proteins clearly implicates CBL in the regulation of numerous signaling processes (Dikic et al., 2003; Schmidt and Dikic, 2005).

Direct effects of individual ESCRTs on EGFR signaling have been first observed in *Tsg101*-deficient mouse fibroblasts. *Tsg101* was originally identified as a gene whose disruption produced transformation of NIH3T3 mouse fibroblasts which grew in soft agar and induced metastatic tumors in nude mice (Li and Cohen, 1996). [However, currently there are more examples in the literature showing increased levels of TSG101 in tumors and its pro-oncogenic activities, indicating that TSG101 is unlikely to be a tumor suppressor (Tanaka et al., 2008). Examples include (Liu et al., 2002; Oh et al., 2007; Zhu et al., 2004).] *Tsg101* mutant cells were defective in the delivery for example of EGF to late endocytic compartments and displayed prolonged activation of ERK1/2 as a consequence of delayed receptor downregulation (Babst et al., 2000). In *Drosophila*, electron microscopy studies of *hrs* mutant larvae (expressing a truncated Hrs protein which still contained the VHS and FYVE domain) revealed an impairment in endosome membrane invagination and formation of MVBs (Lloyd et al., 2002). *hrs* mutant animals failed to degrade active Egfr and the Torso RTK, leading to enhanced signaling shown by elevated phospho-MAPK levels, upregulation of downstream transcription factors, and altered embryonic patterning. These data demonstrated that Hrs and MVB formation function to downregulate RTK signaling in the case of the *Drosophila* Egfr and Torso. Soon thereafter it was shown that Hrs mediates downregulation of multiple signaling receptors (Jekely and Rorth, 2003). *Drosophila* epithelial cells devoid of Hrs accumulated multiple signaling receptors in an endosomal compartment with high levels of ubiquitinated proteins: not only RTKs (Egfr and Pvr) but also Notch and receptors for Hedgehog and Dpp (TGFB-related). However, most Hrs-dependent receptor turnover appeared to be ligand independent, indicating that both active and inactive signaling receptors may be targeted by Hrs for degradation *in vivo*. A number of cell culture-based studies from Harald Stenmark´s lab confirmed the EGF-dependent elevation of active ERK levels upon TSG101 and HRS KD compared to controls (Bache et al., 2006; Malerod et al., 2007). Interestingly, depletion of the ESCRT-III subunit CHMP3/VPS24 and the ESCRT-II subunit EAP30/VPS22 (see chapter 3.1.4.) did not lead to elevated phospho-ERK levels,

suggesting functional differences between individual ESCRTs and that degradation of the receptor is not required *per se* for termination of its signaling (as may be the case for EGFR trapping in ILVs upon RAB7 KD (Vanlandingham and Ceresa, 2009)). However, another study investigating the effect of VPS22 depletion showed no effect on EGF (and major histocompatibility complex class I) degradation, suggesting that mammalian ESCRTII may be redundant, cargo-specific, or not required for protein sorting at the MVB (Bowers et al., 2006). The differential effect of individual ESCRT KDs on EGFR signaling may be explained by the observation that only depletion of HRS or TSG101 caused enhanced recycling of the receptor, whereas this was not the case with depletion of VPS22 or VPS24 (Raiborg et al., 2008). HRS-dependent recycling was also shown for the beta-2 adrenergic receptor, but disruption of HRS prevented recycling and functional re-sensitization of the GPCR, converting the temporal profile of cell signaling from sustained to transient (Hanyaloglu et al., 2005). Thus, in the case of the EGFR, depletion of HRS and TSG101 leads to sustained MAPK activation upon stimulation, whereas in the case of the GPCR, HRS depletion causes a reduction in the ability for re-stimulation. As for TSG101, the involvement of HRS in cancer development is not clear. For example, targeted disruption of HRS attenuated the proliferation, anchorage-independent growth, tumorigenesis, and metastatic potential of HeLa cells *in vitro* and *in vivo* (Toyoshima et al., 2007). The same study also shows that HRS is more strongly expressed in many malignant human cancer tissues compared to normal tissues, in contradiction to the dogma of receptor downregulation and signal attenuation by HRS (Fig. 22) and other ESCRTs.

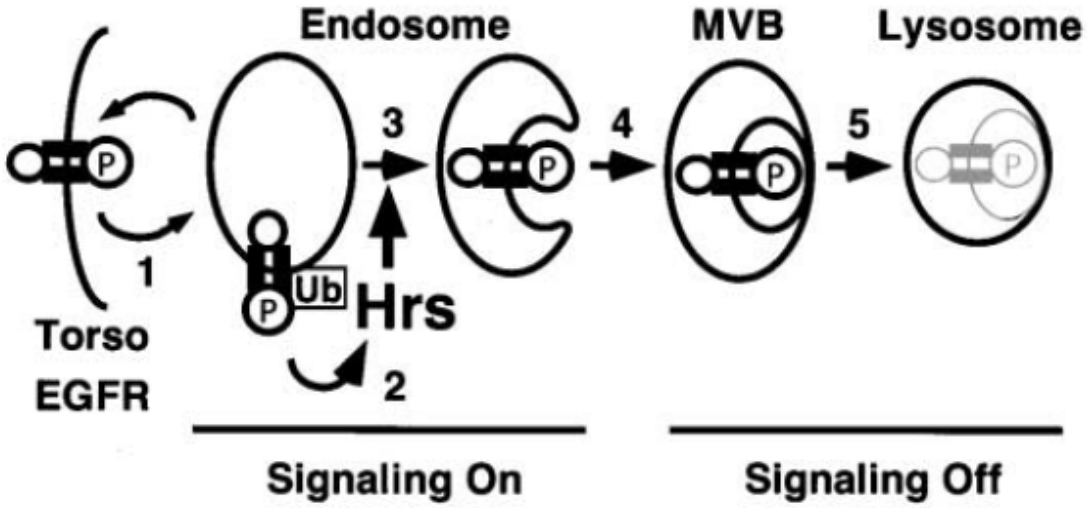

Fig. 22: The dogma of ESCRT-dependent growth factor receptor downregulation and signal attenuation. ESCRT proteins, exemplified here by HRS, mediate inward budding of endosomal membranes, leading to sorting of activated RTKs into internal vesicles of MVBs. This process is required to degrade active RTKs and downregulate RTK signaling (Lloyd et al., 2002).

Several lines of evidence show that the EGFR is active within the cells and signals from intracellular compartments. More than 20 years ago, it was shown for the first time by immunofluorescence, electron microscopy, and subcellular fractionation, that endosomal EGFR is phosphorylated and associates with downstream effectors (Carpentier et al., 1987; Wada et al., 1992). Later it was shown that **endosomal active EGFR** stays associated with a variety of signaling proteins (chapter 2.2.) such as SHC, GRB2, SOS, and hyperphosphorylated RAF1 (Di Guglielmo et al., 1994; Oksvold et al., 2000), RAS GTPase-activating protein 1 or RASA1/RASGAP (Wang et al., 1996), and EPS8 and CBL (Burke et al., 2001; de Melker et al., 2001), reviewed in (Baass et al., 1995; Wiley and Burke, 2001). Interestingly, endosome-localized EGFR can activate RAS as efficiently as surface-localized receptors (Haugh et al., 1999a), but that activation of PLCG1 is restricted to the plasma membrane (Haugh et al., 1999b). This was due to a lack of the appropriate lipid substrate for PLCG1 in the endosomal compartment, suggesting that signaling from endosomes might be qualitatively different from that generated at the cell surface. In an artificial stimulation condition, EGF-bound but inactive EGFR (kinase activity was blocked by the highly selective inhibitor AG1478 or tyrphostin) could be internalized into endosomes. After washout of the drug, the receptor was specifically activated on endosomes, which could completely substitute for plasma membrane activation, as measured by activation of several signaling pathways including cell survival *via* inhibition of apoptosis (Wang et al., 2002). The induction of cell proliferation, however, required a second pulse, which could originate from endosomal EGFR as well (Pennock and Wang, 2003). [Work from another group showed already before that the continuous growth factor requirement for cell cycle entry could be replaced with two short pulses of mitogen, where activation of MEK and induction of the transcription factor MYC were sufficient to drive the first phase, whereas synthetic PI3K lipid products were sufficient to drive the second phase of signaling (Jones and Kazlauskas, 2001)]. The experiments from Wang and Pennock suggest that signals transduced from internalized EGFR, with or without a contribution from the plasma membrane, fully satisfy the physiological requirements for S-phase entry. By expanding their experimental approach, the authors could also demonstrate that endosomal PDGFR signaling is sufficient to generate physiological output including cell proliferation and cell survival (Wang et al., 2004).

Taken together, endosomal EGFR stays active, recruits the downstream signaling machinery, and is able to compensate for plasma membrane activation of the signaling network leading to cell proliferation. But how the pool of active endosomal receptor is regulated, and to what extend it contributes to the biological response under physiological conditions, remain open questions.

4. Project outline

The aim of this study was to correlate endocytic trafficking of the EGFR and different stimulation conditions with downstream signaling events by various approaches. Particularly, EGF-induced signal transduction after interfering with clathrin- and dynamin-dependent endocytosis, CBL-mediated ubiquitination, ESCRT-dependent endosomal sorting (*e.g.* HRS, TSG101, and VPS4), and after depletion of two BRO1 domain-containing proteins (ALIX and HD-PTP), was investigated in detail. In addition, consequences of distinct stimulation conditions, such as low *vs.* high EGF, continuous *vs.* pulse-chase stimulation, EGF *vs.* PMA stimulation, and of EGFR overexpression, were elucidated. Thus, the main questions were, how do cells react to disturbances in EGFR trafficking and how do they adopt their response to various stimulation conditions. Several methods were deployed to measure downstream signaling: 1) the activation status of components of the signaling cascade was determined by immunoblotting for phosphorylated signaling proteins; 2) a live-cell signaling reporter assay was set up to measure the strength and duration of ELK1-dependent transcriptional activation over time; 3) the induction of endogenous target genes downstream of the EGFR-MAPK cascade was detected by quantitative real-time RT-PCR; 4) genome-wide transcriptional profiling using microarrays was performed; and 5) induction of EGF response genes was quantified by the recently developed NanoString nCounter gene expression system were individual mRNA transcripts are counted without enzymatic reactions or bias, a technology more sensitive than microarrays and similar in sensitivity to real-time PCR (Geiss et al., 2008; Malkov et al., 2009). All of these techniques were applied under various KD and stimulation conditions over time, in order to understand the cellular response and its flexibility *vs.* robustness towards perturbations of the EGFR signaling system.

Results

1. Establishing a live-cell signaling assay to measure ELK1-driven transcription

In order to measure EGF-triggered transcriptional activation in living cells over time, we made use of a commercially available HeLa cell line from Stratagene. HLR-ELK1 (HeLa luciferase reporter for ELK1) cells stably express the activator domain of ELK1 (an ERK MAPK downstream ETS family transcription factor, see chapter 2.3.) fused to the Gal4 DNA-binding domain. A second expression cassette contains a luciferase gene under the control of the Gal4 upstream activation sequence (Fig. 1). Upon phosphorylation of ELK1 and dimerization, luciferase is expressed, which we assayed in an incubator equipped for light detection in cell culture dishes.

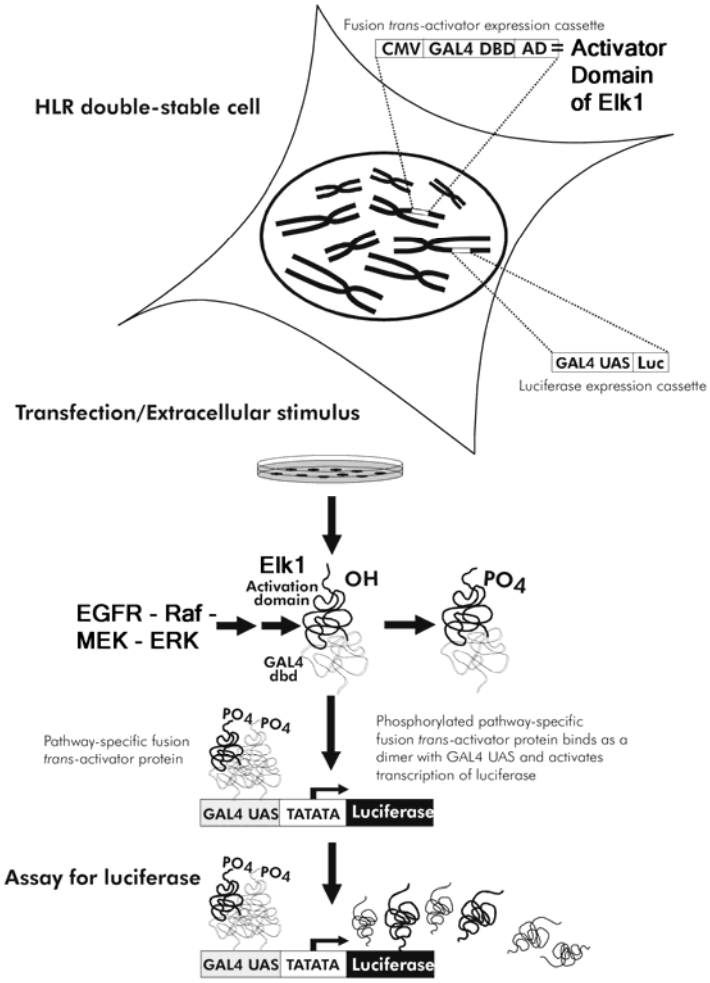

Fig. 1: Schematic representation of the double-stable PathDetect® HLR-ELK1 *trans*-reporter cell line.
The HeLa luciferase reporter cells stably express the activator domain of ELK1 fused to the Gal4 DNA-binding domain (DBD) under the control of the CMV promoter. A second expression cassette contains a luciferase gene under the control of the Gal4 upstream activation sequence (UAS). Upon activation for example of the ERK-MAPK cascade, ELK1 is phosphorylated and dimerizes. The dimeric fusion protein then binds *via* the Gal4 DBD to the Gal4 UAS and induces luciferase expression.

Induction of luciferase expression under our conditions is completely dependent on EGF stimulation and on EGFR kinase activity, since without EGF or upon EGF stimulation in the presence of the specific EGFR kinase inhibitor AG1478 (tyrphostin), only background light production can be observed (Fig. 2 A). The specificity of the inhibitor was confirmed by western blot (Fig. 2 G): AG1478 blocked phosphorylation of the EGFR, MEK1/2 and ERK1/2 only during EGF stimulation, whereas the inhibitor had hardly any effect when cells were stimulated with the phorbol ester phorbol-12-myristate-13-acetate (PMA, activates MEK and ERK *via* PKC and not *via* the EGFR). EGFR-depleted cells display very low luciferase activity (Fig. 2 B and H), and signaling measured by this assay can be increased to about 250% by EGFR overexpression (Fig. 2 C and I). Light production and detection are not limited for example by substrate (luciferin) availability or technical reasons, since PMA stimulation leads to a massive increase of luciferase activity to 400% compared to the standard 100 ng/ml continuous EGF stimulation (Fig. 2 D). On the other hand, signaling is significantly decreased when cells are partially depleted of MEK1 and MEK2 (Fig. 2 E and J), or when MEK activity is interfered with by using the selective inhibitor U0126 (Fig. 2 F). Altogether, these observations indicate that the assay was sensitive and robust, with a wide dynamic range, and that it faithfully reproduced the EGF response along the ERK cascade.

2. EGFR signaling in cells depleted of ESCRTs or ESCRT-associated proteins

We then investigated whether the EGF signal was affected when interfering with EGFR sorting into the multivesicular endosome by siRNA-mediated depletion of ESCRT subunits (chapter 3.1.4.). First, we depleted the ESCRT-0 subunit HRS (initiating the ESCRT sequence responsible for activated receptor sorting into intralumenal vesicles, ILVs), and the ESCRT-I subunit TSG101 (which interacts with HRS and is required for ILV formation). Neither HRS nor TSG101 knockdown (KD) did result in increased or sustained EGF signaling in our assay (Fig. 3 A). If anything, the signal was somewhat decreased.

To confirm these results, we analyzed the transcriptional induction of two endogenous downstream target genes of the pathway, *EGR1* and *FOS*, by quantitative real-time RT-PCR

Fig. 2: Validation of the live-cell signaling assay using HLR-ELK1 cells.
A) Cells were starved over night (16-18 h) and assayed for luciferase activity without (grey) or during continuous EGF stimulation (100 ng/ml as general stimulation condition; black). In addition, EGF stimulation was carried out in the presence of AG1478 (an EGFR kinase inhibitor, 150 nM; red). The data are always normalized to the protein content of the cells in the dish, and represent at least two independent experiments in duplicates. **B)** Luciferase activity in mock-treated (black) *vs.* EGFR-depleted (red) cells. **C)** Comparison between GFP- (black) and GFP-EGFR-expressing (red) cells. Here, four independent experiments in duplicates are additionally normalized to the GFP peak = 100% and "0 min" because of experimental variation. **D)** Comparison between EGF and PMA (10 ng/ml) stimulation (n = 7; normalization to peak of EGF = 100% and "0 min"). **E)** Luciferase activity in mock-treated (black) *vs.* MEK1 and MEK2 double KD (red) cells. **F)** Luciferase induction upon EGF stimulation in the absence (black) or presence (red) of U0126 (MEK inhibitor, 10 µM). **G)** Verification of AG1478 specificity: in 15' EGF, signaling proteins are phosphorylated, whereas in 15' EGF & AG(1478), they are not. In PMA-stimulated cells, the EGFR is not phosphorylated, but MEK and ERK are, and the AG1478 inhibitor has very little effect. **H)** Verification of EGFR KD efficiency by western blot. **I)** Verification of GFP or GFP-EGFR expression. **J)** Verification of MEK1 and MEK2 double KD.

Figure 2 - Results

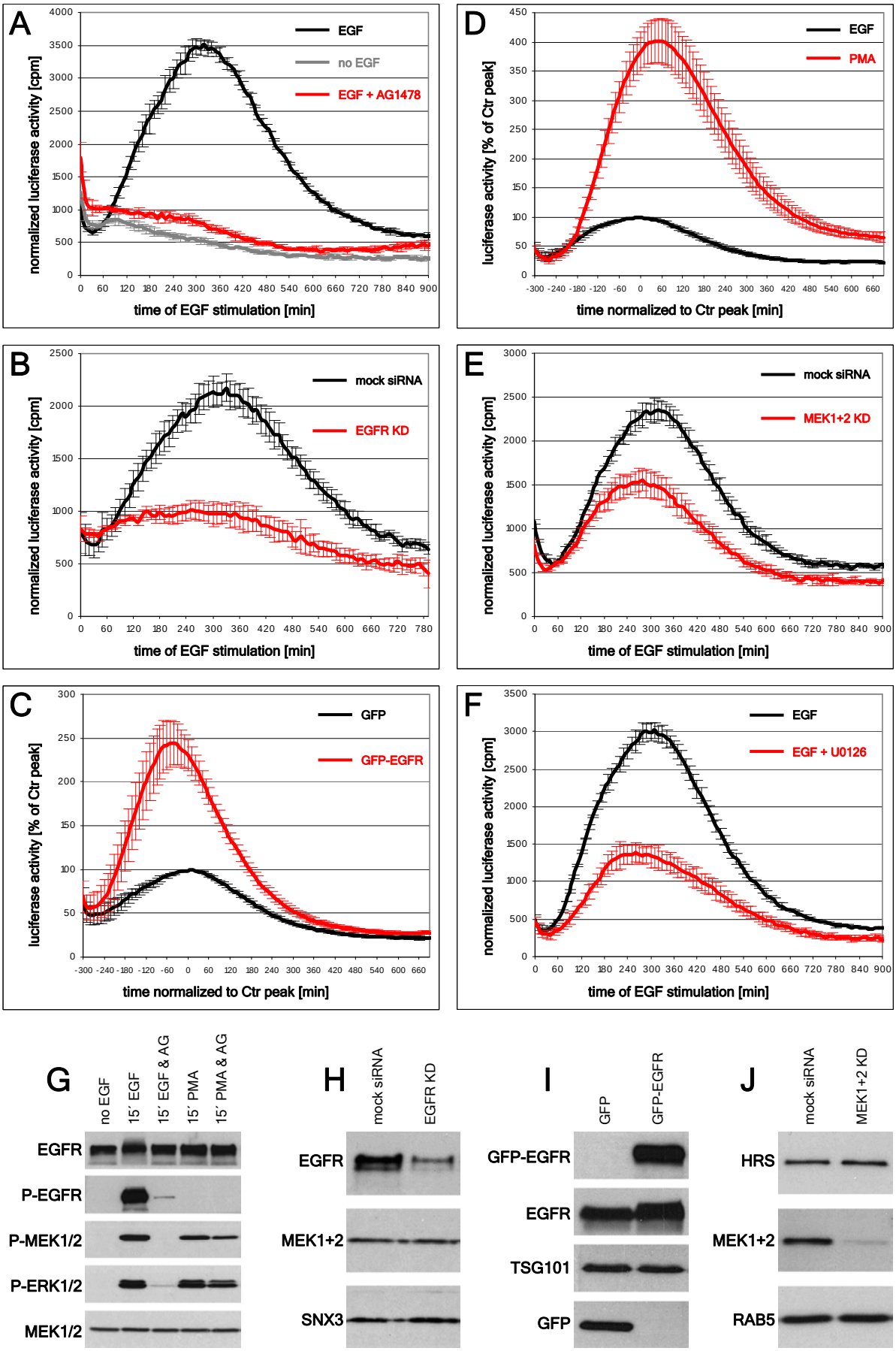

(Fig. 3 B). Again, HRS and TSG101 KD had very little effect on EGF-induced transcription at three time points of stimulation, and the small decrease in *EGR1* or *FOS* mRNA levels was within the error bars. In addition, depletion of the ATPase VPS4A (responsible for the disassembly of ESCRT-III filaments after endosomal inward vesiculation) had no effect on the induction of the immediate early genes *EGR1* and *FOS* downstream of EGF (Fig. 3 B).

Many studies have shown that HRS or TSG101 depletion delays EGFR sorting into MVBs and its degradation, and concomitantly increases the activation state of downstream kinases, as measured by their phosphorylation state (chapter 3.2.4.). Having observed no effect of ESCRT depletion on the signaling output, we wondered whether activity of the EGFR and downstream kinases were affected under our KD conditions. As expected, EGFR levels decreased after EGF addition in mock-treated cells (in the presence of the translation inhibitor cycloheximide, to prevent EGFR re-synthesis), with only about 25% remaining after 5 h (Fig. 3 C, and quantification in Fig 3 D). EGFR degradation was delayed after depletion of HRS, TSG101, or VPS4A to an extent similar to that previously observed by others. The KD of ESCRTs was also accompanied by an increase in the phosphorylation state of the EGFR and its downstream kinases, MEK1/2 and ERK1/2 (Fig. 3 C and D). Our KD conditions thus recapitulated the effects of ESCRT depletion reported by others, which unambiguously demonstrates that the lack of effects on downstream transcriptional induction was not due to incomplete protein depletion.

This apparent discrepancy between the activation status of the EGFR and downstream signaling partners, and the signaling output lead us to investigate the EGF response in more detail. To this end, we measured all EGF-regulated transcripts by genome-wide microarray analysis. We used the HLR-ELK1 cell line and the same stimulation conditions (continuous 100 ng/ml EGF after 16-18 h serum-deprivation, but without cycloheximide, see below), to correlate the data with our previous results. As before, ON-TARGETplus SMARTpool siRNAs from Dharmacon were transfected under identical conditions to deplete HRS, TSG101, VPS4A, and ALIX (an ESCRT-associated protein which regulates ILV formation in late endosomes, see chapter 3.1.5. and 3.2.3). Mock-treated cells were transfected with a non-targeting siRNA pool from the same company. RNA from serum-starved cells and from cells stimulated with EGF for three time points (30, 120, and 360 min) was extracted, analyzed,

---

Fig. 3: EGFR degradation and signaling upon depletion of ESCRT subunits.
A) Signaling assay with HRS (green; n = 5 in duplicates) or TSG101 (blue; n = 10 in duplicates) KD cells, compared to mock (black; normalization as in Fig. 2 C and D). **B)** Real-time qRT-PCR (with QuantiTect SYBR Green PCR Kits from Qiagen) for endogenous *EGR1* and *FOS* mRNAs in mock *vs.* HRS, TSG101, or VPS4A (orange) KD cells at three time points of EGF stimulation. Values are simply expressed as ddCt = number of PCR cycles between non-induced and EGF-induced, normalized to beta-actin. Data are means of at least three independent experiments in triplicates. **C)** EGFR degradation and EGFR, MEK1/2, and ERK1/2 phosphorylation upon EGF stimulation for up to 5 h in HRS, TSG101, or VPS4A KD cells, compared to mock. The standard 100 ng/ml EGF continuous stimulation of serum-starved HLR-ELK1 cells was used in the presence of 10 µg/ml cycloheximide, and cells were harvested and prepared for western blot analysis. **D)** Quantification of C) using ImageJ software. Values represent two to three independent experiments, and are normalized to mock 0 = 100% for EGFR and to mock 1 h = 100% for P-EGFR, P-MEK1/2, and P-ERK1/2.

Figure 3 - Results

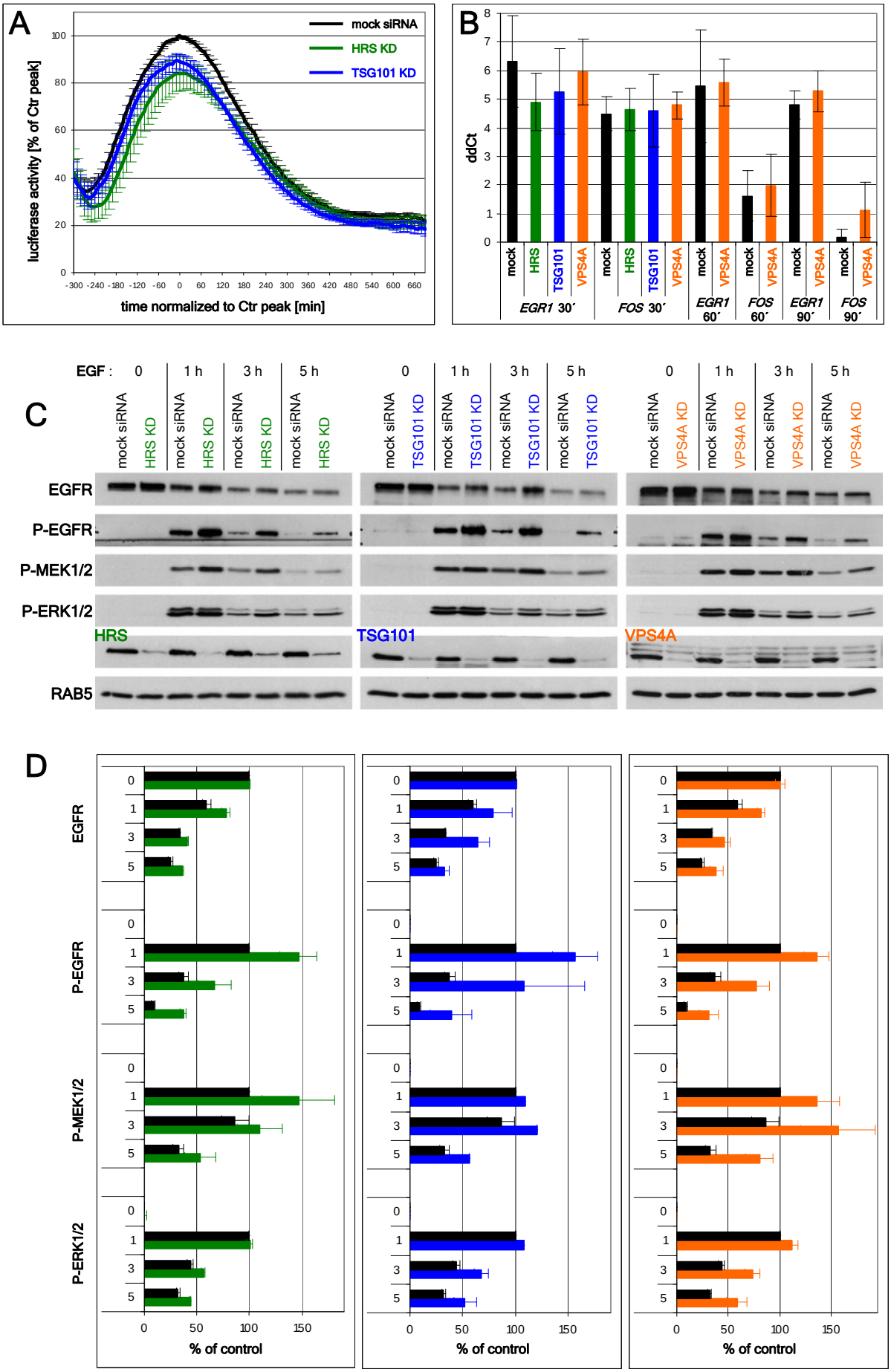

and processed for hybridization with Affymetrix Human Gene 1.0 ST Arrays, in biological (not technical) triplicates. In parallel, one dish per KD condition was harvested for western blot analysis to verify protein depletion.

The addition of EGF caused a strong cellular response, as revealed by changes in the levels of approximately 260 mRNAs about 2-fold above or below their expression in starved-only cells (Fig. 4 A). To illustrate the architecture of the response, data were normalized to values of mock-treated cells at 0 min, grouped and ranked according to their peak and strength of induction, respectively, as described in the legend to Fig. 4. The EGF response was very well orchestrated in time, displaying functional waves of transcription (chapter 2.4.). Immediate early genes, such as classical transcription factors of the AP-1 and EGR families, were strongly upregulated at 30 min EGF and then faded away at later time points (Fig. 4 B and 5 A). Synthesis of those transcription factors involved in subsequent transcriptional control of many late-induced genes is necessary to allow for full EGF-dependent signaling response, therefore cycloheximide should be omitted in such experiments (see also part 3). At the later points of our EGF stimulation time course, a second and then a third wave of transcripts were stimulated, encoding effector proteins but also many feedback regulators of the response (chapter 2.4. and 2.6.1.; see below, Fig. 5).

We then analyzed to what extent the expression of EGF-regulated transcripts was altered after depletion of ESCRT subunits and ESCRT-associated proteins. siRNA-mediated KD efficiently depleted the levels of each mRNA and protein (Fig. 4 C). Some difference between HRS protein and mRNA levels (about 50-60% reduction of *HRS* mRNA, but almost complete depletion of the protein) may be due to mRNA retained in the RNA-induced silencing complex (RISC) during RNA interference (RNAi). In addition, a stronger KD of HRS was toxic to the cells. To evaluate the effects of ESCRT inactivation in the EGF response, mRNA levels for each time point under each KD condition were normalized as the corresponding values for mock-treated cells (to mock 0 min, see above). Data for each of the 260 EGF-induced genes were then plotted next to each other in the heat map shown in Fig. 4 A and B, to allow for direct comparison of all conditions. Strikingly, the analysis of the transcripts showed that the overall EGF-dependent response was not significantly affected under any KD condition at any time-point. The general pattern of transcripts stimulated by EGF remained similar to that of controls, and no general shift or delay was observed in the response.

Fig. 4: Microarray analysis of EGF-induced genes in mock *vs.* HRS-, TSG101-, VPS4A-, and ALIX-depleted cells. **A)** Architecture of the transcriptional EGF response. The heat map (generated with Partek software) shows 263 genes whose transcription was at least 1.8-fold above or below mock 0 min (no EGF). Data represent means of biological triplicates (p-value = 0.05, false discovery rate = 0.05), and are normalized to mock 0 min = 1 (white = 0 in Log2, see scale in B). Genes are further grouped according to the time of their maximal or minimal transcription (30, 120, or 360 min EGF, see B), and ranked within these groups according to decreasing fold difference between mock 30 / 120 / 360 min and mock 0 min. Only properly annotated genes were considered in the heat map (Affymetrix probes without any assigned gene and pseudogenes were omitted). Included genes and their expression values can be found in the appendix. **B)** Immediate and delayed early genes in mock *vs.* ESCRT KD cells (detailed expression profiles in mock-treated cells are shown in Fig. 5). **C)** Verification of KD efficiencies. Shown are mRNA levels for HRS, TSG101, VPS4A, or ALIX, in microarrays *vs.* NanoString (see text; again values are normalized to mock 0 min), and protein levels determined by western blotting.

Figure 4 - Results

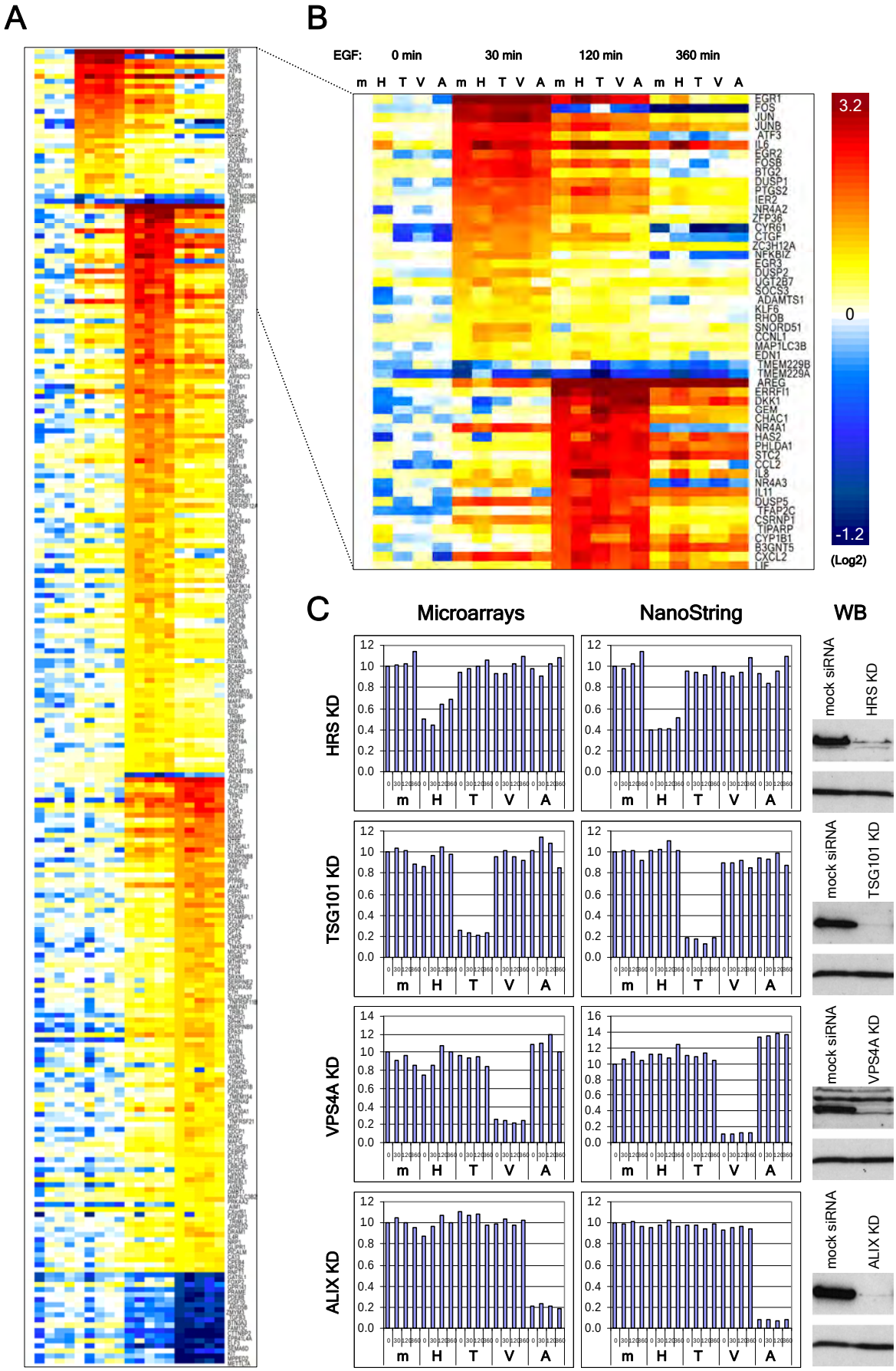

To rationalize the wave-like organization of the response in our data set, a detailed analysis of known regulators of EGFR signaling was carried out. The well-characterized immediate early genes encoding for AP-1 family members (e.g. JUN, FOS, FOSB) and early growth response transcription factors (EGR1-3), whose function is necessary to initiate subsequent waves of transcription, were strongly induced at 30 min EGF (Fig. 5 A). Due to their short half-life, mRNAs of these forward-driving transcriptional activators were quickly downregulated after the initial burst of transcription, but also due to the induction of transcriptional repressors. Some were induced maximally at 30 min EGF, particularly JUNB, ATF3, KLF2/6, and ZFP36, a negative regulator of mRNA stability (Fig. 5 B). Most of the analyzed negative feedback regulators of transcription were peaking at 120 min of EGF in our time course. Examples include CREM, NAB2, FOSL1/2, JUND, and MAFF, many of which interfere with expression and activity of AP-1 and EGR transcription factors (chapter 2.4.).

Positive feedback loops acting on the input layer of the cascade include the very strong upregulation of AREG (Fig. 5 C) and strong induction of HBEGF as well as EREG (Fig. 5 C´), ligands of the EGFR (all peaking at 120 min EGF). The transcription of EGFR itself is slowly increasing upon EGF stimulation, with the maximum of induction at 360 min in our time course (same for the ERBB3 and ERBB4 ligand NRG1, Fig. 5 C´). The transcription of other EGF family ligands or ERBB receptors was not found to respond to EGF.

The well characterized inhibitor of EGFR kinase activity, MIG6 (or ERRFI1/RALT; chapter 2.6.1.) was strongly and maximally induced at 120 min EGF (Fig. 5 D). Transcription of another regulator of EGFR degradation (LRIG1) and modulators of downstream signaling events (the phosphatase PTPRE, Sprouty and SPRED proteins) was also found to peak between 120 and 360 min of EGF (Fig. 5 D´). In addition, multiple genes for SOCS proteins, regulating EGFR degradation and STAT-dependent signaling, are induced maximally between 30 and 120 min of stimulation (Fig. 5 E).

Importantly, almost all ERK-specific DUSPs or MKPs (chapter 2.6.1.) were found to be transcriptionally upregulated, particularly strong at 30 and 120 min EGF (Fig. 5 F). These include all nuclear MKPs of subfamily I (DUSP1, 2, 4, and 5), as well as the cytosolic DUSP6. DUSP10, dephosphorylating preferentially JNK and p38 MAPKs, was also induced by EGF.

Thus, the architecture, and perhaps also the robustness, of the EGF-mediated transcriptional program in our analysis is determined by a fine balance between feed-forward and attenuation mechanisms on several layers of the signaling network.

Fig. 5: EGF-induced transcription of genes known to regulate EGFR signaling.
Shown are data obtained by microarray analysis (Fig. 4) for the mock-treated samples, normalized to the 0 min time point. **A)** Examples of the classical AP-1 and EGR family transcription factors, whose transcription was strongly induced by EGF. **B)** EGF-induced expression of known transcriptional repressors. **C)** and **C´)** The transcription of four EGF ligands and the EGFR itself was induced by EGF. **D)** and **D´)** Induction of known feedback regulators of intracellular EGFR signaling. **E)** Transcription of several SOCS proteins induced by EGF. **F)** Multiple DUSPs are induced as a response to EGF stimulation.

Figure 5 - Results

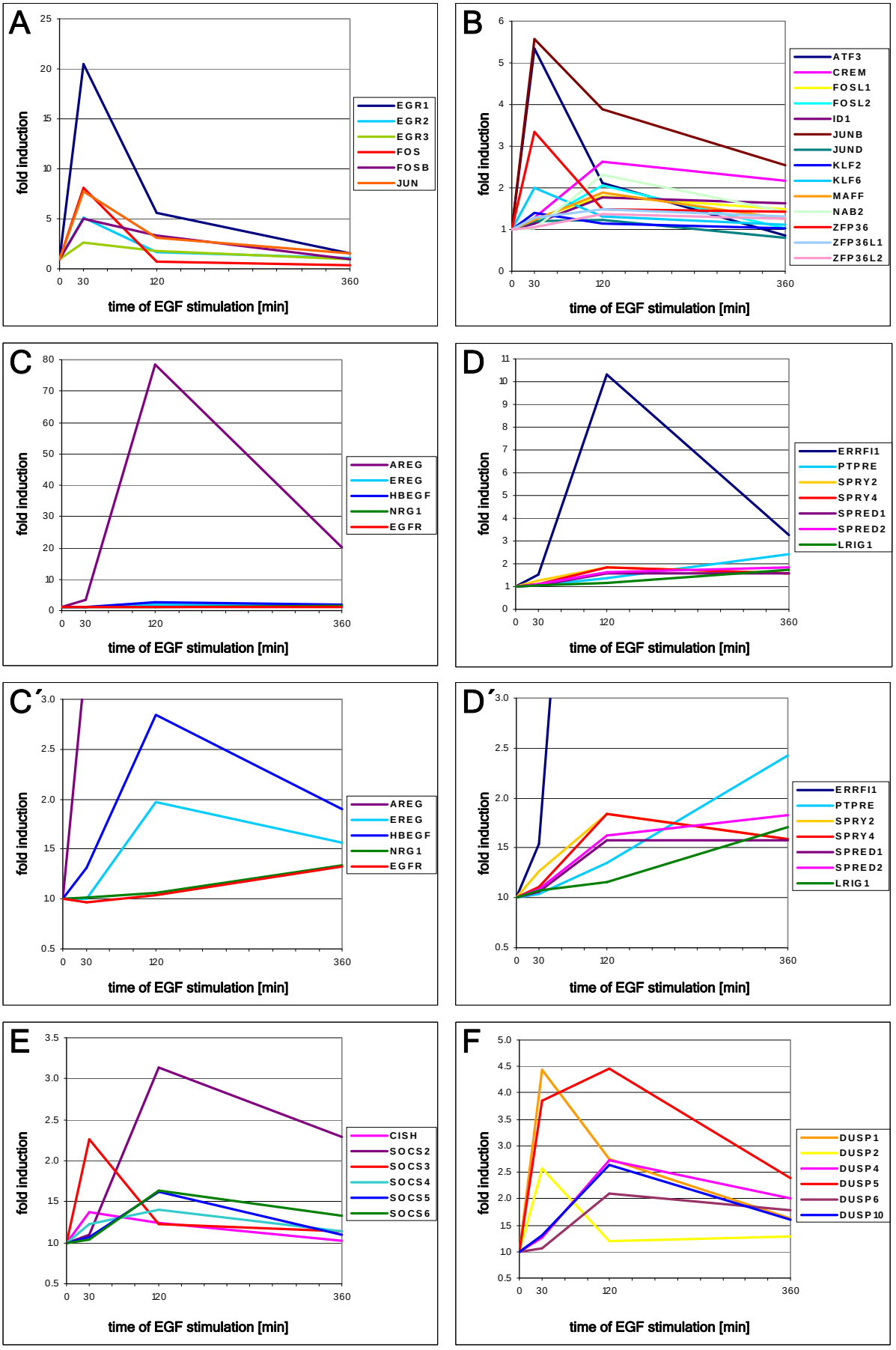

Before further investigation of KD effects, data validity and quality were verified by analyzing the same samples with NanoString, a novel technique that provides high sensitivity and broad dynamic range (chapter 4). Briefly, reporter probes carry unique fluorescent barcodes for each mRNA to be detected, and capture probes allow the complexes between mRNA, reporter and capture probe to be immobilized after hybridization. The complexes are aligned in an electrical field, and single molecule imaging by automated confocal microscopy detects and counts individual complexes without amplification steps. To date, mRNA levels of more than 500 genes can be analyzed in the same sample.

We selected 114 genes for probe design. These include 90 EGF-responsive genes identified in a previous study by Yosef Yarden´s group (discussed in chapter 2.4.), 12 genes whose products participate in signal transduction through the ERK MAPK cascade (ranging from the EGFR itself to the ELK1 transcription factor; chapter 2.2. to 2.3.), and genes for standardization and KD verification. In addition to the samples analyzed by microarrays, we also included the KD of another BRO1 domain-containing protein, HD-PTP, which was reported to control the degradation and signaling of the EGFR (chapter 2.6.1. and 3.2.2.). Depletion of HD-PTP, cell treatments, and RNA preparation was done in the same experiment parallel to the processing of the microarray samples.

The levels of mRNA depletion determined by NanoString were the same or higher (for VPS4A and ALIX KD, Fig. 4 C; HD-PTP mRNA was 20% of mock, not shown), perhaps due to the better dynamic range of the NanoString technique. In the heat map shown in Fig. 6 A, the architecture and magnitude of the transcriptional EGF response determined by microarray and NanoString analyses can be directly compared, since the values were normalized, grouped and ranked in the same way and plotted with the same scale (for details, see legend to Fig. 6). The overall pattern of the NanoString data was essentially identical to that measured in the microarrays, with less than 1% error (1 out of 107 genes displayed a different profile: ATF3 peaking at 120 min instead of 30 min). However, absolute values were often different, especially for very high or very low expression. In general, genes were found to be more induced when measured by NanoString, probably due to the higher dynamic range and better sensitivity of the technique (comparable to quantitative real-time PCR). Thus, for quantitative analysis, values from the NanoString measurement should be preferred, but the microarray data were validated in terms of general tendencies.

Fig. 6: Comparison of microarray and NanoString data and quality controls.
A) Heat map showing EGF-induced transcription determined by microarrays *vs.* NanoString (about 100 genes analyzed by both techniques). The normalization, grouping, and ranking were basically done as in Fig. 4 for the microarray data. Normalization is to mock 0 min (= 1 = 0 in Log2 = white) for both the microarray and NanoString data. But grouping and ranking of the genes were according to the mock time course of microarrays only (far left), to compare directly the architecture and magnitude of the EGF response between the microarrays and the NanoString data. **B)** Principal component analysis (PCA) of microarray data. Genes induced by EGF (Fig. 4 A) were analyzed with Partek; colorization is according to the time points of EGF treatment (0 min = red, 30 min = green, 120 min = blue, and 360 min = violet). **B´)** Same as in B), but triplicates of each condition are plotted with the same color. **C)** PCA of NanoString data (100 genes analyzed) as in B). **C´)** PCA of NanoString data, where triplicates are colored the same as in B´) for the microarrays.

Figure 6 - Results

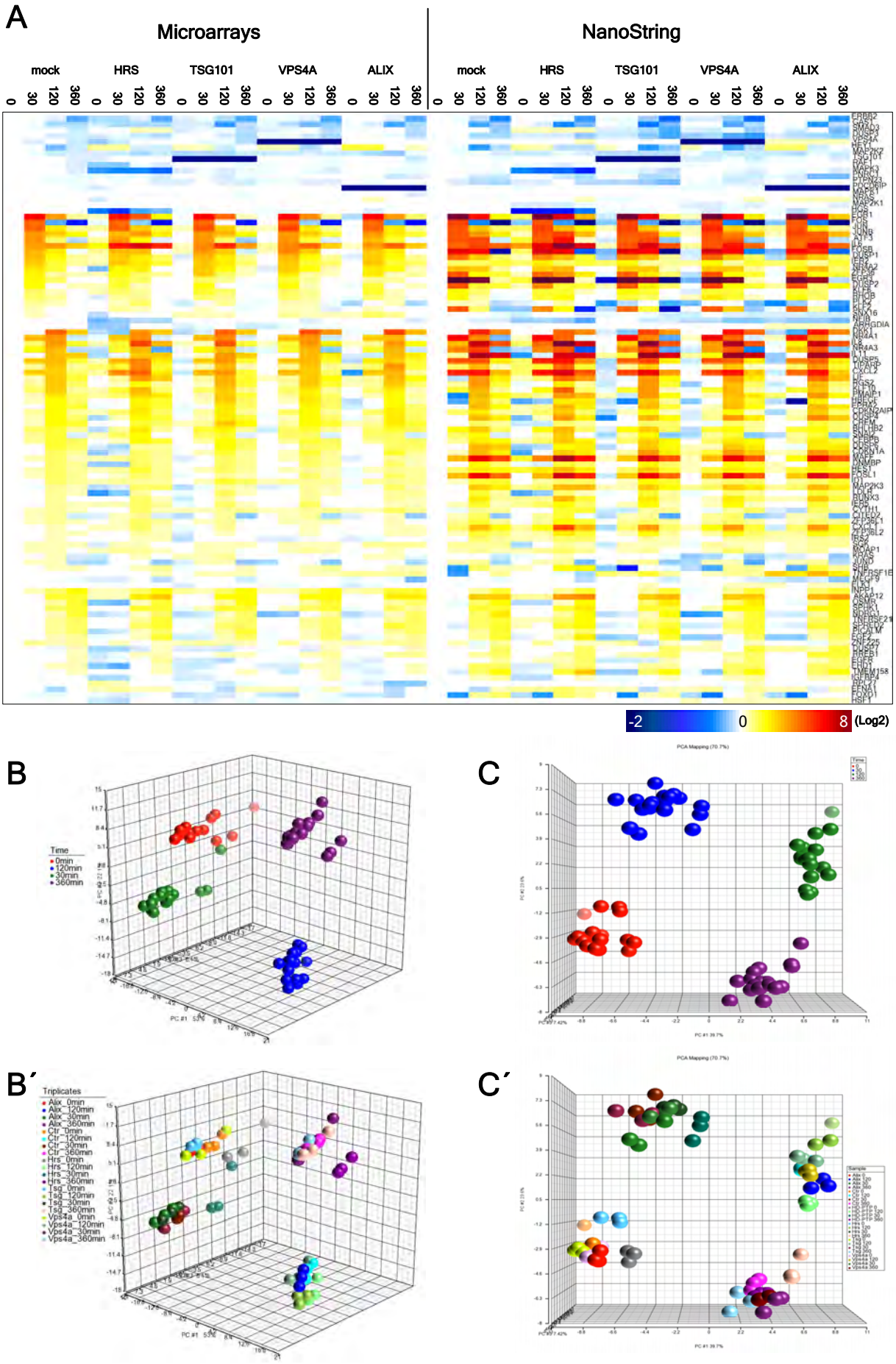

Principle component analysis (PCA, a mathematical procedure allowing to illustrate data variability) of the EGF-induced genes measured by microarrays (Fig. 4 A) revealed that genes affected at the same time of EGF stimulation cluster together (Fig. 6 B). Thus, the major source of variability in the data set originates from EGF stimulation, and not from the KD conditions. Rare outliers are HRS KD conditions. In Fig. 6 B´, the same analysis is color-coded for the triplicates, showing low variability of the replicates for each condition. Fig. 6 C and C´ show the PCA of the approximately 100 genes analyzed by NanoString, demonstrating again that major data variability arises from EGF and not KD conditions.

To better reveal possible changes in gene expression resulting from HRS, TSG101, VPS4A, or ALIX depletion, mRNA levels from the microarray data for each KD condition were normalized to the corresponding mock values at each time point (Fig. 7 A to C). Genes whose transcription was affected by more than 40% compared to mock were ranked according to the strength of the effect, and compared to their behavior in the other KD conditions (see legend to Fig. 7). Then, more significant changes in the levels of transcripts, compared to the other KDs, were indeed observed after depletion of HRS, although the KD seemed less efficient (Fig. 4 C). The relatively high number of genes affected by HRS depletion in unstimulated cells indicates that at least a part of the effects are EGF-independent (Fig. 7 A). But HRS KD was also the condition at 30 min EGF with the most effects (not shown). However, the majority of the observed effects was rather weak (see scale in Fig. 7 A), and relatively few genes were upregulated to more than 200% of the mock values. In addition, gene expression was not uniformly affected by depletion of different ESCRT subunits, although HRS, TSG101 and VPS4A operate together in receptor sorting into MVBs. At later time points of stimulation, the quantity of (probably EGF-dependent) effects becomes smaller, but a number of genes commonly and strongly affected can be observed, particularly between samples from HRS- and TSG101-depleted cells at 120 min EGF (see also Fig. 13).

When the effects of ESCRT protein depletion on transcription are compared between the microarray and the NanoString data, it becomes obvious again that the HRS KD has the most

Fig. 7: Magnitude and comparison of ESCRT KD effects between microarray and NanoString data.
A-C) The magnitude of ESCRT KD effects in the microarray analysis at three different time points is shown. Transcription values are normalized to the mock of each time point (white = 100%), and for effects of the individual KDs, the cut-off is 40% above or below mock. Tables with top KD effects (40 genes up- and downregulated in the corresponding KD condition at each time point) are included in the appendix. In **A)**, KD effects at time 0 (EGF-independent effects) are shown. The red-labeled letters (H for HRS KD on the far left) indicate the KD condition from which the affected genes were selected and ranked according to the strength of the effect. The columns below the black-labeled letters (T for TSG101 KD *etc.* on the far left) show how the genes affected by the HRS KD behave in the other KD conditions. The same is shown for each KD condition: after the genes affected by HRS KD, genes changed in TSG101, VPS4A, or ALIX KD (red letters in A) from left to right) are selected and ranked, and the behavior of the affected genes in the other conditions can be compared (black letters). In **B)**, genes affected by all four KDs can be compared to their transcriptional behavior in the other conditions at 120 min EGF stimulation, and in **C)** the same is shown for 360 min EGF. **D)** The heat map shows the magnitude of ESCRT KD effects in the microarrays compared to data obtained by NanoString for the 100 genes analyzed by both techniques. Again, values from each condition are normalized to the corresponding mock of the same time point (ratio of condition x min / mock x min). The mock time course appears white and was thus omitted.

Figure 7 - Results

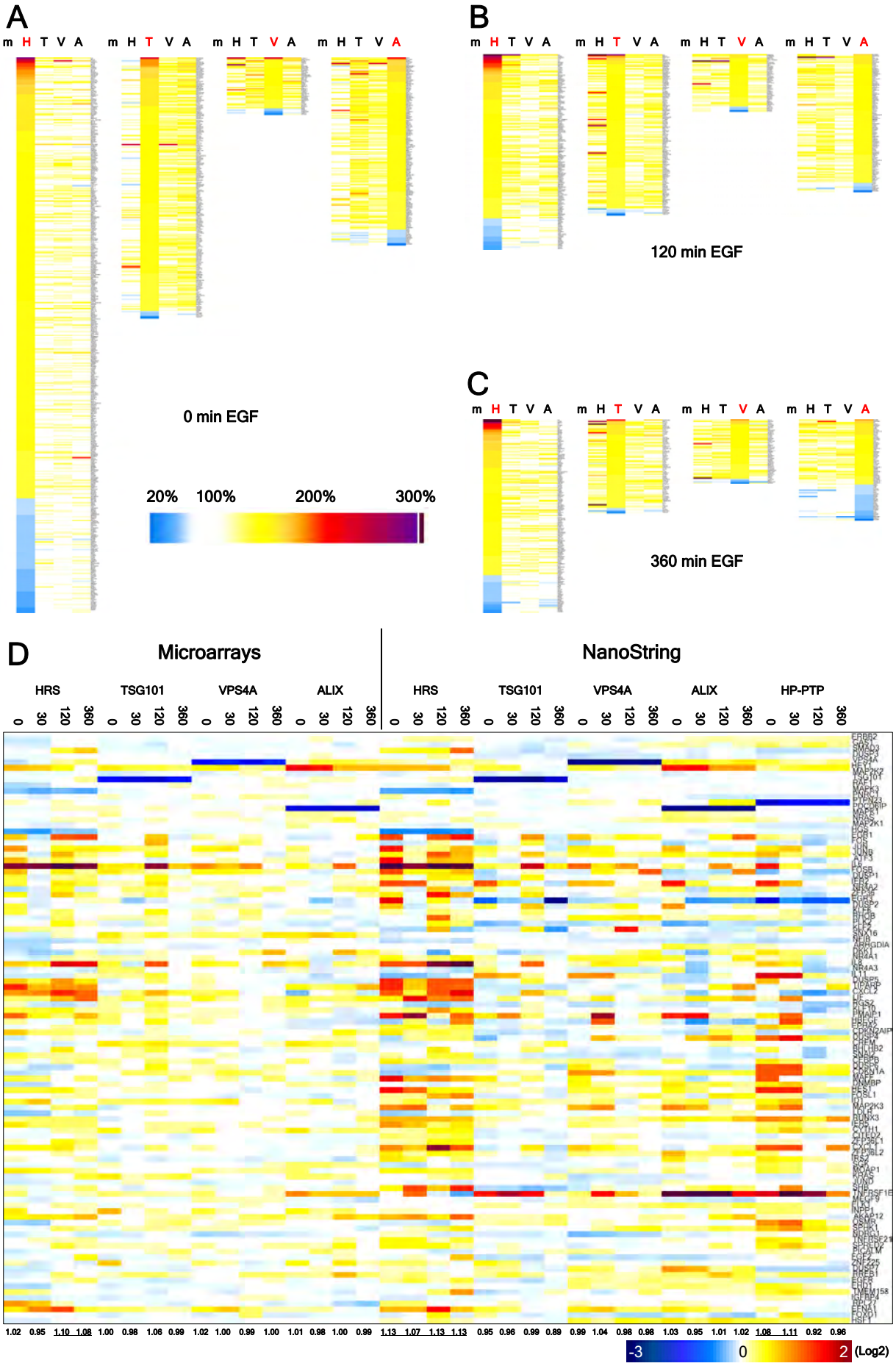

and the strongest effects (Fig. 7 D). Depletion of HD-PTP also has some impact at early time points, compared to TSG101, VPS4A, or ALIX KD. Data for the 100 genes analyzed by both techniques were normalized to the corresponding mock values at each time point, not the mock values for 0 min EGF only as in Fig. 6 A (but otherwise grouped and ranked as in Fig. 6 A; see legend). Despite higher absolute values of the effects in the NanoString analysis, the profiles are very similar to those obtained by the genome-wide transcriptional analysis, thus validating the microarray data. However, it should be pointed out again that the observed KD effects are rather subtle and do not indicate a general change in EGF-induced transcription.

3. EGFR degradation and signaling under different EGF stimulation conditions

Because of the discrepancy between the increased EGFR and MAPK phosphorylation in EGF-stimulated cells depleted of ESCRTs, and the lack of general effects on downstream transcriptional activation, we aimed to elucidate the influence of different stimulation conditions in more detail. First, the effect of cycloheximide was evaluated by western blot analysis of EGF-stimulated cells with a better time resolution. As shown in Fig. 8 A, the EGFR protein is re-synthesized, after initial degradation, starting at approximately 4-5 h of continuous stimulation with 100 ng/ml EGF in the absence of cycloheximide. However, the receptor is much faster dephosphorylated under these conditions, compared to EGF stimulation in the presence of the protein synthesis inhibitor. Apparently, re-synthesized EGFR can be activated at late time points of EGF stimulation, which was not the case when cycloheximide was used. Similarly, MEK1/2 and ERK1/2 are dephosphorylated faster but can be re-phosphorylated at later times of stimulation without cycloheximide (Fig. 8 A). We wondered whether this was due to the continuous presence of ligand, and performed the same experiment under (5 min EGF) pulse-chase conditions (Fig. 8 B). Phosphorylation of MEK and ERK appear the same as upon continuous stimulation, perhaps *via* the induction of autocrine feedback loops (Fig. 5 C). Despite of less pronounced EGFR degradation and strong re-synthesis of the protein without cycloheximide, phospho-EGFR signals are only

Fig. 8: EGFR degradation and signaling in different stimulation conditions.
A) Continuous stimulation with 100 ng/ml EGF was performed for the indicated time points, in the presence or absence of 10 µg/ml cycloheximide, and cells were harvested and prepared for immunoblot analysis to detect EGFR, and phosphorylated EGFR, MEK1/2, and ERK1/2. **B)** Same as in A), but instead of continuous stimulation, a 5 min EGF pulse (100 ng/ml) was followed by washes and a chase with EGF- and serum-free medium. Exposure times are the same in A) and B). In **C)**, continuous stimulation with "high EGF" (100 ng/ml) is compared to stimulation with "low EGF" (1.5 ng/ml) in the presence of cycloheximide for the indicated time points, in mock-treated *vs.* VPS4A KD cells. Signal detection was with the same exposure times between the two conditions. **D)** Luciferase activity in HLR-ELK1 cells stimulated with high (black) *vs.* low (red) EGF concentrations (n = 3 in duplicates). **E)** A second NanoString experiment was performed, where different EGF stimulation conditions were compared (see Fig. 10 for additional conditions tested, and Fig. 11 for quality controls). The transcriptional EGF response is shown for high *vs.* low *vs.* pulse-chase (p-ch, as in B) EGF-stimulated cells (without cycloheximide). Data are normalized, grouped and ranked as in Fig. 4 and 6, and the 0 min normalization time point (white) was omitted. **F)** Effects of the different stimulation conditions on EGF-induced transcription measured by NanoString. Here, the data normalization was to the corresponding time point of the 100 ng/ml continuous EGF stimulation (ratio of condition x min / high EGF x min; high EGF values are 1 = white), to analyze differences between the standard stimulation condition and low or pulse-chase stimulation.

Figure 8 - Results

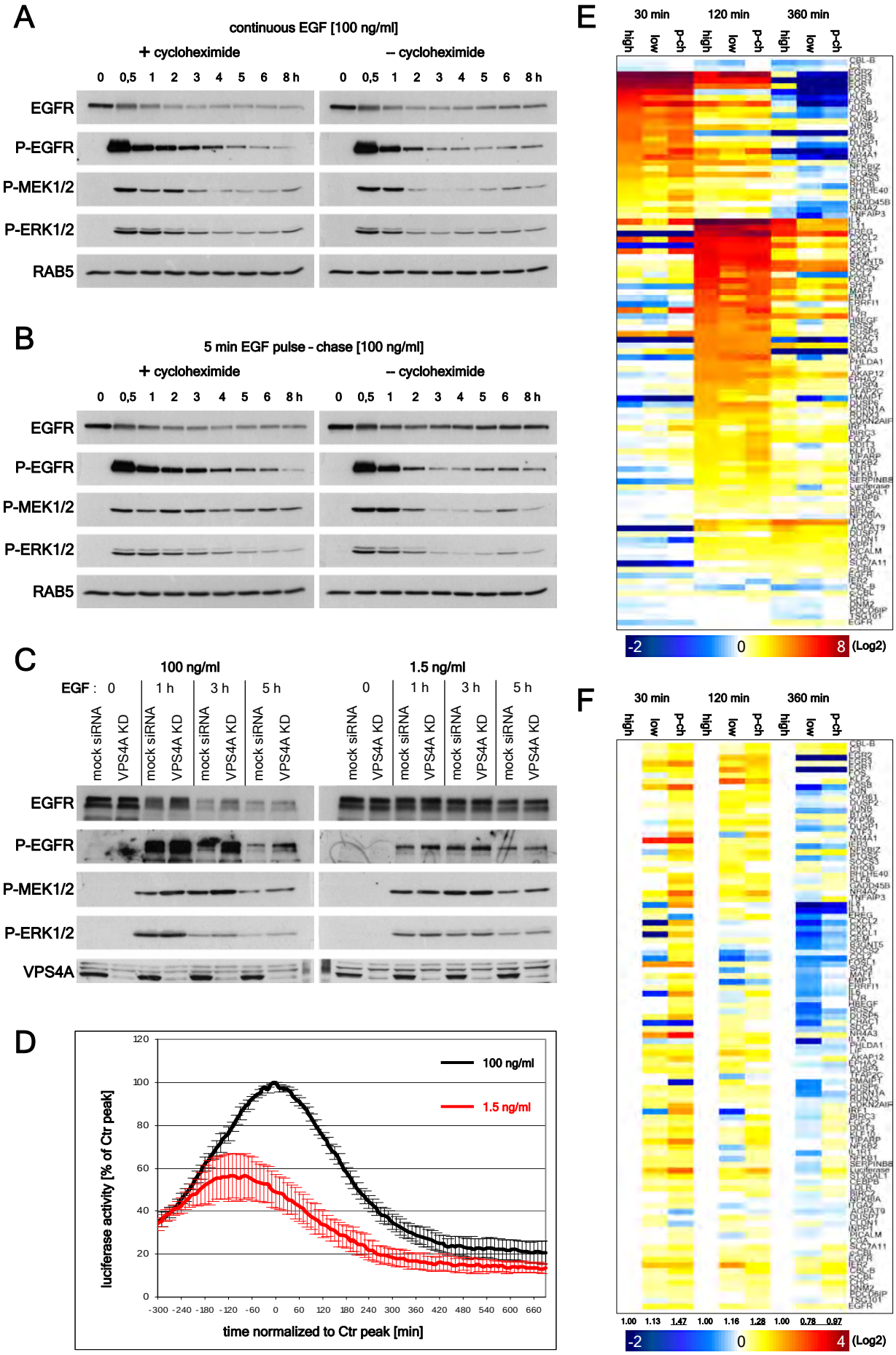

slightly elevated at 5-6 h of EGF treatment. In the presence of cycloheximide, the kinetics of EGFR degradation and phosphorylation, as well as of ERK phosphorylation, look similar between continuous and pulse-chase stimulation conditions (only MEK phosphorylation is enhanced at late time points of pulse-chase stimulation). Thus, the stimulation condition (continuous *vs.* pulse-chase) seems to affect only the levels of EGFR, but has a rather mild impact on the activation status of the cascade. Inhibiting protein synthesis during EGF stimulation, on the other hand, extends the duration of EGFR, MEK and ERK phosphorylation significantly, probably due to the inhibition of negative feedback loops (chapter 2.4. and 2.6.1.; Fig. 5). It should also be noted that despite of re-activation of the cytosolic signal transduction components in the absence of cycloheximide, transcription does not seem to become upregulated again for example at 6 h of EGF stimulation in the luciferase signaling assay or in the microarray analysis.

Next, we compared the EGFR degradation and downstream phosphorylation events in cells stimulated with 100 ng/ml ("high EGF") *vs.* 1.5 ng/ml ("low EGF"). In the preliminary western blot analysis shown in Fig. 8 C (comparing also mock-treated with VPS4A-depleted cells in the presence of cycloheximide), it becomes apparent that the half-life of EGFR is much longer when cells are stimulated with low EGF than under high EGF stimulation conditions, in agreement with previous observations (chapter 3.2.4.). However, the receptor phosphorylation level is significantly lower at 1 and 3 h of stimulation with 1.5 ng/ml EGF, compared to our standard stimulation condition. MEK1/2 activation seems comparable between high and low EGF stimulation, but phospho-ERK1/2 signals are again decreased at 1 h of stimulation with low EGF. In the ELK1-driven reporter signaling assay, low EGF also leads to decreased and shorter induction of luciferase expression than upon high EGF stimulation (Fig. 8 D), in contrast to observations by Sigismund *et al.* (chapter 3.2.4.). Thus, increased levels of EGFR during a stimulation time course with low EGF do not necessarily correlate with prolonged receptor activity and upregulation of downstream signaling.

In order to investigate the impact of different stimulation conditions on the transcriptional induction of endogenous target genes comprehensively, we designed another NanoString experiment (other conditions tested in parallel and quality controls will be presented below in part 4). Probes for 50 genes were in common between the first and the second experiment to compare the EGF response (Fig. 11 C). 40 novel genes, selected from our microarray data, were included in the analysis, and 10 genes for standardization and KD verification.

To illustrate the EGF response, data were normalized to values from unstimulated cells (Fig. 8 E); to visualize possible effects of different stimulation conditions, normalization was to values from the standard ("high") EGF stimulation for each time point (Fig. 8 F). Grouping and ranking of genes was done as in Fig 4 and 6. The analysis of transcripts from cells stimulated with high EGF, low EGF, or (5 min high EGF) pulse-chase conditions revealed little difference

in the architecture of the response (Fig. 8 E). Differences between the stimulation conditions become better visible in Fig. 8 F, where particularly upon stimulation with low EGF the response is ceasing faster. However, pulse-chase stimulation appears to increase the early events of transcriptional induction, for the 30 min EGF time point on average 1.5-fold above the continuous stimulation condition. Taken together, while low EGF stimulation does not increase the transcriptional response as proposed by Sigismund *et al.*, pulse-chase stimulation may have some effects at early times of stimulation.

4. EGF signaling upon interference with EGFR internalization and ubiquitination

Since ESCRT-mediated endosomal sorting of the EGFR does not regulate the transcriptional response to EGF globally, we asked whether interfering with upstream events of EGFR trafficking might lead to stronger and more general effects on signaling. To this end, we depleted cells of clathrin heavy chain (CHC) and dynamin 2 (DNM2) proteins, involved in EGF-induced internalization of the receptor (chapter 3.2.1. and 3.2.4.). In addition, cells were simultaneously depleted of CBL and CBLB, which were shown to cooperate in stimulus-dependent EGFR ubiquitination and degradative sorting (chapter 3.2.1.).

Luciferase activity in our reporter assay was significantly upregulated in CHC or DNM2 KD cells, compared to mock treatment (Fig. 9 A). Simultaneous depletion of the two proteins did not lead to an additive effect, indicating that under our conditions the same pathway of internalization was affected. Protein levels were efficiently downmodulated, as shown in Fig. 9 C (the DNM2-antibody recognizes two bands of which the upper one is unspecific; KD of the lower band is better visible in Fig. 12 A). Double KD of CBL and CBLB also increased ELK1-driven luciferase expression to an extend similar to that observed upon CHC and DNM2 depletion (Fig. 9 B). Simultaneous KD of ALIX and TSG101, in order to interfere with both ESCRT- and LBPA-mediated ILV formation (chapter 3.1.5. and 3.2.3.), did not cause any such effect, despite high efficiency of protein depletion (Fig. 9 C).

EGFR degradation upon EGF stimulation was delayed in both CHC-DNM2 (Fig. 9 D) and CBL-CBLB (Fig. 9 E) double KD cells, particularly in the presence of cycloheximide, although receptor degradation could not be blocked completely (as for ESCRT KDs in Fig. 3 C). Both double KD conditions led to increased phosphorylation of EGFR, MEK, and ERK during the stimulation time course compared to mock, with the strongest effect in CBL-CBLB-depleted

Fig. 9: EGF-induced signaling in cells depleted for various proteins involved in EGFR endocytic trafficking.
A) Signaling assay with HLR-ELK1 cells depleted for CHC (yellow; n = 7), DNM2 (red; n = 7), or both (orange; n = 2), compared to mock-treated cells (black). **B)** Luciferase activity in CBL and CBLB double KD cells (green; n = 6), compared to mock-treated (black) or ALIX and TSG101 double KD cells (blue; n = 3), under standard high EGF continuous stimulation conditions. **C)** Verification of KD efficiencies by western blot: CHC and DNM2 double KD, CBL and CBLB double KD, ALIX and TSG101 double KD (from left to right). EGFR degradation and EGFR, MEK1/2, and ERK1/2 phosphorylation in CHC and DNM2 double KD cells **(D)**, or CBL and CBLB double KD cells **(E)**, compared to mock, in the presence (as in Fig. 3) or absence of 10 µg/ml cycloheximide for the indicated times of EGF stimulation. **F)** EGF stimulation time course and EGFR degradation as well as phosphorylation of signaling components in GFP vs. GFP-EGFR expressing cells, analyzed by western blot.

Figure 9 - Results

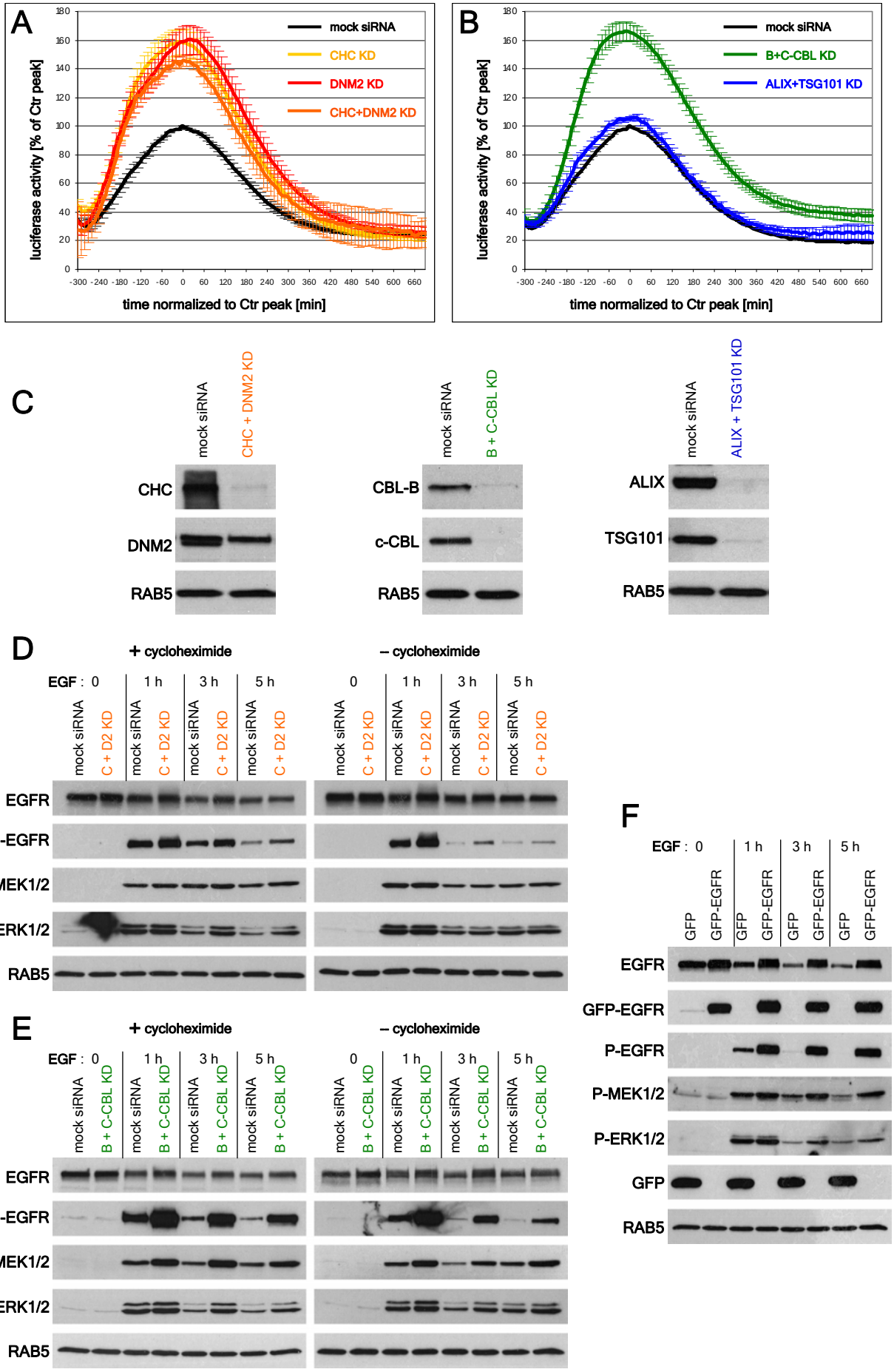

cells (Fig. 9 E). These effects did not depend on the presence of cycloheximide, but for example differences in ERK activation can be less pronounced when cycloheximide is omitted (Fig. 9 D, right). For comparison, EGF stimulation in time was also performed with cells overexpressing the receptor, leading to strong upregulation of luciferase induction in our signaling assay (Fig. 2 C). GFP-EGFR is poorly degraded and highly active even at the longest time point after EGF addition (Fig. 9 F). Phospho-MEK and phospho-ERK signals are also increased, but "only" to an extend similar to the effect of the double KDs, suggesting that levels of active signaling components in the ERK cascade are not directly proportional to each other. In summary, interfering with receptor internalization and ubiquitination, or EGFR overexpression, increases both the activation state of signal transducing proteins and downstream transcriptional induction of the luciferase reporter.

Conditions for measuring EGF-regulated transcription of endogenous target genes in the second NanoString analysis included the above mentioned double KDs (CHC and DNM2, CBL and CBLB, ALIX and TSG101), EGFR overexpression, as well as a PMA stimulation time course, to clarify if and how far the endogenous response can be elevated. The heat map in Fig. 10 A illustrates the EGF response under these conditions (data were normalized to the corresponding 0 min values; see legend for details). At first glance, the overall structure of transcription seems preserved in all conditions except for PMA-stimulated samples: at 120 and 360 min of PMA stimulation, a more or less global boost and shift (both higher and longer transcriptional activity) of the response can be observed, in agreement with the very strong upregulation of luciferase expression in the signaling assay (Fig. 2 D). Data in Fig. 10 B were normalized to the corresponding control values for each time point, to visualize effects of the various conditions compared to the control time course. The general impact of PMA treatment becomes obvious again, showing a general elevation and delay compared to the normal EGF-induced transcription. In addition, the CBL-CBLB and CHC-DNM2 double KDs also lead to a significant upregulation of many, but not all genes in the response. Strikingly, the pattern of affected genes is very similar to effects in EGFR-overexpressing samples (Fig. 10 B, right). ALIX and TSG101 double KD cells display an increase in transcription of some

---

Fig. 10: Transcriptional response in various KD and EGFR-overexpressing cells stimulated with EGF, and upon PMA stimulation, measured by NanoString.
A) Conditions selected for the second NanoString analysis included (10 ng/ml) PMA stimulation, ALIX and TSG101 (A + T), CBLB and CBL (B + C), CHC and DNM2 (C + D2) double KDs, and GFP-EGFR-overexpressing cells (from left to right), compared to (100 ng/ml continuous) EGF-stimulated cells only (Ctr). Values of mRNA transcription were normalized to the corresponding 0 min time points, which are then equal 1 (white) and were omitted. Grouping and ranking of the genes was done as in Fig. 4 and 6 according to the values of the Ctr time course, to illustrate the EGF response comparably. **B)** To visualize effects of the above mentioned conditions compared to Ctr (no other treatment than overnight serum deprivation and subsequent EGF stimulation), the data were normalized to each of the corresponding Ctr time points. **C)** Magnitude of effects of all conditions tested in the first and second NanoString measurements (50 genes were in common between the two analyses; see also Fig. 11 C). Basically, values from the heat maps shown in Fig. 7 D) (right side) for the first NanoString, for low EGF and pulse-chase (p-ch.) stimulation from Fig. 8 F), and from the above heat map 10 B) for PMA, double KDs, and EGFR overexpression, were combined and illustrated using the same scale. The strength of effects can thereby be directly compared. The grouping and ranking of genes was done as in Fig. 11 C).

Figure 10 - Results

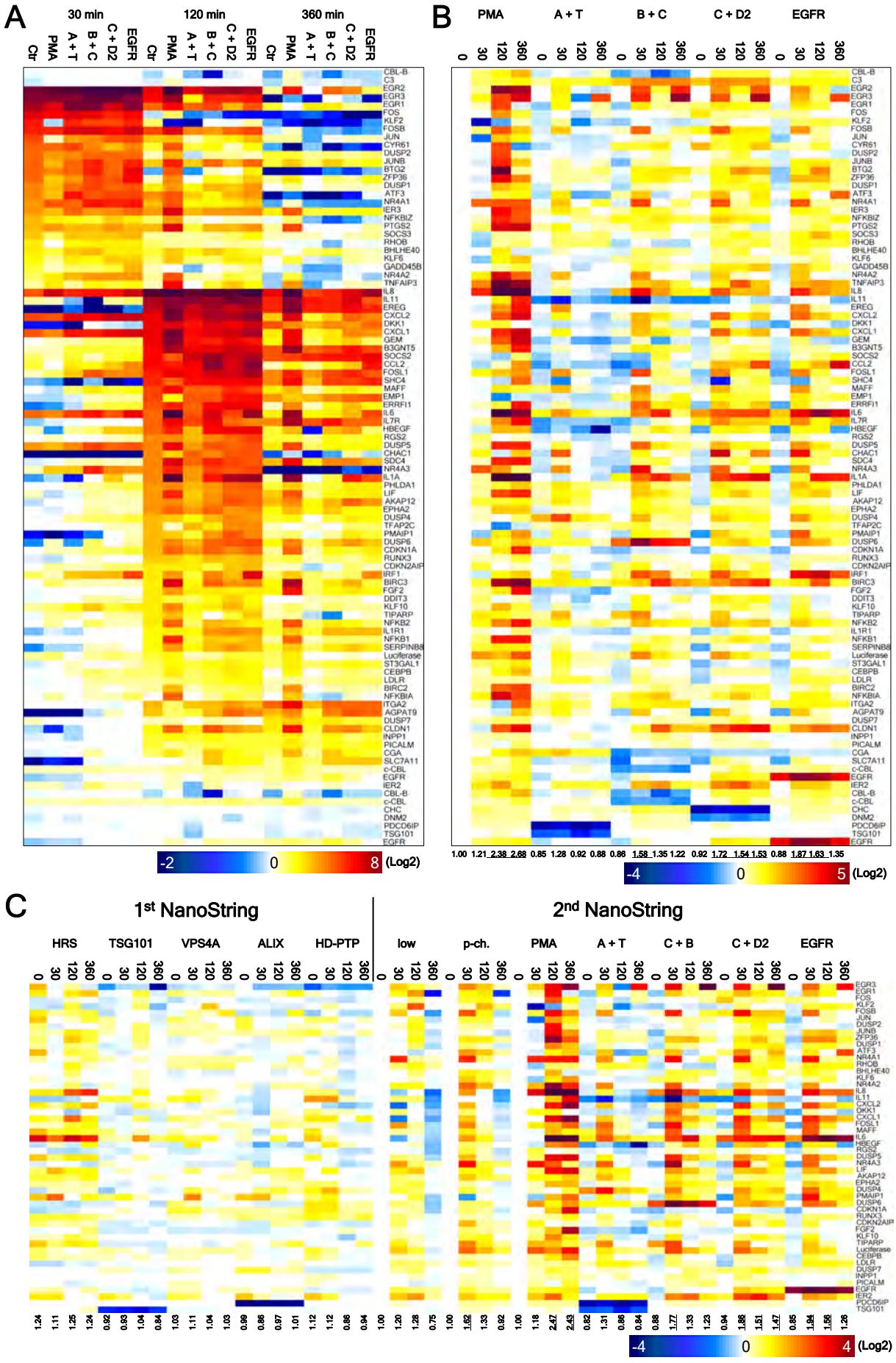

genes at 30 min of EGF stimulation, but the magnitude of effects is rather low and the majority of genes is expressed similarly to controls. Taken together, genes induced by EGF can be globally upregulated, as demonstrated by PMA treatment. Interference with receptor internalization or ubiquitination leads to significant (albeit not general) increase in EGF-mediated transcriptional activity, and the observed effects are reminiscent of those observed upon EGFR overexpression, arguing for specific interference with EGFR sorting.

The heat map in Fig. 10 C allows for a direct comparison of the magnitude of effects between all conditions analyzed by the NanoString technology. On the left, effects of ESCRT, ALIX and HD-PTP KDs from Fig. 7 D (part 2) are shown, effects of different stimulation conditions from Fig. 8 F (part 3) are included in the middle, and on the right, the impact of PMA stimulation, double KDs, and of EGFR overexpression (Fig. 10 B) is illustrated. All values for the 50 genes analyzed in both NanoString measurements are expressed using the same scale and are thus directly comparable. Clearly, PMA treatment has the most potent effect on the transcriptional activity downstream of ERK (although stimulation of other pathways probably contributes to the response). As mentioned above, the CBL-CBLB and CHC-DNM2 double KDs upregulate many genes of the response, clustering together with effects of EGFR overexpression. ALIX-TSG101 double KD and pulse-chase stimulation with EGF have some impact on the transcription of early genes, and depletion of HRS has the relatively strongest impact in the first NanoString experiment, although the magnitude of the effects is rather low compared to conditions analyzed in the second NanoString approach.

Quality control of the data from the second NanoString measurements by PCA demonstrates very low variability within triplicates of each condition and time point of stimulation (Fig. 11 A). By coloring all conditions at each time point the same (Fig. 11 B), it becomes obvious that the major source of variability is the addition of EGF over time (as in Fig. 6 B and C). However, overlay with Fig. 11 B´, where each condition has the same color independent of the time point, reveals that outliers at 120 and 360 min correspond to PMA-stimulated samples (red circles), and that CBL-CBLB and CHC-DNM2 double KD samples cluster away from other conditions but together with EGFR-overexpressing conditions (green circles). Thus, major impacts of the conditions with the strongest effects can be seen already in the PCA.

Fig. 11: Quality controls for the second NanoString experiment and comparison to the first data set.
A to B´) PCA of the second NanoString experiment. In **A)**, triplicates are labeled with the same color; in **B)** all conditions at the same time of EGF stimulation have the same color (0 min = red, 30 min = blue, 120 min = green, and 360 min = violet); and in **B´)** each condition (KDs, EGFR overexpression, and different stimulation conditions) are color-coded the same way. **C)** Heat map showing the comparison of the EGF response between the first and second NanoString experiment in the mock / control samples (100 ng/ml EGF), and mRNA levels of the second controls measured also with the first NanoString code set (CS). The values are normalized to the corresponding control 0 min of each measurement (all white, therefore no data for 0 min is shown). The grouping (peak of transcription) and ranking (decreasing strength of induction) is done as in Fig. 4 and 6, here according to the values of the second controls obtained with the second CS (left lanes at each time point). In the middle lanes of each time point, the second control samples were probed with the first CS (used in experiments shown in Fig. 6 and 7). And for comparison, data from the first experiment are plotted on the right side of each time point.

Figure 11 - Results

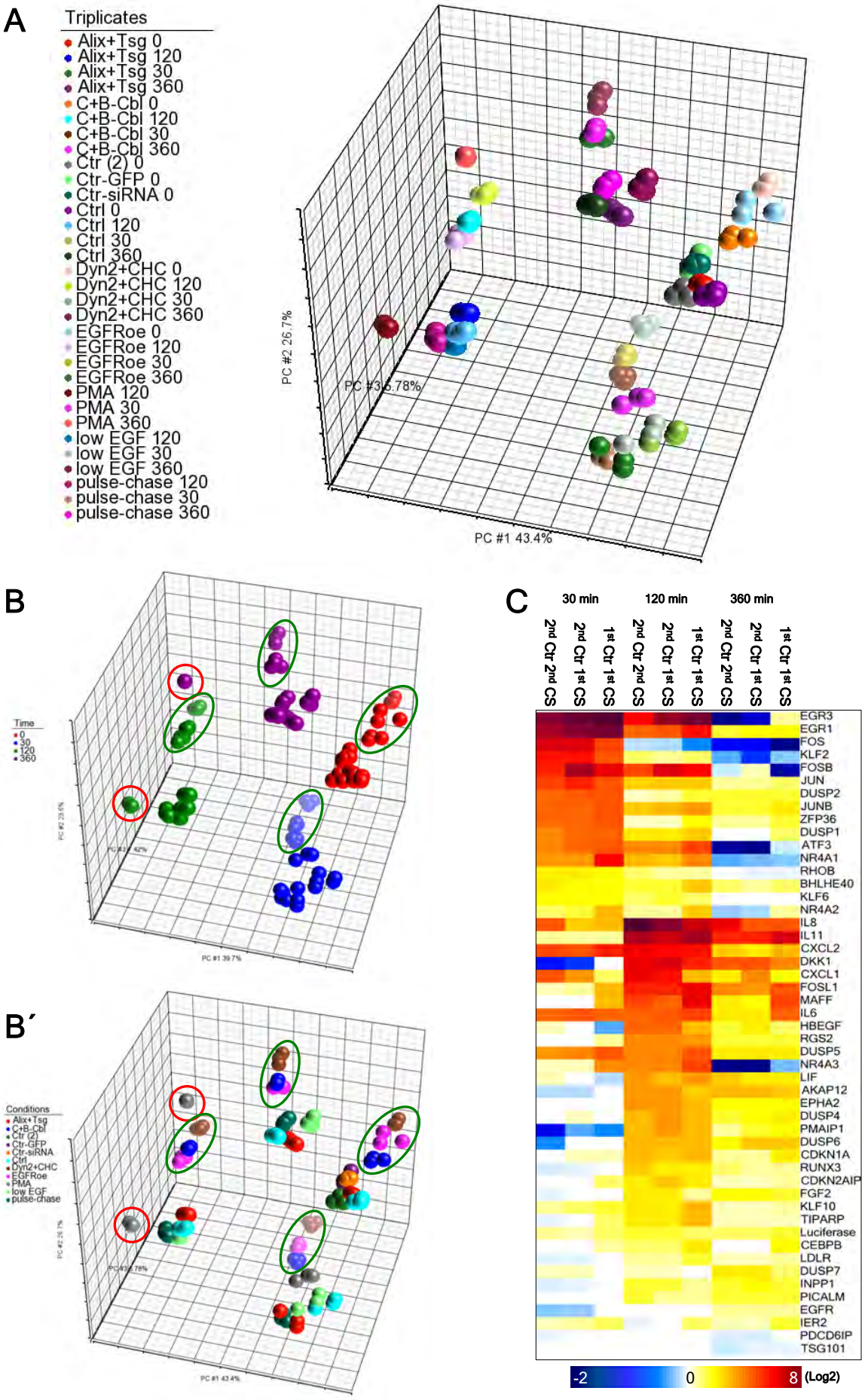

The heat map in Fig. 11 C enables the direct comparison of the EGF response in the mock / control of the first and second NanoString analysis. In addition, mRNA quantities from the second experiment were measured with both code sets (sets of capture and reporter probes), to check for possible differences in hybridization efficiencies. In general, the EGF response was very similar between the two experiments, with some differences concerning absolute values of gene induction but very few changes in the kinetics of transcription. Detailed analysis revealed that the code set had virtually no impact: both kinetics and values of mRNA transcription in the second experiment measured with both code sets were identical, with FOSB as an exception (apparently much stronger induction when measured with the first code set, but this was due to normalization to the very low 0 min values, where a small difference has a large impact on the later time points). More importantly, when both control data sets were measured with the same (the first) code set, only 3 out of 107 genes display significantly different expression kinetics (e.g. peak at 30 min instead of 120 min). Therefore, despite some differences in the absolute values, the kinetics and architecture of the EGF response between the two experiments are well preserved and reproducible.

RNA and protein depletion efficiencies are shown in Fig. 12 . The levels of CHC, DNM2 (Fig. 12 A), ALIX, and TSG101 (Fig. 12 C) mRNAs are reduced to 10-20% of mock, protein depletion is almost complete. CBL and CBLB proteins and mRNAs are less well depleted (60-70% mRNA reduction compared to mock in Fig. 12 B), but higher KD efficiency was toxic (so was increased DNM2 KD). Note that CBLB mRNA seems to be downregulated during EGF treatment, but CBL transcription seems induced by EGF. EGFR mRNA increased about 8-fold upon ectopic expression, but protein overexpression was less pronounced (Fig. 12 D).

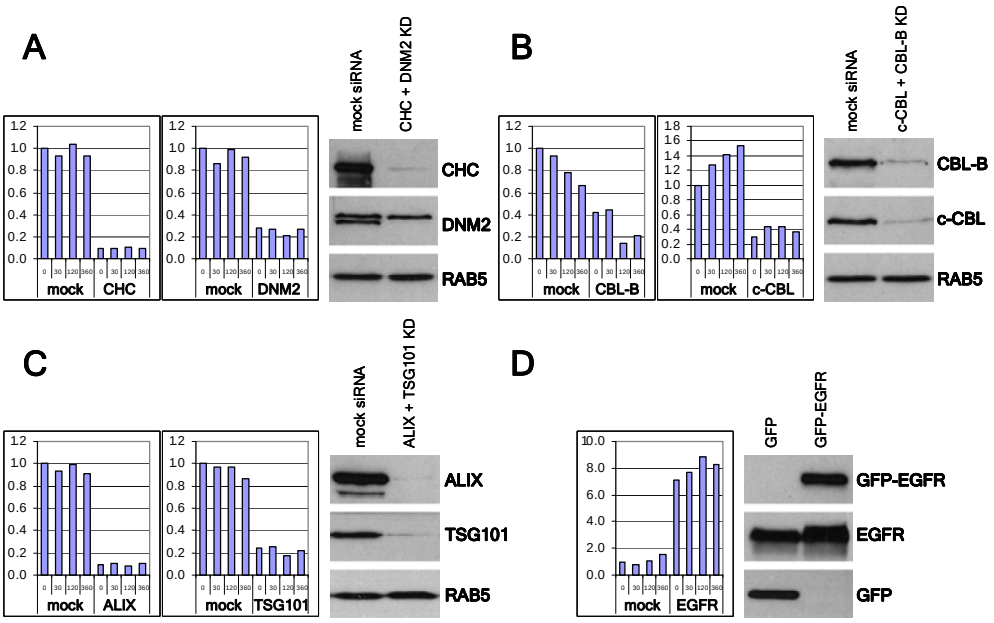

Fig. 12: Verification of double KDs and EGFR overexpression in the second NanoString analysis.
mRNA levels from NanoString data were normalized to mock 0 min (left), and KD of the corresponding proteins were verified by western blot (right), compared to the corresponding mock-treated samples. **A)** CHC and DNM2 double KD; **B)** CBL and CBLB double KD; **C)** ALIX and TSG101 double KD; and **D)** EGFR overexpression.

5. Outlook: specific effects of HRS and TSG101 depletion, and late EGFR activity

In contrast to the dogma of ESCRT function in sequestering the active EGFR into endosomes, thereby uncoupling the receptor kinase from its cytosolic effectors and thus terminating endosomal EGFR signaling, we found no evidence for a general role of ESCRT subunits or accessory proteins in regulating EGF-induced transcriptional responses (part 2, Fig. 3 and 4). Observed effects of ESCRT depletion were not global, rather weak in their intensity, and often not the same between individual KDs (Fig. 7). However, in the microarray analysis we observed a number of genes whose expression was significantly affected at late time points, particularly upon HRS and TSG101 depletion at 120 min of EGF stimulation.

To gain insight into these commonly affected genes and their connection to each other, we performed pathway analysis using the Ingenuity IPA software in an unbiased fashion. A gene list, containing effects of both HRS and TSG101 depletion at 120 min EGF, was used as the basis for pathway or network computation by the software. The most significant network identified by this approach is shown in Fig. 13). It contains many genes involved in NF-kappa-B and cytokine signaling: NFKB (nuclear factor of kappa light polypeptide gene enhancer in B-cells) 1 and 2, NFKBIA (nuclear factor of kappa light polypeptide gene enhancer in B-cells inhibitor, alpha; or I-kappa-B-alpha), TNFAIP3 (tumor necrosis factor, alpha-induced protein 3), BIRC3 (baculoviral IAP repeat-containing 3), IL6 (interleukin 6), PTGS2 (prostaglandin-endoperoxide synthase 2, or cyclooxygenase 2), and CCL2 (chemokine (C-C motif) ligand 2). The network illustrated in Fig. 13 displays expression bar charts next to the gene symbol to visualize the effect over the time of EGF stimulation, and values for the fold-difference at 120 min compared to mock (in Fig. 13 A for the HRS KD, in Fig. 13 B for the TSG101 KD). Manual analysis uncovered more genes involved in NF-kappa-B and cytokine signaling which were transcriptionally affected by both KDs: IL8, CXCL2 (chemokine (C-X-C motif) ligand 2), ZFAND5 (zinc finger, AN1-type domain 5), and IRF1 (interferon regulatory factor). Genes regulating NF-kappa-B signaling which were only affected upon HRS depletion were: NFKBIE (nuclear factor of kappa light polypeptide gene enhancer in B-cells inhibitor, epsilon; or I-kappa-B-epsilon), REL and RELB (v-rel reticuloendotheliosis viral oncogene homolog (B)), as well as RHEBL1 (RAS homolog enriched in brain-like 1). The impact of HRS depletion on the expression of those genes was more pronounced than upon TSG101 KD, as HRS had more and stronger effects in general.

Fig. 13: Pathway or network analysis with Ingenuity IPA software of HRS and TSG101 effects at 120 min EGF from microarray data.
With the GeneSpring GX software (Agilent), a list of genes which were commonly affected by HRS and TSG101 KD, compared to mock, was generated and imported into Ingenuity. Shown is an unbiased, automatically modeled network for this comparison at 120 min of EGF stimulation. In **A)**, values for the HRS KD are shown (fold difference compared to mock 120 min), in **B)** values for Tsg101 KD effects. An expression bar chart (next to the symbol of each gene whose transcription was affected) shows the tendency of the KD effects over the four time points (red: up, blue: down). Pathway components without associated bar chart and values were added by the software to the network. Connecting lines represent various types of interactions based on data from the literature.

Figure 13 - Results

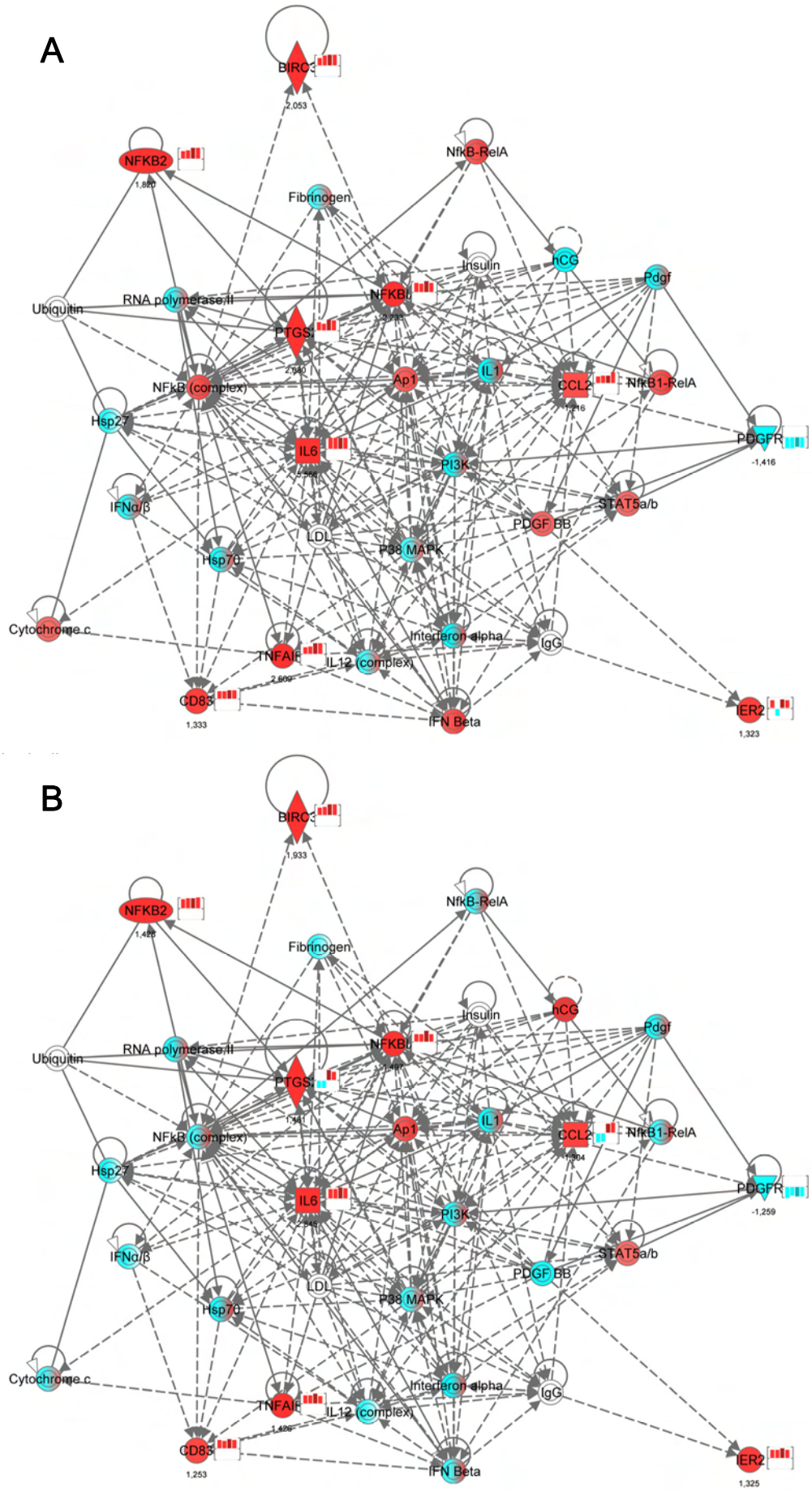

Hence, while depletion of the ESCRT subunits HRS and TSG101 has no overall influence on EGFR signaling, their KD may specifically affect NF-kappa-B and cytokine signaling. However, this observation is difficult to explain and needs to be further characterized.

Another interesting observation was made in experiments where the EGFR inhibitor AG1478 (Fig. 2 A) was added at different times of continuous EGF stimulation. Cells were subjected to EGF for up to 3 h, and then for another 15 min in the absence or presence of the inhibitor. Surprisingly, even at the 3 h time point when the majority of the receptor is degraded or supposed to be trapped within late endosomes, the inhibitor still completely abolishes phosphorylation of MEK and ERK (Fig. 14 A, right). The inhibition was specific for the EGFR kinase, because MEK and ERK kinases were only minimally affected by AG1478 in PMA-stimulated cells (induces the MAPK cascade *via* PKC, circumventing the EGFR).

Luciferase induction in our signaling assay could also be blocked efficiently by adding the inhibitor at late times after initial EGFR stimulation. Cells were pre-stimulated for up to 3 h, and then assayed for luciferase activity in the presence or absence of AG1478 (Fig. 14 B). Even at the latest time point of pre-incubation, the inhibitor leads to an immediate downregulation of luciferase expression, which was not the case when cells were stimulated with PMA (Fig. 14 B´). Thus, for full MEK-ERK phosphorylation and transcriptional induction of the reporter, EGFR kinase activity seems to be required for up to 3 h during stimulation.

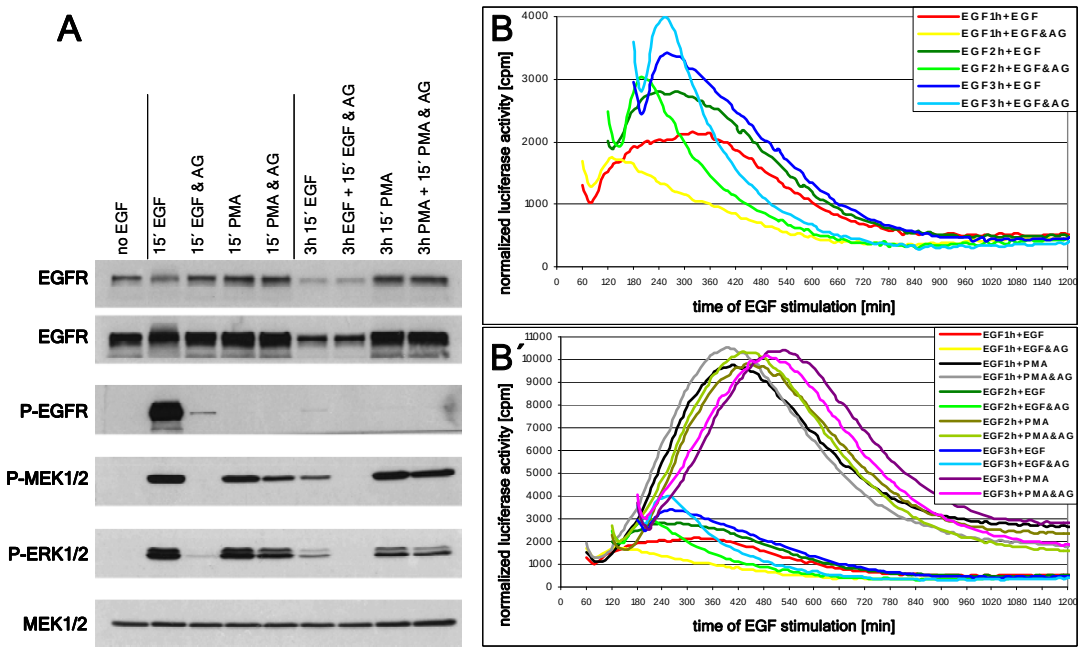

Fig. 14: Late requirement for EGFR activity.
A) Western blot analysis of the EGFR and phosphorylation status of signaling components upon EGF or PMA stimulation, in the presence or absence of the EGFR kinase inhibitor AG1478. Cells were stimulated for 15 min with EGF or PMA, in the absence or presence of the inhibitor. On the right side, cells were stimulated for 3 h with EGF or PMA, and for another 15 min in the absence or presence of AG1478. **B)** Luciferase activity of HLR-ELK1 cells, pre-stimulated for 1, 2, or 3 h with EGF, and subsequently stimulated with EGF in the absence or presence of AG1478. **B´)** In parallel, the cells were subsequently stimulated with PMA in the absence or presence of AG1478. The experiment was done only once, but repeated under EGF pulse-chase stimulation conditions, with the same effect of the EGFR kinase inhibitor (not shown).

Discussion

The EGF-induced removal of the EGFR from the plasma membrane and its endocytic downregulation is a major negative feedback mechanism controlling the intensity and duration of receptor signaling (Carpenter and Cohen, 1976; Wells et al., 1990; Wiley et al., 1991). Different mechanisms of ligand-accelerated endocytosis (Doherty and McMahon, 2009; Mayor and Pagano, 2007; Sorkin and Goh, 2008), rapid ubiquitination of activated EGFR by the ubiquitin ligase CBL (Galcheva-Gargova et al., 1995; Levkowitz et al., 1998; Schmidt and Dikic, 2005), and ESCRT-mediated sorting of the ubiquitinated receptor into MVBs for lysosomal degradation (Hurley and Hanson, 2010; Raiborg and Stenmark, 2009; Williams and Urbe, 2007), are the underlying principles of EGFR downregulation (Fig. I), introduced mainly in chapter 3.1.4 and 3.2.1. This complex cascade of events not only leads to physical degradation of the receptor and desensitization, protecting the cell from excessive stimulation, but is also assumed to turn off intracellular EGFR activity, as discussed in chapter 3.2.4. In this study, we aimed to dissect the precise contribution of endocytic sorting events to the EGF-induced transcriptional response.

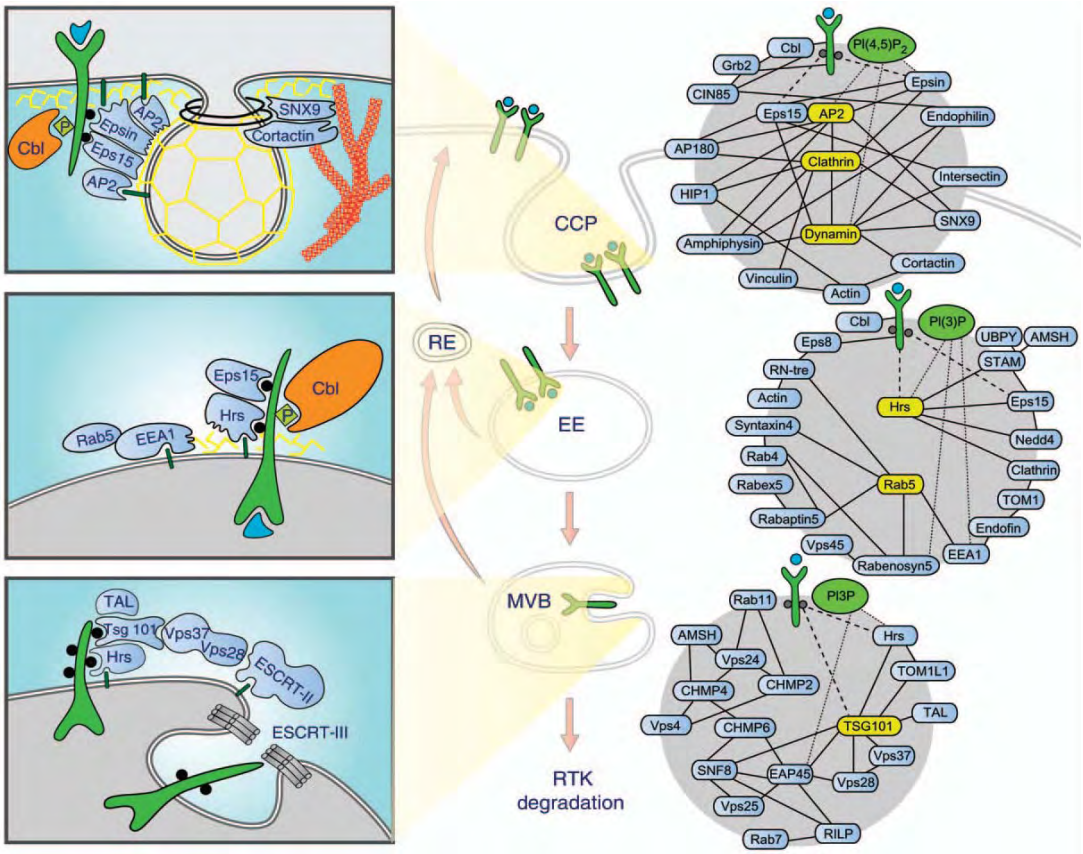

Fig. I: Major processes and molecular players underlying RTK sorting for internalization and degradation.
Three main receptor sorting steps taking place at the plasma membrane (CCP: clathrin-coated pits), EEs and MVBs (middle). The spatial organization and respective molecular assemblies are illustrated on the left. Interactomes of each sorting step are displayed on the right-hand side of the figure. Nodes and their links are shown, and hubs are presented in yellow. Membrane-anchoring lipid molecules are shown in green, and their interactions are presented as dotted lines. Dashed lines represent ubiquitin-mediated protein-protein interactions (Zwang and Yarden, 2009).

To our surprise, depletion of the ESCRT proteins HRS (Raiborg et al., 2002) and TSG101 (Babst et al., 2000), as well as KD of the ESCRT-associated ATPase VPS4A (Lata et al., 2008), did not lead to elevated or sustained signaling in a EGF-inducible reporter system or increased induction of the endogenous target genes *EGR1* and *FOS* (Fig. 3 A and B). This lack of effect was neither due to shortcomings of the signaling assay (Fig. 2), nor to insufficient protein depletion, since EGFR degradation was delayed (although not blocked) and ERK1/2 phosphorylation concomitantly prolonged under our KD conditions (Fig. 3 C and D), in agreement with observations of other groups for HRS and TSG101 depletion (Babst et al., 2000; Bache et al., 2006; Malerod et al., 2007).

We therefore assume that increased levels of phosphorylated EGFR and downstream kinases are not necessarily indicative of enhanced signaling in general and increased transcription in particular. Indeed, phospho-levels are not always interrelated: for instance in Fig 8 C, EGFR is significantly less degraded but also less active upon stimulation with “low” compared to “high” EGF. Phospho-MEK signals are similar between the two conditions, whereas ERK1/2 seem again less active at 1 h of stimulation with low EGF. Moreover, even though MEK1/2 phosphorylation seems comparable, transcriptional induction of our reporter (Fig. 8 D) or of many endogenous target genes (Fig. 8 F, 360 min time point) is decreased and/or shortened upon low EGF stimulation. This is in contrast to previous findings which suggest that stimulation of cells with low EGF leads to stronger signaling (*via* clathrin-mediated receptor recycling), compared to high EGF stimulation conditions (Sigismund et al., 2008; Sigismund et al., 2005). As mentioned in chapter 3.2.1. and 3.2.4., another study found no evidence for different internalization routes and receptor fates, depending on the stimulation conditions (Kazazic et al., 2006). These discrepancies can for the time being only be explained by cell type- or even cell clone-specific effects (Sorkin and Goh, 2008).

Another striking example for the sometimes relatively poor correlation of phospho-levels between different signaling components is shown in Fig. 9 F. Overexpressed GFP-EGFR is highly active throughout the EGF stimulation time course, but levels of phosphorylated MEK and ERK are not proportionally upregulated in comparison to GFP mock-transfected samples, and also compared to effects of CHC-DNM2 and CBL-CBLB double KDs in Fig. 9 D and E, respectively. Finally, PMA stimulation leads to a massive transcriptional activation of luciferase in the signaling assay (Fig. 2 D), but phospho-ERK1/2 signals are similar at 15 min of treatment compared to EGF (Fig. 2 G). However, ERKs stay active for longer in PMA-stimulated cells (Fig. 14 A), and ERK-independent transcriptional induction by PMA (a structural analog of diacylglycerol) *via* PKC activation can not be excluded (Azzi et al., 1992; Castagna et al., 1982). Nevertheless, monitoring only the phosphorylation of the EGFR and downstream kinases does not seem to allow general conclusions about signaling outputs, particularly about transcriptional activity, and other approaches have to be deployed in parallel if for instance “increased signaling” is being postulated.

Experiments aiming to examine effects on EGF-induced EGFR downregulation have to be conducted in the presence of cycloheximide (inhibiting protein translation (Bennett et al., 1965)), otherwise re-synthesis of the receptor will blur the kinetics of receptor degradation. This was already implied even before the receptor was cloned and characterized, as cycloheximide (or actinomycin D, an inhibitor of transcription (Sobell, 1985)) was shown to inhibit the ability of cells to rebind EGF some time after initial stimulation (Carpenter and Cohen, 1976). However, cycloheximide has profound effects on signaling itself. The drug interferes with regulatory feedback loops induced during the response (chapter 2.4. and 2.6.1.; Fig. 5), as shown on the example of EGF-mediated DUSP expression, which, when interfered with, leads to persistent activation of MAPKs (Amit et al., 2007a; Brondello et al., 1997; Sun et al., 1993). Accordingly, phosphorylation of ERK and MEK, but also of the EGFR, was prolonged in the presence of cycloheximide (Fig. 8 A and B). Interfering with EGFR internalization or ubiquitination led to increased phospho-EGFR and phospho-MAPK signals (see below), but this effect was less pronounced when cycloheximide was present during the stimulation time course (Fig. 9 D and E). The same was observed in TSG101-depleted cells (data not shown). Therefore, cycloheximide leads to artifacts in EGFR downstream signaling events, and should be omitted when the EGF response is being explored.

Quantitative analysis of EGF-induced transcription of EGR1 and FOS indicated that the expression of immediate early genes is not affected by HRS, TSG101, or VPS4A depletion (Fig. 3 B). But it is well conceivable, considering the dogma of ESCRT function in signal attenuation (chapter 3.2.4., Fig. 22), that other (for instance late response) genes are upregulated or longer transcribed in ESCRT-depleted cells. To scrutinize a possible role of ESCRT-mediated EGFR sorting in downstream signaling, we performed a genome-wide transcriptional analysis of the EGF response in ESCRT KD cells using microarrays. Data quality was validated by mRNA quantification of about 100 genes utilizing NanoString, a technology more sensitive than microarrays and similar in sensitivity and dynamic range to real-time PCR (Geiss et al., 2008; Malkov et al., 2009) (Fig. 6 A).

The architecture of EGF-induced transcription is well preserved in comparison to the only other comprehensive study on the overall kinetics of the response (Amit et al., 2007a), described in chapter 2.4. Functional waves of transcription (Fig. 4 A), including immediate and delayed early genes as well as late effectors, are connected *via* both positive and negative feedback loops, determining the kinetic profile of gene expression. The initial burst of transcriptional activators (e.g. AP-1 components and EGR family transcription factors, Fig. 4 B and 5 A) drives subsequent expression of genes later in the program (Hess et al., 2004; Shaulian and Karin, 2002). Transcriptional repressors (Fig. 5 B) are responsible for the rapid attenuation of forward-driving transcription factors (Amit et al., 2007b), in conjunction with

their short mRNA half-life (see also Fig. 12 of the introduction). Positive feedbacks such as the induction of EGFR ligands and the receptor itself (Fig. 5 C and C´) may explain the re-phosphorylation of the cytosolic EGFR and MAPKs observed under pulse-chase stimulation conditions in the absence of cycloheximide (Fig. 8 B, right). EGF-induced regulators of EGFR kinase activity, receptor degradation and/or downstream signaling (ERRFI1/MIG6 (Frosi et al., 2010; Zhang and Vande Woude, 2007), LRIG1 (Gur et al., 2004; Laederich et al., 2004), several SOCS proteins (Kario et al., 2005; Xia et al., 2002), PTPRE (Elson and Leder, 1995; Toledano-Katchalski et al., 2003), SPRYs (Kim and Bar-Sagi, 2004; Mason et al., 2006) and SPREDs (Bundschu et al., 2007), Fig. 5 D to E; chapter 2.6.1.) will contribute to the CBL-mediated downregulation of the receptor and of receptor-proximal signaling events. The relatively late maximal induction of many negative feedback regulators at 120 min EGF suggests that at least some of them participate in maintaining a refractory period, terminating prolonged rather than acute signal activation, and avoiding repetitive and excessive stimulation (Amit et al., 2007a; Rubin et al., 2005). This may explain the fact that despite of partial reactivation of cytosolic signal transduction components in the absence of cycloheximide (Fig. 8 A and B, right), transcription is not upregulated concomitantly at late time points of EGF stimulation (Fig. 2, 4, 5 A, and 8 E). Apart from the slow induction of PTPRE (dephosphorylating ERKs) (Toledano-Katchalski et al., 2003; Wabakken et al., 2002), several MAPK phosphatases or DUSPs able to deactivate ERK1/2 (Boutros et al., 2008; Jeffrey et al., 2007; Patterson et al., 2009) are induced maximally at both early and later times after EGF addition (Fig. 5 F). These phosphatases probably cooperate in turning-off the MAPK cascade and prevent inappropriate overstimulation. Interestingly, both CBL and CBLB transcription is directly regulated by EGF (Fig. 12 B; to our knowledge the first observation of this potential feedback mechanism), but the biological significance of that phenomenon is not clear at present.

Thus, the wave-like organization of the transcriptional response to EGF, namely the coordinated and temporally restricted expression of functionally related clusters of genes (Amit et al., 2007b), is defined by the interplay between forward-driving and negative feedback mechanisms (Citri and Yarden, 2006; Kholodenko, 2006; Kholodenko et al., 2010; Lemmon and Schlessinger, 2010; Shilo, 2005). This balance, leading to the definition of an activation interval, may provide significant robustness to the system (Becskei and Serrano, 2000; Freeman, 2000; Kitano, 2004; Pires-daSilva and Sommer, 2003; Stelling et al., 2004). It could explain why increased activation of EGFR and MAPKs upon ESCRT KD (Fig. 3 C and D) does not lead to a global change in the architecture of the EGF response (Fig. 4 and Fig. 10 C). “Buffering” may even happen during the cytosolic signal transduction *via* the MAPK cascade: in Fig. 9 F, even in the presence of cycloheximide (hence, in the absence of negative feedback loops), overexpressed and hyperphosphorylated EGFR did not lead to a proportional upregulation of MEK and ERK activity (see above), which is somewhat

unexpected since enzymatic reactions in the signal processing layer should lead to signal amplification instead of dampening. However, the final transcriptional signaling output is significantly increased upon EGFR overexpression (Fig. 2 C and Fig. 10, see below).

Since sorting of the EGFR into MVBs does not have a general impact on the EGF-induced transcriptional program, we interfered with receptor trafficking events further upstream of ESCRT function, to identify the “point of commitment” from where the receptor is still able to affect gene expression. Utilizing the reporter assay, we demonstrate that impairing clathrin- and dynamin-dependent internalization of the EGFR (chapter 3.2.1.) (Damke et al., 1995; Huang et al., 2004a; Motley et al., 2003; Sorkin and Goh, 2008) increases ELK1-driven transcriptional activation, as shown for CHC and DNM2 single or double KDs (Fig. 9 A). Similarly, simultaneous depletion of CBL and CBLB, which are not necessary for internalization (Duan et al., 2003; Huang et al., 2006) (chapter3.1.4.) but cooperate in ubiquitin-mediated targeting of the receptor for degradative sorting (Pennock and Wang, 2008), leads to increased luciferase induction downstream of EGF (Fig. 9 B). As expected, EGFR degradation is delayed and activity of the receptor and the MAPK cascade is elevated in both double KDs, more or less independently of the presence or absence of cycloheximide (Fig. 9 D and E).

In our second large-scale transcriptional analysis of about 100 EGF-responsive genes using the NanoString technology, we found that CHC-DNM2 as well as CBL-CBLB double KDs lead to strong and significant upregulation of many transcripts (Fig. 10 B). Strikingly, the pattern and strength of effects is very similar to those observed upon EGFR overexpression. Increased transcriptional activity is therefore specifically due to defects in receptor sorting upstream of ESCRTs, since ectopically expressed EGFR is also less efficiently degraded (Fig. 9 F). Similar behavior of CHC-DNM2 and CBL-CBLB double KDs, and of EGFR overexpressing cells could be seen already in the statistical PCA analysis, where samples from these three conditions cluster together (Fig. 11 B and B´, green ovals). However, the overall organization of the EGF response does not appear to be altered even under those conditions (Fig. 10 A), demonstrating again the robustness of the system in HeLa cells. Only PMA stimulation increases both the strength and duration of the response globally, showing that the system can be “pushed” and that the magnitude of transcriptional activity is not limited in general (Fig. 10 A and B). Accordingly, PMA-treated samples at 120 and 360 min can be seen as outliers in the PCA analysis (Fig. 11 B and B´, red circles), indicative of the overall impact of PMA stimulation. The phorbol ester PMA mimics diacylglycerol and activates PKC (Azzi et al., 1992; Castagna et al., 1982), which affects a multitude of cellular signaling pathways (Redig and Platanias, 2007; Rosse et al., 2010). Thus, we can not exclude ERK-independent effects, but PMA stimulation still provides the proof-of-principle that a global change in the expression of EGF-responsive genes can be achieved.

When the magnitude of effects of all tested conditions is compared, the mitogenic potency of PMA treatment becomes obvious again, followed in strength by conditions interfering with receptor internalization and ubiquitination, where effects are reminiscent of those observed upon ectopic EGFR expression (Fig. 10 C). It has been shown that overexpression of EGFR is in itself sufficient to increase the mitogenic or differentiation potency of EGF (Traverse et al., 1994). Increasing the time of active receptor at the plasma membrane is most probably responsible for these effects. Overexpressed EGF receptors at "high" ligand concentrations are internalized significantly slower than endogenous, modestly expressed EGFR due to the limited capacity of (clathrin-dependent) rapid internalization (Lund et al., 1990; Sorkin and Goh, 2008; Wiley, 1988) (chapter 3.2.1.). Depletion of CHC and DNM2 interferes with this rapid internalization mechanism (Huang et al., 2004a; Motley et al., 2003), leading to the same effect (Fig. 10 C). For TGFB-mediated signaling, it has been shown that inhibitors of clathrin-dependent endocytosis lead to accumulation of the receptor at the plasma membrane, enhancing signaling and cellular responses (Chen et al., 2009). Computational modeling suggests that at high EGF concentrations (in the saturation range), internalized receptors contribute very little to the overall signal (Schoeberl et al., 2002), and that ERK activation is robust to parameter perturbations (Birtwistle et al., 2007). Another study proposes that signal output from the MAPK module is sensitive to low level input only at the plasma membrane because of a low threshold for activation, whereas it is high in the cytosol (Harding et al., 2005).

Abrogation of EGFR ubiquitination and CBL functions also lead to increased recycling of ligand-stimulated receptor (Grovdal et al., 2004; Schmidt and Dikic, 2005). In general, the most potent EGF family ligands as well as mitogenic receptor heterodimers are internalization-deficient and/or display increased recycling (chapter 2.5. and 3.2.2.). In addition, CBL stays associated with the EGFR throughout the endocytic route and continues to ubiquitinate the EGFR after internalization, which is required for receptor downregulation (de Melker et al., 2001; Umebayashi et al., 2008). The effects on EGF signaling observed in HRS-depleted cells, rather weak but compared to the other ESCRT KDs still the most significant (Fig. 7 and 10 C), may also be explained by increased EGFR recycling (Hanyaloglu et al., 2005; Raiborg et al., 2008) (chapter 3.2.4.), although some of the observed effects of HRS depletion are likely to be EGF-independent (Fig. 7 A).

Taken together, our observations and a number of reports in the literature argue that conditions increasing the number of active receptors at the plasma membrane, either by interfering with internalization or by increasing EGFR recycling, have the strongest impact on downstream transcriptional activation. More precisely, continuous ubiquitination *via* CBL and CBLB, and to a lesser extend recruitment of the ubiquitinated receptor by HRS for ESCRT-mediated downregulation, seem to define the point after which EGFR sorting events do not influence signaling to the nucleus anymore.

Surprisingly, depletion of VPS4A, mediating the final step of ESCRT disassembly after membrane invagination (Kieffer et al., 2008; Lata et al., 2008; Scott et al., 2005) (chapter 3.1.4.), has the lowest number of effects (Fig. 7). It is possible that the receptor becomes trapped in MVBs and somehow signaling-incompetent. The same has been shown for KD of the ESCRT-II subunit EAP30/VPS22 and the ESCRT-III subunit CHMP3/VPS24, leading to impaired receptor degradation without effects on MEK and ERK phosphorylation (Bache et al., 2006; Malerod et al., 2007). Other conditions tested in our signaling assay supporting this notion were depletion of ANXA2 and RAB7, as well as leupeptin treatment (an inhibitor of lysosomal proteases (Aoyagi et al., 1969; Seglen et al., 1979)), strongly interfering with EGFR degradation but without effect on transcriptional induction of our reporter (data not shown). Here, ILV formation is not affected and the EGFR is presumably sequestered in ILVs (Gruenberg and Stenmark, 2004; Mayran et al., 2003; Vanlandingham and Ceresa, 2009).

The BRO1 domain-containing protein ALIX regulates late endosomal membrane invagination *via* the lipid LBPA (Falguieres et al., 2009; Kobayashi et al., 1999; Matsuo et al., 2004) (chapter 3.1.5. and 3.2.3.). It has been shown that ALIX depletion or internalization of inhibitory anti-LBPA antibodies does not regulate EGFR degradation (Luyet et al., 2008). But because TSG101 and ALIX cooperate in the back-fusion of ILVs and in budding into late endosomes (Falguieres et al., 2008; Luyet et al., 2008), simultaneous depletion of TSG101 and ALIX was included in our analysis. Interfering with both ESCRT- and LBPA-mediated sorting upon TSG101 and ALIX double KD did not lead to significantly increased transcriptional activation upon EGF stimulation in our reporter system (Fig. 9 B) or to elevated expression of endogenous target genes (Fig. 10 B and C). This demonstrates that one pathway of ILV formation can not compensate for the other, and that both pathways or both proteins together do not regulate intracellular EGFR signaling.

HD-PTP/PTPN23, a BRO1 domain-containing phosphatase-defective protein, (Barr et al., 2009; Gingras et al., 2009) (chapter 2.6.1.), is a candidate tumor suppressor (Toyooka et al., 2000) implicated in regulating EGFR degradation (Doyotte et al., 2008). It has been found to contribute to EGF-stimulated motility of carcinoma cells (Mariotti et al., 2009), and to EGFR signaling in *Drosophila* (Miura et al., 2008). However, HD-PTP depletion had only a subtle impact on EGF-induced transcription in comparison to conditions of the second NanoString analysis (Fig. 10 C).

In conclusion, the EGF-induced transcriptional program seems extremely robust and resistant to perturbations in HeLa cells. ESCRT-mediated sorting of the EGFR does not contribute to the overall response, in contrast to the dogma of ESCRT function in attenuating EGFR signaling from endosomes. Interfering with rapid receptor internalization, on the other hand, leads to transcriptional upregulation of many EGF response genes. Impeding EGFR ubiquitination by depletion of CBLs has the same impact on the transcriptional output,

suggesting that receptor ubiquitination might define the crucial point of signal termination. However, even EGFR overexpression does not lead to global disturbances in the architecture of the response, which can only be seen upon massive cell stimulation with PMA.

We do not know if this robustness of the EGF-induced transcriptional response, determined by the balance of positive and negative feedback mechanisms, is specific for our HeLa cell line. It could be a hallmark of cancer cells, or may be even true for primary cells or tissues. Under physiological conditions *in vivo*, many stimuli will shape the biological output together, providing for specific cell fate decisions. Thus, our data on the response downstream of EGF and its receptor provide a snapshot of an isolated signaling cascade rather than a holistic picture. We speculate that the tenacity of an individual cascade may be a general principle to ensure biological robustness, protecting the system from detrimental fluctuations or overreactions, and that biological flexibility and specificity may arise from combinatorial effects of several active signaling cascades.

Our results also question the potential role of HRS and TSG101 as principal regulators of RTK signaling in cancer development. Indeed, many examples from the literature support this view, and their involvement in tumor suppression is controversial (Liu et al., 2002; Oh et al., 2007; Stuffers et al., 2009; Toyoshima et al., 2007; Zhu et al., 2004) (chapter 3.2.4.). However, in our microarray analysis, we found specific effects of HRS and TSG101 depletion. Particularly at later times of EGF stimulation, both HRS and TSG101 KD commonly affect genes regulating the NF-kappa-B system and cytokine signaling, as revealed by unbiased computation using the pathway analysis software Ingenuity. Fig. 13 shows the software-generated network, with genes affected by both KDs at 120 min EGF as initial input. The network contains NFKB1 and NFKB2; transcription of two other NF-kappa-B family members, REL and RELB, where only affected by HRS depletion and are not included in Fig. 13. Thus, the expression of four out of five NF-kappa-B transcription factors is altered upon HRS (and partially TSG101) KD in our EGF stimulation time course. Transcription of NFKBIA/IKBA, a member of the I-kappa-B family of inhibitory proteins, is affected by both ESCRT KDs (Fig. 13). HRS depletion also increased the expression of NFKBIE/IKBE, so two out of three I-kappa-B family genes are stronger induced in HRS KD cells.

Signaling by NF-kappa-B transcription factors and cytokines regulates many physiological processes, including immune responses, inflammation, apoptosis, cell adhesion, and proliferation, reviewed in (Chen, 2005; Hayden and Ghosh, 2008; Perkins, 2007; Skaug et al., 2009). Crosstalk with the MAPK cascade and downstream targets results from the interaction of NF-kappa-B proteins with bZIP (leucine zipper) transcription factors of the AP-1 (JUN, FOS, ATFs), CREB, and EGR family (e.g. EGR1) (Perkins, 2007) (Fig. 5 A). STAT transcription factors directly associate with the EGFR and contribute to the EGF response (Morandell et al., 2008; Schulze et al., 2005; Yuan et al., 2010) (chapter 2.1. and 2.2.).

Particularly STAT3 regulates the non-canonical pathway of NF-kappa-B activation (Perkins, 2007) and links inflammation (Ghosh and Hayden, 2008) to cancer development (Bollrath and Greten, 2009). Conversely, NF-kappa-B signaling regulates the transcription of EGF response genes such as JUNB, JUND, KLF2, and ATFs (transcriptional repressors shown in Fig. 5 B), that are rapidly induced by NF-kappa-B activation (Perkins, 2007). Hence, the EGF and NF-kappa-B signaling systems are closely interlinked, and HRS as well as TSG101 among the ESCRT proteins may have specific functions in this connection.

For instance, the cytokines IL6 and IL8 are induced both by NF-kappa-B proteins (Pahl, 1999) and EGF (Fig. 10 A; effects of HRS and TSG101 KD on the transcription of those two interleukins can be seen in Fig. 7 D and 10 C, with values depicted in Fig 13). The NFKB1- and RELA-regulated gene BIRC3 (Koul et al., 2006; Wang et al., 2003) is, compared to mock, 2- to 3-fold upregulated upon HRS and TSG101 KD at 120 min (Fig. 13) and at 360 min EGF (not shown). BIRC3/IAP2 inhibits apoptosis by binding to the tumor necrosis factor receptor-associated factors TRAF1 and TRAF2 (Li et al., 2002; Liston et al., 1996; Rothe et al., 1995). Another gene strongly and EGF-dependently upregulated by HRS and TSG101 depletion is TNFAIP3/A20 (Fig. 13), shown to inhibit NF-kappa-B activation as well as TNF-mediated apoptosis (Wertz et al., 2004). The related, A20-like protein ZFAND5/ZNF216, interacting with TNFAIP3/A20 and regulating NF-kappa-B activation and apoptosis (Huang et al., 2004b), is affected by both ESCRT KDs as well (not shown). PTGS2/COX2 (cyclooxygenase 2) is induced 4 to 5-fold by EGF (Fig. 10 A), strongly upregulated in HRS and TSG101 KDs (Fig. 13), and its expression can be regulated by NF-kappa-B (Alvarez et al., 2005; Lerebours et al., 2008). The expression of the chemokine ligand CCL2, involved in immunoregulatory and inflammatory processes (Bachmann et al., 2006), was about 20-fold-induced by EGF (Fig. 10 A) and is regulated in part by NF-kappa-B (Hashimoto et al., 2009; Lerebours et al., 2008; Thompson and Van Eldik, 2009). Only a weak effect on CCL2 transcription was observed at 120 min EGF for HRS and TSG101 KDs (Fig. 13), which was much stronger at 360 min EGF (not shown). Finally, transcription of the chemokine CXCL2, induced by EGF about 20-fold (Fig. 10 A), is significantly upregulated in the two ESCRT KDs (not included in the network shown in Fig. 13). It is another downstream target gene of both EGR1 and NF-kappa-B transcription factors (Ha et al., 2010; Wang et al., 2009). In general, many cytokines showing transcriptional activity upon EGF stimulation (Fig. 10 A) and NF-kappa-B signaling (Pahl, 1999) seem to be affected particularly by HRS KD (another two examples are IL1A and IL1B, not shown). Most of these genes are also strongly upregulated upon PMA stimulation (NFKB1 and 2, NFKBIA and Z, TNFAIP3, BIRC3, PTGS2, IL1A, IL6 and IL8, CXCL1 and 2; Fig. 10 B), presumably because PKCs can participate in the activation of NF-kappa-B signaling (Diaz-Meco et al., 1993; Diaz-Meco et al., 1994; Ghosh and Baltimore, 1990; Lin et al., 2000; Manicassamy et al., 2006).

Taken together, the two ESCRT proteins HRS and TSG101 somehow seem to interconnect specific events of EGF and NF-kappa-B and/or cytokine signaling. ESCRT-II-mediated degradation of the chemokine receptor CXCR4 has been demonstrated (Malerod et al., 2007), but the general implications of this observation are not clear. Increased JAK/STAT activity has been found in *Drosophila* upon mutating TSG101 and an ESCRT-II subunit, and enhanced JAK/STAT signaling was also detected outside of the mutant clones due to increased IL6 secretion (Herz and Bergmann, 2009; Herz et al., 2006). However, these are only initial observations regarding the interplay of ESCRT function and cytokine signaling, to date difficult to explain. Further comprehensive studies and modeling approaches are necessary to unravel the complex relationship between EGF- and NF-kappa-B-responsive genes, particularly in the context of ESCRT function.

A last interesting but still preliminary observation is the strong effect of EGFR kinase inhibition at late time points of EGF stimulation shown in Fig. 14. The specific and highly potent EGFR kinase inhibitor AG1478 (tyrphostin) (Gazit et al., 1989; Yaish et al., 1988) caused a dramatic reduction of phosphorylated MEK and ERK levels after 3 h of EGF stimulation (Fig. 14 A). Concomitantly, transcriptional activity in the reporter assay was immediately shut down when AG1478 was added, even up to 3 h after EGF pre-incubation (Fig. 14 B). The effect was specific for EGFR inhibition, as it was not seen in PMA-treated cells. At that time of EGF stimulation, more than 60% of the receptor is degraded under our conditions (Fig. 3 D), and EGFR is supposed to be sorted into MVBs for sequestering the kinase away from its cytosolic substrates (Fig. 22 in the introduction). The full extent of downstream signaling events may require the contribution of ligand-bound receptor, which escaped the ESCRT-mediated downregulation and recycled back to the plasma membrane. Alternatively, a subpopulation of active, perhaps non- or de-ubiquitinated EGF receptors may not be subject to endosomal sorting and downregulation *via* the ESCRT machinery. This explanation could resolve the contradiction between the late requirement for EGFR activity and the lack of general effects of ESCRT depletion on the signaling response. Indeed, many studies show that at least a part of endosomal EGFR stays active and associates with downstream effectors (Burke et al., 2001; de Melker et al., 2001; Di Guglielmo et al., 1994; Oksvold et al., 2000; Wang et al., 1996) (chapter 3.2.4.). Moreover, the endosomal receptor is fully capable of substituting for signaling from the plasma membrane (Haugh et al., 1999; Pennock and Wang, 2003; Wang et al., 2002). But whether EGFR signaling from intracellular compartments really contributes to the overall response, or whether it can only compensate for plasma membrane signaling, remains an open question. In any case, the experiment shown in Fig. 14 demonstrates that continuous EGFR activity is crucial to ensure the full magnitude of EGF signaling, and that the activation state of the participating components are ultimately linked long after the initial stimulation.

Materials and Methods

1. Reagents, antibodies, siRNAs and constructs

For cell culture, DMEM (Dulbecco's Modified Eagle Medium) from Sigma-Aldrich (St. Louis, MO) was used. FCS (fetal calf serum) was from Brunschwig (Basel, Switzerland), L-glutamine, penicillin and streptomycin, phenol red-free DMEM (high glucose, 25 mM HEPES-buffered, without sodium pyruvate) and Opti-MEM Reduced Serum Medium, were all from Gibco-BRL (Gaithersburg, MD). Human EGF (epidermal growth factor, used at 1.5 or 100 ng/ml), AG1478 (tyrphostin, 150 nM final concentration), PMA (phorbol-12-myristate-13-acetate, used at 10 ng/ml), and cycloheximide (10 µg/ml final) were from Sigma. U0126 (10 µM final) was from Cell Signaling Technology (Danvers, MA), and luciferin (0.1 mM final) from Promega (Madison, WI). Transfection of cells with siRNAs (small interfering RNAs) was performed with Lipofectamine RNAiMAX (Invitrogen, Carlsbad, CA), and plasmid transfection was done with FuGENE HD Transfection Reagent (Roche Diagnostics, Basel, Switzerland).

Antibodies used were the following: sheep anti-EGFR (BD Biosciences, San Diego, CA); mouse anti-phospho-EGFR (Tyr1173) [9H2] (Upstate, Lake Placid, NY); mouse anti-MEK1/2, rabbit anti-phospho-MEK1/2, rabbit anti-ERK1/2, mouse anti-phospho-ERK1/2 [E10] (all from Cell Signaling); mouse anti-RAB5 (a kind gift from Reinhard Jahn, Göttingen, Germany); rabbit anti-SNX3 (a kind gift from Wanjin Hong, Singapore); mouse anti-TSG101 (GeneTex, San Antonio, TX); rabbit anti-HRS (a kind gift from Harald Stenmark, Oslo, Norway); mouse anti-GFP (Roche); rabbit anti-ALIX (a kind gift from Rémy Sadoul, Grenoble, France); rabbit anti-DNM2 and rabbit anti-CHC (Abcam, Cambridge, UK); rabbit anti-VPS4A [H-165], rabbit anti-CBL [C-15], and rabbit anti-CBLB [H-121] (all from Santa Cruz Biotechnology, Santa Cruz, CA). Horseradish peroxidase (HRP)-conjugated secondary antibodies were from Invitrogen or GE Healthcare (Chalfont St. Giles, UK).

Protein depletion was performed with ON-TARGETplus SMART pool siRNAs from Dharmacon (Thermo Fisher Scientific, Lafayette, CO). Target sequences of all siRNAs can be found in the appendix. Plasmids used were pEGFP-N1-EGFR (a kind gift from Alexander Sorkin, Pittsburgh, PA) and the parental vector pEGFP-N1 (Clonetech, Mountain View, CA).

2. Cell culture, transfection, EGF stimulation, and harvest of cells

HeLa luciferase reporter for ELK1 (HLR-ELK1) cells (Stratagene, La Jolla, CA) were maintained in 10 cm dishes at 37°C and 5% CO_2 in DMEM, supplemented with 10% FCS, 2 mM L-glutamine, penicillin and streptomycin.

The day before transfection, confluent cells were diluted and seeded into 6 cm dishes. Transfection of siRNAs was performed using Lipofectamine RNAiMAX according to manufacturer´s instructions. Briefly, 10 µl Lipofectamine RNAiMAX were diluted in 500 µl Opti-MEM Reduced Serum Medium, and incubated for 5 min at room temperature. ON-TARGETplus SMART pool siRNAs from Dharmacon were diluted in 500 µl Opti-MEM as well, and were combined with the diluted Lipofectamine RNAiMAX. As control, ON-TARGETplus Non-Targeting siRNA pool from Dharmacon was used. The siRNA duplex-Lipofectamine RNAiMAX complexes were incubated for 20 min at room temperature, during which time the medium in the dishes was changed to 3 ml DMEM without antibiotics. The complexes were added to the dishes to a final siRNA concentration of 35-50 nM. After 6 h of incubation, the medium was changed back to 5 ml DMEM with 10% FCS and antibiotics, and the cells were grown for two days to a confluency of about 80%.

Plasmid transfection with FuGENE HD Transfection Reagent, according to manufacturer´s instructions, was as follows: 4.5 µl FuGENE reagent were diluted in 200 µl Opti-MEM and incubated for 5 min. Then, between 1 and 1.5 µg of DNA was added, and the mixture was incubated for another 15 min at room temperature. Medium in the dishes was changed to antibiotics-free DMEM before the plasmid-FuGENE complexes were added to the cells. After 6 h incubation, the medium was changed back to complete DMEM.

Before EGF stimulation, cells were starved for 16-18 h in DMEM without FCS, and then continuously stimulated (3 days after transfection) for the indicated times with 100 ng/ml EGF. Other stimulation conditions were 5 min EGF pulse followed by washes and a chase with serum-free medium, continuous stimulation with 1.5 ng/ml ("low") EGF, or PMA treatment at a final concentration of 10 ng/ml. For EGFR degradation time courses, cycloheximide was added to a final concentration of 10 µg/ml. The cells were washed twice with PBS at 4°C, and harvested in cell lysis buffer (Cell Signaling). Protein quantification was with the protein assay reagent from Bio-Rad Laboratories (Hercules, CA), as described (Bradford, 1976). Samples were then processed for standard SDS-PAGE (Laemmli, 1970; Shapiro et al., 1967) and western blotting analysis (Burnette, 1981; Towbin et al., 1979). Where indicated, quantification of western blots was done with ImageJ v1.43r (Wayne Rasband, NIH, Bethesda, MD). For RNA extraction, cells were scraped in 350 µl RLT lysis buffer (Qiagen, Valencia, CA), snap-frozen and stored at -80°C until RNA purification.

3. Live-cell signaling assay and quantitative real-time RT-PCR

To measure EGF-induced luciferase activity, HLR-ELK1 cells were split one day after transfection into 3.5 cm dishes in duplicates. The next day, cells were starved for 8 h in serum-free DMEM, and then washed with phenol red-free DMEM supplemented with

penicillin and streptomycin. Stimulation was in the same phenol red-free, HEPES-buffered medium containing 0.1 mM luciferin and 100 ng/ml EGF. In some experiments, inhibitors (AG1478 or U0126, see above) were present, and PMA stimulation was as described above. Cultures were maintained at 37°C in a light-tight incubator, and bioluminescence was monitored continuously for up to 16 h using Hamamatsu photomultiplier tube detector assemblies as reported by (Yamazaki et al., 2000; Yoo et al., 2004). Photon counts were integrated over 10 min intervals. Data were analyzed with the LumiCycle v1.4 software (Actimetrics, Wilmette, IL) and MS Excel 2003 (Microsoft, Redmond, WA).

For quantitative real-time RT-PCR, purification of total RNA using the RNeasy Mini Kit from Qiagen was done according to manufacturer´s instructions. RNA concentrations were measured with the NanoDrop ND-1000 UV/Vis Spectrophotometer (NanoDrop Technologies, Wilmington, DE). 1 µg of RNA was used for primer annealing (with QuantiTect Primer Assays for human *EGR1*, *FOS*, and *ACTB* (actin, beta) from Qiagen). Reverse transcription (with SuperScript enzyme, Invitrogen), and PCR with QuantiTect SYBR Green PCR Kits (Qiagen), was done according to manufacturer´s instructions. Monitoring of cDNA amplification was with the iCycler from Bio-Rad, and data were analyzed with the iCycler IQ v3.1 software.

4. Sample preparation for microarray analysis

HLR-ELK1 cells were grown, transfected, starved for 16-18 h, stimulated, and harvested in RLT buffer as described above. Five transfection conditions (mock / non-targeting siRNA pool and siRNA pools for HRS, TSG101, VPS4A, and ALIX; HD-PTP knockdown was performed in parallel but analyzed only by NanoString, see below) and four time points of stimulation (0, 30, 120, and 360 min) were assayed in biological triplicates (60 dishes or samples in total; 72 including the HD-PTP knockdown). One dish per transfection condition was prepared simultaneously for verification of protein depletion by Western blotting (see above). The same lots of media, FCS, transfection reagents, siRNAs, and EGF were used throughout the procedure, to exclude any possible batch effects.

The following experimental steps were done together with Sven Wichert and in collaboration with Moritz Rossner at the Max Planck Institute of Experimental Medicine in Göttingen, Germany. Purification of total RNA was again with the RNeasy Mini Kit from Qiagen. Concentration, purity and integrity of the RNA were measured with the Picodrop Microliter UV/Vis Spectrophotometer (Picodrop, Saffron Walden, UK), and the Agilent 2100 Bioanalyzer (Agilent Technologies, Santa Clara, CA), together with the RNA 6000 Series II Nano Kit (Agilent) according to manufacturer´s instructions.

ss- and ds-cDNA synthesis, cRNA *in vitro* transcription (amplification step), cRNA cleanup, second cycle cDNA synthesis, cRNA hydrolysis, ss-cDNA cleanup, fragmentation,

terminal labeling, and hybridization (with GeneChip Hybridization Oven 645, Affymetrix, High Wycombe, Buckinghamshire, UK), were done using the Human Gene 1.0 ST Array Reagent Kit and the GeneChip Whole Transcript Sense Target Labeling Assay, according to Affymetrix protocols. Washing and staining (with the GeneChip Fluidics Station 450, Affymetrix), as well as scanning (using the GeneChip Scanner 3000 7G from Affymetrix), were done according to manufacturer´s instructions as well. The raw microarray data were managed with the Affymetrix GeneChip Operating Software (GCOS) before further analysis.

In general, all samples were processed simultaneously, except for cleanup steps and the hybridization till scanning procedure. There, one replicate of each condition was processed at the same time, in order to minimize possible batch effects due to sample handling. Sample preparation was according to the 100 ng Total RNA Labeling Protocol. Differing from the protocol, 200 ng of total RNA were used as starting material for the first-strand cDNA synthesis. After cRNA *in vitro* transcription and cleanup, samples were stored at -80°C. cRNA concentration and purity was measured with the Picodrop spectrophotometer, and 10 µg of cRNA were used for the second cycle, first-strand cDNA synthesis. After hydrolysis of the cRNA, samples were stored at -20°C. ss-cDNA was purified and quantified, then again frozen at -20°C. For the fragmentation and terminal labeling, 5.5 µg of ss-cDNA were used, and samples ready for hybridization were kept at -20°C. The hybridization cocktail was prepared according to the 169 Format Array Protocol. In addition, BSA (bovine serum albumin, from Invitrogen) and herring sperm DNA (Promega) were included, and the final volume of the hybridization mix was adjusted to 110 µl.

5. mRNA measurements using the NanoString technology

The same samples analyzed by microarrays were also measured for data validation with the NanoString nCounter gene expression system (Geiss et al., 2008; Malkov et al., 2009) from NanoString Technologies (Seattle, WA). In addition, knockdown of HD-PTP was included in the first NanoString analysis. Target sequences for the probe design by the company can be found in the appendix.

NanoString was also used as an investigative tool in a second large-scale experiment. Conditions included a control time course (100 ng/ml continuous EGF), EGF pulse-chase stimulation, low EGF, and PMA stimulation (see 2. above). Transfection conditions were CHC-DNM2, CBL-CBLB, and ALIX-TSG101 double knockdowns, as well as overexpression of EGFR from the pEGFP-N1-EGFR vector. To check for possible effects of the transfection procedure, cells were also transfected with the non-targeting siRNA pool, or with the GFP-expressing plasmid pEGFP-N1. Otherwise, the general procedure of cell growth, transfection, starvation, stimulation, and harvest was identical to the microarray experiment described

above. Triplicates were prepared for each of the eight conditions and four time points, therefore a total of 96 dishes or samples was processed.

RNA extraction for the second NanoString experiment was done with the automated QIAcube station from Qiagen. Concentration, purity and integrity of the RNA were measured as described above. Assay set-up (combining reporter probes, mRNA, and capture probes), hybridization at 65°C for at least 12 h, post-hybridization processing using the nCounter Prep Station, and scanning with the nCounter Digital Analyzer (NanoString) were done according to manufacturer´s instructions, only that 300 ng of mRNA was used as starting material. The NanoString measurements were done with the help of Mylène Docquier and Didier Chollet, under supervision of Patrick Descombes, at the local Genomics platform (CMU, Geneva).

6. Software used for data analysis

The microarray data were normalized with Partek Genomics Suite v6.5 (St. Louis, MO) according to the RMA procedure (Robust Multichip Average, consisting of background adjustment, quantile normalization, and summarization) (Bolstad et al., 2003), and a batch removal step was performed to eliminate possible effects of the scan date. For further analysis, data of one replicate (HRS knockdown at 30 min EGF #1) was not considered because of frequent outliers (but was included in the NanoString analysis where it behaved similar to the other replicates of this condition). For reasons of data import and handling, an artificial replicate (with the mean values of the other two replicates) had to be created and included in the microarray analysis. Further normalization (to the mock-treated sample at time 0, or to the corresponding mock values at each time point), defining a cut-off (1.8-fold difference to mock 0 min EGF), grouping (according to the peak of expression) and ranking (according to the strength of induction) of genes was done with R.2.6 (a programming language; www.r-project.org) and MS Excel 2003 (see also figure legends). Other softwares used were Bioconductor packages (Fred Hutchinson Cancer Research Center, Seattle, WA) and GSEA v2.0 (Gene Set Enrichment Analysis, Broad Institute, Cambridge, MA).

Values from NanoString measurements were normalized to multiple housekeeping genes (Vandesompele et al., 2002) using an Excel-based macro written by Céline Delucinge Vivier at the Genomics platform. Further normalization, grouping and ranking was as above.

Heat maps were created with Partek, and additionally processed for visualization with Adobe Illustrator CS4 v14.0 (Adobe, San Jose, CA). GeneSpring GX v7.3 (Agilent) was used to create lists of affected genes in knockdown conditions, and pathway analysis was performed for those genes with Ingenuity pathway analysis IPA v7.6 software (Ingenuity Systems, Redwood City, CA). Lists of EGF-induced genes and of genes affected by knockdowns in the microarray analysis can be found in the appendix. The complete data sets for the microarray and NanoString analyses will be made available online upon publication.

Bibliography

Acconcia, F., Sigismund, S., and Polo, S. (2009). Ubiquitin in trafficking: the network at work. Exp Cell Res *315*, 1610-1618.

Adams, T.E., Hansen, J.A., Starr, R., Nicola, N.A., Hilton, D.J., and Billestrup, N. (1998). Growth hormone preferentially induces the rapid, transient expression of SOCS-3, a novel inhibitor of cytokine receptor signaling. J Biol Chem *273*, 1285-1287.

Agazie, Y.M., and Hayman, M.J. (2003). Development of an efficient "substrate-trapping" mutant of Src homology phosphotyrosine phosphatase 2 and identification of the epidermal growth factor receptor, Gab1, and three other proteins as target substrates. J Biol Chem *278*, 13952-13958.

Agromayor, M., and Martin-Serrano, J. (2006). Interaction of AMSH with ESCRT-III and deubiquitination of endosomal cargo. J Biol Chem *281*, 23083-23091.

Alam, S.L., Langelier, C., Whitby, F.G., Koirala, S., Robinson, H., Hill, C.P., and Sundquist, W.I. (2006). Structural basis for ubiquitin recognition by the human ESCRT-II EAP45 GLUE domain. Nat Struct Mol Biol *13*, 1029-1030.

Alessi, D.R., Smythe, C., and Keyse, S.M. (1993). The human CL100 gene encodes a Tyr/Thr-protein phosphatase which potently and specifically inactivates MAP kinase and suppresses its activation by oncogenic ras in Xenopus oocyte extracts. Oncogene *8*, 2015-2020.

Alexander, W.S. (2002). Suppressors of cytokine signalling (SOCS) in the immune system. Nat Rev Immunol *2*, 410-416.

Alvarez, S., Serramia, M.J., Fresno, M., and Munoz-Fernandez, M. (2005). Human immunodeficiency virus type 1 envelope glycoprotein 120 induces cyclooxygenase-2 expression in neuroblastoma cells through a nuclear factor-kappaB and activating protein-1 mediated mechanism. J Neurochem *94*, 850-861.

Amidon, B., Schmitt, J.D., Thuren, T., King, L., and Waite, M. (1995). Biosynthetic conversion of phosphatidylglycerol to sn-1:sn-1' bis(monoacylglycerol) phosphate in a macrophage-like cell line. Biochemistry *34*, 5554-5560.

Amit, I., Citri, A., Shay, T., Lu, Y., Katz, M., Zhang, F., Tarcic, G., Siwak, D., Lahad, J., Jacob-Hirsch, J.*, et al.* (2007a). A module of negative feedback regulators defines growth factor signaling. Nat Genet *39*, 503-512.

Amit, I., Wides, R., and Yarden, Y. (2007b). Evolvable signaling networks of receptor tyrosine kinases: relevance of robustness to malignancy and to cancer therapy. Mol Syst Biol *3*, 151.

Amit, I., Yakir, L., Katz, M., Zwang, Y., Marmor, M.D., Citri, A., Shtiegman, K., Alroy, I., Tuvia, S., Reiss, Y.*, et al.* (2004). Tal, a Tsg101-specific E3 ubiquitin ligase, regulates receptor endocytosis and retrovirus budding. Genes Dev *18*, 1737-1752.

Anastasi, S., Baietti, M.F., Frosi, Y., Alema, S., and Segatto, O. (2007). The evolutionarily conserved EBR module of RALT/MIG6 mediates suppression of the EGFR catalytic activity. Oncogene *26*, 7833-7846.

Anastasi, S., Fiorentino, L., Fiorini, M., Fraioli, R., Sala, G., Castellani, L., Alema, S., Alimandi, M., and Segatto, O. (2003). Feedback inhibition by RALT controls signal output by the ErbB network. Oncogene *22*, 4221-4234.

Anklesaria, P., Teixido, J., Laiho, M., Pierce, J.H., Greenberger, J.S., and Massague, J. (1990). Cell-cell adhesion mediated by binding of membrane-anchored transforming growth factor alpha to epidermal growth factor receptors promotes cell proliferation. Proc Natl Acad Sci U S A *87*, 3289-3293.

Aoyagi, T., Miyata, S., Nanbo, M., Kojima, F., and Matsuzaki, M. (1969). Biological activities of leupeptins. J Antibiot (Tokyo) *22*, 558-568.

Attar, N., and Cullen, P.J. (2010). The retromer complex. Adv Enzyme Regul *50*, 216-236.

Audhya, A., McLeod, I.X., Yates, J.R., and Oegema, K. (2007). MVB-12, a fourth subunit of metazoan ESCRT-I, functions in receptor downregulation. PLoS One *2*, e956.

Austin, C.D., De Maziere, A.M., Pisacane, P.I., van Dijk, S.M., Eigenbrot, C., Sliwkowski, M.X., Klumperman, J., and Scheller, R.H. (2004). Endocytosis and sorting of ErbB2 and the site of action of cancer therapeutics trastuzumab and geldanamycin. Mol Biol Cell *15*, 5268-5282.

Azzi, A., Boscoboinik, D., and Hensey, C. (1992). The protein kinase C family. Eur J Biochem *208*, 547-557.

Baass, P.C., Di Guglielmo, G.M., Authier, F., Posner, B.I., and Bergeron, J.J. (1995). Compartmentalized signal transduction by receptor tyrosine kinases. Trends Cell Biol *5*, 465-470.

Babst, M., Katzmann, D.J., Estepa-Sabal, E.J., Meerloo, T., and Emr, S.D. (2002). Escrt-III: an endosome-associated heterooligomeric protein complex required for mvb sorting. Dev Cell *3*, 271-282.

Babst, M., Odorizzi, G., Estepa, E.J., and Emr, S.D. (2000). Mammalian tumor susceptibility gene 101 (TSG101) and the yeast homologue, Vps23p, both function in late endosomal trafficking. Traffic *1*, 248-258.

Bache, K.G., Brech, A., Mehlum, A., and Stenmark, H. (2003a). Hrs regulates multivesicular body formation via ESCRT recruitment to endosomes. J Cell Biol *162*, 435-442.

Bache, K.G., Raiborg, C., Mehlum, A., Madshus, I.H., and Stenmark, H. (2002). Phosphorylation of Hrs downstream of the epidermal growth factor receptor. Eur J Biochem *269*, 3881-3887.

Bache, K.G., Raiborg, C., Mehlum, A., and Stenmark, H. (2003b). STAM and Hrs are subunits of a multivalent ubiquitin-binding complex on early endosomes. J Biol Chem *278*, 12513-12521.

Bache, K.G., Stuffers, S., Malerod, L., Slagsvold, T., Raiborg, C., Lechardeur, D., Walchli, S., Lukacs, G.L., Brech, A., and Stenmark, H. (2006). The ESCRT-III subunit hVps24 is required for degradation but not silencing of the epidermal growth factor receptor. Mol Biol Cell *17*, 2513-2523.

Bachmann, M.F., Kopf, M., and Marsland, B.J. (2006). Chemokines: more than just road signs. Nat Rev Immunol *6*, 159-164.

Bainton, D.F. (1981). The discovery of lysosomes. J Cell Biol *91*, 66s-76s.

Balbis, A., Parmar, A., Wang, Y., Baquiran, G., and Posner, B.I. (2007). Compartmentalization of signaling-competent epidermal growth factor receptors in endosomes. Endocrinology *148*, 2944-2954.

Balbis, A., and Posner, B.I. (2010). Compartmentalization of EGFR in cellular membranes: role of membrane rafts. J Cell Biochem *109*, 1103-1108.

Baldys, A., Gooz, M., Morinelli, T.A., Lee, M.H., Raymond, J.R., Jr., Luttrell, L.M., and Raymond, J.R., Sr. (2009). Essential role of c-Cbl in amphiregulin-induced recycling and signaling of the endogenous epidermal growth factor receptor. Biochemistry *48*, 1462-1473.

Barbieri, M.A., Roberts, R.L., Gumusboga, A., Highfield, H., Alvarez-Dominguez, C., Wells, A., and Stahl, P.D. (2000). Epidermal growth factor and membrane trafficking. EGF receptor activation of endocytosis requires Rab5a. J Cell Biol *151*, 539-550.

Barr, A.J., Ugochukwu, E., Lee, W.H., King, O.N., Filippakopoulos, P., Alfano, I., Savitsky, P., Burgess-Brown, N.A., Muller, S., and Knapp, S. (2009). Large-scale structural analysis of the classical human protein tyrosine phosphatome. Cell *136*, 352-363.

Baulida, J., and Carpenter, G. (1997). Heregulin degradation in the absence of rapid receptor-mediated internalization. Exp Cell Res *232*, 167-172.

Baulida, J., Kraus, M.H., Alimandi, M., Di Fiore, P.P., and Carpenter, G. (1996). All ErbB receptors other than the epidermal growth factor receptor are endocytosis impaired. J Biol Chem *271*, 5251-5257.

Becskei, A., and Serrano, L. (2000). Engineering stability in gene networks by autoregulation. Nature *405*, 590-593.

Beguinot, L., Lyall, R.M., Willingham, M.C., and Pastan, I. (1984). Down-regulation of the epidermal growth factor receptor in KB cells is due to receptor internalization and subsequent degradation in lysosomes. Proc Natl Acad Sci U S A *81*, 2384-2388.

Behnia, R., and Munro, S. (2005). Organelle identity and the signposts for membrane traffic. Nature *438*, 597-604.

Belgareh-Touze, N., Leon, S., Erpapazoglou, Z., Stawiecka-Mirota, M., Urban-Grimal, D., and Haguenauer-Tsapis, R. (2008). Versatile role of the yeast ubiquitin ligase Rsp5p in intracellular trafficking. Biochem Soc Trans *36*, 791-796.

Bennasroune, A., Fickova, M., Gardin, A., Dirrig-Grosch, S., Aunis, D., Cremel, G., and Hubert, P. (2004). Transmembrane peptides as inhibitors of ErbB receptor signaling. Mol Biol Cell *15*, 3464-3474.

Bennett, L.L., Jr., Ward, V.L., and Brockman, R.W. (1965). Inhibition of protein synthesis in vitro by cycloheximide and related glutarimide antibiotics. Biochim Biophys Acta *103*, 478-485.

Bhola, N.E., and Grandis, J.R. (2008). Crosstalk between G-protein-coupled receptors and epidermal growth factor receptor in cancer. Front Biosci *13*, 1857-1865.

Birtwistle, M.R., Hatakeyama, M., Yumoto, N., Ogunnaike, B.A., Hoek, J.B., and Kholodenko, B.N. (2007). Ligand-dependent responses of the ErbB signaling network: experimental and modeling analyses. Mol Syst Biol *3*, 144.

Bivona, T.G., Perez De Castro, I., Ahearn, I.M., Grana, T.M., Chiu, V.K., Lockyer, P.J., Cullen, P.J., Pellicer, A., Cox, A.D., and Philips, M.R. (2003). Phospholipase Cgamma activates Ras on the Golgi apparatus by means of RasGRP1. Nature *424*, 694-698.

Blagoev, B., Ong, S.E., Kratchmarova, I., and Mann, M. (2004). Temporal analysis of phosphotyrosine-dependent signaling networks by quantitative proteomics. Nat Biotechnol *22*, 1139-1145.

Blake, T.J., Shapiro, M., Morse, H.C., 3rd, and Langdon, W.Y. (1991). The sequences of the human and mouse c-cbl proto-oncogenes show v-cbl was generated by a large truncation encompassing a proline-rich domain and a leucine zipper-like motif. Oncogene *6*, 653-657.

Blomberg, J., Reynolds, F.H., Jr., Van de Ven, W.J., and Stephenson, J.R. (1980). Abelson murine leukaemia virus transformation involves loss of epidermal growth factor-binding sites. Nature *286*, 504-507.

Bocharov, E.V., Mineev, K.S., Volynsky, P.E., Ermolyuk, Y.S., Tkach, E.N., Sobol, A.G., Chupin, V.V., Kirpichnikov, M.P., Efremov, R.G., and Arseniev, A.S. (2008). Spatial structure of the dimeric transmembrane domain of the growth factor receptor ErbB2 presumably corresponding to the receptor active state. J Biol Chem *283*, 6950-6956.

Bohmann, D., Bos, T.J., Admon, A., Nishimura, T., Vogt, P.K., and Tjian, R. (1987). Human proto-oncogene c-jun encodes a DNA binding protein with structural and functional properties of transcription factor AP-1. Science *238*, 1386-1392.

Bohn, G., Allroth, A., Brandes, G., Thiel, J., Glocker, E., Schaffer, A.A., Rathinam, C., Taub, N., Teis, D., Zeidler, C.*, et al.* (2007). A novel human primary immunodeficiency syndrome caused by deficiency of the endosomal adaptor protein p14. Nat Med *13*, 38-45.

Bollrath, J., and Greten, F.R. (2009). IKK/NF-kappaB and STAT3 pathways: central signalling hubs in inflammation-mediated tumour promotion and metastasis. EMBO Rep *10*, 1314-1319.

Bolstad, B.M., Irizarry, R.A., Astrand, M., and Speed, T.P. (2003). A comparison of normalization methods for high density oligonucleotide array data based on variance and bias. Bioinformatics *19*, 185-193.

Bonifacino, J.S. (2004). The GGA proteins: adaptors on the move. Nat Rev Mol Cell Biol *5*, 23-32.

Bonifacino, J.S., and Hurley, J.H. (2008). Retromer. Curr Opin Cell Biol *20*, 427-436.

Bonifacino, J.S., and Traub, L.M. (2003). Signals for sorting of transmembrane proteins to endosomes and lysosomes. Annu Rev Biochem *72*, 395-447.

Booth, A.M., Fang, Y., Fallon, J.K., Yang, J.M., Hildreth, J.E., and Gould, S.J. (2006). Exosomes and HIV Gag bud from endosome-like domains of the T cell plasma membrane. J Cell Biol *172*, 923-935.

Bose, R., and Zhang, X. (2009). The ErbB kinase domain: structural perspectives into kinase activation and inhibition. Exp Cell Res *315*, 649-658.

Boulton, T.G., Nye, S.H., Robbins, D.J., Ip, N.Y., Radziejewska, E., Morgenbesser, S.D., DePinho, R.A., Panayotatos, N., Cobb, M.H., and Yancopoulos, G.D. (1991). ERKs: a family of protein-serine/threonine kinases that are activated and tyrosine phosphorylated in response to insulin and NGF. Cell *65*, 663-675.

Boulton, T.G., Yancopoulos, G.D., Gregory, J.S., Slaughter, C., Moomaw, C., Hsu, J., and Cobb, M.H. (1990). An insulin-stimulated protein kinase similar to yeast kinases involved in cell cycle control. Science *249*, 64-67.

Boutros, T., Chevet, E., and Metrakos, P. (2008). Mitogen-activated protein (MAP) kinase/MAP kinase phosphatase regulation: roles in cell growth, death, and cancer. Pharmacol Rev *60*, 261-310.

Bouyain, S., and Leahy, D.J. (2007). Structure-based mutagenesis of the substrate-recognition domain of Nrdp1/FLRF identifies the binding site for the receptor tyrosine kinase ErbB3. Protein Sci *16*, 654-661.

Bouyain, S., Longo, P.A., Li, S., Ferguson, K.M., and Leahy, D.J. (2005). The extracellular region of ErbB4 adopts a tethered conformation in the absence of ligand. Proc Natl Acad Sci U S A *102*, 15024-15029.

Bowers, K., Piper, S.C., Edeling, M.A., Gray, S.R., Owen, D.J., Lehner, P.J., and Luzio, J.P. (2006). Degradation of endocytosed epidermal growth factor and virally ubiquitinated major histocompatibility complex class I is independent of mammalian ESCRTII. J Biol Chem *281*, 5094-5105.

Bowtell, D., Fu, P., Simon, M., and Senior, P. (1992). Identification of murine homologues of the Drosophila son of sevenless gene: potential activators of ras. Proc Natl Acad Sci U S A *89*, 6511-6515.

Bradford, M.M. (1976). A rapid and sensitive method for the quantitation of microgram quantities of protein utilizing the principle of protein-dye binding. Anal Biochem *72*, 248-254.

Brahma, A., and Dalby, K.N. (2007). Regulation of protein phosphorylation within the MKK1-ERK2 complex by MP1 and the MP1*P14 heterodimer. Arch Biochem Biophys *460*, 85-91.

Braulke, T., and Bonifacino, J.S. (2009). Sorting of lysosomal proteins. Biochim Biophys Acta *1793*, 605-614.

Briggs, M.W., and Sacks, D.B. (2003). IQGAP proteins are integral components of cytoskeletal regulation. EMBO Rep *4*, 571-574.

Bright, N.A., Gratian, M.J., and Luzio, J.P. (2005). Endocytic delivery to lysosomes mediated by concurrent fusion and kissing events in living cells. Curr Biol *15*, 360-365.

Britsch, S., Li, L., Kirchhoff, S., Theuring, F., Brinkmann, V., Birchmeier, C., and Riethmacher, D. (1998). The ErbB2 and ErbB3 receptors and their ligand, neuregulin-1, are essential for development of the sympathetic nervous system. Genes Dev *12*, 1825-1836.

Brondello, J.M., Brunet, A., Pouyssegur, J., and McKenzie, F.R. (1997). The dual specificity mitogen-activated protein kinase phosphatase-1 and -2 are induced by the p42/p44MAPK cascade. J Biol Chem *272*, 1368-1376.

Brondello, J.M., Pouyssegur, J., and McKenzie, F.R. (1999). Reduced MAP kinase phosphatase-1 degradation after p42/p44MAPK-dependent phosphorylation. Science *286*, 2514-2517.

Brotherus, J., Renkonen, O., Fischer, W., and Herrmann, J. (1974). Novel stereoconfiguration in lyso-bis-phosphatidic acid of cultured BHK-cells. Chem Phys Lipids *13*, 178-182.

Brown, M.D., and Sacks, D.B. (2006). IQGAP1 in cellular signaling: bridging the GAP. Trends Cell Biol *16*, 242-249.

Brunet, A., Roux, D., Lenormand, P., Dowd, S., Keyse, S., and Pouyssegur, J. (1999). Nuclear translocation of p42/p44 mitogen-activated protein kinase is required for growth factor-induced gene expression and cell cycle entry. EMBO J *18*, 664-674.

Bucci, C., Lutcke, A., Steele-Mortimer, O., Olkkonen, V.M., Dupree, P., Chiariello, M., Bruni, C.B., Simons, K., and Zerial, M. (1995). Co-operative regulation of endocytosis by three Rab5 isoforms. FEBS Lett *366*, 65-71.

Bucci, C., Thomsen, P., Nicoziani, P., McCarthy, J., and van Deurs, B. (2000). Rab7: a key to lysosome biogenesis. Mol Biol Cell *11*, 467-480.

Buday, L., and Downward, J. (1993). Epidermal growth factor regulates p21ras through the formation of a complex of receptor, Grb2 adapter protein, and Sos nucleotide exchange factor. Cell *73*, 611-620.

Bullock, A.N., Rodriguez, M.C., Debreczeni, J.E., Songyang, Z., and Knapp, S. (2007). Structure of the SOCS4-ElonginB/C complex reveals a distinct SOCS box interface and the molecular basis for SOCS-dependent EGFR degradation. Structure *15*, 1493-1504.

Bundschu, K., Walter, U., and Schuh, K. (2007). Getting a first clue about SPRED functions. Bioessays *29*, 897-907.

Burden, S., and Yarden, Y. (1997). Neuregulins and their receptors: a versatile signaling module in organogenesis and oncogenesis. Neuron *18*, 847-855.

Burgess, A.W., Cho, H.S., Eigenbrot, C., Ferguson, K.M., Garrett, T.P., Leahy, D.J., Lemmon, M.A., Sliwkowski, M.X., Ward, C.W., and Yokoyama, S. (2003). An open-and-shut case? Recent insights into the activation of EGF/ErbB receptors. Mol Cell *12*, 541-552.

Burke, C.L., and Stern, D.F. (1998). Activation of Neu (ErbB-2) mediated by disulfide bond-induced dimerization reveals a receptor tyrosine kinase dimer interface. Mol Cell Biol *18*, 5371-5379.

Burke, P., Schooler, K., and Wiley, H.S. (2001). Regulation of epidermal growth factor receptor signaling by endocytosis and intracellular trafficking. Mol Biol Cell *12*, 1897-1910.

Burnette, W.N. (1981). "Western blotting": electrophoretic transfer of proteins from sodium dodecyl sulfate--polyacrylamide gels to unmodified nitrocellulose and radiographic detection with antibody and radioiodinated protein A. Anal Biochem *112*, 195-203.

Cacace, A.M., Michaud, N.R., Therrien, M., Mathes, K., Copeland, T., Rubin, G.M., and Morrison, D.K. (1999). Identification of constitutive and ras-inducible phosphorylation sites of KSR: implications for 14-3-3 binding, mitogen-activated protein kinase binding, and KSR overexpression. Mol Cell Biol *19*, 229-240.

Cacalano, N.A., Sanden, D., and Johnston, J.A. (2001). Tyrosine-phosphorylated SOCS-3 inhibits STAT activation but binds to p120 RasGAP and activates Ras. Nat Cell Biol *3*, 460-465.

Callus, B.A., and Mathey-Prevot, B. (2002). SOCS36E, a novel Drosophila SOCS protein, suppresses JAK/STAT and EGF-R signalling in the imaginal wing disc. Oncogene *21*, 4812-4821.

Camps, M., Nichols, A., Gillieron, C., Antonsson, B., Muda, M., Chabert, C., Boschert, U., and Arkinstall, S. (1998). Catalytic activation of the phosphatase MKP-3 by ERK2 mitogen-activated protein kinase. Science *280*, 1262-1265.

Cantalupo, G., Alifano, P., Roberti, V., Bruni, C.B., and Bucci, C. (2001). Rab-interacting lysosomal protein (RILP): the Rab7 effector required for transport to lysosomes. EMBO J *20*, 683-693.

Cao, L., Zhang, L., Ruiz-Lozano, P., Yang, Q., Chien, K.R., Graham, R.M., and Zhou, M. (1998). A novel putative protein-tyrosine phosphatase contains a BRO1-like domain and suppresses Ha-ras-mediated transformation. J Biol Chem *273*, 21077-21083.

Cao, W., Bao, C., Padalko, E., and Lowenstein, C.J. (2008). Acetylation of mitogen-activated protein kinase phosphatase-1 inhibits Toll-like receptor signaling. J Exp Med *205*, 1491-1503.

Cao, Z., Wu, X., Yen, L., Sweeney, C., and Carraway, K.L., 3rd (2007). Neuregulin-induced ErbB3 downregulation is mediated by a protein stability cascade involving the E3 ubiquitin ligase Nrdp1. Mol Cell Biol *27*, 2180-2188.

Carlton, J.G., and Martin-Serrano, J. (2007). Parallels between cytokinesis and retroviral budding: a role for the ESCRT machinery. Science *316*, 1908-1912.

Carpenter, G., and Cohen, S. (1976). 125I-labeled human epidermal growth factor. Binding, internalization, and degradation in human fibroblasts. J Cell Biol *71*, 159-171.

Carpenter, G., King, L., Jr., and Cohen, S. (1978). Epidermal growth factor stimulates phosphorylation in membrane preparations in vitro. Nature *276*, 409-410.

Carpentier, J.L., Gorden, P., Anderson, R.G., Goldstein, J.L., Brown, M.S., Cohen, S., and Orci, L. (1982). Co-localization of 125I-epidermal growth factor and ferritin-low density lipoprotein in coated pits: a quantitative electron microscopic study in normal and mutant human fibroblasts. J Cell Biol *95*, 73-77.

Carpentier, J.L., White, M.F., Orci, L., and Kahn, R.C. (1987). Direct visualization of the phosphorylated epidermal growth factor receptor during its internalization in A-431 cells. J Cell Biol *105*, 2751-2762.

Casci, T., Vinos, J., and Freeman, M. (1999). Sprouty, an intracellular inhibitor of Ras signaling. Cell *96*, 655-665.

Castagna, M., Takai, Y., Kaibuchi, K., Sano, K., Kikkawa, U., and Nishizuka, Y. (1982). Direct activation of calcium-activated, phospholipid-dependent protein kinase by tumor-promoting phorbol esters. J Biol Chem *257*, 7847-7851.

Castiglioni, S., Maier, J.A., and Mariotti, M. (2007). The tyrosine phosphatase HD-PTP: A novel player in endothelial migration. Biochem Biophys Res Commun *364*, 534-539.

Ceresa, B.P. (2006). Regulation of EGFR endocytic trafficking by rab proteins. Histol Histopathol *21*, 987-993.

Ceresa, B.P., and Bahr, S.J. (2006). rab7 activity affects epidermal growth factor:epidermal growth factor receptor degradation by regulating endocytic trafficking from the late endosome. J Biol Chem *281*, 1099-1106.

Chang, C.P., Lazar, C.S., Walsh, B.J., Komuro, M., Collawn, J.F., Kuhn, L.A., Tainer, J.A., Trowbridge, I.S., Farquhar, M.G., Rosenfeld, M.G.*, et al.* (1993). Ligand-induced internalization of the epidermal growth factor receptor is mediated by multiple endocytic codes analogous to the tyrosine motif found in constitutively internalized receptors. J Biol Chem *268*, 19312-19320.

Chang, E.H., Gonda, M.A., Ellis, R.W., Scolnick, E.M., and Lowy, D.R. (1982). Human genome contains four genes homologous to transforming genes of Harvey and Kirsten murine sarcoma viruses. Proc Natl Acad Sci U S A *79*, 4848-4852.

Chardin, P., Camonis, J.H., Gale, N.W., van Aelst, L., Schlessinger, J., Wigler, M.H., and Bar-Sagi, D. (1993). Human Sos1: a guanine nucleotide exchange factor for Ras that binds to GRB2. Science *260*, 1338-1343.

Chavrier, P., Parton, R.G., Hauri, H.P., Simons, K., and Zerial, M. (1990). Localization of low molecular weight GTP binding proteins to exocytic and endocytic compartments. Cell *62*, 317-329.

Chen, C.L., Hou, W.H., Liu, I.H., Hsiao, G., Huang, S.S., and Huang, J.S. (2009a). Inhibitors of clathrin-dependent endocytosis enhance TGFbeta signaling and responses. J Cell Sci *122*, 1863-1871.

Chen, P., Hutter, D., Yang, X., Gorospe, M., Davis, R.J., and Liu, Y. (2001). Discordance between the binding affinity of mitogen-activated protein kinase subfamily members for MAP kinase phosphatase-2 and their ability to activate the phosphatase catalytically. J Biol Chem *276*, 29440-29449.

Chen, P.I., Kong, C., Su, X., and Stahl, P.D. (2009b). Rab5 isoforms differentially regulate the trafficking and degradation of epidermal growth factor receptors. J Biol Chem *284*, 30328-30338.

Chen, R.H., Sarnecki, C., and Blenis, J. (1992). Nuclear localization and regulation of erk- and rsk-encoded protein kinases. Mol Cell Biol *12*, 915-927.

Chen, Z.J. (2005). Ubiquitin signalling in the NF-kappaB pathway. Nat Cell Biol *7*, 758-765.

Chevallier, J., Chamoun, Z., Jiang, G., Prestwich, G., Sakai, N., Matile, S., Parton, R.G., and Gruenberg, J. (2008). Lysobisphosphatidic acid controls endosomal cholesterol levels. J Biol Chem *283*, 27871-27880.

Chinkers, M., McKanna, J.A., and Cohen, S. (1979). Rapid induction of morphological changes in human carcinoma cells A-431 by epidermal growth factors. J Cell Biol *83*, 260-265.

Chiu, V.K., Bivona, T., Hach, A., Sajous, J.B., Silletti, J., Wiener, H., Johnson, R.L., 2nd, Cox, A.D., and Philips, M.R. (2002). Ras signalling on the endoplasmic reticulum and the Golgi. Nat Cell Biol *4*, 343-350.

Cho, H.S., and Leahy, D.J. (2002). Structure of the extracellular region of HER3 reveals an interdomain tether. Science *297*, 1330-1333.

Cho, H.S., Mason, K., Ramyar, K.X., Stanley, A.M., Gabelli, S.B., Denney, D.W., Jr., and Leahy, D.J. (2003). Structure of the extracellular region of HER2 alone and in complex with the Herceptin Fab. Nature *421*, 756-760.

Choi, K.Y., Satterberg, B., Lyons, D.M., and Elion, E.A. (1994). Ste5 tethers multiple protein kinases in the MAP kinase cascade required for mating in S. cerevisiae. Cell *78*, 499-512.

Choudhary, C., and Mann, M. (2010). Decoding signalling networks by mass spectrometry-based proteomics. Nat Rev Mol Cell Biol *11*, 427-439.

Choy, E., Chiu, V.K., Silletti, J., Feoktistov, M., Morimoto, T., Michaelson, D., Ivanov, I.E., and Philips, M.R. (1999). Endomembrane trafficking of ras: the CAAX motif targets proteins to the ER and Golgi. Cell *98*, 69-80.

Chu, T., Sun, J., Saksena, S., and Emr, S.D. (2006). New component of ESCRT-I regulates endosomal sorting complex assembly. J Cell Biol *175*, 815-823.

Chung, E., Graves-Deal, R., Franklin, J.L., and Coffey, R.J. (2005). Differential effects of amphiregulin and TGF-alpha on the morphology of MDCK cells. Exp Cell Res *309*, 149-160.

Citri, A., Skaria, K.B., and Yarden, Y. (2003). The deaf and the dumb: the biology of ErbB-2 and ErbB-3. Exp Cell Res *284*, 54-65.

Citri, A., and Yarden, Y. (2006). EGF-ERBB signalling: towards the systems level. Nat Rev Mol Cell Biol *7*, 505-516.

Claas, C., Stipp, C.S., and Hemler, M.E. (2001). Evaluation of prototype transmembrane 4 superfamily protein complexes and their relation to lipid rafts. J Biol Chem *276*, 7974-7984.

Cohen, S. (1962). Isolation of a mouse submaxillary gland protein accelerating incisor eruption and eyelid opening in the new-born animal. J Biol Chem *237*, 1555-1562.

Cohen, S. (1965). The stimulation of epidermal proliferation by a specific protein (EGF). Dev Biol *12*, 394-407.

Cohen, S., and Carpenter, G. (1975). Human epidermal growth factor: isolation and chemical and biological properties. Proc Natl Acad Sci U S A *72*, 1317-1321.

Cohen, S., Carpenter, G., and King, L., Jr. (1980). Epidermal growth factor-receptor-protein kinase interactions. Co-purification of receptor and epidermal growth factor-enhanced phosphorylation activity. J Biol Chem *255*, 4834-4842.

Conner, S.D., and Schmid, S.L. (2003). Regulated portals of entry into the cell. Nature *422*, 37-44.

Countaway, J.L., McQuilkin, P., Girones, N., and Davis, R.J. (1990). Multisite phosphorylation of the epidermal growth factor receptor. Use of site-directed mutagenesis to examine the role of serine/threonine phosphorylation. J Biol Chem *265*, 3407-3416.

Crews, C.M., Alessandrini, A., and Erikson, R.L. (1992). The primary structure of MEK, a protein kinase that phosphorylates the ERK gene product. Science *258*, 478-480.

Crone, S.A., and Lee, K.F. (2002). Gene targeting reveals multiple essential functions of the neuregulin signaling system during development of the neuroendocrine and nervous systems. Ann N Y Acad Sci *971*, 547-553.

Cunnick, J.M., Dorsey, J.F., Munoz-Antonia, T., Mei, L., and Wu, J. (2000). Requirement of SHP2 binding to Grb2-associated binder-1 for mitogen-activated protein kinase activation in response to lysophosphatidic acid and epidermal growth factor. J Biol Chem *275*, 13842-13848.

Cunningham, B.C., Ultsch, M., De Vos, A.M., Mulkerrin, M.G., Clauser, K.R., and Wells, J.A. (1991). Dimerization of the extracellular domain of the human growth hormone receptor by a single hormone molecule. Science *254*, 821-825.

Curtiss, M., Jones, C., and Babst, M. (2007). Efficient cargo sorting by ESCRT-I and the subsequent release of ESCRT-I from multivesicular bodies requires the subunit Mvb12. Mol Biol Cell *18*, 636-645.

Daaka, Y., Luttrell, L.M., Ahn, S., Della Rocca, G.J., Ferguson, S.S., Caron, M.G., and Lefkowitz, R.J. (1998). Essential role for G protein-coupled receptor endocytosis in the activation of mitogen-activated protein kinase. J Biol Chem *273*, 685-688.

Damke, H., Gossen, M., Freundlieb, S., Bujard, H., and Schmid, S.L. (1995). Tightly regulated and inducible expression of dominant interfering dynamin mutant in stably transformed HeLa cells. Methods Enzymol *257*, 209-220.

Davies, G.C., Ryan, P.E., Rahman, L., Zajac-Kaye, M., and Lipkowitz, S. (2006). EGFRvIII undergoes activation-dependent downregulation mediated by the Cbl proteins. Oncogene *25*, 6497-6509.

de Duve, C. (2005). The lysosome turns fifty. Nat Cell Biol *7*, 847-849.

De Duve, C., Pressman, B.C., Gianetto, R., Wattiaux, R., and Appelmans, F. (1955). Tissue fractionation studies. 6. Intracellular distribution patterns of enzymes in rat-liver tissue. Biochem J *60*, 604-617.

de Larco, J.E., and Todaro, G.J. (1978). Epithelioid and fibroblastic rat kidney cell clones: epidermal growth factor (EGF) receptors and the effect of mouse sarcoma virus transformation. J Cell Physiol *94*, 335-342.

de Lartigue, J., Polson, H., Feldman, M., Shokat, K., Tooze, S.A., Urbe, S., and Clague, M.J. (2009). PIKfyve regulation of endosome-linked pathways. Traffic *10*, 883-893.

de Melker, A.A., van der Horst, G., Calafat, J., Jansen, H., and Borst, J. (2001). c-Cbl ubiquitinates the EGF receptor at the plasma membrane and remains receptor associated throughout the endocytic route. J Cell Sci *114*, 2167-2178.

de Vos, A.M., Ultsch, M., and Kossiakoff, A.A. (1992). Human growth hormone and extracellular domain of its receptor: crystal structure of the complex. Science *255*, 306-312.

Deakin, N.O., and Turner, C.E. (2008). Paxillin comes of age. J Cell Sci *121*, 2435-2444.

Defea, K. (2008). Beta-arrestins and heterotrimeric G-proteins: collaborators and competitors in signal transduction. Br J Pharmacol *153 Suppl 1*, S298-309.

DeFea, K.A., Zalevsky, J., Thoma, M.S., Dery, O., Mullins, R.D., and Bunnett, N.W. (2000). beta-arrestin-dependent endocytosis of proteinase-activated receptor 2 is required for intracellular targeting of activated ERK1/2. J Cell Biol *148*, 1267-1281.

DeFeo, D., Gonda, M.A., Young, H.A., Chang, E.H., Lowy, D.R., Scolnick, E.M., and Ellis, R.W. (1981). Analysis of two divergent rat genomic clones homologous to the transforming gene of Harvey murine sarcoma virus. Proc Natl Acad Sci U S A *78*, 3328-3332.

Deneka, M., Pelchen-Matthews, A., Byland, R., Ruiz-Mateos, E., and Marsh, M. (2007). In macrophages, HIV-1 assembles into an intracellular plasma membrane domain containing the tetraspanins CD81, CD9, and CD53. J Cell Biol *177*, 329-341.

Dengjel, J., Akimov, V., Olsen, J.V., Bunkenborg, J., Mann, M., Blagoev, B., and Andersen, J.S. (2007). Quantitative proteomic assessment of very early cellular signaling events. Nat Biotechnol *25*, 566-568.

Di Fiore, P.P., Pierce, J.H., Kraus, M.H., Segatto, O., King, C.R., and Aaronson, S.A. (1987). erbB-2 is a potent oncogene when overexpressed in NIH/3T3 cells. Science *237*, 178-182.

Di Guglielmo, G.M., Baass, P.C., Ou, W.J., Posner, B.I., and Bergeron, J.J. (1994). Compartmentalization of SHC, GRB2 and mSOS, and hyperphosphorylation of Raf-1 by EGF but not insulin in liver parenchyma. EMBO J *13*, 4269-4277.

Diaz-Meco, M.T., Berra, E., Municio, M.M., Sanz, L., Lozano, J., Dominguez, I., Diaz-Golpe, V., Lain de Lera, M.T., Alcami, J., Paya, C.V.*, et al.* (1993). A dominant negative protein kinase C zeta subspecies blocks NF-kappa B activation. Mol Cell Biol *13*, 4770-4775.

Diaz-Meco, M.T., Dominguez, I., Sanz, L., Dent, P., Lozano, J., Municio, M.M., Berra, E., Hay, R.T., Sturgill, T.W., and Moscat, J. (1994). zeta PKC induces phosphorylation and inactivation of I kappa B-alpha in vitro. EMBO J *13*, 2842-2848.

Dickson, R.B., Hanover, J.A., Willingham, M.C., and Pastan, I. (1983). Prelysosomal divergence of transferrin and epidermal growth factor during receptor-mediated endocytosis. Biochemistry *22*, 5667-5674.

Dikic, I. (2002). CIN85/CMS family of adaptor molecules. FEBS Lett *529*, 110-115.

Dikic, I., Szymkiewicz, I., and Soubeyran, P. (2003). Cbl signaling networks in the regulation of cell function. Cell Mol Life Sci *60*, 1805-1827.

Dinneen, J.L., and Ceresa, B.P. (2004). Expression of dominant negative rab5 in HeLa cells regulates endocytic trafficking distal from the plasma membrane. Exp Cell Res *294*, 509-522.

Doherty, G.J., and McMahon, H.T. (2009). Mechanisms of endocytosis. Annu Rev Biochem *78*, 857-902.

Dowd, S., Sneddon, A.A., and Keyse, S.M. (1998). Isolation of the human genes encoding the pyst1 and Pyst2 phosphatases: characterisation of Pyst2 as a cytosolic dual-specificity MAP kinase phosphatase and its catalytic activation by both MAP and SAP kinases. J Cell Sci *111 (Pt 22)*, 3389-3399.

Doyotte, A., Mironov, A., McKenzie, E., and Woodman, P. (2008). The Bro1-related protein HD-PTP/PTPN23 is required for endosomal cargo sorting and multivesicular body morphogenesis. Proc Natl Acad Sci U S A *105*, 6308-6313.

Dreux, A.C., Lamb, D.J., Modjtahedi, H., and Ferns, G.A. (2006). The epidermal growth factor receptors and their family of ligands: their putative role in atherogenesis. Atherosclerosis *186*, 38-53.

Duan, L., Miura, Y., Dimri, M., Majumder, B., Dodge, I.L., Reddi, A.L., Ghosh, A., Fernandes, N., Zhou, P., Mullane-Robinson, K.*, et al.* (2003). Cbl-mediated ubiquitinylation is required for lysosomal sorting of epidermal growth factor receptor but is dispensable for endocytosis. J Biol Chem *278*, 28950-28960.

Dunn, W.A., Connolly, T.P., and Hubbard, A.L. (1986). Receptor-mediated endocytosis of epidermal growth factor by rat hepatocytes: receptor pathway. J Cell Biol *102*, 24-36.

Ebner, R., and Derynck, R. (1991). Epidermal growth factor and transforming growth factor-alpha: differential intracellular routing and processing of ligand-receptor complexes. Cell Regul *2*, 599-612.

Edeling, M.A., Smith, C., and Owen, D. (2006). Life of a clathrin coat: insights from clathrin and AP structures. Nat Rev Mol Cell Biol *7*, 32-44.

Eden, E.R., White, I.J., Tsapara, A., and Futter, C.E. (2010). Membrane contacts between endosomes and ER provide sites for PTP1B-epidermal growth factor receptor interaction. Nat Cell Biol *12*, 267-272.

Edwards, D.R., Handsley, M.M., and Pennington, C.J. (2008). The ADAM metalloproteinases. Mol Aspects Med *29*, 258-289.

Edwin, F., Anderson, K., Ying, C., and Patel, T.B. (2009). Intermolecular interactions of Sprouty proteins and their implications in development and disease. Mol Pharmacol *76*, 679-691.

Edwin, F., and Patel, T.B. (2008). A novel role of Sprouty 2 in regulating cellular apoptosis. J Biol Chem *283*, 3181-3190.

Egan, J.E., Hall, A.B., Yatsula, B.A., and Bar-Sagi, D. (2002). The bimodal regulation of epidermal growth factor signaling by human Sprouty proteins. Proc Natl Acad Sci U S A *99*, 6041-6046.

Ekerot, M., Stavridis, M.P., Delavaine, L., Mitchell, M.P., Staples, C., Owens, D.M., Keenan, I.D., Dickinson, R.J., Storey, K.G., and Keyse, S.M. (2008). Negative-feedback regulation of FGF signalling by DUSP6/MKP-3 is driven by ERK1/2 and mediated by Ets factor binding to a conserved site within the DUSP6/MKP-3 gene promoter. Biochem J *412*, 287-298.

Elson, A., and Leder, P. (1995). Identification of a cytoplasmic, phorbol ester-inducible isoform of protein tyrosine phosphatase epsilon. Proc Natl Acad Sci U S A *92*, 12235-12239.

Endo, T.A., Masuhara, M., Yokouchi, M., Suzuki, R., Sakamoto, H., Mitsui, K., Matsumoto, A., Tanimura, S., Ohtsubo, M., Misawa, H.*, et al.* (1997). A new protein containing an SH2 domain that inhibits JAK kinases. Nature *387*, 921-924.

Erickson, J.W., Cerione, R.A., and Hart, M.J. (1997a). Identification of an actin cytoskeletal complex that includes IQGAP and the Cdc42 GTPase. J Biol Chem *272*, 24443-24447.

Erickson, S.L., O'Shea, K.S., Ghaboosi, N., Loverro, L., Frantz, G., Bauer, M., Lu, L.H., and Moore, M.W. (1997b). ErbB3 is required for normal cerebellar and cardiac development: a comparison with ErbB2-and heregulin-deficient mice. Development *124*, 4999-5011.

Falguieres, T., Luyet, P.P., Bissig, C., Scott, C.C., Velluz, M.C., and Gruenberg, J. (2008). In vitro budding of intralumenal vesicles into late endosomes is regulated by Alix and Tsg101. Mol Biol Cell *19*, 4942-4955.

Falguieres, T., Luyet, P.P., and Gruenberg, J. (2009). Molecular assemblies and membrane domains in multivesicular endosome dynamics. Exp Cell Res *315*, 1567-1573.

Feng, Y., Press, B., and Wandinger-Ness, A. (1995). Rab 7: an important regulator of late endocytic membrane traffic. J Cell Biol *131*, 1435-1452.

Ferby, I., Reschke, M., Kudlacek, O., Knyazev, P., Pante, G., Amann, K., Sommergruber, W., Kraut, N., Ullrich, A., Fassler, R.*, et al.* (2006). Mig6 is a negative regulator of EGF receptor-mediated skin morphogenesis and tumor formation. Nat Med *12*, 568-573.

Ferguson, K.M., Berger, M.B., Mendrola, J.M., Cho, H.S., Leahy, D.J., and Lemmon, M.A. (2003). EGF activates its receptor by removing interactions that autoinhibit ectodomain dimerization. Mol Cell *11*, 507-517.

Fernandes, H., Cohen, S., and Bishayee, S. (2001). Glycosylation-induced conformational modification positively regulates receptor-receptor association: a study with an aberrant epidermal growth factor receptor (EGFRvIII/DeltaEGFR) expressed in cancer cells. J Biol Chem *276*, 5375-5383.

Filimonenko, M., Stuffers, S., Raiborg, C., Yamamoto, A., Malerod, L., Fisher, E.M., Isaacs, A., Brech, A., Stenmark, H., and Simonsen, A. (2007). Functional multivesicular bodies are required for autophagic clearance of protein aggregates associated with neurodegenerative disease. J Cell Biol *179*, 485-500.

Fiorentino, L., Pertica, C., Fiorini, M., Talora, C., Crescenzi, M., Castellani, L., Alema, S., Benedetti, P., and Segatto, O. (2000). Inhibition of ErbB-2 mitogenic and transforming activity by RALT, a mitogen-induced signal transducer which binds to the ErbB-2 kinase domain. Mol Cell Biol *20*, 7735-7750.

Fiorini, M., Ballaro, C., Sala, G., Falcone, G., Alema, S., and Segatto, O. (2002). Expression of RALT, a feedback inhibitor of ErbB receptors, is subjected to an integrated transcriptional and post-translational control. Oncogene *21*, 6530-6539.

Fisher, R.D., Chung, H.Y., Zhai, Q., Robinson, H., Sundquist, W.I., and Hill, C.P. (2007). Structural and biochemical studies of ALIX/AIP1 and its role in retrovirus budding. Cell *128*, 841-852.

Fivaz, M., Vilbois, F., Thurnheer, S., Pasquali, C., Abrami, L., Bickel, P.E., Parton, R.G., and van der Goot, F.G. (2002). Differential sorting and fate of endocytosed GPI-anchored proteins. EMBO J *21*, 3989-4000.

Flint, A.J., Tiganis, T., Barford, D., and Tonks, N.K. (1997). Development of "substrate-trapping" mutants to identify physiological substrates of protein tyrosine phosphatases. Proc Natl Acad Sci U S A *94*, 1680-1685.

Freeman, M. (2000). Feedback control of intercellular signalling in development. Nature *408*, 313-319.

French, A.R., Sudlow, G.P., Wiley, H.S., and Lauffenburger, D.A. (1994). Postendocytic trafficking of epidermal growth factor-receptor complexes is mediated through saturable and specific endosomal interactions. J Biol Chem *269*, 15749-15755.

French, A.R., Tadaki, D.K., Niyogi, S.K., and Lauffenburger, D.A. (1995). Intracellular trafficking of epidermal growth factor family ligands is directly influenced by the pH sensitivity of the receptor/ligand interaction. J Biol Chem *270*, 4334-4340.

Frosi, Y., Anastasi, S., Ballaro, C., Varsano, G., Castellani, L., Maspero, E., Polo, S., Alema, S., and Segatto, O. (2010). A two-tiered mechanism of EGFR inhibition by RALT/MIG6 via kinase suppression and receptor degradation. J Cell Biol *189*, 557-571.

Furthauer, M., Lin, W., Ang, S.L., Thisse, B., and Thisse, C. (2002). Sef is a feedback-induced antagonist of Ras/MAPK-mediated FGF signalling. Nat Cell Biol *4*, 170-174.

Futter, C.E., Felder, S., Schlessinger, J., Ullrich, A., and Hopkins, C.R. (1993). Annexin I is phosphorylated in the multivesicular body during the processing of the epidermal growth factor receptor. J Cell Biol *120*, 77-83.

Galcheva-Gargova, Z., Theroux, S.J., and Davis, R.J. (1995). The epidermal growth factor receptor is covalently linked to ubiquitin. Oncogene *11*, 2649-2655.

Gale, N.W., Kaplan, S., Lowenstein, E.J., Schlessinger, J., and Bar-Sagi, D. (1993). Grb2 mediates the EGF-dependent activation of guanine nucleotide exchange on Ras. Nature *363*, 88-92.

Gan, Z., Ram, S., Vaccaro, C., Ober, R.J., and Ward, E.S. (2009). Analyses of the recycling receptor, FcRn, in live cells reveal novel pathways for lysosomal delivery. Traffic *10*, 600-614.

Garrett, T.P., McKern, N.M., Lou, M., Elleman, T.C., Adams, T.E., Lovrecz, G.O., Kofler, M., Jorissen, R.N., Nice, E.C., Burgess, A.W.*, et al.* (2003). The crystal structure of a truncated ErbB2 ectodomain reveals an active conformation, poised to interact with other ErbB receptors. Mol Cell *11*, 495-505.

Garrett, T.P., McKern, N.M., Lou, M., Elleman, T.C., Adams, T.E., Lovrecz, G.O., Zhu, H.J., Walker, F., Frenkel, M.J., Hoyne, P.A.*, et al.* (2002). Crystal structure of a truncated epidermal growth factor receptor extracellular domain bound to transforming growth factor alpha. Cell *110*, 763-773.

Gassmann, M., Casagranda, F., Orioli, D., Simon, H., Lai, C., Klein, R., and Lemke, G. (1995). Aberrant neural and cardiac development in mice lacking the ErbB4 neuregulin receptor. Nature *378*, 390-394.

Gazit, A., Yaish, P., Gilon, C., and Levitzki, A. (1989). Tyrphostins I: synthesis and biological activity of protein tyrosine kinase inhibitors. J Med Chem *32*, 2344-2352.

Geiss, G.K., Bumgarner, R.E., Birditt, B., Dahl, T., Dowidar, N., Dunaway, D.L., Fell, H.P., Ferree, S., George, R.D., Grogan, T.*, et al.* (2008). Direct multiplexed measurement of gene expression with color-coded probe pairs. Nat Biotechnol *26*, 317-325.

Ghiglione, C., Amundadottir, L., Andresdottir, M., Bilder, D., Diamonti, J.A., Noselli, S., Perrimon, N., and Carraway, I.K. (2003). Mechanism of inhibition of the Drosophila and mammalian EGF receptors by the transmembrane protein Kekkon 1. Development *130*, 4483-4493.

Ghiglione, C., Carraway, K.L., 3rd, Amundadottir, L.T., Boswell, R.E., Perrimon, N., and Duffy, J.B. (1999). The transmembrane molecule kekkon 1 acts in a feedback loop to negatively regulate the activity of the Drosophila EGF receptor during oogenesis. Cell *96*, 847-856.

Ghosh, S., and Baltimore, D. (1990). Activation in vitro of NF-kappa B by phosphorylation of its inhibitor I kappa B. Nature *344*, 678-682.

Ghosh, S., and Hayden, M.S. (2008). New regulators of NF-kappaB in inflammation. Nat Rev Immunol *8*, 837-848.

Gilmore, J.L., Scott, J.A., Bouizar, Z., Robling, A., Pitfield, S.E., Riese, D.J., 2nd, and Foley, J. (2008). Amphiregulin-EGFR signaling regulates PTHrP gene expression in breast cancer cells. Breast Cancer Res Treat *110*, 493-505.

Gingras, M.C., Kharitidi, D., Chenard, V., Uetani, N., Bouchard, M., Tremblay, M.L., and Pause, A. (2009a). Expression analysis and essential role of the putative tyrosine phosphatase His-domain-containing protein tyrosine phosphatase (HD-PTP). Int J Dev Biol *53*, 1069-1074.

Gingras, M.C., Zhang, Y.L., Kharitidi, D., Barr, A.J., Knapp, S., Tremblay, M.L., and Pause, A. (2009b). HD-PTP is a catalytically inactive tyrosine phosphatase due to a conserved divergence in its phosphatase domain. PLoS One *4*, e5105.

Glenney, J.R., Jr., and Zokas, L. (1989). Novel tyrosine kinase substrates from Rous sarcoma virus-transformed cells are present in the membrane skeleton. J Cell Biol *108*, 2401-2408.

Goldoni, S., Iozzo, R.A., Kay, P., Campbell, S., McQuillan, A., Agnew, C., Zhu, J.X., Keene, D.R., Reed, C.C., and Iozzo, R.V. (2007). A soluble ectodomain of LRIG1 inhibits cancer cell growth by attenuating basal and ligand-dependent EGFR activity. Oncogene *26*, 368-381.

Gorden, P., Carpentier, J.L., Cohen, S., and Orci, L. (1978). Epidermal growth factor: morphological demonstration of binding, internalization, and lysosomal association in human fibroblasts. Proc Natl Acad Sci U S A *75*, 5025-5029.

Gotoh, N., Tojo, A., Hino, M., Yazaki, Y., and Shibuya, M. (1992). A highly conserved tyrosine residue at codon 845 within the kinase domain is not required for the transforming activity of human epidermal growth factor receptor. Biochem Biophys Res Commun *186*, 768-774.

Grant, B.D., and Donaldson, J.G. (2009). Pathways and mechanisms of endocytic recycling. Nat Rev Mol Cell Biol *10*, 597-608.

Graus-Porta, D., Beerli, R.R., Daly, J.M., and Hynes, N.E. (1997). ErbB-2, the preferred heterodimerization partner of all ErbB receptors, is a mediator of lateral signaling. EMBO J *16*, 1647-1655.

Grovdal, L.M., Stang, E., Sorkin, A., and Madshus, I.H. (2004). Direct interaction of Cbl with pTyr 1045 of the EGF receptor (EGFR) is required to sort the EGFR to lysosomes for degradation. Exp Cell Res *300*, 388-395.

Gruenberg, J. (2001). The endocytic pathway: a mosaic of domains. Nat Rev Mol Cell Biol *2*, 721-730.

Gruenberg, J. (2003). Lipids in endocytic membrane transport and sorting. Curr Opin Cell Biol *15*, 382-388.

Gruenberg, J. (2009). Viruses and endosome membrane dynamics. Curr Opin Cell Biol *21*, 582-588.

Gruenberg, J., and Maxfield, F.R. (1995). Membrane transport in the endocytic pathway. Curr Opin Cell Biol *7*, 552-563.

Gruenberg, J., and Stenmark, H. (2004). The biogenesis of multivesicular endosomes. Nat Rev Mol Cell Biol *5*, 317-323.

Gruenberg, J., and van der Goot, F.G. (2006). Mechanisms of pathogen entry through the endosomal compartments. Nat Rev Mol Cell Biol *7*, 495-504.

Gu, H., and Neel, B.G. (2003). The "Gab" in signal transduction. Trends Cell Biol *13*, 122-130.

Gullick, W.J. (1994). A new model for the interaction of EGF-like ligands with their receptors: the new one-two. Eur J Cancer *30A*, 2186.

Guo, D., Holmlund, C., Henriksson, R., and Hedman, H. (2004). The LRIG gene family has three vertebrate paralogs widely expressed in human and mouse tissues and a homolog in Ascidiacea. Genomics *84*, 157-165.

Gur, G., Rubin, C., Katz, M., Amit, I., Citri, A., Nilsson, J., Amariglio, N., Henriksson, R., Rechavi, G., Hedman, H., *et al.* (2004). LRIG1 restricts growth factor signaling by enhancing receptor ubiquitylation and degradation. EMBO J *23*, 3270-3281.

Guy, P.M., Platko, J.V., Cantley, L.C., Cerione, R.A., and Carraway, K.L., 3rd (1994). Insect cell-expressed p180erbB3 possesses an impaired tyrosine kinase activity. Proc Natl Acad Sci U S A *91*, 8132-8136.

Ha, J., Choi, H.S., Lee, Y., Kwon, H.J., Song, Y.W., and Kim, H.H. (2010). CXC chemokine ligand 2 induced by receptor activator of NF-kappa B ligand enhances osteoclastogenesis. J Immunol *184*, 4717-4724.

Hackel, P.O., Gishizky, M., and Ullrich, A. (2001). Mig-6 is a negative regulator of the epidermal growth factor receptor signal. Biol Chem *382*, 1649-1662.

Hacohen, N., Kramer, S., Sutherland, D., Hiromi, Y., and Krasnow, M.A. (1998). sprouty encodes a novel antagonist of FGF signaling that patterns apical branching of the Drosophila airways. Cell *92*, 253-263.

Haglund, K., Schmidt, M.H., Wong, E.S., Guy, G.R., and Dikic, I. (2005). Sprouty2 acts at the Cbl/CIN85 interface to inhibit epidermal growth factor receptor downregulation. EMBO Rep *6*, 635-641.

Haglund, K., Sigismund, S., Polo, S., Szymkiewicz, I., Di Fiore, P.P., and Dikic, I. (2003). Multiple monoubiquitination of RTKs is sufficient for their endocytosis and degradation. Nat Cell Biol *5*, 461-466.

Haigler, H., Ash, J.F., Singer, S.J., and Cohen, S. (1978). Visualization by fluorescence of the binding and internalization of epidermal growth factor in human carcinoma cells A-431. Proc Natl Acad Sci U S A *75*, 3317-3321.

Haigler, H.T., McKanna, J.A., and Cohen, S. (1979). Direct visualization of the binding and internalization of a ferritin conjugate of epidermal growth factor in human carcinoma cells A-431. J Cell Biol *81*, 382-395.

Haj, F.G., Markova, B., Klaman, L.D., Bohmer, F.D., and Neel, B.G. (2003). Regulation of receptor tyrosine kinase signaling by protein tyrosine phosphatase-1B. J Biol Chem *278*, 739-744.

Haj, F.G., Verveer, P.J., Squire, A., Neel, B.G., and Bastiaens, P.I. (2002). Imaging sites of receptor dephosphorylation by PTP1B on the surface of the endoplasmic reticulum. Science *295*, 1708-1711.

Hall, A., Marshall, C.J., Spurr, N.K., and Weiss, R.A. (1983). Identification of transforming gene in two human sarcoma cell lines as a new member of the ras gene family located on chromosome 1. Nature *303*, 396-400.

Hall, A.B., Jura, N., DaSilva, J., Jang, Y.J., Gong, D., and Bar-Sagi, D. (2003). hSpry2 is targeted to the ubiquitin-dependent proteasome pathway by c-Cbl. Curr Biol *13*, 308-314.

Han, W., Zhang, T., Yu, H., Foulke, J.G., and Tang, C.K. (2006). Hypophosphorylation of residue Y1045 leads to defective downregulation of EGFRvIII. Cancer Biol Ther *5*, 1361-1368.

Hancock, J.F., Cadwallader, K., Paterson, H., and Marshall, C.J. (1991). A CAAX or a CAAL motif and a second signal are sufficient for plasma membrane targeting of ras proteins. EMBO J *10*, 4033-4039.

Hanover, J.A., Beguinot, L., Willingham, M.C., and Pastan, I.H. (1985). Transit of receptors for epidermal growth factor and transferrin through clathrin-coated pits. Analysis of the kinetics of receptor entry. J Biol Chem *260*, 15938-15945.

Hanover, J.A., Willingham, M.C., and Pastan, I. (1984). Kinetics of transit of transferrin and epidermal growth factor through clathrin-coated membranes. Cell *39*, 283-293.

Hanson, P.I., Roth, R., Lin, Y., and Heuser, J.E. (2008). Plasma membrane deformation by circular arrays of ESCRT-III protein filaments. J Cell Biol *180*, 389-402.

Hanyaloglu, A.C., McCullagh, E., and von Zastrow, M. (2005). Essential role of Hrs in a recycling mechanism mediating functional resensitization of cell signaling. EMBO J *24*, 2265-2283.

Harding, A., Tian, T., Westbury, E., Frische, E., and Hancock, J.F. (2005). Subcellular localization determines MAP kinase signal output. Curr Biol *15*, 869-873.

Harris, R.C., Chung, E., and Coffey, R.J. (2003). EGF receptor ligands. Exp Cell Res *284*, 2-13.

Hart, M.J., Callow, M.G., Souza, B., and Polakis, P. (1996). IQGAP1, a calmodulin-binding protein with a rasGAP-related domain, is a potential effector for cdc42Hs. EMBO J *15*, 2997-3005.

Harte, M.T., and Gentry, L.E. (1995). Mutations within subdomain II of the extracellular region of epidermal growth factor receptor selectively alter TGF alpha binding. Arch Biochem Biophys *322*, 378-389.

Hashimoto, K., Ichiyama, T., Hasegawa, M., Hasegawa, S., Matsubara, T., and Furukawa, S. (2009). Cysteinyl leukotrienes induce monocyte chemoattractant protein-1 in human monocyte/macrophages via mitogen-activated protein kinase and nuclear factor-kappaB pathways. Int Arch Allergy Immunol *149*, 275-282.

Haslekas, C., Breen, K., Pedersen, K.W., Johannessen, L.E., Stang, E., and Madshus, I.H. (2005). The inhibitory effect of ErbB2 on epidermal growth factor-induced formation of clathrin-coated pits correlates with retention of epidermal growth factor receptor-ErbB2 oligomeric complexes at the plasma membrane. Mol Biol Cell *16*, 5832-5842.

Haugh, J.M., Huang, A.C., Wiley, H.S., Wells, A., and Lauffenburger, D.A. (1999a). Internalized epidermal growth factor receptors participate in the activation of p21(ras) in fibroblasts. J Biol Chem *274*, 34350-34360.

Haugh, J.M., Schooler, K., Wells, A., Wiley, H.S., and Lauffenburger, D.A. (1999b). Effect of epidermal growth factor receptor internalization on regulation of the phospholipase C-gamma1 signaling pathway. J Biol Chem *274*, 8958-8965.

Havrylov, S., Redowicz, M.J., and Buchman, V.L. (2010). Emerging roles of Ruk/CIN85 in vesicle-mediated transport, adhesion, migration and malignancy. Traffic *11*, 721-731.

Hayden, M.S., and Ghosh, S. (2008). Shared principles in NF-kappaB signaling. Cell *132*, 344-362.

Hedman, H., and Henriksson, R. (2007). LRIG inhibitors of growth factor signalling - double-edged swords in human cancer? Eur J Cancer *43*, 676-682.

Herbst, J.J., Opresko, L.K., Walsh, B.J., Lauffenburger, D.A., and Wiley, H.S. (1994). Regulation of postendocytic trafficking of the epidermal growth factor receptor through endosomal retention. J Biol Chem *269*, 12865-12873.

Herz, H.M., and Bergmann, A. (2009). Genetic analysis of ESCRT function in Drosophila: a tumour model for human Tsg101. Biochem Soc Trans *37*, 204-207.

Herz, H.M., Chen, Z., Scherr, H., Lackey, M., Bolduc, C., and Bergmann, A. (2006). vps25 mosaics display non-autonomous cell survival and overgrowth, and autonomous apoptosis. Development *133*, 1871-1880.

Hess, J., Angel, P., and Schorpp-Kistner, M. (2004). AP-1 subunits: quarrel and harmony among siblings. J Cell Sci *117*, 5965-5973.

Hicke, L., and Riezman, H. (1996). Ubiquitination of a yeast plasma membrane receptor signals its ligand-stimulated endocytosis. Cell *84*, 277-287.

Hilton, D.J., Richardson, R.T., Alexander, W.S., Viney, E.M., Willson, T.A., Sprigg, N.S., Starr, R., Nicholson, S.E., Metcalf, D., and Nicola, N.A. (1998). Twenty proteins containing a C-terminal SOCS box form five structural classes. Proc Natl Acad Sci U S A *95*, 114-119.

Hirano, S., Kawasaki, M., Ura, H., Kato, R., Raiborg, C., Stenmark, H., and Wakatsuki, S. (2006a). Double-sided ubiquitin binding of Hrs-UIM in endosomal protein sorting. Nat Struct Mol Biol *13*, 272-277.

Hirano, S., Suzuki, N., Slagsvold, T., Kawasaki, M., Trambaiolo, D., Kato, R., Stenmark, H., and Wakatsuki, S. (2006b). Structural basis of ubiquitin recognition by mammalian Eap45 GLUE domain. Nat Struct Mol Biol *13*, 1031-1032.

Hislop, J.N., Marley, A., and Von Zastrow, M. (2004). Role of mammalian vacuolar protein-sorting proteins in endocytic trafficking of a non-ubiquitinated G protein-coupled receptor to lysosomes. J Biol Chem *279*, 22522-22531.

Hoepfner, S., Severin, F., Cabezas, A., Habermann, B., Runge, A., Gillooly, D., Stenmark, H., and Zerial, M. (2005). Modulation of receptor recycling and degradation by the endosomal kinesin KIF16B. Cell *121*, 437-450.

Holgado-Madruga, M., Emlet, D.R., Moscatello, D.K., Godwin, A.K., and Wong, A.J. (1996). A Grb2-associated docking protein in EGF- and insulin-receptor signalling. Nature *379*, 560-564.

Honegger, A.M., Dull, T.J., Felder, S., Van Obberghen, E., Bellot, F., Szapary, D., Schmidt, A., Ullrich, A., and Schlessinger, J. (1987). Point mutation at the ATP binding site of EGF receptor abolishes protein-tyrosine kinase activity and alters cellular routing. Cell *51*, 199-209.

Huang, F., Khvorova, A., Marshall, W., and Sorkin, A. (2004a). Analysis of clathrin-mediated endocytosis of epidermal growth factor receptor by RNA interference. J Biol Chem *279*, 16657-16661.

Huang, F., Kirkpatrick, D., Jiang, X., Gygi, S., and Sorkin, A. (2006). Differential regulation of EGF receptor internalization and degradation by multiubiquitination within the kinase domain. Mol Cell *21*, 737-748.

Huang, J., Teng, L., Li, L., Liu, T., Chen, D., Xu, L.G., Zhai, Z., and Shu, H.B. (2004b). ZNF216 Is an A20-like and IkappaB kinase gamma-interacting inhibitor of NFkappaB activation. J Biol Chem *279*, 16847-16853.

Hubbard, S.R. (2004). Juxtamembrane autoinhibition in receptor tyrosine kinases. Nat Rev Mol Cell Biol *5*, 464-471.

Hubbard, S.R. (2006). EGF receptor activation: push comes to shove. Cell *125*, 1029-1031.

Hunter, T., Ling, N., and Cooper, J.A. (1984). Protein kinase C phosphorylation of the EGF receptor at a threonine residue close to the cytoplasmic face of the plasma membrane. Nature *311*, 480-483.

Hurley, J.H. (2008). ESCRT complexes and the biogenesis of multivesicular bodies. Curr Opin Cell Biol *20*, 4-11.

Hurley, J.H., and Hanson, P.I. (2010). Membrane budding and scission by the ESCRT machinery: it's all in the neck. Nat Rev Mol Cell Biol *11*, 556-566.

Huse, M., and Kuriyan, J. (2002). The conformational plasticity of protein kinases. Cell *109*, 275-282.

Hutter, D., Chen, P., Barnes, J., and Liu, Y. (2000). Catalytic activation of mitogen-activated protein (MAP) kinase phosphatase-1 by binding to p38 MAP kinase: critical role of the p38 C-terminal domain in its negative regulation. Biochem J *352 Pt 1*, 155-163.

Hynes, N.E., Horsch, K., Olayioye, M.A., and Badache, A. (2001). The ErbB receptor tyrosine family as signal integrators. Endocr Relat Cancer *8*, 151-159.

Hynes, N.E., and Lane, H.A. (2005). ERBB receptors and cancer: the complexity of targeted inhibitors. Nat Rev Cancer *5*, 341-354.

Ichioka, F., Takaya, E., Suzuki, H., Kajigaya, S., Buchman, V.L., Shibata, H., and Maki, M. (2007). HD-PTP and Alix share some membrane-traffic related proteins that interact with their Bro1 domains or proline-rich regions. Arch Biochem Biophys *457*, 142-149.

Im, Y.J., Wollert, T., Boura, E., and Hurley, J.H. (2009). Structure and function of the ESCRT-II-III interface in multivesicular body biogenesis. Dev Cell *17*, 234-243.

Impagnatiello, M.A., Weitzer, S., Gannon, G., Compagni, A., Cotten, M., and Christofori, G. (2001). Mammalian sprouty-1 and -2 are membrane-anchored phosphoprotein inhibitors of growth factor signaling in endothelial cells. J Cell Biol *152*, 1087-1098.

Ishibe, S., Joly, D., Liu, Z.X., and Cantley, L.G. (2004). Paxillin serves as an ERK-regulated scaffold for coordinating FAK and Rac activation in epithelial morphogenesis. Mol Cell *16*, 257-267.

Ishibe, S., Joly, D., Zhu, X., and Cantley, L.G. (2003). Phosphorylation-dependent paxillin-ERK association mediates hepatocyte growth factor-stimulated epithelial morphogenesis. Mol Cell *12*, 1275-1285.

Ito, M., Tchoua, U., Okamoto, M., and Tojo, H. (2002). Purification and properties of a phospholipase A2/lipase preferring phosphatidic acid, bis(monoacylglycerol) phosphate, and monoacylglycerol from rat testis. J Biol Chem *277*, 43674-43681.

Iwamoto, R., Handa, K., and Mekada, E. (1999). Contact-dependent growth inhibition and apoptosis of epidermal growth factor (EGF) receptor-expressing cells by the membrane-anchored form of heparin-binding EGF-like growth factor. J Biol Chem *274*, 25906-25912.

Iwamoto, Y., Chin, Y.E., Peng, X., and Fu, X.Y. (1998). Identification of a membrane-associated inhibitor(s) of epidermal growth factor-induced signal transducer and activator of transcription activation. J Biol Chem *273*, 18198-18204.

Iyer, V.R., Eisen, M.B., Ross, D.T., Schuler, G., Moore, T., Lee, J.C., Trent, J.M., Staudt, L.M., Hudson, J., Jr., Boguski, M.S.*, et al.* (1999). The transcriptional program in the response of human fibroblasts to serum. Science *283*, 83-87.

Jaaro, H., Rubinfeld, H., Hanoch, T., and Seger, R. (1997). Nuclear translocation of mitogen-activated protein kinase kinase (MEK1) in response to mitogenic stimulation. Proc Natl Acad Sci U S A *94*, 3742-3747.

Jahn, R., and Scheller, R.H. (2006). SNAREs--engines for membrane fusion. Nat Rev Mol Cell Biol *7*, 631-643.

Jansen, S.M., Sleumer, L.S., Damen, E., Meijer, I.M., van Zoelen, E.J., and van Leeuwen, J.E. (2009). ErbB2 and ErbB4 Cbl binding sites can functionally replace the ErbB1 Cbl binding site. Cell Signal *21*, 810-818.

Jeffrey, K.L., Camps, M., Rommel, C., and Mackay, C.R. (2007). Targeting dual-specificity phosphatases: manipulating MAP kinase signalling and immune responses. Nat Rev Drug Discov *6*, 391-403.

Jekely, G., and Rorth, P. (2003). Hrs mediates downregulation of multiple signalling receptors in Drosophila. EMBO Rep *4*, 1163-1168.

Jiang, X., Huang, F., Marusyk, A., and Sorkin, A. (2003). Grb2 regulates internalization of EGF receptors through clathrin-coated pits. Mol Biol Cell *14*, 858-870.

Jiang, X., and Sorkin, A. (2003). Epidermal growth factor receptor internalization through clathrin-coated pits requires Cbl RING finger and proline-rich domains but not receptor polyubiquitylation. Traffic *4*, 529-543.

Joazeiro, C.A., Wing, S.S., Huang, H., Leverson, J.D., Hunter, T., and Liu, Y.C. (1999). The tyrosine kinase negative regulator c-Cbl as a RING-type, E2-dependent ubiquitin-protein ligase. Science *286*, 309-312.

Johannessen, L.E., Pedersen, N.M., Pedersen, K.W., Madshus, I.H., and Stang, E. (2006). Activation of the epidermal growth factor (EGF) receptor induces formation of EGF receptor- and Grb2-containing clathrin-coated pits. Mol Cell Biol *26*, 389-401.

Jones, R.B., Gordus, A., Krall, J.A., and MacBeath, G. (2006). A quantitative protein interaction network for the ErbB receptors using protein microarrays. Nature *439*, 168-174.

Jones, S.M., and Kazlauskas, A. (2001). Growth-factor-dependent mitogenesis requires two distinct phases of signalling. Nat Cell Biol *3*, 165-172.

Jongeward, G.D., Clandinin, T.R., and Sternberg, P.W. (1995). sli-1, a negative regulator of let-23-mediated signaling in C. elegans. Genetics *139*, 1553-1566.

Jordens, I., Fernandez-Borja, M., Marsman, M., Dusseljee, S., Janssen, L., Calafat, J., Janssen, H., Wubbolts, R., and Neefjes, J. (2001). The Rab7 effector protein RILP controls lysosomal transport by inducing the recruitment of dynein-dynactin motors. Curr Biol *11*, 1680-1685.

Joutti, A., Brotherus, J., Renkonen, O., Laine, R., and Fischer, W. (1976). The stereochemical configuration of lysobisphosphatidic acid from rat liver, rabbit lung and pig lung. Biochim Biophys Acta *450*, 206-209.

Jouve, M., Sol-Foulon, N., Watson, S., Schwartz, O., and Benaroch, P. (2007). HIV-1 buds and accumulates in "nonacidic" endosomes of macrophages. Cell Host Microbe *2*, 85-95.

Jura, N., Endres, N.F., Engel, K., Deindl, S., Das, R., Lamers, M.H., Wemmer, D.E., Zhang, X., and Kuriyan, J. (2009). Mechanism for activation of the EGF receptor catalytic domain by the juxtamembrane segment. Cell *137*, 1293-1307.

Kamata, T., and Feramisco, J.R. (1984). Epidermal growth factor stimulates guanine nucleotide binding activity and phosphorylation of ras oncogene proteins. Nature *310*, 147-150.

Kamura, T., Burian, D., Yan, Q., Schmidt, S.L., Lane, W.S., Querido, E., Branton, P.E., Shilatifard, A., Conaway, R.C., and Conaway, J.W. (2001). Muf1, a novel Elongin BC-interacting leucine-rich repeat protein that can assemble with Cul5 and Rbx1 to reconstitute a ubiquitin ligase. J Biol Chem *276*, 29748-29753.

Kamura, T., Sato, S., Haque, D., Liu, L., Kaelin, W.G., Jr., Conaway, R.C., and Conaway, J.W. (1998). The Elongin BC complex interacts with the conserved SOCS-box motif present in members of the SOCS, ras, WD-40 repeat, and ankyrin repeat families. Genes Dev *12*, 3872-3881.

Kario, E., Marmor, M.D., Adamsky, K., Citri, A., Amit, I., Amariglio, N., Rechavi, G., and Yarden, Y. (2005). Suppressors of cytokine signaling 4 and 5 regulate epidermal growth factor receptor signaling. J Biol Chem *280*, 7038-7048.

Karlsson, M., Mathers, J., Dickinson, R.J., Mandl, M., and Keyse, S.M. (2004). Both nuclear-cytoplasmic shuttling of the dual specificity phosphatase MKP-3 and its ability to anchor MAP kinase in the cytoplasm are mediated by a conserved nuclear export signal. J Biol Chem *279*, 41882-41891.

Karnoub, A.E., and Weinberg, R.A. (2008). Ras oncogenes: split personalities. Nat Rev Mol Cell Biol *9*, 517-531.

Karten, B., Peake, K.B., and Vance, J.E. (2009). Mechanisms and consequences of impaired lipid trafficking in Niemann-Pick type C1-deficient mammalian cells. Biochim Biophys Acta *1791*, 659-670.

Kato, R., Nonami, A., Taketomi, T., Wakioka, T., Kuroiwa, A., Matsuda, Y., and Yoshimura, A. (2003). Molecular cloning of mammalian Spred-3 which suppresses tyrosine kinase-mediated Erk activation. Biochem Biophys Res Commun *302*, 767-772.

Katzmann, D.J., Babst, M., and Emr, S.D. (2001). Ubiquitin-dependent sorting into the multivesicular body pathway requires the function of a conserved endosomal protein sorting complex, ESCRT-I. Cell *106*, 145-155.

Katzmann, D.J., Odorizzi, G., and Emr, S.D. (2002). Receptor downregulation and multivesicular-body sorting. Nat Rev Mol Cell Biol *3*, 893-905.

Kaufmann, S.H. (2008). Immunology's foundation: the 100-year anniversary of the Nobel Prize to Paul Ehrlich and Elie Metchnikoff. Nat Immunol *9*, 705-712.

Kaushansky, A., Gordus, A., Budnik, B.A., Lane, W.S., Rush, J., and MacBeath, G. (2008). System-wide investigation of ErbB4 reveals 19 sites of Tyr phosphorylation that are unusually selective in their recruitment properties. Chem Biol *15*, 808-817.

Kazazic, M., Roepstorff, K., Johannessen, L.E., Pedersen, N.M., van Deurs, B., Stang, E., and Madshus, I.H. (2006). EGF-induced activation of the EGF receptor does not trigger mobilization of caveolae. Traffic *7*, 1518-1527.

Keilhack, H., Tenev, T., Nyakatura, E., Godovac-Zimmermann, J., Nielsen, L., Seedorf, K., and Bohmer, F.D. (1998). Phosphotyrosine 1173 mediates binding of the protein-tyrosine phosphatase SHP-1 to the epidermal growth factor receptor and attenuation of receptor signaling. J Biol Chem *273*, 24839-24846.

Keshet, Y., and Seger, R. (2010). The MAP kinase signaling cascades: a system of hundreds of components regulates a diverse array of physiological functions. Methods Mol Biol *661*, 3-38.

Keyse, S.M. (2000). Protein phosphatases and the regulation of mitogen-activated protein kinase signalling. Curr Opin Cell Biol *12*, 186-192.

Keyse, S.M., and Emslie, E.A. (1992). Oxidative stress and heat shock induce a human gene encoding a protein-tyrosine phosphatase. Nature *359*, 644-647.

Kholodenko, B.N. (2006). Cell-signalling dynamics in time and space. Nat Rev Mol Cell Biol *7*, 165-176.

Kholodenko, B.N., Hancock, J.F., and Kolch, W. (2010). Signalling ballet in space and time. Nat Rev Mol Cell Biol *11*, 414-426.

Kieffer, C., Skalicky, J.J., Morita, E., De Domenico, I., Ward, D.M., Kaplan, J., and Sundquist, W.I. (2008). Two distinct modes of ESCRT-III recognition are required for VPS4 functions in lysosomal protein targeting and HIV-1 budding. Dev Cell *15*, 62-73.

Kim, H.J., and Bar-Sagi, D. (2004). Modulation of signalling by Sprouty: a developing story. Nat Rev Mol Cell Biol *5*, 441-450.

Kim, J., Sitaraman, S., Hierro, A., Beach, B.M., Odorizzi, G., and Hurley, J.H. (2005). Structural basis for endosomal targeting by the Bro1 domain. Dev Cell *8*, 937-947.

King, J.A., Straffon, A.F., D'Abaco, G.M., Poon, C.L., I, S.T., Smith, C.M., Buchert, M., Corcoran, N.M., Hall, N.E., Callus, B.A.*, et al.* (2005). Distinct requirements for the Sprouty domain for functional activity of Spred proteins. Biochem J *388*, 445-454.

Kitano, H. (2004). Biological robustness. Nat Rev Genet *5*, 826-837.

Klein, D.E., Nappi, V.M., Reeves, G.T., Shvartsman, S.Y., and Lemmon, M.A. (2004). Argos inhibits epidermal growth factor receptor signalling by ligand sequestration. Nature *430*, 1040-1044.

Klingler-Hoffmann, M., Fodero-Tavoletti, M.T., Mishima, K., Narita, Y., Cavenee, W.K., Furnari, F.B., Huang, H.J., and Tiganis, T. (2001). The protein tyrosine phosphatase TCPTP suppresses the tumorigenicity of glioblastoma cells expressing a mutant epidermal growth factor receptor. J Biol Chem *276*, 46313-46318.

Kobayashi, T., Beuchat, M.H., Chevallier, J., Makino, A., Mayran, N., Escola, J.M., Lebrand, C., Cosson, P., and Gruenberg, J. (2002). Separation and characterization of late endosomal membrane domains. J Biol Chem *277*, 32157-32164.

Kobayashi, T., Beuchat, M.H., Lindsay, M., Frias, S., Palmiter, R.D., Sakuraba, H., Parton, R.G., and Gruenberg, J. (1999). Late endosomal membranes rich in lysobisphosphatidic acid regulate cholesterol transport. Nat Cell Biol *1*, 113-118.

Kobayashi, T., Stang, E., Fang, K.S., de Moerloose, P., Parton, R.G., and Gruenberg, J. (1998). A lipid associated with the antiphospholipid syndrome regulates endosome structure and function. Nature *392*, 193-197.

Kobayashi, T., Vischer, U.M., Rosnoblet, C., Lebrand, C., Lindsay, M., Parton, R.G., Kruithof, E.K., and Gruenberg, J. (2000). The tetraspanin CD63/lamp3 cycles between endocytic and secretory compartments in human endothelial cells. Mol Biol Cell *11*, 1829-1843.

Kochupurakkal, B.S., Harari, D., Di-Segni, A., Maik-Rachline, G., Lyass, L., Gur, G., Kerber, G., Citri, A., Lavi, S., Eilam, R.*, et al.* (2005). Epigen, the last ligand of ErbB receptors, reveals intricate relationships between affinity and mitogenicity. J Biol Chem *280*, 8503-8512.

Kolch, W. (2005). Coordinating ERK/MAPK signalling through scaffolds and inhibitors. Nat Rev Mol Cell Biol *6*, 827-837.

Kolling, R., and Hollenberg, C.P. (1994). The ABC-transporter Ste6 accumulates in the plasma membrane in a ubiquitinated form in endocytosis mutants. EMBO J *13*, 3261-3271.

Komada, M., and Kitamura, N. (1995). Growth factor-induced tyrosine phosphorylation of Hrs, a novel 115-kilodalton protein with a structurally conserved putative zinc finger domain. Mol Cell Biol *15*, 6213-6221.

Komander, D., Clague, M.J., and Urbe, S. (2009). Breaking the chains: structure and function of the deubiquitinases. Nat Rev Mol Cell Biol *10*, 550-563.

Kornfeld, K., Hom, D.B., and Horvitz, H.R. (1995). The ksr-1 gene encodes a novel protein kinase involved in Ras-mediated signaling in C. elegans. Cell *83*, 903-913.

Kornilova, E.S., Taverna, D., Hoeck, W., and Hynes, N.E. (1992). Surface expression of erbB-2 protein is post-transcriptionally regulated in mammary epithelial cells by epidermal growth factor and by the culture density. Oncogene *7*, 511-519.

Kortum, R.L., and Lewis, R.E. (2004). The molecular scaffold KSR1 regulates the proliferative and oncogenic potential of cells. Mol Cell Biol *24*, 4407-4416.

Koul, D., Takada, Y., Shen, R., Aggarwal, B.B., and Yung, W.K. (2006). PTEN enhances TNF-induced apoptosis through modulation of nuclear factor-kappaB signaling pathway in human glioma cells. Biochem Biophys Res Commun *350*, 463-471.

Kramer, S., Okabe, M., Hacohen, N., Krasnow, M.A., and Hiromi, Y. (1999). Sprouty: a common antagonist of FGF and EGF signaling pathways in Drosophila. Development *126*, 2515-2525.

Kranz, J.E., Satterberg, B., and Elion, E.A. (1994). The MAP kinase Fus3 associates with and phosphorylates the upstream signaling component Ste5. Genes Dev *8*, 313-327.

Kraut-Cohen, J., Muller, W.J., and Elson, A. (2008). Protein-tyrosine phosphatase epsilon regulates Shc signaling in a kinase-specific manner: increasing coherence in tyrosine phosphatase signaling. J Biol Chem *283*, 4612-4621.

Kumar, N., Wolf-Yadlin, A., White, F.M., and Lauffenburger, D.A. (2007). Modeling HER2 effects on cell behavior from mass spectrometry phosphotyrosine data. PLoS Comput Biol *3*, e4.

Kyuuma, M., Kikuchi, K., Kojima, K., Sugawara, Y., Sato, M., Mano, N., Goto, J., Takeshita, T., Yamamoto, A., Sugamura, K.*, et al.* (2007). AMSH, an ESCRT-III associated enzyme, deubiquitinates cargo on MVB/late endosomes. Cell Struct Funct *31*, 159-172.

Laederich, M.B., Funes-Duran, M., Yen, L., Ingalla, E., Wu, X., Carraway, K.L., 3rd, and Sweeney, C. (2004). The leucine-rich repeat protein LRIG1 is a negative regulator of ErbB family receptor tyrosine kinases. J Biol Chem *279*, 47050-47056.

Laemmli, U.K. (1970). Cleavage of structural proteins during the assembly of the head of bacteriophage T4. Nature *227*, 680-685.

Lakadamyali, M., Rust, M.J., and Zhuang, X. (2006). Ligands for clathrin-mediated endocytosis are differentially sorted into distinct populations of early endosomes. Cell *124*, 997-1009.

Lander, E.S., Linton, L.M., Birren, B., Nusbaum, C., Zody, M.C., Baldwin, J., Devon, K., Dewar, K., Doyle, M., FitzHugh, W.*, et al.* (2001). Initial sequencing and analysis of the human genome. Nature *409*, 860-921.

Langdon, W.Y. (1995). The cbl oncogene: a novel substrate of protein tyrosine kinases. Aust N Z J Med *25*, 859-864.

Langdon, W.Y., Hartley, J.W., Klinken, S.P., Ruscetti, S.K., and Morse, H.C., 3rd (1989). v-cbl, an oncogene from a dual-recombinant murine retrovirus that induces early B-lineage lymphomas. Proc Natl Acad Sci U S A *86*, 1168-1172.

Langelier, C., von Schwedler, U.K., Fisher, R.D., De Domenico, I., White, P.L., Hill, C.P., Kaplan, J., Ward, D., and Sundquist, W.I. (2006). Human ESCRT-II complex and its role in human immunodeficiency virus type 1 release. J Virol *80*, 9465-9480.

Laplante, M., and Sabatini, D.M. (2009). mTOR signaling at a glance. J Cell Sci *122*, 3589-3594.

Lata, S., Schoehn, G., Jain, A., Pires, R., Piehler, J., Gottlinger, H.G., and Weissenhorn, W. (2008). Helical structures of ESCRT-III are disassembled by VPS4. Science *321*, 1354-1357.

Le Blanc, I., Luyet, P.P., Pons, V., Ferguson, C., Emans, N., Petiot, A., Mayran, N., Demaurex, N., Faure, J., Sadoul, R.*, et al.* (2005). Endosome-to-cytosol transport of viral nucleocapsids. Nat Cell Biol *7*, 653-664.

Le Roy, C., and Wrana, J.L. (2005). Clathrin- and non-clathrin-mediated endocytic regulation of cell signalling. Nat Rev Mol Cell Biol *6*, 112-126.

Lebrand, C., Corti, M., Goodson, H., Cosson, P., Cavalli, V., Mayran, N., Faure, J., and Gruenberg, J. (2002). Late endosome motility depends on lipids via the small GTPase Rab7. EMBO J *21*, 1289-1300.

Lee, J.A., Beigneux, A., Ahmad, S.T., Young, S.G., and Gao, F.B. (2007a). ESCRT-III dysfunction causes autophagosome accumulation and neurodegeneration. Curr Biol *17*, 1561-1567.

Lee, K.F., Simon, H., Chen, H., Bates, B., Hung, M.C., and Hauser, C. (1995). Requirement for neuregulin receptor erbB2 in neural and cardiac development. Nature *378*, 394-398.

Lee, S., Joshi, A., Nagashima, K., Freed, E.O., and Hurley, J.H. (2007b). Structural basis for viral late-domain binding to Alix. Nat Struct Mol Biol *14*, 194-199.

Leevers, S.J., and Marshall, C.J. (1992). Activation of extracellular signal-regulated kinase, ERK2, by p21ras oncoprotein. EMBO J *11*, 569-574.

Lefkowitz, R.J., and Whalen, E.J. (2004). beta-arrestins: traffic cops of cell signaling. Curr Opin Cell Biol *16*, 162-168.

Lehr, S., Kotzka, J., Herkner, A., Klein, E., Siethoff, C., Knebel, B., Noelle, V., Bruning, J.C., Klein, H.W., Meyer, H.E.*, et al.* (1999). Identification of tyrosine phosphorylation sites in human Gab-1 protein by EGF receptor kinase in vitro. Biochemistry *38*, 151-159.

Lemmon, M.A. (2009). Ligand-induced ErbB receptor dimerization. Exp Cell Res *315*, 638-648.

Lemmon, M.A., Bu, Z., Ladbury, J.E., Zhou, M., Pinchasi, D., Lax, I., Engelman, D.M., and Schlessinger, J. (1997). Two EGF molecules contribute additively to stabilization of the EGFR dimer. EMBO J *16*, 281-294.

Lemmon, M.A., and Schlessinger, J. (2010). Cell signaling by receptor tyrosine kinases. Cell *141*, 1117-1134.

Lenferink, A.E., Pinkas-Kramarski, R., van de Poll, M.L., van Vugt, M.J., Klapper, L.N., Tzahar, E., Waterman, H., Sela, M., van Zoelen, E.J., and Yarden, Y. (1998). Differential endocytic routing of homo- and hetero-dimeric ErbB tyrosine kinases confers signaling superiority to receptor heterodimers. EMBO J *17*, 3385-3397.

Leprince, D., Gegonne, A., Coll, J., de Taisne, C., Schneeberger, A., Lagrou, C., and Stehelin, D. (1983). A putative second cell-derived oncogene of the avian leukaemia retrovirus E26. Nature *306*, 395-397.

Lerebours, F., Vacher, S., Andrieu, C., Espie, M., Marty, M., Lidereau, R., and Bieche, I. (2008). NF-kappa B genes have a major role in inflammatory breast cancer. BMC Cancer *8*, 41.

Levchenko, A., Bruck, J., and Sternberg, P.W. (2000). Scaffold proteins may biphasically affect the levels of mitogen-activated protein kinase signaling and reduce its threshold properties. Proc Natl Acad Sci U S A *97*, 5818-5823.

Levkowitz, G., Klapper, L.N., Tzahar, E., Freywald, A., Sela, M., and Yarden, Y. (1996). Coupling of the c-Cbl protooncogene product to ErbB-1/EGF-receptor but not to other ErbB proteins. Oncogene *12*, 1117-1125.

Levkowitz, G., Waterman, H., Ettenberg, S.A., Katz, M., Tsygankov, A.Y., Alroy, I., Lavi, S., Iwai, K., Reiss, Y., Ciechanover, A.*, et al.* (1999). Ubiquitin ligase activity and tyrosine phosphorylation underlie suppression of growth factor signaling by c-Cbl/Sli-1. Mol Cell *4*, 1029-1040.

Levkowitz, G., Waterman, H., Zamir, E., Kam, Z., Oved, S., Langdon, W.Y., Beguinot, L., Geiger, B., and Yarden, Y. (1998). c-Cbl/Sli-1 regulates endocytic sorting and ubiquitination of the epidermal growth factor receptor. Genes Dev *12*, 3663-3674.

Li, L., and Cohen, S.N. (1996). Tsg101: a novel tumor susceptibility gene isolated by controlled homozygous functional knockout of allelic loci in mammalian cells. Cell *85*, 319-329.

Li, N., Batzer, A., Daly, R., Yajnik, V., Skolnik, E., Chardin, P., Bar-Sagi, D., Margolis, B., and Schlessinger, J. (1993). Guanine-nucleotide-releasing factor hSos1 binds to Grb2 and links receptor tyrosine kinases to Ras signalling. Nature *363*, 85-88.

Li, X., Yang, Y., and Ashwell, J.D. (2002). TNF-RII and c-IAP1 mediate ubiquitination and degradation of TRAF2. Nature *416*, 345-347.

Lim, J., Yusoff, P., Wong, E.S., Chandramouli, S., Lao, D.H., Fong, C.W., and Guy, G.R. (2002). The cysteine-rich sprouty translocation domain targets mitogen-activated protein kinase inhibitory proteins to phosphatidylinositol 4,5-bisphosphate in plasma membranes. Mol Cell Biol *22*, 7953-7966.

Lin, C.H., MacGurn, J.A., Chu, T., Stefan, C.J., and Emr, S.D. (2008). Arrestin-related ubiquitin-ligase adaptors regulate endocytosis and protein turnover at the cell surface. Cell *135*, 714-725.

Lin, C.R., Chen, W.S., Lazar, C.S., Carpenter, C.D., Gill, G.N., Evans, R.M., and Rosenfeld, M.G. (1986). Protein kinase C phosphorylation at Thr 654 of the unoccupied EGF receptor and EGF binding regulate functional receptor loss by independent mechanisms. Cell *44*, 839-848.

Lin, X., O'Mahony, A., Mu, Y., Geleziunas, R., and Greene, W.C. (2000). Protein kinase C-theta participates in NF-kappaB activation induced by CD3-CD28 costimulation through selective activation of IkappaB kinase beta. Mol Cell Biol *20*, 2933-2940.

Linding, R., Jensen, L.J., Ostheimer, G.J., van Vugt, M.A., Jorgensen, C., Miron, I.M., Diella, F., Colwill, K., Taylor, L., Elder, K.*, et al.* (2007). Systematic discovery of in vivo phosphorylation networks. Cell *129*, 1415-1426.

Liston, P., Roy, N., Tamai, K., Lefebvre, C., Baird, S., Cherton-Horvat, G., Farahani, R., McLean, M., Ikeda, J.E., MacKenzie, A.*, et al.* (1996). Suppression of apoptosis in mammalian cells by NAIP and a related family of IAP genes. Nature *379*, 349-353.

Liu, F., and Chernoff, J. (1997). Protein tyrosine phosphatase 1B interacts with and is tyrosine phosphorylated by the epidermal growth factor receptor. Biochem J *327 (Pt 1)*, 139-145.

Liu, R.T., Huang, C.C., You, H.L., Chou, F.F., Hu, C.C., Chao, F.P., Chen, C.M., and Cheng, J.T. (2002). Overexpression of tumor susceptibility gene TSG101 in human papillary thyroid carcinomas. Oncogene *21*, 4830-4837.

Lloyd, T.E., Atkinson, R., Wu, M.N., Zhou, Y., Pennetta, G., and Bellen, H.J. (2002). Hrs regulates endosome membrane invagination and tyrosine kinase receptor signaling in Drosophila. Cell *108*, 261-269.

Lock, P., I, S.T., Straffon, A.F., Schieb, H., Hovens, C.M., and Stylli, S.S. (2006). Spred-2 steady-state levels are regulated by phosphorylation and Cbl-mediated ubiquitination. Biochem Biophys Res Commun *351*, 1018-1023.

Lombardi, D., Soldati, T., Riederer, M.A., Goda, Y., Zerial, M., and Pfeffer, S.R. (1993). Rab9 functions in transport between late endosomes and the trans Golgi network. EMBO J *12*, 677-682.

Longva, K.E., Blystad, F.D., Stang, E., Larsen, A.M., Johannessen, L.E., and Madshus, I.H. (2002). Ubiquitination and proteasomal activity is required for transport of the EGF receptor to inner membranes of multivesicular bodies. J Cell Biol *156*, 843-854.

Luetteke, N.C., Qiu, T.H., Fenton, S.E., Troyer, K.L., Riedel, R.F., Chang, A., and Lee, D.C. (1999). Targeted inactivation of the EGF and amphiregulin genes reveals distinct roles for EGF receptor ligands in mouse mammary gland development. Development *126*, 2739-2750.

Lund, K.A., Opresko, L.K., Starbuck, C., Walsh, B.J., and Wiley, H.S. (1990). Quantitative analysis of the endocytic system involved in hormone-induced receptor internalization. J Biol Chem *265*, 15713-15723.

Luttrell, L.M. (2008). Reviews in molecular biology and biotechnology: transmembrane signaling by G protein-coupled receptors. Mol Biotechnol *39*, 239-264.

Luttrell, L.M., Ferguson, S.S., Daaka, Y., Miller, W.E., Maudsley, S., Della Rocca, G.J., Lin, F., Kawakatsu, H., Owada, K., Luttrell, D.K.*, et al.* (1999). Beta-arrestin-dependent formation of beta2 adrenergic receptor-Src protein kinase complexes. Science *283*, 655-661.

Luttrell, L.M., Roudabush, F.L., Choy, E.W., Miller, W.E., Field, M.E., Pierce, K.L., and Lefkowitz, R.J. (2001). Activation and targeting of extracellular signal-regulated kinases by beta-arrestin scaffolds. Proc Natl Acad Sci U S A *98*, 2449-2454.

Luyet, P.P., Falguieres, T., Pons, V., Pattnaik, A.K., and Gruenberg, J. (2008). The ESCRT-I subunit TSG101 controls endosome-to-cytosol release of viral RNA. Traffic *9*, 2279-2290.

Luzio, J.P., Parkinson, M.D., Gray, S.R., and Bright, N.A. (2009). The delivery of endocytosed cargo to lysosomes. Biochem Soc Trans *37*, 1019-1021.

Luzio, J.P., Pryor, P.R., and Bright, N.A. (2007). Lysosomes: fusion and function. Nat Rev Mol Cell Biol *8*, 622-632.

Luzio, J.P., Pryor, P.R., Gray, S.R., Gratian, M.J., Piper, R.C., and Bright, N.A. (2005). Membrane traffic to and from lysosomes. Biochem Soc Symp, 77-86.

Macdonald-Obermann, J.L., and Pike, L.J. (2009). The intracellular juxtamembrane domain of the epidermal growth factor (EGF) receptor is responsible for the allosteric regulation of EGF binding. J Biol Chem *284*, 13570-13576.

Malerod, L., Stuffers, S., Brech, A., and Stenmark, H. (2007). Vps22/EAP30 in ESCRT-II mediates endosomal sorting of growth factor and chemokine receptors destined for lysosomal degradation. Traffic *8*, 1617-1629.

Malkov, V.A., Serikawa, K.A., Balantac, N., Watters, J., Geiss, G., Mashadi-Hossein, A., and Fare, T. (2009). Multiplexed measurements of gene signatures in different analytes using the Nanostring nCounter Assay System. BMC Res Notes *2*, 80.

Manicassamy, S., Gupta, S., and Sun, Z. (2006). Selective function of PKC-theta in T cells. Cell Mol Immunol *3*, 263-270.

Mann, G.B., Fowler, K.J., Gabriel, A., Nice, E.C., Williams, R.L., and Dunn, A.R. (1993). Mice with a null mutation of the TGF alpha gene have abnormal skin architecture, wavy hair, and curly whiskers and often develop corneal inflammation. Cell *73*, 249-261.

Mariotti, M., Castiglioni, S., Garcia-Manteiga, J.M., Beguinot, L., and Maier, J.A. (2009a). HD-PTP inhibits endothelial migration through its interaction with Src. Int J Biochem Cell Biol *41*, 687-693.

Mariotti, M., Castiglioni, S., and Maier, J.A. (2009b). Inhibition of T24 human bladder carcinoma cell migration by RNA interference suppressing the expression of HD-PTP. Cancer Lett *273*, 155-163.

Marsh, M., Theusner, K., and Pelchen-Matthews, A. (2009). HIV assembly and budding in macrophages. Biochem Soc Trans *37*, 185-189.

Marshall, C.J. (1995). Specificity of receptor tyrosine kinase signaling: transient versus sustained extracellular signal-regulated kinase activation. Cell *80*, 179-185.

Marti, U., Burwen, S.J., Wells, A., Barker, M.E., Huling, S., Feren, A.M., and Jones, A.L. (1991). Localization of epidermal growth factor receptor in hepatocyte nuclei. Hepatology *13*, 15-20.

Mason, J.M., Morrison, D.J., Bassit, B., Dimri, M., Band, H., Licht, J.D., and Gross, I. (2004). Tyrosine phosphorylation of Sprouty proteins regulates their ability to inhibit growth factor signaling: a dual feedback loop. Mol Biol Cell *15*, 2176-2188.

Mason, J.M., Morrison, D.J., Basson, M.A., and Licht, J.D. (2006). Sprouty proteins: multifaceted negative-feedback regulators of receptor tyrosine kinase signaling. Trends Cell Biol *16*, 45-54.

Masuda, K., Shima, H., Watanabe, M., and Kikuchi, K. (2001). MKP-7, a novel mitogen-activated protein kinase phosphatase, functions as a shuttle protein. J Biol Chem *276*, 39002-39011.

Matheny, S.A., Chen, C., Kortum, R.L., Razidlo, G.L., Lewis, R.E., and White, M.A. (2004). Ras regulates assembly of mitogenic signalling complexes through the effector protein IMP. Nature *427*, 256-260.

Matsuo, H., Chevallier, J., Mayran, N., Le Blanc, I., Ferguson, C., Faure, J., Blanc, N.S., Matile, S., Dubochet, J., Sadoul, R.*, et al.* (2004). Role of LBPA and Alix in multivesicular liposome formation and endosome organization. Science *303*, 531-534.

Mattoon, D.R., Lamothe, B., Lax, I., and Schlessinger, J. (2004). The docking protein Gab1 is the primary mediator of EGF-stimulated activation of the PI-3K/Akt cell survival pathway. BMC Biol *2*, 24.

Maxfield, F.R., and McGraw, T.E. (2004). Endocytic recycling. Nat Rev Mol Cell Biol *5*, 121-132.

Mayor, S., and Pagano, R.E. (2007). Pathways of clathrin-independent endocytosis. Nat Rev Mol Cell Biol *8*, 603-612.

Mayran, N., Parton, R.G., and Gruenberg, J. (2003). Annexin II regulates multivesicular endosome biogenesis in the degradation pathway of animal cells. EMBO J *22*, 3242-3253.

McCallum, S.J., Wu, W.J., and Cerione, R.A. (1996). Identification of a putative effector for Cdc42Hs with high sequence similarity to the RasGAP-related protein IQGAP1 and a Cdc42Hs binding partner with similarity to IQGAP2. J Biol Chem *271*, 21732-21737.

McCubrey, J.A., Steelman, L.S., Chappell, W.H., Abrams, S.L., Wong, E.W., Chang, F., Lehmann, B., Terrian, D.M., Milella, M., Tafuri, A.*, et al.* (2007). Roles of the Raf/MEK/ERK pathway in cell growth, malignant transformation and drug resistance. Biochim Biophys Acta *1773*, 1263-1284.

McCullough, J., Clague, M.J., and Urbe, S. (2004). AMSH is an endosome-associated ubiquitin isopeptidase. J Cell Biol *166*, 487-492.

McCullough, J., Fisher, R.D., Whitby, F.G., Sundquist, W.I., and Hill, C.P. (2008). ALIX-CHMP4 interactions in the human ESCRT pathway. Proc Natl Acad Sci U S A *105*, 7687-7691.

McCullough, J., Row, P.E., Lorenzo, O., Doherty, M., Beynon, R., Clague, M.J., and Urbe, S. (2006). Activation of the endosome-associated ubiquitin isopeptidase AMSH by STAM, a component of the multivesicular body-sorting machinery. Curr Biol *16*, 160-165.

McDonald, P.H., Chow, C.W., Miller, W.E., Laporte, S.A., Field, M.E., Lin, F.T., Davis, R.J., and Lefkowitz, R.J. (2000). Beta-arrestin 2: a receptor-regulated MAPK scaffold for the activation of JNK3. Science *290*, 1574-1577.

McNatt, M.W., McKittrick, I., West, M., and Odorizzi, G. (2007). Direct binding to Rsp5 mediates ubiquitin-independent sorting of Sna3 via the multivesicular body pathway. Mol Biol Cell *18*, 697-706.

Mellman, I. (1996). Endocytosis and molecular sorting. Annu Rev Cell Dev Biol *12*, 575-625.

Mellman, I., Fuchs, R., and Helenius, A. (1986). Acidification of the endocytic and exocytic pathways. Annu Rev Biochem *55*, 663-700.

Melman, L., Geuze, H.J., Li, Y., McCormick, L.M., Van Kerkhof, P., Strous, G.J., Schwartz, A.L., and Bu, G. (2002). Proteasome regulates the delivery of LDL receptor-related protein into the degradation pathway. Mol Biol Cell *13*, 3325-3335.

Mendrola, J.M., Berger, M.B., King, M.C., and Lemmon, M.A. (2002). The single transmembrane domains of ErbB receptors self-associate in cell membranes. J Biol Chem *277*, 4704-4712.

Meyer, D., and Birchmeier, C. (1995). Multiple essential functions of neuregulin in development. Nature *378*, 386-390.

Miaczynska, M., Pelkmans, L., and Zerial, M. (2004). Not just a sink: endosomes in control of signal transduction. Curr Opin Cell Biol *16*, 400-406.

Miaczynska, M., and Zerial, M. (2002). Mosaic organization of the endocytic pathway. Exp Cell Res *272*, 8-14.

Michaud, N.R., Therrien, M., Cacace, A., Edsall, L.C., Spiegel, S., Rubin, G.M., and Morrison, D.K. (1997). KSR stimulates Raf-1 activity in a kinase-independent manner. Proc Natl Acad Sci U S A *94*, 12792-12796.

Miettinen, P.J., Berger, J.E., Meneses, J., Phung, Y., Pedersen, R.A., Werb, Z., and Derynck, R. (1995). Epithelial immaturity and multiorgan failure in mice lacking epidermal growth factor receptor. Nature *376*, 337-341.

Minogue, S., Waugh, M.G., De Matteis, M.A., Stephens, D.J., Berditchevski, F., and Hsuan, J.J. (2006). Phosphatidylinositol 4-kinase is required for endosomal trafficking and degradation of the EGF receptor. J Cell Sci *119*, 571-581.

Minowada, G., Jarvis, L.A., Chi, C.L., Neubuser, A., Sun, X., Hacohen, N., Krasnow, M.A., and Martin, G.R. (1999). Vertebrate Sprouty genes are induced by FGF signaling and can cause chondrodysplasia when overexpressed. Development *126*, 4465-4475.

Mittal, R., and McMahon, H.T. (2009). Arrestins as adaptors for ubiquitination in endocytosis and sorting. EMBO Rep *10*, 41-43.

Miura, G.I., Roignant, J.Y., Wassef, M., and Treisman, J.E. (2008). Myopic acts in the endocytic pathway to enhance signaling by the Drosophila EGF receptor. Development *135*, 1913-1922.

Mobius, W., van Donselaar, E., Ohno-Iwashita, Y., Shimada, Y., Heijnen, H.F., Slot, J.W., and Geuze, H.J. (2003). Recycling compartments and the internal vesicles of multivesicular bodies harbor most of the cholesterol found in the endocytic pathway. Traffic *4*, 222-231.

Moodie, S.A., Willumsen, B.M., Weber, M.J., and Wolfman, A. (1993). Complexes of Ras.GTP with Raf-1 and mitogen-activated protein kinase kinase. Science *260*, 1658-1661.

Morandell, S., Stasyk, T., Skvortsov, S., Ascher, S., and Huber, L.A. (2008). Quantitative proteomics and phosphoproteomics reveal novel insights into complexity and dynamics of the EGFR signaling network. Proteomics *8*, 4383-4401.

Morel, E., Parton, R.G., and Gruenberg, J. (2009). Annexin A2-dependent polymerization of actin mediates endosome biogenesis. Dev Cell *16*, 445-457.

Mori, S., Heldin, C.H., and Claesson-Welsh, L. (1992). Ligand-induced polyubiquitination of the platelet-derived growth factor beta-receptor. J Biol Chem *267*, 6429-6434.

Morita, E., Sandrin, V., Alam, S.L., Eckert, D.M., Gygi, S.P., and Sundquist, W.I. (2007a). Identification of human MVB12 proteins as ESCRT-I subunits that function in HIV budding. Cell Host Microbe *2*, 41-53.

Morita, E., Sandrin, V., Chung, H.Y., Morham, S.G., Gygi, S.P., Rodesch, C.K., and Sundquist, W.I. (2007b). Human ESCRT and ALIX proteins interact with proteins of the midbody and function in cytokinesis. EMBO J *26*, 4215-4227.

Morrison, D.K. (2001). KSR: a MAPK scaffold of the Ras pathway? J Cell Sci *114*, 1609-1612.

Mosesson, Y., Shtiegman, K., Katz, M., Zwang, Y., Vereb, G., Szollosi, J., and Yarden, Y. (2003). Endocytosis of receptor tyrosine kinases is driven by monoubiquitylation, not polyubiquitylation. J Biol Chem *278*, 21323-21326.

Motley, A., Bright, N.A., Seaman, M.N., and Robinson, M.S. (2003). Clathrin-mediated endocytosis in AP-2-depleted cells. J Cell Biol *162*, 909-918.

Mukherjee, S., Soe, T.T., and Maxfield, F.R. (1999). Endocytic sorting of lipid analogues differing solely in the chemistry of their hydrophobic tails. J Cell Biol *144*, 1271-1284.

Mukhopadhyay, A., Funato, K., and Stahl, P.D. (1997). Rab7 regulates transport from early to late endocytic compartments in Xenopus oocytes. J Biol Chem *272*, 13055-13059.

Muller, J., Ory, S., Copeland, T., Piwnica-Worms, H., and Morrison, D.K. (2001). C-TAK1 regulates Ras signaling by phosphorylating the MAPK scaffold, KSR1. Mol Cell *8*, 983-993.

Mullock, B.M., Bright, N.A., Fearon, C.W., Gray, S.R., and Luzio, J.P. (1998). Fusion of lysosomes with late endosomes produces a hybrid organelle of intermediate density and is NSF dependent. J Cell Biol *140*, 591-601.

Murphy, L.O., MacKeigan, J.P., and Blenis, J. (2004). A network of immediate early gene products propagates subtle differences in mitogen-activated protein kinase signal amplitude and duration. Mol Cell Biol *24*, 144-153.

Murphy, L.O., Smith, S., Chen, R.H., Fingar, D.C., and Blenis, J. (2002). Molecular interpretation of ERK signal duration by immediate early gene products. Nat Cell Biol *4*, 556-564.

Nada, S., Hondo, A., Kasai, A., Koike, M., Saito, K., Uchiyama, Y., and Okada, M. (2009). The novel lipid raft adaptor p18 controls endosome dynamics by anchoring the MEK-ERK pathway to late endosomes. EMBO J *28*, 477-489.

Nagashima, T., Shimodaira, H., Ide, K., Nakakuki, T., Tani, Y., Takahashi, K., Yumoto, N., and Hatakeyama, M. (2007). Quantitative transcriptional control of ErbB receptor signaling undergoes graded to biphasic response for cell differentiation. J Biol Chem *282*, 4045-4056.

Naka, T., Narazaki, M., Hirata, M., Matsumoto, T., Minamoto, S., Aono, A., Nishimoto, N., Kajita, T., Taga, T., Yoshizaki, K.*, et al.* (1997). Structure and function of a new STAT-induced STAT inhibitor. Nature *387*, 924-929.

Nguyen, D.G., Booth, A., Gould, S.J., and Hildreth, J.E. (2003). Evidence that HIV budding in primary macrophages occurs through the exosome release pathway. J Biol Chem *278*, 52347-52354.

Nicholson, S.E., Metcalf, D., Sprigg, N.S., Columbus, R., Walker, F., Silva, A., Cary, D., Willson, T.A., Zhang, J.G., Hilton, D.J.*, et al.* (2005). Suppressor of cytokine signaling (SOCS)-5 is a potential negative regulator of epidermal growth factor signaling. Proc Natl Acad Sci U S A *102*, 2328-2333.

Nickas, M.E., and Yaffe, M.P. (1996). BRO1, a novel gene that interacts with components of the Pkc1p-mitogen-activated protein kinase pathway in Saccharomyces cerevisiae. Mol Cell Biol *16*, 2585-2593.

Nikko, E., Sullivan, J.A., and Pelham, H.R. (2008). Arrestin-like proteins mediate ubiquitination and endocytosis of the yeast metal transporter Smf1. EMBO Rep *9*, 1216-1221.

Nilsson, J., Vallbo, C., Guo, D., Golovleva, I., Hallberg, B., Henriksson, R., and Hedman, H. (2001). Cloning, characterization, and expression of human LIG1. Biochem Biophys Res Commun *284*, 1155-1161.

Nonami, A., Kato, R., Taniguchi, K., Yoshiga, D., Taketomi, T., Fukuyama, S., Harada, M., Sasaki, A., and Yoshimura, A. (2004). Spred-1 negatively regulates interleukin-3-mediated ERK/mitogen-activated protein (MAP) kinase activation in hematopoietic cells. J Biol Chem *279*, 52543-52551.

Normanno, N., Bianco, C., De Luca, A., and Salomon, D.S. (2001). The role of EGF-related peptides in tumor growth. Front Biosci *6*, D685-707.

Normanno, N., Bianco, C., Strizzi, L., Mancino, M., Maiello, M.R., De Luca, A., Caponigro, F., and Salomon, D.S. (2005). The ErbB receptors and their ligands in cancer: an overview. Curr Drug Targets *6*, 243-257.

Normanno, N., De Luca, A., Bianco, C., Strizzi, L., Mancino, M., Maiello, M.R., Carotenuto, A., De Feo, G., Caponigro, F., and Salomon, D.S. (2006). Epidermal growth factor receptor (EGFR) signaling in cancer. Gene *366*, 2-16.

Northwood, I.C., Gonzalez, F.A., Wartmann, M., Raden, D.L., and Davis, R.J. (1991). Isolation and characterization of two growth factor-stimulated protein kinases that phosphorylate the epidermal growth factor receptor at threonine 669. J Biol Chem *266*, 15266-15276.

Novikoff, A.B., Beaufay, H., and De Duve, C. (1956). Electron microscopy of lysosomerich fractions from rat liver. J Biophys Biochem Cytol *2*, 179-184.

Nunn, M.F., Seeburg, P.H., Moscovici, C., and Duesberg, P.H. (1983). Tripartite structure of the avian erythroblastosis virus E26 transforming gene. Nature *306*, 391-395.

Obita, T., Saksena, S., Ghazi-Tabatabai, S., Gill, D.J., Perisic, O., Emr, S.D., and Williams, R.L. (2007). Structural basis for selective recognition of ESCRT-III by the AAA ATPase Vps4. Nature *449*, 735-739.

Oestreich, A.J., Aboian, M., Lee, J., Azmi, I., Payne, J., Issaka, R., Davies, B.A., and Katzmann, D.J. (2007a). Characterization of multiple multivesicular body sorting determinants within Sna3: a role for the ubiquitin ligase Rsp5. Mol Biol Cell *18*, 707-720.

Oestreich, A.J., Davies, B.A., Payne, J.A., and Katzmann, D.J. (2007b). Mvb12 is a novel member of ESCRT-I involved in cargo selection by the multivesicular body pathway. Mol Biol Cell *18*, 646-657.

Offterdinger, M., and Bastiaens, P.I. (2008). Prolonged EGFR signaling by ERBB2-mediated sequestration at the plasma membrane. Traffic *9*, 147-155.

Ogiso, H., Ishitani, R., Nureki, O., Fukai, S., Yamanaka, M., Kim, J.H., Saito, K., Sakamoto, A., Inoue, M., Shirouzu, M.*, et al.* (2002). Crystal structure of the complex of human epidermal growth factor and receptor extracellular domains. Cell *110*, 775-787.

Oh, K.B., Stanton, M.J., West, W.W., Todd, G.L., and Wagner, K.U. (2007). Tsg101 is upregulated in a subset of invasive human breast cancers and its targeted overexpression in transgenic mice reveals weak oncogenic properties for mammary cancer initiation. Oncogene *26*, 5950-5959.

Ohtsu, H., Dempsey, P.J., and Eguchi, S. (2006). ADAMs as mediators of EGF receptor transactivation by G protein-coupled receptors. Am J Physiol Cell Physiol *291*, C1-10.

Oksvold, M.P., Skarpen, E., Lindeman, B., Roos, N., and Huitfeldt, H.S. (2000). Immunocytochemical localization of Shc and activated EGF receptor in early endosomes after EGF stimulation of HeLa cells. J Histochem Cytochem *48*, 21-33.

Olayioye, M.A., Beuvink, I., Horsch, K., Daly, J.M., and Hynes, N.E. (1999). ErbB receptor-induced activation of stat transcription factors is mediated by Src tyrosine kinases. J Biol Chem *274*, 17209-17218.

Olayioye, M.A., Graus-Porta, D., Beerli, R.R., Rohrer, J., Gay, B., and Hynes, N.E. (1998). ErbB-1 and ErbB-2 acquire distinct signaling properties dependent upon their dimerization partner. Mol Cell Biol *18*, 5042-5051.

Olsen, J.V., Blagoev, B., Gnad, F., Macek, B., Kumar, C., Mortensen, P., and Mann, M. (2006). Global, in vivo, and site-specific phosphorylation dynamics in signaling networks. Cell *127*, 635-648.

Omerovic, J., Santangelo, L., Puggioni, E.M., Marrocco, J., Dall'Armi, C., Palumbo, C., Belleudi, F., Di Marcotullio, L., Frati, L., Torrisi, M.R.*, et al.* (2007). The E3 ligase Aip4/Itch ubiquitinates and targets ErbB-4 for degradation. FASEB J *21*, 2849-2862.

Ono, A., and Freed, E.O. (2004). Cell-type-dependent targeting of human immunodeficiency virus type 1 assembly to the plasma membrane and the multivesicular body. J Virol *78*, 1552-1563.

Orth, J.D., Krueger, E.W., Weller, S.G., and McNiven, M.A. (2006). A novel endocytic mechanism of epidermal growth factor receptor sequestration and internalization. Cancer Res *66*, 3603-3610.

Ory, S., Zhou, M., Conrads, T.P., Veenstra, T.D., and Morrison, D.K. (2003). Protein phosphatase 2A positively regulates Ras signaling by dephosphorylating KSR1 and Raf-1 on critical 14-3-3 binding sites. Curr Biol *13*, 1356-1364.

Ozaki, K., Miyazaki, S., Tanimura, S., and Kohno, M. (2005). Efficient suppression of FGF-2-induced ERK activation by the cooperative interaction among mammalian Sprouty isoforms. J Cell Sci *118*, 5861-5871.

Pahl, H.L. (1999). Activators and target genes of Rel/NF-kappaB transcription factors. Oncogene *18*, 6853-6866.

Pan, B., Sengoku, K., Goishi, K., Takuma, N., Yamashita, T., Wada, K., and Ishikawa, M. (2002). The soluble and membrane-anchored forms of heparin-binding epidermal growth factor-like growth factor appear to play opposing roles in the survival and apoptosis of human luteinized granulosa cells. Mol Hum Reprod *8*, 734-741.

Patterson, K.I., Brummer, T., O'Brien, P.M., and Daly, R.J. (2009). Dual-specificity phosphatases: critical regulators with diverse cellular targets. Biochem J *418*, 475-489.

Pawson, T. (2007). Dynamic control of signaling by modular adaptor proteins. Curr Opin Cell Biol *19*, 112-116.

Peck, J.W., Bowden, E.T., and Burbelo, P.D. (2004). Structure and function of human Vps20 and Snf7 proteins. Biochem J *377*, 693-700.

Pelchen-Matthews, A., Kramer, B., and Marsh, M. (2003). Infectious HIV-1 assembles in late endosomes in primary macrophages. J Cell Biol *162*, 443-455.

Pelchen-Matthews, A., Raposo, G., and Marsh, M. (2004). Endosomes, exosomes and Trojan viruses. Trends Microbiol *12*, 310-316.

Pennock, S., and Wang, Z. (2003). Stimulation of cell proliferation by endosomal epidermal growth factor receptor as revealed through two distinct phases of signaling. Mol Cell Biol *23*, 5803-5815.

Pennock, S., and Wang, Z. (2008). A tale of two Cbls: interplay of c-Cbl and Cbl-b in epidermal growth factor receptor downregulation. Mol Cell Biol *28*, 3020-3037.

Perkins, N.D. (2007). Integrating cell-signalling pathways with NF-kappaB and IKK function. Nat Rev Mol Cell Biol *8*, 49-62.

Perret, E., Lakkaraju, A., Deborde, S., Schreiner, R., and Rodriguez-Boulan, E. (2005). Evolving endosomes: how many varieties and why? Curr Opin Cell Biol *17*, 423-434.

Petiot, A., Faure, J., Stenmark, H., and Gruenberg, J. (2003). PI3P signaling regulates receptor sorting but not transport in the endosomal pathway. J Cell Biol *162*, 971-979.

Pierce, K.L., Luttrell, L.M., and Lefkowitz, R.J. (2001). New mechanisms in heptahelical receptor signaling to mitogen activated protein kinase cascades. Oncogene *20*, 1532-1539.

Piessevaux, J., Lavens, D., Peelman, F., and Tavernier, J. (2008). The many faces of the SOCS box. Cytokine Growth Factor Rev *19*, 371-381.

Pinkas-Kramarski, R., Soussan, L., Waterman, H., Levkowitz, G., Alroy, I., Klapper, L., Lavi, S., Seger, R., Ratzkin, B.J., Sela, M.*, et al.* (1996). Diversification of Neu differentiation factor and epidermal growth factor signaling by combinatorial receptor interactions. EMBO J *15*, 2452-2467.

Pires-daSilva, A., and Sommer, R.J. (2003). The evolution of signalling pathways in animal development. Nat Rev Genet *4*, 39-49.

Pitfield, S.E., Bryant, I., Penington, D.J., Park, G., and Riese, D.J., 2nd (2006). Phosphorylation of ErbB4 on tyrosine 1056 is critical for ErbB4 coupling to inhibition of colony formation by human mammary cell lines. Oncol Res *16*, 179-193.

Pons, V., Luyet, P.P., Morel, E., Abrami, L., van der Goot, F.G., Parton, R.G., and Gruenberg, J. (2008). Hrs and SNX3 functions in sorting and membrane invagination within multivesicular bodies. PLoS Biol *6*, e214.

Popov, S., Popova, E., Inoue, M., and Gottlinger, H.G. (2009). Divergent Bro1 domains share the capacity to bind human immunodeficiency virus type 1 nucleocapsid and to enhance virus-like particle production. J Virol *83*, 7185-7193.

Pornillos, O., Higginson, D.S., Stray, K.M., Fisher, R.D., Garrus, J.E., Payne, M., He, G.P., Wang, H.E., Morham, S.G., and Sundquist, W.I. (2003). HIV Gag mimics the Tsg101-recruiting activity of the human Hrs protein. J Cell Biol *162*, 425-434.

Press, B., Feng, Y., Hoflack, B., and Wandinger-Ness, A. (1998). Mutant Rab7 causes the accumulation of cathepsin D and cation-independent mannose 6-phosphate receptor in an early endocytic compartment. J Cell Biol *140*, 1075-1089.

Printen, J.A., and Sprague, G.F., Jr. (1994). Protein-protein interactions in the yeast pheromone response pathway: Ste5p interacts with all members of the MAP kinase cascade. Genetics *138*, 609-619.

Pryor, P.R., Mullock, B.M., Bright, N.A., Gray, S.R., and Luzio, J.P. (2000). The role of intraorganellar Ca(2+) in late endosome-lysosome heterotypic fusion and in the reformation of lysosomes from hybrid organelles. J Cell Biol *149*, 1053-1062.

Pryor, P.R., Mullock, B.M., Bright, N.A., Lindsay, M.R., Gray, S.R., Richardson, S.C., Stewart, A., James, D.E., Piper, R.C., and Luzio, J.P. (2004). Combinatorial SNARE complexes with VAMP7 or VAMP8 define different late endocytic fusion events. EMBO Rep *5*, 590-595.

Pullikuth, A., McKinnon, E., Schaeffer, H.J., and Catling, A.D. (2005). The MEK1 scaffolding protein MP1 regulates cell spreading by integrating PAK1 and Rho signals. Mol Cell Biol *25*, 5119-5133.

Pullikuth, A.K., and Catling, A.D. (2007). Scaffold mediated regulation of MAPK signaling and cytoskeletal dynamics: a perspective. Cell Signal *19*, 1621-1632.

Qiu, C., Tarrant, M.K., Choi, S.H., Sathyamurthy, A., Bose, R., Banjade, S., Pal, A., Bornmann, W.G., Lemmon, M.A., Cole, P.A.*, et al.* (2008). Mechanism of activation and inhibition of the HER4/ErbB4 kinase. Structure *16*, 460-467.

Qiu, X.B., and Goldberg, A.L. (2002). Nrdp1/FLRF is a ubiquitin ligase promoting ubiquitination and degradation of the epidermal growth factor receptor family member, ErbB3. Proc Natl Acad Sci U S A *99*, 14843-14848.

Raiborg, C., Bache, K.G., Gillooly, D.J., Madshus, I.H., Stang, E., and Stenmark, H. (2002). Hrs sorts ubiquitinated proteins into clathrin-coated microdomains of early endosomes. Nat Cell Biol *4*, 394-398.

Raiborg, C., Bache, K.G., Mehlum, A., Stang, E., and Stenmark, H. (2001a). Hrs recruits clathrin to early endosomes. EMBO J *20*, 5008-5021.

Raiborg, C., Bremnes, B., Mehlum, A., Gillooly, D.J., D'Arrigo, A., Stang, E., and Stenmark, H. (2001b). FYVE and coiled-coil domains determine the specific localisation of Hrs to early endosomes. J Cell Sci *114*, 2255-2263.

Raiborg, C., Malerod, L., Pedersen, N.M., and Stenmark, H. (2008). Differential functions of Hrs and ESCRT proteins in endocytic membrane trafficking. Exp Cell Res *314*, 801-813.

Raiborg, C., Rusten, T.E., and Stenmark, H. (2003). Protein sorting into multivesicular endosomes. Curr Opin Cell Biol *15*, 446-455.

Raiborg, C., and Stenmark, H. (2009). The ESCRT machinery in endosomal sorting of ubiquitylated membrane proteins. Nature *458*, 445-452.

Raiborg, C., Wesche, J., Malerod, L., and Stenmark, H. (2006). Flat clathrin coats on endosomes mediate degradative protein sorting by scaffolding Hrs in dynamic microdomains. J Cell Sci *119*, 2414-2424.

Raposo, G., Moore, M., Innes, D., Leijendekker, R., Leigh-Brown, A., Benaroch, P., and Geuze, H. (2002). Human macrophages accumulate HIV-1 particles in MHC II compartments. Traffic *3*, 718-729.

Rapp, U.R., Goldsborough, M.D., Mark, G.E., Bonner, T.I., Groffen, J., Reynolds, F.H., Jr., and Stephenson, J.R. (1983). Structure and biological activity of v-raf, a unique oncogene transduced by a retrovirus. Proc Natl Acad Sci U S A *80*, 4218-4222.

Rawlings, J.S., Rennebeck, G., Harrison, S.M., Xi, R., and Harrison, D.A. (2004). Two Drosophila suppressors of cytokine signaling (SOCS) differentially regulate JAK and EGFR pathway activities. BMC Cell Biol *5*, 38.

Ray, L.B., and Sturgill, T.W. (1987). Rapid stimulation by insulin of a serine/threonine kinase in 3T3-L1 adipocytes that phosphorylates microtubule-associated protein 2 in vitro. Proc Natl Acad Sci U S A *84*, 1502-1506.

Raymond, C.K., Howald-Stevenson, I., Vater, C.A., and Stevens, T.H. (1992). Morphological classification of the yeast vacuolar protein sorting mutants: evidence for a prevacuolar compartment in class E vps mutants. Mol Biol Cell *3*, 1389-1402.

Razi, M., and Futter, C.E. (2006). Distinct roles for Tsg101 and Hrs in multivesicular body formation and inward vesiculation. Mol Biol Cell *17*, 3469-3483.

Red Brewer, M., Choi, S.H., Alvarado, D., Moravcevic, K., Pozzi, A., Lemmon, M.A., and Carpenter, G. (2009). The juxtamembrane region of the EGF receptor functions as an activation domain. Mol Cell *34*, 641-651.

Redig, A.J., and Platanias, L.C. (2007). The protein kinase C (PKC) family of proteins in cytokine signaling in hematopoiesis. J Interferon Cytokine Res *27*, 623-636.

Reggiori, F., and Pelham, H.R. (2001). Sorting of proteins into multivesicular bodies: ubiquitin-dependent and -independent targeting. EMBO J *20*, 5176-5186.

Reich, A., Sapir, A., and Shilo, B. (1999). Sprouty is a general inhibitor of receptor tyrosine kinase signaling. Development *126*, 4139-4147.

Reiss, K., and Saftig, P. (2009). The "a disintegrin and metalloprotease" (ADAM) family of sheddases: physiological and cellular functions. Semin Cell Dev Biol *20*, 126-137.

Revillion, F., Lhotellier, V., Hornez, L., Bonneterre, J., and Peyrat, J.P. (2008). ErbB/HER ligands in human breast cancer, and relationships with their receptors, the bio-pathological features and prognosis. Ann Oncol *19*, 73-80.

Riethmacher, D., Sonnenberg-Riethmacher, E., Brinkmann, V., Yamaai, T., Lewin, G.R., and Birchmeier, C. (1997). Severe neuropathies in mice with targeted mutations in the ErbB3 receptor. Nature *389*, 725-730.

Rink, J., Ghigo, E., Kalaidzidis, Y., and Zerial, M. (2005). Rab conversion as a mechanism of progression from early to late endosomes. Cell *122*, 735-749.

Ritter, S.L., and Hall, R.A. (2009). Fine-tuning of GPCR activity by receptor-interacting proteins. Nat Rev Mol Cell Biol *10*, 819-830.

Roberts, P.J., and Der, C.J. (2007). Targeting the Raf-MEK-ERK mitogen-activated protein kinase cascade for the treatment of cancer. Oncogene *26*, 3291-3310.

Rodrigues, G.A., Falasca, M., Zhang, Z., Ong, S.H., and Schlessinger, J. (2000). A novel positive feedback loop mediated by the docking protein Gab1 and phosphatidylinositol 3-kinase in epidermal growth factor receptor signaling. Mol Cell Biol *20*, 1448-1459.

Roepstorff, K., Grandal, M.V., Henriksen, L., Knudsen, S.L., Lerdrup, M., Grovdal, L., Willumsen, B.M., and van Deurs, B. (2009). Differential effects of EGFR ligands on endocytic sorting of the receptor. Traffic *10*, 1115-1127.

Rosse, C., Linch, M., Kermorgant, S., Cameron, A.J., Boeckeler, K., and Parker, P.J. (2010). PKC and the control of localized signal dynamics. Nat Rev Mol Cell Biol *11*, 103-112.

Rothe, M., Pan, M.G., Henzel, W.J., Ayres, T.M., and Goeddel, D.V. (1995). The TNFR2-TRAF signaling complex contains two novel proteins related to baculoviral inhibitor of apoptosis proteins. Cell *83*, 1243-1252.

Row, P.E., Liu, H., Hayes, S., Welchman, R., Charalabous, P., Hofmann, K., Clague, M.J., Sanderson, C.M., and Urbe, S. (2007). The MIT domain of UBPY constitutes a CHMP binding and endosomal localization signal required for efficient epidermal growth factor receptor degradation. J Biol Chem *282*, 30929-30937.

Roy, M., Li, Z., and Sacks, D.B. (2004). IQGAP1 binds ERK2 and modulates its activity. J Biol Chem *279*, 17329-17337.

Roy, M., Li, Z., and Sacks, D.B. (2005). IQGAP1 is a scaffold for mitogen-activated protein kinase signaling. Mol Cell Biol *25*, 7940-7952.

Rozakis-Adcock, M., Fernley, R., Wade, J., Pawson, T., and Bowtell, D. (1993). The SH2 and SH3 domains of mammalian Grb2 couple the EGF receptor to the Ras activator mSos1. Nature *363*, 83-85.

Rubin, C., Gur, G., and Yarden, Y. (2005a). Negative regulation of receptor tyrosine kinases: unexpected links to c-Cbl and receptor ubiquitylation. Cell Res *15*, 66-71.

Rubin, C., Zwang, Y., Vaisman, N., Ron, D., and Yarden, Y. (2005b). Phosphorylation of carboxyl-terminal tyrosines modulates the specificity of Sprouty-2 inhibition of different signaling pathways. J Biol Chem *280*, 9735-9744.

Rubinfeld, H., and Seger, R. (2005). The ERK cascade: a prototype of MAPK signaling. Mol Biotechnol *31*, 151-174.

Sachse, M., Urbe, S., Oorschot, V., Strous, G.J., and Klumperman, J. (2002). Bilayered clathrin coats on endosomal vacuoles are involved in protein sorting toward lysosomes. Mol Biol Cell *13*, 1313-1328.

Sahin, U., Weskamp, G., Kelly, K., Zhou, H.M., Higashiyama, S., Peschon, J., Hartmann, D., Saftig, P., and Blobel, C.P. (2004). Distinct roles for ADAM10 and ADAM17 in ectodomain shedding of six EGFR ligands. J Cell Biol *164*, 769-779.

Salazar, G., and Gonzalez, A. (2002). Novel mechanism for regulation of epidermal growth factor receptor endocytosis revealed by protein kinase A inhibition. Mol Biol Cell *13*, 1677-1693.

Sancak, Y., Bar-Peled, L., Zoncu, R., Markhard, A.L., Nada, S., and Sabatini, D.M. (2010). Ragulator-Rag complex targets mTORC1 to the lysosomal surface and is necessary for its activation by amino acids. Cell *141*, 290-303.

Santos, S.D., Verveer, P.J., and Bastiaens, P.I. (2007). Growth factor-induced MAPK network topology shapes Erk response determining PC-12 cell fate. Nat Cell Biol *9*, 324-330.

Sasaki, A., Taketomi, T., Kato, R., Saeki, K., Nonami, A., Sasaki, M., Kuriyama, M., Saito, N., Shibuya, M., and Yoshimura, A. (2003). Mammalian Sprouty4 suppresses Ras-independent ERK activation by binding to Raf1. Nat Cell Biol *5*, 427-432.

Sasaki, A., Taketomi, T., Wakioka, T., Kato, R., and Yoshimura, A. (2001). Identification of a dominant negative mutant of Sprouty that potentiates fibroblast growth factor- but not epidermal growth factor-induced ERK activation. J Biol Chem *276*, 36804-36808.

Schaeffer, H.J., Catling, A.D., Eblen, S.T., Collier, L.S., Krauss, A., and Weber, M.J. (1998). MP1: a MEK binding partner that enhances enzymatic activation of the MAP kinase cascade. Science *281*, 1668-1671.

Scheid, M.P., and Woodgett, J.R. (2001). PKB/AKT: functional insights from genetic models. Nat Rev Mol Cell Biol *2*, 760-768.

Schlessinger, J., and Lemmon, M.A. (2003). SH2 and PTB domains in tyrosine kinase signaling. Sci STKE *2003*, RE12.

Schmidt, M.H., and Dikic, I. (2005). The Cbl interactome and its functions. Nat Rev Mol Cell Biol *6*, 907-918.

Schmidt, M.H., Hoeller, D., Yu, J., Furnari, F.B., Cavenee, W.K., Dikic, I., and Bogler, O. (2004). Alix/AIP1 antagonizes epidermal growth factor receptor downregulation by the Cbl-SETA/CIN85 complex. Mol Cell Biol *24*, 8981-8993.

Schneider, M.R., and Wolf, E. (2009). The epidermal growth factor receptor ligands at a glance. J Cell Physiol *218*, 460-466.

Schoeberl, B., Eichler-Jonsson, C., Gilles, E.D., and Muller, G. (2002). Computational modeling of the dynamics of the MAP kinase cascade activated by surface and internalized EGF receptors. Nat Biotechnol *20*, 370-375.

Schulze, A., Lehmann, K., Jefferies, H.B., McMahon, M., and Downward, J. (2001). Analysis of the transcriptional program induced by Raf in epithelial cells. Genes Dev *15*, 981-994.

Schulze, A., Nicke, B., Warne, P.H., Tomlinson, S., and Downward, J. (2004). The transcriptional response to Raf activation is almost completely dependent on Mitogen-activated Protein Kinase Kinase activity and shows a major autocrine component. Mol Biol Cell *15*, 3450-3463.

Schulze, W.X., Deng, L., and Mann, M. (2005). Phosphotyrosine interactome of the ErbB-receptor kinase family. Mol Syst Biol *1*, 2005 0008.

Schwartz, M.A., and Madhani, H.D. (2004). Principles of MAP kinase signaling specificity in Saccharomyces cerevisiae. Annu Rev Genet *38*, 725-748.

Schweighofer, B., Testori, J., Sturtzel, C., Sattler, S., Mayer, H., Wagner, O., Bilban, M., and Hofer, E. (2009). The VEGF-induced transcriptional response comprises gene clusters at the crossroad of angiogenesis and inflammation. Thromb Haemost *102*, 544-554.

Schweitzer, R., Howes, R., Smith, R., Shilo, B.Z., and Freeman, M. (1995). Inhibition of Drosophila EGF receptor activation by the secreted protein Argos. Nature *376*, 699-702.

Scita, G., and Di Fiore, P.P. (2010). The endocytic matrix. Nature *463*, 464-473.

Scott, A., Chung, H.Y., Gonciarz-Swiatek, M., Hill, G.C., Whitby, F.G., Gaspar, J., Holton, J.M., Viswanathan, R., Ghaffarian, S., Hill, C.P.*, et al.* (2005). Structural and mechanistic studies of VPS4 proteins. EMBO J *24*, 3658-3669.

Seet, B.T., Dikic, I., Zhou, M.M., and Pawson, T. (2006). Reading protein modifications with interaction domains. Nat Rev Mol Cell Biol *7*, 473-483.

Seglen, P.O., Grinde, B., and Solheim, A.E. (1979). Inhibition of the lysosomal pathway of protein degradation in isolated rat hepatocytes by ammonia, methylamine, chloroquine and leupeptin. Eur J Biochem *95*, 215-225.

Shapiro, A.L., Vinuela, E., and Maizel, J.V., Jr. (1967). Molecular weight estimation of polypeptide chains by electrophoresis in SDS-polyacrylamide gels. Biochem Biophys Res Commun *28*, 815-820.

Sharma, C., Vomastek, T., Tarcsafalvi, A., Catling, A.D., Schaeffer, H.J., Eblen, S.T., and Weber, M.J. (2005). MEK partner 1 (MP1): regulation of oligomerization in MAP kinase signaling. J Cell Biochem *94*, 708-719.

Sharrocks, A.D. (2001). The ETS-domain transcription factor family. Nat Rev Mol Cell Biol *2*, 827-837.

Shattuck, D.L., Miller, J.K., Laederich, M., Funes, M., Petersen, H., Carraway, K.L., 3rd, and Sweeney, C. (2007). LRIG1 is a novel negative regulator of the Met receptor and opposes Met and Her2 synergy. Mol Cell Biol *27*, 1934-1946.

Shaul, Y.D., and Seger, R. (2007). The MEK/ERK cascade: from signaling specificity to diverse functions. Biochim Biophys Acta *1773*, 1213-1226.

Shaulian, E., and Karin, M. (2002). AP-1 as a regulator of cell life and death. Nat Cell Biol *4*, E131-136.

Shen, F., Lin, Q., Gu, Y., Childress, C., and Yang, W. (2007). Activated Cdc42-associated kinase 1 is a component of EGF receptor signaling complex and regulates EGF receptor degradation. Mol Biol Cell *18*, 732-742.

Shenoy, S.K., and Lefkowitz, R.J. (2005). Seven-transmembrane receptor signaling through beta-arrestin. Sci STKE *2005*, cm10.

Shilo, B.Z. (2003). Signaling by the Drosophila epidermal growth factor receptor pathway during development. Exp Cell Res *284*, 140-149.

Shilo, B.Z. (2005). Regulating the dynamics of EGF receptor signaling in space and time. Development *132*, 4017-4027.

Shim, S., Kimpler, L.A., and Hanson, P.I. (2007). Structure/function analysis of four core ESCRT-III proteins reveals common regulatory role for extreme C-terminal domain. Traffic *8*, 1068-1079.

Shimizu, K., Goldfarb, M., Suard, Y., Perucho, M., Li, Y., Kamata, T., Feramisco, J., Stavnezer, E., Fogh, J., and Wigler, M.H. (1983). Three human transforming genes are related to the viral ras oncogenes. Proc Natl Acad Sci U S A *80*, 2112-2116.

Sibilia, M., Steinbach, J.P., Stingl, L., Aguzzi, A., and Wagner, E.F. (1998). A strain-independent postnatal neurodegeneration in mice lacking the EGF receptor. EMBO J *17*, 719-731.

Sibilia, M., and Wagner, E.F. (1995). Strain-dependent epithelial defects in mice lacking the EGF receptor. Science *269*, 234-238.

Sigismund, S., Argenzio, E., Tosoni, D., Cavallaro, E., Polo, S., and Di Fiore, P.P. (2008). Clathrin-mediated internalization is essential for sustained EGFR signaling but dispensable for degradation. Dev Cell *15*, 209-219.

Sigismund, S., Woelk, T., Puri, C., Maspero, E., Tacchetti, C., Transidico, P., Di Fiore, P.P., and Polo, S. (2005). Clathrin-independent endocytosis of ubiquitinated cargos. Proc Natl Acad Sci U S A *102*, 2760-2765.

Silverstein, S.C., Steinman, R.M., and Cohn, Z.A. (1977). Endocytosis. Annu Rev Biochem *46*, 669-722.

Simons, K., and Gerl, M.J. (2010). Revitalizing membrane rafts: new tools and insights. Nat Rev Mol Cell Biol *11*, 688-699.

Simons, K., and Ikonen, E. (1997). Functional rafts in cell membranes. Nature *387*, 569-572.

Singh, A.B., and Harris, R.C. (2005). Autocrine, paracrine and juxtacrine signaling by EGFR ligands. Cell Signal *17*, 1183-1193.

Singh, A.B., Tsukada, T., Zent, R., and Harris, R.C. (2004). Membrane-associated HB-EGF modulates HGF-induced cellular responses in MDCK cells. J Cell Sci *117*, 1365-1379.

Skaug, B., Jiang, X., and Chen, Z.J. (2009). The role of ubiquitin in NF-kappaB regulatory pathways. Annu Rev Biochem *78*, 769-796.

Slagsvold, T., Aasland, R., Hirano, S., Bache, K.G., Raiborg, C., Trambaiolo, D., Wakatsuki, S., and Stenmark, H. (2005). Eap45 in mammalian ESCRT-II binds ubiquitin via a phosphoinositide-interacting GLUE domain. J Biol Chem *280*, 19600-19606.

Slamon, D.J., Clark, G.M., Wong, S.G., Levin, W.J., Ullrich, A., and McGuire, W.L. (1987). Human breast cancer: correlation of relapse and survival with amplification of the HER-2/neu oncogene. Science *235*, 177-182.

Slamon, D.J., Godolphin, W., Jones, L.A., Holt, J.A., Wong, S.G., Keith, D.E., Levin, W.J., Stuart, S.G., Udove, J., Ullrich, A.*, et al.* (1989). Studies of the HER-2/neu proto-oncogene in human breast and ovarian cancer. Science *244*, 707-712.

Smith, E.R., Smedberg, J.L., Rula, M.E., and Xu, X.X. (2004). Regulation of Ras-MAPK pathway mitogenic activity by restricting nuclear entry of activated MAPK in endoderm differentiation of embryonic carcinoma and stem cells. J Cell Biol *164*, 689-699.

Smith, T.G., Karlsson, M., Lunn, J.S., Eblaghie, M.C., Keenan, I.D., Farrell, E.R., Tickle, C., Storey, K.G., and Keyse, S.M. (2006). Negative feedback predominates over cross-regulation to control ERK MAPK activity in response to FGF signalling in embryos. FEBS Lett *580*, 4242-4245.

Sobell, H.M. (1985). Actinomycin and DNA transcription. Proc Natl Acad Sci U S A *82*, 5328-5331.

Sobo, K., Chevallier, J., Parton, R.G., Gruenberg, J., and van der Goot, F.G. (2007a). Diversity of raft-like domains in late endosomes. PLoS One *2*, e391.

Sobo, K., Le Blanc, I., Luyet, P.P., Fivaz, M., Ferguson, C., Parton, R.G., Gruenberg, J., and van der Goot, F.G. (2007b). Late endosomal cholesterol accumulation leads to impaired intra-endosomal trafficking. PLoS One *2*, e851.

Sorkin, A., Di Fiore, P.P., and Carpenter, G. (1993). The carboxyl terminus of epidermal growth factor receptor/erbB-2 chimerae is internalization impaired. Oncogene *8*, 3021-3028.

Sorkin, A., and Goh, L.K. (2008). Endocytosis and intracellular trafficking of ErbBs. Exp Cell Res *314*, 3093-3106.

Sorkin, A., Krolenko, S., Kudrjavtceva, N., Lazebnik, J., Teslenko, L., Soderquist, A.M., and Nikolsky, N. (1991a). Recycling of epidermal growth factor-receptor complexes in A431 cells: identification of dual pathways. J Cell Biol *112*, 55-63.

Sorkin, A., and Von Zastrow, M. (2002). Signal transduction and endocytosis: close encounters of many kinds. Nat Rev Mol Cell Biol *3*, 600-614.

Sorkin, A., and von Zastrow, M. (2009). Endocytosis and signalling: intertwining molecular networks. Nat Rev Mol Cell Biol *10*, 609-622.

Sorkin, A., Waters, C., Overholser, K.A., and Carpenter, G. (1991b). Multiple autophosphorylation site mutations of the epidermal growth factor receptor. Analysis of kinase activity and endocytosis. J Biol Chem *266*, 8355-8362.

Sorkin, A.D., Teslenko, L.V., and Nikolsky, N.N. (1988). The endocytosis of epidermal growth factor in A431 cells: a pH of microenvironment and the dynamics of receptor complex dissociation. Exp Cell Res *175*, 192-205.

Sorkina, T., Huang, F., Beguinot, L., and Sorkin, A. (2002). Effect of tyrosine kinase inhibitors on clathrin-coated pit recruitment and internalization of epidermal growth factor receptor. J Biol Chem *277*, 27433-27441.

Soubeyran, P., Kowanetz, K., Szymkiewicz, I., Langdon, W.Y., and Dikic, I. (2002). Cbl-CIN85-endophilin complex mediates ligand-induced downregulation of EGF receptors. Nature *416*, 183-187.

Speight, P., and Silverman, M. (2005). Diacylglycerol-activated Hmunc13 serves as an effector of the GTPase Rab34. Traffic *6*, 858-865.

Sporn, M.B., and Todaro, G.J. (1980). Autocrine secretion and malignant transformation of cells. N Engl J Med *303*, 878-880.

Stamos, J., Sliwkowski, M.X., and Eigenbrot, C. (2002). Structure of the epidermal growth factor receptor kinase domain alone and in complex with a 4-anilinoquinazoline inhibitor. J Biol Chem *277*, 46265-46272.

Stang, E., Blystad, F.D., Kazazic, M., Bertelsen, V., Brodahl, T., Raiborg, C., Stenmark, H., and Madshus, I.H. (2004). Cbl-dependent ubiquitination is required for progression of EGF receptors into clathrin-coated pits. Mol Biol Cell *15*, 3591-3604.

Starkey, R.H., Cohen, S., and Orth, D.N. (1975). Epidermal growth factor: identification of a new hormone in human urine. Science *189*, 800-802.

Starr, R., Willson, T.A., Viney, E.M., Murray, L.J., Rayner, J.R., Jenkins, B.J., Gonda, T.J., Alexander, W.S., Metcalf, D., Nicola, N.A.*, et al.* (1997). A family of cytokine-inducible inhibitors of signalling. Nature *387*, 917-921.

Stelling, J., Sauer, U., Szallasi, Z., Doyle, F.J., 3rd, and Doyle, J. (2004). Robustness of cellular functions. Cell *118*, 675-685.

Stenmark, H. (2009). Rab GTPases as coordinators of vesicle traffic. Nat Rev Mol Cell Biol *10*, 513-525.

Stern, K.A., Place, T.L., and Lill, N.L. (2008). EGF and amphiregulin differentially regulate Cbl recruitment to endosomes and EGF receptor fate. Biochem J *410*, 585-594.

Stern, K.A., Visser Smit, G.D., Place, T.L., Winistorfer, S., Piper, R.C., and Lill, N.L. (2007). Epidermal growth factor receptor fate is controlled by Hrs tyrosine phosphorylation sites that regulate Hrs degradation. Mol Cell Biol *27*, 888-898.

Sternberg, P.W., Lesa, G., Lee, J., Katz, W.S., Yoon, C., Clandinin, T.R., Huang, L.S., Chamberlin, H.M., and Jongeward, G. (1995). LET-23-mediated signal transduction during Caenorhabditis elegans development. Mol Reprod Dev *42*, 523-528.

Stoscheck, C.M., and Carpenter, G. (1984a). Characterization of the metabolic turnover of epidermal growth factor receptor protein in A-431 cells. J Cell Physiol *120*, 296-302.

Stoscheck, C.M., and Carpenter, G. (1984b). Down regulation of epidermal growth factor receptors: direct demonstration of receptor degradation in human fibroblasts. J Cell Biol *98*, 1048-1053.

Strack, B., Calistri, A., Craig, S., Popova, E., and Gottlinger, H.G. (2003). AIP1/ALIX is a binding partner for HIV-1 p6 and EIAV p9 functioning in virus budding. Cell *114*, 689-699.

Stuchell-Brereton, M.D., Skalicky, J.J., Kieffer, C., Karren, M.A., Ghaffarian, S., and Sundquist, W.I. (2007). ESCRT-III recognition by VPS4 ATPases. Nature *449*, 740-744.

Stuffers, S., Brech, A., and Stenmark, H. (2009a). ESCRT proteins in physiology and disease. Exp Cell Res *315*, 1619-1626.

Stuffers, S., Sem Wegner, C., Stenmark, H., and Brech, A. (2009b). Multivesicular endosome biogenesis in the absence of ESCRTs. Traffic *10*, 925-937.

Stutz, M.A., Shattuck, D.L., Laederich, M.B., Carraway, K.L., 3rd, and Sweeney, C. (2008). LRIG1 negatively regulates the oncogenic EGF receptor mutant EGFRvIII. Oncogene *27*, 5741-5752.

Sun, H., Charles, C.H., Lau, L.F., and Tonks, N.K. (1993). MKP-1 (3CH134), an immediate early gene product, is a dual specificity phosphatase that dephosphorylates MAP kinase in vivo. Cell *75*, 487-493.

Sundaram, M., and Han, M. (1995). The C. elegans ksr-1 gene encodes a novel Raf-related kinase involved in Ras-mediated signal transduction. Cell *83*, 889-901.

Sundquist, W.I., Schubert, H.L., Kelly, B.N., Hill, G.C., Holton, J.M., and Hill, C.P. (2004). Ubiquitin recognition by the human TSG101 protein. Mol Cell *13*, 783-789.

Sundvall, M., Korhonen, A., Paatero, I., Gaudio, E., Melino, G., Croce, C.M., Aqeilan, R.I., and Elenius, K. (2008). Isoform-specific monoubiquitination, endocytosis, and degradation of alternatively spliced ErbB4 isoforms. Proc Natl Acad Sci U S A *105*, 4162-4167.

Suzuki, M., Raab, G., Moses, M.A., Fernandez, C.A., and Klagsbrun, M. (1997). Matrix metalloproteinase-3 releases active heparin-binding EGF-like growth factor by cleavage at a specific juxtamembrane site. J Biol Chem *272*, 31730-31737.

Szymkiewicz, I., Shupliakov, O., and Dikic, I. (2004). Cargo- and compartment-selective endocytic scaffold proteins. Biochem J *383*, 1-11.

Tanaka, N., Kyuuma, M., and Sugamura, K. (2008). Endosomal sorting complex required for transport proteins in cancer pathogenesis, vesicular transport, and non-endosomal functions. Cancer Sci *99*, 1293-1303.

Tarrega, C., and Pulido, R. (2009). A one-step method to identify MAP kinase residues involved in inactivation by tyrosine- and dual-specificity protein phosphatases. Anal Biochem *394*, 81-86.

Tauchi, T., Feng, G.S., Marshall, M.S., Shen, R., Mantel, C., Pawson, T., and Broxmeyer, H.E. (1994). The ubiquitously expressed Syp phosphatase interacts with c-kit and Grb2 in hematopoietic cells. J Biol Chem *269*, 25206-25211.

Teis, D., Saksena, S., and Emr, S.D. (2008). Ordered assembly of the ESCRT-III complex on endosomes is required to sequester cargo during MVB formation. Dev Cell *15*, 578-589.

Teis, D., Saksena, S., Judson, B.L., and Emr, S.D. (2010). ESCRT-II coordinates the assembly of ESCRT-III filaments for cargo sorting and multivesicular body vesicle formation. EMBO J *29*, 871-883.

Teis, D., Taub, N., Kurzbauer, R., Hilber, D., de Araujo, M.E., Erlacher, M., Offterdinger, M., Villunger, A., Geley, S., Bohn, G.*, et al.* (2006). p14-MP1-MEK1 signaling regulates endosomal traffic and cellular proliferation during tissue homeostasis. J Cell Biol *175*, 861-868.

Teis, D., Wunderlich, W., and Huber, L.A. (2002). Localization of the MP1-MAPK scaffold complex to endosomes is mediated by p14 and required for signal transduction. Dev Cell *3*, 803-814.

Teng, C.H., Huang, W.N., and Meng, T.C. (2007). Several dual specificity phosphatases coordinate to control the magnitude and duration of JNK activation in signaling response to oxidative stress. J Biol Chem *282*, 28395-28407.

Theos, A.C., Truschel, S.T., Tenza, D., Hurbain, I., Harper, D.C., Berson, J.F., Thomas, P.C., Raposo, G., and Marks, M.S. (2006). A lumenal domain-dependent pathway for sorting to intralumenal vesicles of multivesicular endosomes involved in organelle morphogenesis. Dev Cell *10*, 343-354.

Therrien, M., Chang, H.C., Solomon, N.M., Karim, F.D., Wassarman, D.A., and Rubin, G.M. (1995). KSR, a novel protein kinase required for RAS signal transduction. Cell *83*, 879-888.

Therrien, M., Michaud, N.R., Rubin, G.M., and Morrison, D.K. (1996). KSR modulates signal propagation within the MAPK cascade. Genes Dev *10*, 2684-2695.

Thiel, K.W., and Carpenter, G. (2007). Epidermal growth factor receptor juxtamembrane region regulates allosteric tyrosine kinase activation. Proc Natl Acad Sci U S A *104*, 19238-19243.

Thien, C.B., and Langdon, W.Y. (2001). Cbl: many adaptations to regulate protein tyrosine kinases. Nat Rev Mol Cell Biol *2*, 294-307.

Thompson, S.A., Higashiyama, S., Wood, K., Pollitt, N.S., Damm, D., McEnroe, G., Garrick, B., Ashton, N., Lau, K., Hancock, N.*, et al.* (1994). Characterization of sequences within heparin-binding EGF-like growth factor that mediate interaction with heparin. J Biol Chem *269*, 2541-2549.

Thompson, W.L., and Van Eldik, L.J. (2009). Inflammatory cytokines stimulate the chemokines CCL2/MCP-1 and CCL7/MCP-3 through NFkB and MAPK dependent pathways in rat astrocytes [corrected]. Brain Res *1287*, 47-57.

Thorne, B.A., and Plowman, G.D. (1994). The heparin-binding domain of amphiregulin necessitates the precursor pro-region for growth factor secretion. Mol Cell Biol *14*, 1635-1646.

Threadgill, D.W., Dlugosz, A.A., Hansen, L.A., Tennenbaum, T., Lichti, U., Yee, D., LaMantia, C., Mourton, T., Herrup, K., Harris, R.C.*, et al.* (1995). Targeted disruption of mouse EGF receptor: effect of genetic background on mutant phenotype. Science *269*, 230-234.

Tiganis, T., Bennett, A.M., Ravichandran, K.S., and Tonks, N.K. (1998). Epidermal growth factor receptor and the adaptor protein p52Shc are specific substrates of T-cell protein tyrosine phosphatase. Mol Cell Biol *18*, 1622-1634.

Tiganis, T., Kemp, B.E., and Tonks, N.K. (1999). The protein-tyrosine phosphatase TCPTP regulates epidermal growth factor receptor-mediated and phosphatidylinositol 3-kinase-dependent signaling. J Biol Chem *274*, 27768-27775.

Tohgo, A., Choy, E.W., Gesty-Palmer, D., Pierce, K.L., Laporte, S., Oakley, R.H., Caron, M.G., Lefkowitz, R.J., and Luttrell, L.M. (2003). The stability of the G protein-coupled receptor-beta-arrestin interaction determines the mechanism and functional consequence of ERK activation. J Biol Chem *278*, 6258-6267.

Tohgo, A., Pierce, K.L., Choy, E.W., Lefkowitz, R.J., and Luttrell, L.M. (2002). beta-Arrestin scaffolding of the ERK cascade enhances cytosolic ERK activity but inhibits ERK-mediated transcription following angiotensin AT1a receptor stimulation. J Biol Chem *277*, 9429-9436.

Toledano-Katchalski, H., and Elson, A. (1999). The transmembranal and cytoplasmic forms of protein tyrosine phosphatase epsilon physically associate with the adaptor molecule Grb2. Oncogene *18*, 5024-5031.

Toledano-Katchalski, H., Kraut, J., Sines, T., Granot-Attas, S., Shohat, G., Gil-Henn, H., Yung, Y., and Elson, A. (2003). Protein tyrosine phosphatase epsilon inhibits signaling by mitogen-activated protein kinases. Mol Cancer Res *1*, 541-550.

Torii, S., Kusakabe, M., Yamamoto, T., Maekawa, M., and Nishida, E. (2004). Sef is a spatial regulator for Ras/MAP kinase signaling. Dev Cell *7*, 33-44.

Towbin, H., Staehelin, T., and Gordon, J. (1979). Electrophoretic transfer of proteins from polyacrylamide gels to nitrocellulose sheets: procedure and some applications. Proc Natl Acad Sci U S A *76*, 4350-4354.

Touchot, N., Chardin, P., and Tavitian, A. (1987). Four additional members of the ras gene superfamily isolated by an oligonucleotide strategy: molecular cloning of YPT-related cDNAs from a rat brain library. Proc Natl Acad Sci U S A *84*, 8210-8214.

Toyooka, S., Ouchida, M., Jitsumori, Y., Tsukuda, K., Sakai, A., Nakamura, A., Shimizu, N., and Shimizu, K. (2000). HD-PTP: A novel protein tyrosine phosphatase gene on human chromosome 3p21.3. Biochem Biophys Res Commun *278*, 671-678.

Toyoshima, M., Tanaka, N., Aoki, J., Tanaka, Y., Murata, K., Kyuuma, M., Kobayashi, H., Ishii, N., Yaegashi, N., and Sugamura, K. (2007). Inhibition of tumor growth and metastasis by depletion of vesicular sorting protein Hrs: its regulatory role on E-cadherin and beta-catenin. Cancer Res *67*, 5162-5171.

Trang, S.H., Joyner, D.E., Damron, T.A., Aboulafia, A.J., and Randall, R.L. (2010). Potential for functional redundancy in EGF and TGFalpha signaling in desmoid cells: a cDNA microarray analysis. Growth Factors *28*, 10-23.

Traub, L.M. (2009). Tickets to ride: selecting cargo for clathrin-regulated internalization. Nat Rev Mol Cell Biol *10*, 583-596.

Traverse, S., Seedorf, K., Paterson, H., Marshall, C.J., Cohen, P., and Ullrich, A. (1994). EGF triggers neuronal differentiation of PC12 cells that overexpress the EGF receptor. Curr Biol *4*, 694-701.

Troyer, K.L., Luetteke, N.C., Saxon, M.L., Qiu, T.H., Xian, C.J., and Lee, D.C. (2001). Growth retardation, duodenal lesions, and aberrant ileum architecture in triple null mice lacking EGF, amphiregulin, and TGF-alpha. Gastroenterology *121*, 68-78.

Tsang, M., and Dawid, I.B. (2004). Promotion and attenuation of FGF signaling through the Ras-MAPK pathway. Sci STKE *2004*, pe17.

Tsang, M., Friesel, R., Kudoh, T., and Dawid, I.B. (2002). Identification of Sef, a novel modulator of FGF signalling. Nat Cell Biol *4*, 165-169.

Turner, C.E. (2000). Paxillin interactions. J Cell Sci *113 Pt 23*, 4139-4140.

Turner, C.E., Glenney, J.R., Jr., and Burridge, K. (1990). Paxillin: a new vinculin-binding protein present in focal adhesions. J Cell Biol *111*, 1059-1068.

Tzahar, E., Pinkas-Kramarski, R., Moyer, J.D., Klapper, L.N., Alroy, I., Levkowitz, G., Shelly, M., Henis, S., Eisenstein, M., Ratzkin, B.J.*, et al.* (1997). Bivalence of EGF-like ligands drives the ErbB signaling network. EMBO J *16*, 4938-4950.

Tzahar, E., Waterman, H., Chen, X., Levkowitz, G., Karunagaran, D., Lavi, S., Ratzkin, B.J., and Yarden, Y. (1996). A hierarchical network of interreceptor interactions determines signal transduction by Neu differentiation factor/neuregulin and epidermal growth factor. Mol Cell Biol *16*, 5276-5287.

Ullrich, A., Coussens, L., Hayflick, J.S., Dull, T.J., Gray, A., Tam, A.W., Lee, J., Yarden, Y., Libermann, T.A., Schlessinger, J.*, et al.* (1984). Human epidermal growth factor receptor cDNA sequence and aberrant expression of the amplified gene in A431 epidermoid carcinoma cells. Nature *309*, 418-425.

Umebayashi, K., Stenmark, H., and Yoshimori, T. (2008). Ubc4/5 and c-Cbl continue to ubiquitinate EGF receptor after internalization to facilitate polyubiquitination and degradation. Mol Biol Cell *19*, 3454-3462.

Ushiro, H., and Cohen, S. (1980). Identification of phosphotyrosine as a product of epidermal growth factor-activated protein kinase in A-431 cell membranes. J Biol Chem *255*, 8363-8365.

Ussar, S., and Voss, T. (2004). MEK1 and MEK2, different regulators of the G1/S transition. J Biol Chem *279*, 43861-43869.

Valesini, G., and Alessandri, C. (2005). New facet of antiphospholipid antibodies. Ann N Y Acad Sci *1051*, 487-497.

Van Beveren, C., van Straaten, F., Curran, T., Muller, R., and Verma, I.M. (1983). Analysis of FBJ-MuSV provirus and c-fos (mouse) gene reveals that viral and cellular fos gene products have different carboxy termini. Cell *32*, 1241-1255.

van der Goot, F.G., and Gruenberg, J. (2006). Intra-endosomal membrane traffic. Trends Cell Biol *16*, 514-521.

van Kerkhof, P., Alves dos Santos, C.M., Sachse, M., Klumperman, J., Bu, G., and Strous, G.J. (2001). Proteasome inhibitors block a late step in lysosomal transport of selected membrane but not soluble proteins. Mol Biol Cell *12*, 2556-2566.

Vandesompele, J., De Preter, K., Pattyn, F., Poppe, B., Van Roy, N., De Paepe, A., and Speleman, F. (2002). Accurate normalization of real-time quantitative RT-PCR data by geometric averaging of multiple internal control genes. Genome Biol *3*, RESEARCH0034.

Vanhaesebroeck, B., Guillermet-Guibert, J., Graupera, M., and Bilanges, B. (2010). The emerging mechanisms of isoform-specific PI3K signalling. Nat Rev Mol Cell Biol *11*, 329-341.

Vanlandingham, P.A., and Ceresa, B.P. (2009). Rab7 regulates late endocytic trafficking downstream of multivesicular body biogenesis and cargo sequestration. J Biol Chem *284*, 12110-12124.

Venter, J.C., Adams, M.D., Myers, E.W., Li, P.W., Mural, R.J., Sutton, G.G., Smith, H.O., Yandell, M., Evans, C.A., Holt, R.A.*, et al.* (2001). The sequence of the human genome. Science *291*, 1304-1351.

Vidricaire, G., Imbeault, M., and Tremblay, M.J. (2004). Endocytic host cell machinery plays a dominant role in intracellular trafficking of incoming human immunodeficiency virus type 1 in human placental trophoblasts. J Virol *78*, 11904-11915.

Vidricaire, G., and Tremblay, M.J. (2005). Rab5 and Rab7, but not ARF6, govern the early events of HIV-1 infection in polarized human placental cells. J Immunol *175*, 6517-6530.

Vieira, A.V., Lamaze, C., and Schmid, S.L. (1996). Control of EGF receptor signaling by clathrin-mediated endocytosis. Science *274*, 2086-2089.

Vojtek, A.B., Hollenberg, S.M., and Cooper, J.A. (1993). Mammalian Ras interacts directly with the serine/threonine kinase Raf. Cell *74*, 205-214.

Volmat, V., Camps, M., Arkinstall, S., Pouyssegur, J., and Lenormand, P. (2001). The nucleus, a site for signal termination by sequestration and inactivation of p42/p44 MAP kinases. J Cell Sci *114*, 3433-3443.

Vomastek, T., Iwanicki, M.P., Schaeffer, H.J., Tarcsafalvi, A., Parsons, J.T., and Weber, M.J. (2007). RACK1 targets the extracellular signal-regulated kinase/mitogen-activated protein kinase pathway to link integrin engagement with focal adhesion disassembly and cell motility. Mol Cell Biol *27*, 8296-8305.

Vomastek, T., Schaeffer, H.J., Tarcsafalvi, A., Smolkin, M.E., Bissonette, E.A., and Weber, M.J. (2004). Modular construction of a signaling scaffold: MORG1 interacts with components of the ERK cascade and links ERK signaling to specific agonists. Proc Natl Acad Sci U S A *101*, 6981-6986.

von Schwedler, U.K., Stuchell, M., Muller, B., Ward, D.M., Chung, H.Y., Morita, E., Wang, H.E., Davis, T., He, G.P., Cimbora, D.M.*, et al.* (2003). The protein network of HIV budding. Cell *114*, 701-713.

von Zastrow, M., and Sorkin, A. (2007). Signaling on the endocytic pathway. Curr Opin Cell Biol *19*, 436-445.

Wabakken, T., Hauge, H., Finne, E.F., Wiedlocha, A., and Aasheim, H. (2002). Expression of human protein tyrosine phosphatase epsilon in leucocytes: a potential ERK pathway-regulating phosphatase. Scand J Immunol *56*, 195-203.

Wada, I., Lai, W.H., Posner, B.I., and Bergeron, J.J. (1992). Association of the tyrosine phosphorylated epidermal growth factor receptor with a 55-kD tyrosine phosphorylated protein at the cell surface and in endosomes. J Cell Biol *116*, 321-330.

Wakioka, T., Sasaki, A., Kato, R., Shouda, T., Matsumoto, A., Miyoshi, K., Tsuneoka, M., Komiya, S., Baron, R., and Yoshimura, A. (2001). Spred is a Sprouty-related suppressor of Ras signalling. Nature *412*, 647-651.

Wallasch, C., Weiss, F.U., Niederfellner, G., Jallal, B., Issing, W., and Ullrich, A. (1995). Heregulin-dependent regulation of HER2/neu oncogenic signaling by heterodimerization with HER3. EMBO J *14*, 4267-4275.

Walton, G.M., Chen, W.S., Rosenfeld, M.G., and Gill, G.N. (1990). Analysis of deletions of the carboxyl terminus of the epidermal growth factor receptor reveals self-phosphorylation at tyrosine 992 and enhanced in vivo tyrosine phosphorylation of cell substrates. J Biol Chem *265*, 1750-1754.

Wang, B., Khachigian, L.M., Esau, L., Birrer, M.J., Zhao, X., Parker, M.I., and Hendricks, D.T. (2009). A key role for early growth response-1 and nuclear factor-kappaB in mediating and maintaining GRO/CXCR2 proliferative signaling in esophageal cancer. Mol Cancer Res *7*, 755-764.

Wang, Q., Villeneuve, G., and Wang, Z. (2005). Control of epidermal growth factor receptor endocytosis by receptor dimerization, rather than receptor kinase activation. EMBO Rep *6*, 942-948.

Wang, Q., Wang, X., and Evers, B.M. (2003). Induction of cIAP-2 in human colon cancer cells through PKC delta/NF-kappa B. J Biol Chem *278*, 51091-51099.

Wang, S.C., and Hung, M.C. (2009). Nuclear translocation of the epidermal growth factor receptor family membrane tyrosine kinase receptors. Clin Cancer Res *15*, 6484-6489.

Wang, T., and Hong, W. (2002). Interorganellar regulation of lysosome positioning by the Golgi apparatus through Rab34 interaction with Rab-interacting lysosomal protein. Mol Biol Cell *13*, 4317-4332.

Wang, Y., Pennock, S., Chen, X., and Wang, Z. (2002). Internalization of inactive EGF receptor into endosomes and the subsequent activation of endosome-associated EGF receptors. Epidermal growth factor. Sci STKE *2002*, pl17.

Wang, Y., Pennock, S.D., Chen, X., Kazlauskas, A., and Wang, Z. (2004). Platelet-derived growth factor receptor-mediated signal transduction from endosomes. J Biol Chem *279*, 8038-8046.

Wang, Z., Tung, P.S., and Moran, M.F. (1996). Association of p120 ras GAP with endocytic components and colocalization with epidermal growth factor (EGF) receptor in response to EGF stimulation. Cell Growth Differ *7*, 123-133.

Wang, Z., Zhang, L., Yeung, T.K., and Chen, X. (1999). Endocytosis deficiency of epidermal growth factor (EGF) receptor-ErbB2 heterodimers in response to EGF stimulation. Mol Biol Cell *10*, 1621-1636.

Ward, C.W., Hoyne, P.A., and Flegg, R.H. (1995). Insulin and epidermal growth factor receptors contain the cysteine repeat motif found in the tumor necrosis factor receptor. Proteins *22*, 141-153.

Ward, Y., Gupta, S., Jensen, P., Wartmann, M., Davis, R.J., and Kelly, K. (1994). Control of MAP kinase activation by the mitogen-induced threonine/tyrosine phosphatase PAC1. Nature *367*, 651-654.

Waterman, H., Alroy, I., Strano, S., Seger, R., and Yarden, Y. (1999). The C-terminus of the kinase-defective neuregulin receptor ErbB-3 confers mitogenic superiority and dictates endocytic routing. EMBO J *18*, 3348-3358.

Waterman, H., Sabanai, I., Geiger, B., and Yarden, Y. (1998). Alternative intracellular routing of ErbB receptors may determine signaling potency. J Biol Chem *273*, 13819-13827.

Watson, H., and Bonifacino, J.S. (2007). Direct binding to Rsp5p regulates ubiquitination-independent vacuolar transport of Sna3p. Mol Biol Cell *18*, 1781-1789.

Wei, H., Ahn, S., Shenoy, S.K., Karnik, S.S., Hunyady, L., Luttrell, L.M., and Lefkowitz, R.J. (2003). Independent beta-arrestin 2 and G protein-mediated pathways for angiotensin II activation of extracellular signal-regulated kinases 1 and 2. Proc Natl Acad Sci U S A *100*, 10782-10787.

Weissbach, L., Settleman, J., Kalady, M.F., Snijders, A.J., Murthy, A.E., Yan, Y.X., and Bernards, A. (1994). Identification of a human rasGAP-related protein containing calmodulin-binding motifs. J Biol Chem *269*, 20517-20521.

Wellbrock, C., Karasarides, M., and Marais, R. (2004). The RAF proteins take centre stage. Nat Rev Mol Cell Biol *5*, 875-885.

Wells, A., Welsh, J.B., Lazar, C.S., Wiley, H.S., Gill, G.N., and Rosenfeld, M.G. (1990). Ligand-induced transformation by a noninternalizing epidermal growth factor receptor. Science *247*, 962-964.

Wertz, I.E., O'Rourke, K.M., Zhou, H., Eby, M., Aravind, L., Seshagiri, S., Wu, P., Wiesmann, C., Baker, R., Boone, D.L.*, et al.* (2004). De-ubiquitination and ubiquitin ligase domains of A20 downregulate NF-kappaB signalling. Nature *430*, 694-699.

Wherrett, J.R., and Huterer, S. (1972). Enrichment of bis-(monoacylglyceryl) phosphate in lysosomes from rat liver. J Biol Chem *247*, 4114-4120.

Whistler, J.L., Enquist, J., Marley, A., Fong, J., Gladher, F., Tsuruda, P., Murray, S.R., and Von Zastrow, M. (2002). Modulation of postendocytic sorting of G protein-coupled receptors. Science *297*, 615-620.

White, I.J., Bailey, L.M., Aghakhani, M.R., Moss, S.E., and Futter, C.E. (2006). EGF stimulates annexin 1-dependent inward vesiculation in a multivesicular endosome subpopulation. EMBO J *25*, 1-12.

Whitmarsh, A.J., Cavanagh, J., Tournier, C., Yasuda, J., and Davis, R.J. (1998). A mammalian scaffold complex that selectively mediates MAP kinase activation. Science *281*, 1671-1674.

Wick, M., Burger, C., Funk, M., and Muller, R. (1995). Identification of a novel mitogen-inducible gene (mig-6): regulation during G1 progression and differentiation. Exp Cell Res *219*, 527-535.

Wiley, H.S. (1988). Anomalous binding of epidermal growth factor to A431 cells is due to the effect of high receptor densities and a saturable endocytic system. J Cell Biol *107*, 801-810.

Wiley, H.S. (2003). Trafficking of the ErbB receptors and its influence on signaling. Exp Cell Res *284*, 78-88.

Wiley, H.S., and Burke, P.M. (2001). Regulation of receptor tyrosine kinase signaling by endocytic trafficking. Traffic *2*, 12-18.

Wiley, H.S., Herbst, J.J., Walsh, B.J., Lauffenburger, D.A., Rosenfeld, M.G., and Gill, G.N. (1991). The role of tyrosine kinase activity in endocytosis, compartmentation, and down-regulation of the epidermal growth factor receptor. J Biol Chem *266*, 11083-11094.

Williams, R.L., and Urbe, S. (2007). The emerging shape of the ESCRT machinery. Nat Rev Mol Cell Biol *8*, 355-368.

Willmarth, N.E., and Ethier, S.P. (2006). Autocrine and juxtacrine effects of amphiregulin on the proliferative, invasive, and migratory properties of normal and neoplastic human mammary epithelial cells. J Biol Chem *281*, 37728-37737.

Wilson, K.J., Gilmore, J.L., Foley, J., Lemmon, M.A., and Riese, D.J., 2nd (2009). Functional selectivity of EGF family peptide growth factors: implications for cancer. Pharmacol Ther *122*, 1-8.

Winkles, J.A. (1998). Serum- and polypeptide growth factor-inducible gene expression in mouse fibroblasts. Prog Nucleic Acid Res Mol Biol *58*, 41-78.

Wolf-Yadlin, A., Kumar, N., Zhang, Y., Hautaniemi, S., Zaman, M., Kim, H.D., Grantcharova, V., Lauffenburger, D.A., and White, F.M. (2006). Effects of HER2 overexpression on cell signaling networks governing proliferation and migration. Mol Syst Biol *2*, 54.

Wollert, T., Wunder, C., Lippincott-Schwartz, J., and Hurley, J.H. (2009). Membrane scission by the ESCRT-III complex. Nature *458*, 172-177.

Wong, E.S., Fong, C.W., Lim, J., Yusoff, P., Low, B.C., Langdon, W.Y., and Guy, G.R. (2002). Sprouty2 attenuates epidermal growth factor receptor ubiquitylation and endocytosis, and consequently enhances Ras/ERK signalling. EMBO J *21*, 4796-4808.

Wong, E.S., Lim, J., Low, B.C., Chen, Q., and Guy, G.R. (2001). Evidence for direct interaction between Sprouty and Cbl. J Biol Chem *276*, 5866-5875.

Wood, E.R., Truesdale, A.T., McDonald, O.B., Yuan, D., Hassell, A., Dickerson, S.H., Ellis, B., Pennisi, C., Horne, E., Lackey, K.*, et al.* (2004). A unique structure for epidermal growth factor receptor bound to GW572016 (Lapatinib): relationships among protein conformation, inhibitor off-rate, and receptor activity in tumor cells. Cancer Res *64*, 6652-6659.

Wood, K.W., Sarnecki, C., Roberts, T.M., and Blenis, J. (1992). ras mediates nerve growth factor receptor modulation of three signal-transducing protein kinases: MAP kinase, Raf-1, and RSK. Cell *68*, 1041-1050.

Worthylake, R., Opresko, L.K., and Wiley, H.S. (1999). ErbB-2 amplification inhibits down-regulation and induces constitutive activation of both ErbB-2 and epidermal growth factor receptors. J Biol Chem *274*, 8865-8874.

Worthylake, R., and Wiley, H.S. (1997). Structural aspects of the epidermal growth factor receptor required for transmodulation of erbB-2/neu. J Biol Chem *272*, 8594-8601.

Wu, S.L., Kim, J., Bandle, R.W., Liotta, L., Petricoin, E., and Karger, B.L. (2006). Dynamic profiling of the post-translational modifications and interaction partners of epidermal growth factor receptor signaling after stimulation by epidermal growth factor using Extended Range Proteomic Analysis (ERPA). Mol Cell Proteomics *5*, 1610-1627.

Wunderlich, W., Fialka, I., Teis, D., Alpi, A., Pfeifer, A., Parton, R.G., Lottspeich, F., and Huber, L.A. (2001). A novel 14-kilodalton protein interacts with the mitogen-activated protein kinase scaffold mp1 on a late endosomal/lysosomal compartment. J Cell Biol *152*, 765-776.

Xia, L., Wang, L., Chung, A.S., Ivanov, S.S., Ling, M.Y., Dragoi, A.M., Platt, A., Gilmer, T.M., Fu, X.Y., and Chin, Y.E. (2002). Identification of both positive and negative domains within the epidermal growth factor receptor COOH-terminal region for signal transducer and activator of transcription (STAT) activation. J Biol Chem *277*, 30716-30723.

Xu, S., Furukawa, T., Kanai, N., Sunamura, M., and Horii, A. (2005). Abrogation of DUSP6 by hypermethylation in human pancreatic cancer. J Hum Genet *50*, 159-167.

Yaish, P., Gazit, A., Gilon, C., and Levitzki, A. (1988). Blocking of EGF-dependent cell proliferation by EGF receptor kinase inhibitors. Science *242*, 933-935.

Yamauchi, T., Ueki, K., Tobe, K., Tamemoto, H., Sekine, N., Wada, M., Honjo, M., Takahashi, M., Takahashi, T., Hirai, H.*, et al.* (1997). Tyrosine phosphorylation of the EGF receptor by the kinase Jak2 is induced by growth hormone. Nature *390*, 91-96.

Yamazaki, S., Numano, R., Abe, M., Hida, A., Takahashi, R., Ueda, M., Block, G.D., Sakaki, Y., Menaker, M., and Tei, H. (2000). Resetting central and peripheral circadian oscillators in transgenic rats. Science *288*, 682-685.

Yamazaki, T., Zaal, K., Hailey, D., Presley, J., Lippincott-Schwartz, J., and Samelson, L.E. (2002). Role of Grb2 in EGF-stimulated EGFR internalization. J Cell Sci *115*, 1791-1802.

Yao, Z., and Seger, R. (2009). The ERK signaling cascade--views from different subcellular compartments. Biofactors *35*, 407-416.

Yarden, Y., and Schlessinger, J. (1985). The EGF receptor kinase: evidence for allosteric activation and intramolecular self-phosphorylation. Ciba Found Symp *116*, 23-45.

Yarden, Y., and Schlessinger, J. (1987a). Epidermal growth factor induces rapid, reversible aggregation of the purified epidermal growth factor receptor. Biochemistry *26*, 1443-1451.

Yarden, Y., and Schlessinger, J. (1987b). Self-phosphorylation of epidermal growth factor receptor: evidence for a model of intermolecular allosteric activation. Biochemistry *26*, 1434-1442.

Yarden, Y., and Sliwkowski, M.X. (2001). Untangling the ErbB signalling network. Nat Rev Mol Cell Biol *2*, 127-137.

Yoo, S.H., Yamazaki, S., Lowrey, P.L., Shimomura, K., Ko, C.H., Buhr, E.D., Siepka, S.M., Hong, H.K., Oh, W.J., Yoo, O.J.*, et al.* (2004). PERIOD2::LUCIFERASE real-time reporting of circadian dynamics reveals persistent circadian oscillations in mouse peripheral tissues. Proc Natl Acad Sci U S A *101*, 5339-5346.

Yoon, C.H., Lee, J., Jongeward, G.D., and Sternberg, P.W. (1995). Similarity of sli-1, a regulator of vulval development in C. elegans, to the mammalian proto-oncogene c-cbl. Science *269*, 1102-1105.

Yoon, S., and Seger, R. (2006). The extracellular signal-regulated kinase: multiple substrates regulate diverse cellular functions. Growth Factors *24*, 21-44.

Yorikawa, C., Shibata, H., Waguri, S., Hatta, K., Horii, M., Katoh, K., Kobayashi, T., Uchiyama, Y., and Maki, M. (2005). Human CHMP6, a myristoylated ESCRT-III protein, interacts directly with an ESCRT-II component EAP20 and regulates endosomal cargo sorting. Biochem J *387*, 17-26.

Yoshimura, A., Ohkubo, T., Kiguchi, T., Jenkins, N.A., Gilbert, D.J., Copeland, N.G., Hara, T., and Miyajima, A. (1995). A novel cytokine-inducible gene CIS encodes an SH2-containing protein that binds to tyrosine-phosphorylated interleukin 3 and erythropoietin receptors. EMBO J *14*, 2816-2826.

Yu, W., Fantl, W.J., Harrowe, G., and Williams, L.T. (1998). Regulation of the MAP kinase pathway by mammalian Ksr through direct interaction with MEK and ERK. Curr Biol *8*, 56-64.

Yu, W.H., Woessner, J.F., Jr., McNeish, J.D., and Stamenkovic, I. (2002). CD44 anchors the assembly of matrilysin/MMP-7 with heparin-binding epidermal growth factor precursor and ErbB4 and regulates female reproductive organ remodeling. Genes Dev *16*, 307-323.

Yuan, T., Wang, Y., Zhao, Z.J., and Gu, H. (2010). Protein-tyrosine phosphatase PTPN9 negatively regulates ErbB2 and epidermal growth factor receptor signaling in breast cancer cells. J Biol Chem *285*, 14861-14870.

Zacharias, D.A., Violin, J.D., Newton, A.C., and Tsien, R.Y. (2002). Partitioning of lipid-modified monomeric GFPs into membrane microdomains of live cells. Science *296*, 913-916.

Zamborlini, A., Usami, Y., Radoshitzky, S.R., Popova, E., Palu, G., and Gottlinger, H. (2006). Release of autoinhibition converts ESCRT-III components into potent inhibitors of HIV-1 budding. Proc Natl Acad Sci U S A *103*, 19140-19145.

Zehorai, E., Yao, Z., Plotnikov, A., and Seger, R. (2010). The subcellular localization of MEK and ERK--a novel nuclear translocation signal (NTS) paves a way to the nucleus. Mol Cell Endocrinol *314*, 213-220.

Zeng, F., Xu, J., and Harris, R.C. (2009). Nedd4 mediates ErbB4 JM-a/CYT-1 ICD ubiquitination and degradation in MDCK II cells. FASEB J *23*, 1935-1945.

Zerial, M., and McBride, H. (2001). Rab proteins as membrane organizers. Nat Rev Mol Cell Biol *2*, 107-117.

Zhang, X., Gureasko, J., Shen, K., Cole, P.A., and Kuriyan, J. (2006). An allosteric mechanism for activation of the kinase domain of epidermal growth factor receptor. Cell *125*, 1137-1149.

Zhang, X., Pickin, K.A., Bose, R., Jura, N., Cole, P.A., and Kuriyan, J. (2007a). Inhibition of the EGF receptor by binding of MIG6 to an activating kinase domain interface. Nature *450*, 741-744.

Zhang, X.F., Settleman, J., Kyriakis, J.M., Takeuchi-Suzuki, E., Elledge, S.J., Marshall, M.S., Bruder, J.T., Rapp, U.R., and Avruch, J. (1993). Normal and oncogenic p21ras proteins bind to the amino-terminal regulatory domain of c-Raf-1. Nature *364*, 308-313.

Zhang, Y., Blattman, J.N., Kennedy, N.J., Duong, J., Nguyen, T., Wang, Y., Davis, R.J., Greenberg, P.D., Flavell, R.A., and Dong, C. (2004). Regulation of innate and adaptive immune responses by MAP kinase phosphatase 5. Nature *430*, 793-797.

Zhang, Y.W., Staal, B., Su, Y., Swiatek, P., Zhao, P., Cao, B., Resau, J., Sigler, R., Bronson, R., and Vande Woude, G.F. (2007b). Evidence that MIG-6 is a tumor-suppressor gene. Oncogene *26*, 269-276.

Zhang, Y.W., and Vande Woude, G.F. (2007). Mig-6, signal transduction, stress response and cancer. Cell Cycle *6*, 507-513.

Zhen, Y., Caprioli, R.M., and Staros, J.V. (2003). Characterization of glycosylation sites of the epidermal growth factor receptor. Biochemistry *42*, 5478-5492.

Zheng, C.F., and Guan, K.L. (1993). Cloning and characterization of two distinct human extracellular signal-regulated kinase activator kinases, MEK1 and MEK2. J Biol Chem *268*, 11435-11439.

Zhu, G., Gilchrist, R., Borley, N., Chng, H.W., Morgan, M., Marshall, J.F., Camplejohn, R.S., Muir, G.H., and Hart, I.R. (2004). Reduction of TSG101 protein has a negative impact on tumor cell growth. Int J Cancer *109*, 541-547.

Zwang, Y., and Yarden, Y. (2009). Systems biology of growth factor-induced receptor endocytosis. Traffic *10*, 349-363.

Appendix

1. List of abbreviations

°C	degree Celsius
7MSR	seven membrane spanning receptor
A + T	ALIX + TSG101
A431	human epidermoid carcinoma A431
AAA+	ATPases associated with various cellular activities
ACK1	activated CDC42-associated kinase 1, official symbol TNK2
ACTB	actin, beta
ADAM	a disintegrin and metalloproteinase
ADP	adenosine diphosphate
AG1478	tyrphostin
AGTR1	angiotensin II receptor, type 1
AIP1	ALG-2 interacting protein 1, also ALIX, official symbol PDCD6IP
AKT	v-akt murine thymoma viral oncogene homolog, also PKB
ALG-2	apoptosis-linked gene 2, official symbol PDCD6 (programmed cell death 6)
ALIX	ALG-2 interacting protein X, also AIP1, official symbol PDCD6IP
AMSH	associated molecule with the SH3 domain of STAM, official symbol STAMBP (STAM binding protein)
anti-	antibody against
ANXA1	annexin A1
ANXA2	annexin A2
AP	adaptor protein (complex)
AP-	activator protein
AREG	amphiregulin
ARF	ADP ribosylation factor
ARRB	arrestin, beta
ART	arrestin-related trafficking adaptor
ASK1	apoptosis signal-regulating kinase 1, official symbol MAP3K5
ATF	activating transcription factor
ATP	adenosine triphosphate
ATPase	adenosine triphosphatase
B + C	CBLB + CBL
BHK	new born / baby hamster kidney
BIRC3	baculoviral IAP repeat-containing 3, also IAP2 (inhibitor of apoptosis protein 2)
BMP	bis(monoacylglyceryl)phosphate
BRO	BCK1-like resistance to osmotic shock
BROX	BRO1 domain-containing protein X, official designation C1orf58
BSA	bovine serum albumin
BTC	betacellulin
bZIP	leucine zipper
C	carboxy
C + D2	CHC + DNM2
Ca2+	calcium
CAMK1	calcium/calmodulin-dependent protein kinase 1
CAV1	caveolin 1
CBL	casitas B-lineage lymphoma proto-oncogene, also C-CBL
CBLB	casitas B-lineage lymphoma proto-oncogene b, also CBL-B
CCL	chemokine (C-C motif) ligand
CCP	clathrin-coated pit
CCV	clathrin-coated vesicle
CD	cluster of differentiation
CDC42	cell division cycle 42
CDK	cyclin-dependent kinase
cDNA	complementary DNA
CHC	clathrin heavy chain, official symbol CLTC
CHMP	charged multivesicular body protein, or chromatin modifying protein
Chol.	cholesterol
CIE	clathrin-independent endocytosis
CIN85	CBL-interacting protein of 85 kDa, official symbol SH3KBP1
CIS	cytokine inducible SH2-containing protein, official symbol CISH
CLIC	clathrin-independent carrier
cm	centimeter
CME	clathrin-mediated endocytosis
CMU	Centre médical universitaire
CMV	cytomegalovirus
CO_2	carbon dioxide
COS	CV-1 (simian) in origin, carrying the SV40 genetic material
cpm	counts per minute

CREM	cAMP responsive element modulator
cRNA	complementary RNA
CS	code set
Ctr	control
CXCL	chemokine (C-X-C motif) ligand
CXCR4	chemokine (C-X-C motif) receptor 4
DAG	diacylglycerol
DBD	DNA binding domain
ddCt	number of PCR cycles between non- and EGF-induced, normalized to actin
DEG	delayed early gene
DMEM	Dulbecco's Modified Eagle Medium
DNA	deoxyribonucleic acid
DNM	dynamin
ds-	double-stranded
DUB	deubiquitinase
DUSP	dual-specificity phosphatase
e.g.	*exempli gratia*
EAP	ELL-associating protein
EE	early endosome
EGF	epidermal growth factor
EGFR	epidermal growth factor receptor
EGR	early growth response
ELF	E74-like factor (ETS domain transcription factor)
ELK	ETS domain-containing protein ELK
EPGN	epigen
EPS15	EGFR pathway substrate 15
EPS15R	EGFR pathway substrate EPS15R, official symbol EPS15L1
ER	endoplasmic reticulum
ERBB	v-erb-b erythroblastic leukemia viral oncogene homolog
ERC	endocytic recycling compartment
EREG	epiregulin
ERK	extracellular signal-regulated kinase
ERK1	extracellular signal-regulated kinase 1, official symbol MAPK3
ERK2	extracellular signal-regulated kinase 2, official symbol MAPK1
ERRFI1	ERBB receptor feedback inhibitor 1, also MIG6 or RALT
ESCRT	endosomal sorting complex required for transport
et al.	*et alii*
ETS	E-twenty six
F-actin	fibrous actin
FAK	focal adhesion kinase, official symbol PTK2
FCS	fetal calf serum
FGF	fibroblast growth factor
Fig.	figure
FOS	FBJ murine osteosarcoma viral oncogene homolog
FOSL	FOS-like antigen
FYVE	Fab1p (yeast orthologue of PIKFYVE), YOTB, Vac1p, EEA1
GAB1	GRB2-associated binding protein 1
Gag	group-specific antigen
GAP	GTPase-activating protein
GASP	G protein-coupled receptor associated sorting protein, official symbol GPRASP1
GDF	GDI displacement factor
GDI	GDP dissociation inhibitor
GDP	guanosine diphosphate
GEEC	GPI-AP-enriched early endosomal compartment
GEF	guanine nucleotide exchange factor
GFP	green fluorescent protein
GGA	golgi-associated, gamma adaptin ear containing, ARF binding protein
GH1	growth hormone 1
GHR	growth hormone receptor
GLUE	GRAM-Like ubiquitin-binding in EAP45
GPCR	G protein-coupled receptor
GPI-AP	glycosylphosphatidylinositol-anchored protein
GRAM	glucosyltransferases, Rab-like GTPase activators and myotubularins
GRB2	growth factor receptor-bound protein 2
GTP	guanosine triphosphate
GTPase	guanosine triphosphatase
h	hour(s)
HBEGF	heparin-binding EGF-like growth factor
HD-PTP	His-domain protein tyrosine phosphatase, official symbol PTPN23
HeLa	Henrietta Lacks
HEp2	human epidermoid cancer
HEPES	4-(2-hydroxyethyl)-1-piperazineethanesulfonic acid
HER	human EGF receptor
HGF	hepatocyte growth factor
HIV	human immunodeficiency virus
HLR-ELK1	HeLa luciferase reporter for ELK1

HMEC	human mammary epithelial cell
HOPS	homotypic fusion and vacuole protein sorting
HRAS	Harvey rat sarcoma viral oncogene homolog
HRG	heregulin, Type I NRG1
HRP	horseradish peroxidase
HRS	hepatocyte growth factor-regulated tyrosine kinase substrate, official symbol HGS
ID1	inhibitor of DNA binding 1
IEG	immediate early gene
IGF1R	insulin-like growth factor 1 receptor
IKB	I-kappa-B, or NF-kappa-B inhibitor
IL	interleukin
ILV	intraluminal vesicle
IMP	impedes mitogenic signal propagation, official symbol BRAP
Ins(1,4,5)P3	inositol-1,4,5-triphosphate, also IP3
IQGAP	IQ motif containing GTPase activating protein
IRF1	interferon regulatory factor 1
JAK	Janus kinase
JDP	JUN dimerization protein
JIP1	JNK-interacting protein 1, official symbol MAPK8IP1
JM	juxtamembrane
JNK	c-JUN N-terminal kinase
JUN	v-jun avian sarcoma virus 17 oncogene homolog
JUNB	jun B proto-oncogene
JUND	jun D proto-oncogene
KD	knockdown
KIF16B	kinesin family member 16B
KLF	Kruppel-like factor
KRAS	Kirsten rat sarcoma viral oncogene homolog
KSR1	kinase suppressor of RAS 1
LAMP	lysosomal-associated membrane protein
LBPA	lysobisphosphatidic acid, also BMP
LDL	low density lipoprotein
LDLR	low density lipoprotein receptor
LE	late endosome
Log2	logarithm base 2
LPA	lysophosphatidic acid
LPAR	lysophosphatidic acid receptor
LRIG1	leucine-rich repeats and immunoglobulin-like domains 1
LRP1	low density lipoprotein receptor-related protein 1
LZ	leucine zipper
M6P	mannose 6-phosphate
M6PR	mannose-6-phosphate receptor (cation-dependent)
MAFF	v-maf avian musculoaponeurotic fibrosarcoma oncogene homolog F
MAPK	mitogen-activated protein kinase
MAPKK	MAPK kinase
MAPKKK	MAPK kinase kinase
MDCK	Madin-Darby canine kidney
MDM2	Mdm2 p53 binding protein homolog (mouse)
MEK	MAPK/ERK kinase
MEK1	MAPK/ERK kinase 1, official symbol MAP2K1
MEK2	MAPK/ERK kinase 2, official symbol MAP2K2
MET	met proto-oncogene, or hepatocyte growth factor receptor
mg	milligram
µg	microgram
µl	microliter
µM	micromolar
MIG6	mitogen-inducible gene 6 protein, official symbol ERRFI1
min (´)	minute(s)
MKP	MAPK phosphatase
ml	milliliter
mM	millimolar
MMP	matrix metalloproteinase
MORG1	MAPK organizer 1, official symbol WDR83
MP1	MEK1 partner 1, official symbol MAPKSP1 for MAPK scaffold protein 1
mRNA	messenger RNA
MTORC1	mammalian target of rapamycin complex 1, official symbol MTOR
MVB	multivesicular body
MYC	v-myc myelocytomatosis viral oncogene homolog (avian)
N	amino
n =	number of experiments

NAB2	NGFI-A binding protein 2 (also EGR1 binding protein 2)
NCE	non-clathrin-mediated endocytosis
NEDD4	neural precursor cell expressed, developmentally down-regulated 4
NFKB	NF-kappa-B, or nuclear factor of kappa light polypeptide gene enhancer in B-cells
NFKBIA	nuclear factor of kappa light polypeptide gene enhancer in B-cells inhibitor alpha, also IKBA
NFKBIE	nuclear factor of kappa light polypeptide gene enhancer in B-cells inhibitor epsilon, also IKBE
ng	nanogram
NGF	nerve growth factor
NIH	National Institute of Health
NIH3T3	mouse embryonic fibroblast cell line, established from an NIH mouse embryo
nM	nanomolar
NOTCH	Notch homolog (*Drosophila*)
NPC	Niemann-Pick type C
NRAS	neuroblastoma RAS viral oncogene homolog
NRG	neuregulin
NRK	normal rat kidney
NSF	N-ethylmaleimide-sensitive factor
NTRK1	neurotrophic tyrosine kinase receptor type 1, also TRKA
P-	phosphorylated
p14	endosome-associated protein of 14 kDa, official symbol ROBLD3
p38	p38 mitogen activated protein kinase, official symbol MAPK14
PAK1	p21 protein (CDC42/RAC)-activated kinase 1
PAR2	protease-activated receptor 2, official symbol F2RL1
PBS	phosphate-buffered saline
PCA	principal component analysis
p-ch	pulse-chase
PCR	polymerase chain reaction
PDCD6IP	programmed cell death 6 interacting protein, also ALIX or AIP1
PDGF	platelet derived growth factor
PDK	3-phosphoinositide-dependent protein kinase 1, official symbol PDPK1
PH	pleckstrin homology
phospho-	phosphorylated
PI(3)P	phosphatidylinositol 3-phosphate
PI(3,4,5)P3	phosphatidylinositol 3,4,5-triphosphate
PI(3,5)P2	phosphatidylinositol 3,5-bisphosphate
PI(4)P	phosphatidylinositol 4-phosphate
PI(4,5)P2	phosphatidylinositol 4,5-bisphosphate, also PIP2
PI3K	phosphatidylinositol-3-kinase
PI4KA	phosphatidylinositol 4-kinase alpha
PIKFYVE	phosphoinositide kinase, FYVE finger containing
PKA	protein kinase A (cAMP-dependent)
PKB	protein kinase B
PKC	protein kinase C
PLA2	phospholipase A2
PLCG1	phospholipase C, gamma 1
PLD2	phospholipase D2
PMA	phorbol 12-myristate 13-acetate
PMEL17	melanocyte protein 17, official symbol SILV
PP2A	protein phosphatase 2A
PRD	proline-rich domain
PTB	phosphotyrosine binding
PTEN	phosphatase and tensin homolog
PTGS2	prostaglandin-endoperoxide synthase 2, also COX2 (cyclooxygenase 2)
PTP	protein tyrosine phosphatase
PTPN	protein tyrosine phosphatase, non-receptor type
PTPR	protein tyrosine phosphatase, receptor type
PX	phox homology
qRT-PCR	quantitative reverse transcription polymerase chain reaction
RAB	RAS-related in brain
RACGAP1	Rac GTPase activating protein 1
RACK1	receptor of activated protein kinase C 1, official symbol GNB2L1
RAF	v-raf-1 murine leukemia viral oncogene homolog
RALT	receptor-associated late transducer, official symbol ERRFI1
RAS	rat sarcoma
RASA1	RAS p21 protein activator (GTPase activating protein) 1, also RASGAP
RASGRP1	RAS guanyl releasing protein 1

RBX1	ring-box 1, E3 ubiquitin protein ligase, also ROC1
RE	recycling endosome
REL	v-rel reticuloendotheliosis viral oncogene homolog
RHEBL1	RAS homolog enriched in brain-like 1
RHOA	RAS homolog A
RILP	RAB-interacting lysosomal protein
RING	really interesting new gene
RISC	RNA-induced silencing complex
RNA	ribonucleic acid
RNAi	RNA interference
R-SNARE	arginine-containing SNARE
RTK	receptor tyrosine kinase
RT-PCR	reverse transcription polymerase chain reaction
SCF	stem cell factor
SDS-PAGE	sodium dodecyl sulfate polyacrylamide gel electrophoresis
SEF	similar expression to *FGF* genes, official symbol IL17RD
sEGFR	secreted, truncated extracellular domain of the EGFR
Ser	serine
SH	SRC homology
SHC	Src homology 2 domain containing
SHP1	SH2 domain-containing protein tyrosine phosphatase, official symbol PTPN6
SHP2	SH2 domain-containing protein tyrosine phosphatase, official symbol PTPN11
siRNA	small interfering RNA
SNARE	soluble N-ethylmaleimide-sensitive fusion protein attachment protein receptor
SNX16	sorting nexin 16
SNX3	sorting nexin 3
SOCS	suppressor of cytokine signaling
SOS	son of sevenless homolog (*Drosophila*)
S-phase	synthesis phase
SPRED	sprouty-related, EVH1 domain containing
SPRY	sprouty homolog (*Drosophila*)
SRC	viral sarcoma oncogene homolog
ss-	single-stranded
STAM	signal transducing adaptor molecule
STAT	signal transducer and activator of transcription
TACE	TNF-alpha converting enzyme
TAL	Tsg101-associated ligase, official symbol LRSAM1
TCPTP	T-cell protein tyrosine phosphatase, official symbol PTPN2
TF	transcription factor
TGFA	transforming growth factor-alpha
TGFB	transforming growth factor, beta
TGN	*trans*-Golgi network
Thr	threonine
TIP47	tail-interacting protein of 47 kDa, official symbol PLIN3 for perilipin 3
TKB	tyrosine kinase-binding
TNF	tumor necrosis factor
TNFAIP3	tumor necrosis factor, alpha-induced protein 3, also A20
TNK2	tyrosine kinase, non-receptor, 2
TRAF	tumor necrosis factor receptor-associated factor
TRF	transferrin receptor
TSG101	tumor susceptibility gene 101
Tyr	tyrosine, also Y
UAS	upstream activation sequence
Ub	ubiquitin
UBA	ubiquitin-associated
UEV	ubiquitin E2 variant
UIM	ubiquitin-interacting motif
VAMP	vesicle-associated membrane protein
VEGF	vascular endothelial growth factor
VEGFR	VEGF receptor
VHS	Vps27p, HRS and STAM
VPS	vacuolar protein sorting
vs.	*versus*
VSV	vesicular stomatitis virus
VTI1B	vesicle transport through interaction with t-SNAREs homolog 1B
WB	western blot
ZFAND5	zinc finger, AN1-type domain 5, also ZNF216
ZFP	zinc finger protein

2. Target sequences of ON-TARGETplus SMARTpool siRNAs from Dharmacon

- **EGFR / ERBB1 siRNA pool**

  Target sequence 1: 5´-CAAAGTGTGTAACGGAATA-3´ Target sequence 3: 5´-GTAACAAGCTCACGCAGTT-3´
  Target sequence 2: 5´-CCATAAATGCTACGAATAT-3´ Target sequence 4: 5´-CAGAGGATGTTCAATAACT-3´

- **MEK1 / MAP2K1 siRNA pool**

  Target sequence 1: 5´-CCATGCTGCTGGCGTCTAA-3´ Target sequence 3: 5´-CGACGGCTCTGCAGTTAAC-3´
  Target sequence 2: 5´-GAGGTTCTCTGGATCAAGT-3´ Target sequence 4: 5´-GCACAAGGTCCTACATGTC-3´

- **MEK2 / MAP2K2 siRNA pool**

  Target sequence 1: 5´-CGACAGCGCATGCAGGAAC-3´ Target sequence 3: 5´-GGTCCGAGGTGGAAGAAGT-3´
  Target sequence 2: 5´-GATCAGCATTTGCATGGAA-3´ Target sequence 4: 5´-TCTTTGAACTCCTGGACTA-3´

- **HRS / HGS siRNA pool**

  Target sequence 1: 5´-GAGGTAAACGTCCGTAACA-3´ Target sequence 3: 5´-AAAGAACTGTGGCCAGACA-3´
  Target sequence 2: 5´-GCACGTCTTTCCAGAATTC-3´ Target sequence 4: 5´-GAACCCACACGTCGCCTTG -3´

- **TSG101 siRNA pool**

  Target sequence 1: 5´-CCGTTTAGATCAAGAAGTA-3´ Target sequence 3: 5´-CCACAACAAGTTCTCAGTA-3´
  Target sequence 2: 5´-CTCCATACCCATCCGGATA-3´ Target sequence 4: 5´-CCAAATACTTCCTACATGC -3´

- **VPS4A siRNA pool**

  Target sequence 1: 5´-CCACAAACATCCCATGGGT-3´ Target sequence 3: 5´-TCAAAGAGAACCAGAGTGA-3´
  Target sequence 2: 5´-CCGAGAAGCTGAAGGATTA-3´ Target sequence 4: 5´-GAATAACAATGATGGGACT-3´

- **ALIX / PDCD6IP / AIP1 siRNA pool**

  Target sequence 1: 5´-CAGATCTGCTTGACATTTA-3´ Target sequence 3: 5´-GCGTATGGCCAGTATAATA-3´
  Target sequence 2: 5´-TCGAGACGCTCCTGAGATA-3´ Target sequence 4: 5´-GTACCTCAGTCTATATTGA-3´

- **HD(-)PTP / PTPN23 siRNA pool**

  Target sequence 1: 5´-GTGCACAGGTGGTAGATTA-3´ Target sequence 3: 5´-GCATGAAGGTCTCCTGTAC-3´
  Target sequence 2: 5´-GCAAACAGCGGATGAGCAA-3´ Target sequence 4: 5´-GTAGTGTCCTCCGCAAGTA-3´

- **CHC / CLTC siRNA pool**

  Target sequence 1: 5´-GAGAATGGCTGTACGTAAT-3´ Target sequence 3: 5´-GCAGAAGAATCAACGTTAT-3´
  Target sequence 2: 5´-TGAGAAATGTAATGCGAAT-3´ Target sequence 4: 5´-CGTAAGAAGGCTCGAGAGT-3´

- **DNM2 / DYN2 siRNA pool**

  Target sequence 1: 5´-GGCCCTACGTAGCAAACTA-3´ Target sequence 3: 5´-CCGAATCAATCGCATCTTC-3´
  Target sequence 2: 5´-GAGATCAGGTGGACACTCT-3´ Target sequence 4: 5´-GAGCGAATCGTCACCACTT-3´

- **CBL / C-CBL siRNA pool**

  Target sequence 1: 5´-AATCAACTCTGAACGGAAA-3´ Target sequence 3: 5´-TAGCCCACCTTATATCTTA-3´
  Target sequence 2: 5´-GACAATCCCTCACAATAAA-3´ Target sequence 4: 5´-GGAGACACATTTCGGATTA-3´

- **CBLB / CBL-B siRNA pool**

  Target sequence 1: 5´-GAACATCACAGGACTATGA-3´ Target sequence 3: 5´-GGTCGAATTTTGGGTATTA-3´
  Target sequence 2: 5´-GTACTGGTCCGTTAGCAAA-3´ Target sequence 4: 5´-TATCAGCATTTACGACTTA-3´

3. Target sequences of NanoString probes

Table 1: Target sequences of the first NanoString code sets

Gene	Accession #	Region	Target Sequence
ACTB	NM_001101.2	1010-1110	TGCAGAAGGAGATCACTGCCCTGGCACCCAGCACAATGAAGATCAAGATCATTGCTCCTCCTGAGCGCAAGTACTCCGTGTGGATCGGCGGCTCCATCCT
AKAP12	NM_005100.3	640-740	TCACAGATGATGGGCAGGAGGAGACACCCGAAATAATCGAACAGATTCCTTCTTCAGAAAGCAATTTAGAAGAGCTAACACAACCCACTGAGTCCCAGGC
ARHGDIA	NM_004309.3	6-106	CCGACGACGTTCGTCATTTAGTGCGGGAGGGATCCTGAACCGCGCGGCCGAACCCTCCGGTGTCCCGACCCAGGCTAAGCTTGAGCATGGCTGAGCAGGA
ATF3	NM_001674.2	705-805	TTTGATATACATGCTCAACCTTCATCGGCCCACGTGTATTGTCCGGGCTCAGAATGGGAGGACTCCAGAAGATGAGAGAAACCTCTTTATCCAACAGATA
BHLHB2	NM_003670.1	560-660	AGAGTGGTTTACAAGCTGGTGAGCTGTCAGGGAGAAATGTCGAAACAGGTCAAGAGATGTTCTGCTCAGGTTTCCAGACATGTGCCCGGGAGGTGCTTCA
C1orf58	NM_144695.2	426-526	AAGCCACAGCTCCTGTGTCTTTTAATTACTATGGTGTAGTCACTGGCCCTTCTGCTTCAAAAATATGCAATGACTTGAGGTCATCCAGGGCACGACTCCT
CDKN1A	NM_000389.2	1975-2075	CATGTGTCCTGGTTCCCGTTTCTCCACCTAGACTGTAAACCTCTCGAGGGCAGGGACCACACCCTGTACTGTTCTGTGTCTTTCACAGCTCCTCCCACAA
CDKN2AIP	NM_017632.2	485-585	AGTGACAGATGCTCCAACCTATACAACAAGAGATGAACTGGTTGCCAAGGTGAAGAAAAGAGGGATATCGAGTAGCAATGAAGGGGTAGAAGAGCCATCC
CEBPB	NM_005194.2	1420-1520	CAACCGCACATGCAGATGGGGCTCCCGCCCGTGGTGTTATTTAAAGAAGAAACGTCTATGTGTACAGATGAATGATAAACTCTCTGCTTCTCCCTCTGCC
CITED2	NM_006079.3	965-1065	AGGAGCTGCCCGAACTCTGGCTGGGGCAAAACGAGTTTGATTTTATGACGGACTTCGTGTGCAAACAGCAGCCCAGCAGAGTGAGCTGTTGACTCGATCG
CREM	NM_001881.2	260-360	CTCCACCTCCTCGCGTCCGTAATCAGTGACGAGGTCCGCTACGTAAATCCCTTTGCGGCGGACAAATGACCATGGAAACAGTTGAATCCCAGCATGATGG
CXCL1	NM_001511.1	445-545	AGGCCCTGCCCTTATAGGAACAGAAGAGGAAAGAGAGACACAGCTGCAGAGGCCACCTGGATTGTGCCTAATGTGTTTGAGCATCGCTTAGGAGAAGTCT
CXCL2	NM_002089.1	435-535	GAAGGAGGCCCTGCCTTACAGGAACAGAAGAGGAAAGAGAGACACAGCTGCAGAGGCCACCTGGCTTGCGCCTAATGTGTTTGAGCATACTTAGGAGAAG
CYTH1	NM_004762.2	1195-1295	CATCAGCAGGGACCCTTTCTACGAAATGCTCGCAGCACGGAAAAAGAAGGTCTCCTCCACGAAGCGACACTGAGCGTGCAGCCAAGGGCGTTGGTCTGCG
DKK1	NM_012242.2	75-175	CGGCACGGTTTCGTGGGGACCCAGGCTTGCAAAGTGACGGTCATTTTCTCTTTCTTTCTCCCTCTTGAGTCCTTCTGAGATGATGGCTCTGGGCGCAGCG
DNMBP	NM_015221.2	5120-5220	GAAGCCCAGTGTCCTATGTATGCAGGAAGCTGTGCTCTAGCAATAGACAGTGTTGGTAATGGTTGTGCTGTACGGCGTTTGGGGTGGCCCCATGTTCCAT
DUSP1	NM_004417.2	987-1087	TCAAGAATGCTGGAGGAAGGGTGTTTGTCCACTGCCAGGCAGGCATTTCCCGGTCAGCCACCATCTGCCTTGCTTACCTTATGAGGACTAATCGAGTCAA
DUSP2	NM_004418.3	1235-1335	CTGGCCCTCATTCGGGGTCGGGAACCAAGGGTGTGTCTGCTCTTTCCCTCCCCATCCTCTGGCAGAAATCAGCTAGACGCTATACCGTGGACTCTCCCTG
DUSP3	NM_004090.3	3430-3530	AATCTTAAAGCAGTATACCTTTCCACAGGCTCGTCTGTGTCCCTGCCACTCTGAGTTATCCAGAAACCACCACCTACAAATGAGGGGACTCATCTAGAAG
DUSP4	NM_001394.5	45-145	GCGACAGGAGCCGCGCGACCGGCAAAAATACACGGGAGGCCGTCGCCGAAAAGAGTCCGCGGTCCTCTCTCGTAAACACACTCTCCTCCACCGGCGCCTC
DUSP5	NM_004419.3	675-775	GTGGATGTAAAACCCATTTCACAAGAGAAGATTGAGAGTGAGAGAGCCCTCATCAGCCAGTGTGGAAAACCAGTGGTAAATGTCAGCTACAGGCCAGCTT
DUSP6	NM_001946.2	1535-1635	ATGTGACAACAGGGTTCCAGCACAGCAGCTGTATTTTACCACCCCTTCCAACCAGAATGTATACCAGGTGGACTCTCTGCAATCTACGTGAAAGACCCCA
DUSP7	NM_001947.2	1065-1165	CTAAGCAGCCCGTGCGACAACCACGCGTCGAGTGAGCAGCTCTACTTTTCCACGCCCACCAACCACAACCTGTTCCCACTCAATACGCTGGAGTCCACGT
EFNA1	NM_004428.2	650-750	TGCTGCCCCACGCCTCTTCCCACTTGCCTGGACTGTGCTGCTCCTTCCACTTCTGCTGCTGCAAACCCCGTGAAGGTGTATGCCACACCTGGCCTTAAAG
EGF	NM_001963.3	3930-4030	TAATGGAGCGAAGCTTTCATATGCCCTCCTATGGGACACAGACCCTTGAAGGGGGTGTCGAGAAGCCCCATTCTCTCCTATCAGCTAACCCATTATGGCA
EGFR	NM_005228.3	2760-2860	GCAGCCAGGAACGTACTGGTGAAAACACCGCAGCATGTCAAGATCACAGATTTTGGGCTGGCCAAACTGCTGGGTGCGGAAGAGAAAGAATACCATGCAG
EGR1	NM_001964.2	1505-1605	GAGGCATACCAAGATCCACTTGCGGCAGAAGGACAAGAAAGCAGACAAAAGTGTTGTGGCCTCTTCGGCCACCTCCTCTCTCTCTTCCTACCCGTCCCCG
EGR3	NM_004430.2	3170-3270	CGTACAGGGTGGCTCCTTTGAAGTGGAGTAATAGGGAAGGTTGCTCTCTGCCACAGCTTGCAGCATGGTCTTGACTGAATGTACTGTTCCTGTTAGCGTT
EHD1	NM_006795.2	2965-3065	TACCTTCCTTCCTCCTCTGTTTAGCAAAGGAGGGCAGCTCACTTGGATGTCCTTACAACGCCCCTGGCCCCCAGGTTGAGCAATAAGAAACCAGAACCTT
ELK1	NM_005229.3	2350-2450	TTTTCAATAGGGGAGAGGGAGTCATCTCTTCCTATATTTGGTGGGGTGGGTGGGAAGGAAGGGATTTGGGGGGGAATCTTCCTGCCGCCTCCCCCACTCC
EPHA2	NM_004431.2	1525-1625	GAGCCGAGTGTGGAAGTACGAGGTCACTTACCGCAAGAAGGGAGACTCCAACAGCTACAATGTGCGCCGCACCGAGGGTTTCTCCGTGACCCTGGACGAC
ERBB2	NM_004448.2	2380-2480	CTGAAAGAGACGGAGCTGAGGAAGGTGAAGGTGCTTGGATCTGGCGCTTTTGGCACAGTCTACAAGGGCATCTGGATCCCTGATGGGGAGAATGTGAAAA
FGF2	NM_002006.4	620-720	GTCCGGGAGAAGAGCGACCCTCACATCAAGCTACAACTTCAAGCAGAAGAGAGAGGAGTTGTGTCTATCAAAGGAGTGTGTGCTAACCGTTACCTGGCTA
FOS	NM_005252.2	1475-1575	ACTCAAGTCCTTACCTCTTCCGGAGATGTAGCAAAACGCATGGAGTGTGTATTGTTCCCAGTGACACTTCAGAGAGCTGGTAGTTAGTAGCATGTTGAGC
FOSB	NM_006732.1	3200-3300	ATATATGGATGTGTGTGTGTGCGTGCGCGTGAGTGTGTGAGCGCTTCTGCAGCCTCGGCCTAGGTCACGTTGGCCCTCAAAGCGAGCCGTTGAATTGGAA
FOSL1	NM_005438.2	280-380	CAGCAGAAGTTCCACCTGGTGCCAAGCATCAACACCATGAGTGGCAGTCAGGAGCTGCAGTGGATGGTACAGCCTCATTTCCTGGGGCCCAGCAGTTACC
FOXD1	NM_004472.2	1607-1707	CTCCTTTTCTCGTCTTGGTGGTTCGGTGTTTTGTTCGCTCCTCCAGGCGCGGCCCCTCTCGACCTCGCGCGCCCATTTTCGCCGCTGCGAATTCTCGGAC
GAPDH	NM_002046.3	35-135	TCCTCCTGTTCGACAGTCAGCCGCATCTTCTTTTGCGTCGCCAGCCGAGCCACATCGCTCAGACACCATGGGGAAGGTGAAGGTCGGAGTCAACGGATTT
GAS1	NM_002048.2	1525-1625	CTGTGGCTTGGGACAGATAGAAGGGATGGTTGGGGATACTTCCCAAAACTTTTTCCAAGTCAACTTGGTGTAGCCGGTTCCCCGGCCACGACTCTGGGCA
GPR34	NM_001097579.1	15-115	GACCGGATGGAAGAGCCCAGCTGACACAACCAAGACGAGTCTCAGTGTCTAGGGAAGCTTGGGGTTCTGCTCCTTTTACTTCAGGCGAACCTGAACTCAG
HBEGF	NM_001945.1	475-575	TGAGAGTCACTTTATCCTCCAAGCCACAAGCACTGGCCACACCAAACAAGGAGGAGCACGGGAAAAGAAAGAAGAAAGGCAAGGGGCTAGGGAAGAAGAG
HES1	NM_005524.2	860-960	GCTGGAGAGGCGGCTAAGGTGTTTGGAGGCTTCCAGGTGGTACCGGCTCCCGATGGCCAGTTTGCTTTCCTCATTCCCAACGGGGCCTTCGCGCACAGCG
HEY1	NM_001040708.1	515-615	AAAATGCTGCATACGGCAGGAGGGAAAGGTTACTTTGACGCGCACGCCCTTGCTATGGACTATCGGAGTTTGGGATTTCGGGAATGCCTGGCAGAAGTTG
HGS	NM_004712.3	175-275	CCTGATCCGCCAAGGGGACACACAAGCAAAATATGCTGTGAATTCCATCAAGAAGAAAGTCAACGACAAGAACCCACACGTCGCCTTGTATGCCCTGGAG
HRAS	NM_005343.2	396-496	AGTACATGCGCACCGGGGAGGGCTTCCTGTGTGTGTTTGCCATCAACAACACCAAGTCTTTTGAGGACATCCACCAGTACAGGGAGCAGATCAAACGGGT
HSF1	NM_005526.2	692-792	CTTCGGCAGAAGCATGCCCAGCAACAGAAAGTCGTCAACAAGCTCATTCAGTTCCTGATCTCACTGGTGCAGTCAAACCGGATCCTGGGGGTGAAGAGAA
ID1	NM_002165.2	345-445	CTGCCCCAGAACCGCAAGGTGAGCAAGGTGGAGATTCTCCAGCACGTCATCGACTACATCAGGGACCTTCAGTTGGAGCTGAACTCGGAATCCGAAGTTG
ID3	NM_002167.3	195-295	AGGAAGCCTGTTTGCAATTTAAGCGGGCTGTGAACGCCCAGGGCCGGCGGGGGCAGGGCCGAGGCGGGCCATTTTGAATAAAGAGGCGTGCCTTCCAGGC
IER2	NM_004907.2	1-101	GTCCGAGTTCGGAATTTCGGTTCAAGGCCCAGTTCCTCGGATTGTTCCTGCGCAACTTCAGTTTCCCTTCCAGGCACGGGCAATGAGTGTTTGGCCGCGA
IER5	NM_016545.4	260-360	GCGCGTCACCAGAGTCGTTTCTCTTCGGAGTCTTAGGTGATCGAGGGTGTGCCCAGGGGGCGGACTTGTTTGCGCCTCCCGTTCCCTCCCAATTTCCAAA
IGFBP4	NM_001552.2	1520-1620	TGGAGACACTCCTATAAGGAGAGTTCAAGCCTGTGGGAGTAGAAAAATCTCATTCCCAGAGTCAGAGGAGAAGAGACATGTACCTTGACCATCGTCCTTC
IL11	NM_000641.2	1145-1245	TGAGACAGAGAACAGGGAATTAAATGTGTCATACATATCCACTTGAGGGCGATTTGTCTGAGAGCTGGGGCTGGATGCTTGGGTAACTGGGGCAGGGCAG
IL6	NM_000600.1	220-320	TGACAAACAAATTCGGTACATCCTCGACGGCATCTCAGCCCTGAGAAAGGAGACATGTAACAAGAGTAACATGTGTGAAAGCAGCAAAGAGGCACTGGCA
IL8	NM_000584.2	25-125	ACAGCAGAGCACACAAGCTTCTAGGACAAGAGCCAGGAAGAAACCACCGGAAGGAACCATCTCACTGTGTGTAAACATGACTTCCAAGCTGGCCGTGGCT
INPP1	NM_002194.3	1370-1470	TCAAAGCTGCATTGTCACGTGTGTGTGGAGATCGCATATTTGGGGCAGCTGGGGCTGGTTATAAGAGCCTATGTGTTGTCCAAGGCCTCGTTGACATTTA

IRS2	NM_003749.2	775-875	GCGCCGAAACGGGTGATCGCTCTCGACTGCTGCCTGAACATCAACAAGCGCGCCGACGCCAAGCACAAGTACCTGATCGCCCTCTACACCAAGGACGAGT
ITGB3	NM_000212.2	4485-4585	GAATAAGCCTTGGAATTAGATATGGGGCAATGACTGAGCCCTGTCTCACCCATGGATTACTCCTTACTGTAGGGAATGGCAGTATGGTAGAGGGATAAAT
JUN	NM_002228.3	140-240	ACACAGCCAGCCAGCCAGGTCGGCAGTATAGTCCGAACTGCAAATCTTATTTTCTTTTCACCTTCTCTCTAACTGCCCAGAGCTAGCGCCTGTGGCTCCC
JUNB	NM_002229.2	1155-1255	GCGCGCCTGGAGGACAAGGTGAAGACGCTCAAGGCCGAGAACGCGGGGCTGTCGAGTACCGCCGGCCTCCTCCGGGAGCAGGTGGCCCAGCTCAAACAGA
JUND	NM_005354.4	955-1055	GCAAGCGGCTGCGCAACCGCATCGCCGCCTCCAAGTGCCGCAAGCGCAAGCTGGAGCGCATCTCGCGCCTGGAAGAGAAAGTGAAGACCCTCAAGAGTCA
KLF10	NM_005655.1	570-670	GCTCAGGCAACAAGTGTGATTCGTCATACAGCTGATGCCCAGCTATGTAACCACCAGACCTGCCCAATGAAAGCAGCCAGCATCCTCAACTATCAGAACA
KLF2	NM_016270.2	1015-1115	GGAAGTTTGCGCGCTCAGACGAGCTCACGCGCCACTACCGAAAGCACACGGGCCACCGGCCATTCCAGTGCCATCTGTGCGATCGTGCCTTCTCGCGCTC
KLF6	NM_001300.4	1339-1439	CGGCGCCTAAGCCTTTGCCGTGAGCATGCACACTGAGAATGCTAATGGTTGGGTTGATTGTATGTTGAGGATCTATTACTGACCGTATGATGAGGCCAAC
KRAS	NM_004985.3	1790-1890	GCATGGACTGTGTCCCCACGGTCATCCAGTGTTGTCATGCATTGGTTAGTCAAAATGGGGAGGGACTAGGGCAGTTTGGATAGCTCAACAAGATACAATC
LDLR	NM_000527.2	4625-4725	TTTCTGAAATCGCCGTGTTACTGTTGCACTGATGTCCGGAGAGACAGTGACAGCCTCCGTCAGACTCCCGCGTGAAGATGTCACAAGGGATTGGCAATTG
LIF	NM_002309.2	180-280	ATGTCACAACAACCTCATGAACCAGATCAGGAGCCAACTGGCACAGCTCAATGGCAGTGCCAATGCCCTCTTTATTCTCTATTACACAGCCCAGGGGGAG
Luciferase	DES_00001.1	139-239	TCGAGGTGAACATCACGTACGCGGAATACTTCGAAATGTCCGTTCGGTTGGCAGAAGCTATGAAACGATATGGGCTGAATACAAATCACAGAATCGTCGT
MAFF	NM_012323.2	210-310	GCCCAGAAGCGGGTCTGCAGCCCAGAGGGCACCTTCTGCAAACATGTCTGTGGATCCCCTATCCAGCAAAGCTCTAAAGATCAAGCGAGAGCTGAGCGAG
MAP2K1	NM_002755.2	970-1070	ACGGAATGGACAGCCGACCTCCCATGGCAATTTTTGAGTTGTTGGATTACATAGTCAACGAGCCTCCTCCAAAACTGCCCAGTGGAGTGTTCAGTCTGGA
MAP2K2	NM_030662.2	1325-1425	GCGGACCTGAAGATGCTCACAAACCACACCTTCATCAAGCGGTCCGAGGTGGAAGAAGTGGATTTTGCCGGCTGGTTGTGTAAAACCCTGCGGCTGAACC
MAP2K3	NM_002756.3	234-334	TGAACCCTGTGCTGAGCACCTTGCAGACGTGATCTTGCTTCGTCCTGCAGCACTGTGCGGGGCAGGAAAATCCAAGAGGA
MAPK1	NM_002745.4	2230-2330	AACTCCACATGCTGGTGCATATACGCCCTTGAGCTACTTCAAATGTGGGTGTTTCAGTAACCACGTTCCATGCCTGAGGATTTAGCAGAGAGGAACACTG
MAPK3	NM_001040056.1	580-680	AACGTGCTCCACCGAGATCTAAAGCCCTCCAACCTGCTCATCAACACCACCTGCGACCTTAAGATTTGTGATTTCGGCCTGGCCCGGATTGCCGATCCTG
MEGF9	NM_001080497.1	875-975	CTGTAGTCCACATGGAGCTCTCAGCATACCGTGCAACAGTTCTGGGAAATGCCAGTGCAAAGTGGGTGTCATTGGCTCTATATGTGACCGATGCCAAGAT
MOAP1	NM_022151.4	1195-1295	TTACAGAAGCTGGTACAGAGAGGAGCAATTGAGAGAGATGCTGTGAATCAGGCCCGCCTAGACCAAGTCATTGCTGGGGCAGTCCACAAAACAATTCGCA
NDRG1	NM_006096.2	565-665	CGCCTACATCCTAACTCGATTTGCTCTAAACAACCCTGAGATGGTGGAGGGCCTTGTCCTTATCAACGTGAACCCTTGTGCGGAAGGCTGGATGGACTGG
NFIB	NM_005596.2	3830-3930	GGCTGCAAAGCGACTGTTCTGCCTACTGTGACAAACTTCAACTTACACAGGTTCCCCTCTCTAACTTCCCACCTGGGTTGCAAGCTGAACTCATTACTGG
NR4A1	NM_002135.3	155-255	CGGCCGGGTAGGGTGCAGCCTGAGGCTTGTTCAGCAGAACAGGTGCAAGCCACATTGTTGCCAAGACCTGCCTGAAGCCGGATTCTCCCCACTGCCTCCT
NR4A2	NM_006186.3	1380-1480	TTCAGAAGTGCCTGGCTGTTGGGATGGTCAAAGAAGTGGTTCGCACAGACAGTTTAAAAGGCCGGAGAGGTCGTTTGCCCTCGAAACCGAAGAGCCCACA
NR4A3	NM_006981.2	1840-1940	GAGGTCGTCTGCCTTCCAAACCAAAGAGCCCATTACAACAGGAACCTTCTCAGCCCTCTCCACCTTCTCCTCCAATCTGCATGATGAATGCCCTTGTCCG
NRAS	NM_002524.3	877-977	ACCCTGGTCCTGACTTCCCTGGAGGAGAAGTATTCCTGTTGCTGTCTTCAGTCTCACAGAGAAGCTCCTGCTACTTCCCCAGCTCTCAGTAGTTTAGTAC
OSMR	NM_003999.1	2920-3020	CCCTGCATCTGTTTTGAGAACTTGACCTATAACCAGGCAGCTTCTGACTCTGGCTCTTGTGGCCATGTTCCAGTATCCCCAAAAGCCCCAAGTATGCTGG
PDCD6IP	NM_013374.3	1350-1450	ACAGTGTCAATACAAAGATACTCTCCCCAAGGAGGTGTTCCCTGTCTTGGCTGCAAAGCACTGTATCATGCAGGCCAATGCTGAGTACCATCAGTCTATC
PICALM	NM_001008660.1	1505-1605	CTATGTCAACTGCTTCTCAGGTAGCAAGTACATGGGGAGGATTCACTCCTTCTCCAGTTGCACAGCCACACCCTTCAGCTGGCCTTAATGTTGACTTTGA
PLK2	NM_006622.2	1395-1495	TACCACCACAGTTGCCAGGTCTGGAACACCCGCAGTAGAAAACAAGCAGCAGATTGGGGATGCTATTCGGATGATAGTCAGAGGGACTCTTGGCAGCTGT
PMAIP1	NM_021127.2	7-107	AAAAGCGTGGTCTCTGGCGCGGGGATCTCAGAGTTTCCCGGGCACTCACCGTGTGTAGTTGGCATCTCCGCGCGTCCGGA
PNRC1	NM_006813.1	965-1065	AGTGATCCACCTTCTCCTAGTGTTCTTCCAAAGCCTCCTAGTCACTGGATGGGAAGCACTGTTGAAAATTCCAACCAAAACAGGGAGCTGATGGCAGTAC
PTPN23	NM_015466.2	1000-1100	TGGATGTCATTGGGGGAAAGTACAATTCTGCCAAGAAGGACAACGACTTCATTTACCATGAGGCTGTCCCAGCATTGGACACTCTTCAGCCTGTAAAAGG
RAF1	NM_002880.2	1990-2090	CCTATGGCATCGTATTGTATGAACTGATGACGGGGGAGCTTCCTTATTCTCACATCAACAACCGAGATCAGATCATCTTCATGGTGGGCCGAGGATATGC
RGS2	NM_002923.1	855-955	AACAGCTTCCCTCACTGTGTACAGAACGCAAGAAGGGAATAGGTGGTCTGAACGTGGTGTCTCACTCTGAAAAGCAGGAATGTAAGATGATGAAAGAGAC
RHOB	NM_004040.2	870-970	CTGCCAAGACCAAGGAAGGCGTGCGCGAGGTCTTCGAGACGGCCACGCGCGCCGCGCTGCAGAAGCGCTACGGCTCCCAGAACGGCTGCATCAACTGCTG
RPL27	NM_000988.3	23-123	GGGCCGGGTGGTTGCTGCCGAAATGGGCAAGTTCATGAAACCTGGGAAGGTGGTGCTTGTCCTGGCTGGACGCTACTCCGGACGCAAAGCTGTCATCGTG
RREB1	NM_001003698.2	1120-1220	TTCGAACACATCGAGGACTGCTGCGTCACAACGCGCTTGTCCACAAACAACTTCCCAGGGATGCAATGGGCAGACCTTTCATACAGAACAACCCTTCAAT
RUNX3	NM_004350.1	2085-2185	GTGGTCTCATAATTCCATTTGTGGAGAGAACAGGAGGGCCAGATAGATAGGTCCTAGCAGAAGGCATTGAGGTGAGGGATCATTTTGGGTCAGACATCAA
SGK	NM_005627.2	1790-1890	GTGTGAACCGTCGTGTGAGTGTGGTATGCCTGATCACAGATGGATTTTGTTATAAGCATCAATGTGACACTTGCAGGACACTACAACGTGGGACATTGTT
SHB	NM_003028.2	3200-3300	TGTAGGGAAAGGGAGACAGAGAAGGAACGTCATTTGCCCAAAGCCACACAGCTCACCAGCAGCAGAGCGGTTCTGCAGCCAATGCTCTTTCGTTGGTTCT
SMAD3	NM_005902.3	4220-4320	TTAAAGGACAGTTGAAAAGGGCAAGAGGAAACCAGGGCAGTTCTAGAGGAGTGCTGGTGACTGGATAGCAGTTTTAAGTGGCGTTCACCTAGTCAACACG
SNAI2	NM_003068.3	740-840	GCGTTTTCCAGACCCTGGTTGCTTCAAGGACACATTAGAACTCACACGGGGGAGAAGCCTTTTTCTTGCCCTCACTGCAACAGAGCATTTGCAGACAGGT
SNX12	NM_013346.2	310-410	AAAATGAGCTGGAGAGAGATAGCAAGATTGTAGTACCACCACTGCCTGGGAAAGCCTTGAAGCGGCAGCTCCCTTTCCGAGGAGATGAAGGGATCTTTGA
SNX16	NM_022133.3	768-868	ACTAGACCAAGAGACACTGAAGAACAAAATCCGGAAACAGTGAATTGGGAAGATAGACCATCTACACCTACTATACTGGGTTATGAAGTGATGGAAGAAA
SNX3	NM_003795.3	412-512	CAGCAACTTCCTCGAGATCGATGTGAGCAACCCGCAAACGGTGGGGGTCGGCCGGGGCCGCTTCACCACTTACGAAATCAGGGTCAAGACAAATCTTCCT
SPHK1	NM_021972.2	895-995	TTCGGGGCTGCGCCTCTTCTCTGTGCTCAGCCTGGCCTGGGGCTTCATTGCTGATGTGGACCTAGAGAGTGAGAAGTATCGGCGTCTGGGGGAGATGCGC
SPRED2	NM_001128210.1	1890-1990	CGCTAGCAAGCATCTGGTTCAGCGGAAATGGGATGTGAGAATGATGAAACCCGACAGAAGTATCTCAGCCTGCAGTCAGTTATTATGTATAGGAGGTGAG
TBP	NM_003194.3	25-125	CGCCGGCTGTTTAACTTCGCTTCCGCTGGCCCATAGTGATCTTTGCAGTGACCCAGCAGCATCACTGTTTCTTGGCGTGTGAAGATAACCCAAGGAATTG
TIPARP	NM_015508.3	835-935	CCAATACATTCTGGACACCAGTGATAAGCTGAGTACTGAGCTCTTTCAGGACAAAAGTGAAGAGGCTTCCCTTGACCTCGTGTTTGAGCTGGTGAACCAG
TMEM158	NM_015444.2	1270-1370	GTGTGCTTCGTGCTGTAGTTATCGTTAGTTCCTCTTCCCGAGATGGGGCCGCCGAGAGACCCCAGCGCCTTTGAAAAGCAAGGTTTGTGCTGCGCTTCCA
TNFRSF1B	NM_001066.2	2835-2935	TTGGTACATGGCCAGTGTGATCCCAAGTGCCAGTCTTGTGTCTGCGTCTGTGTTGCGTGTCGTGGGTGTGTGTAGCCAAGGTCGGTAAGTTGAATGGCCT
TNFRSF21	NM_014452.3	735-835	TGGCATAGAGAAATGCCATGACTGTAGTCAGCCATGCCCATGGCCAATGATTGAGAAATTACCTTGTGCTGCCTTGACTGACCGAGAATGCACTTGCCCA
TSG101	NM_006292.2	1205-1305	GAAGCATGTACGTCTTCTGTCCCGTAAACAGTTCCAGCTGAGGGCACTAATGCAAAAAGCAAGAAAGACTGCCGGTCTCAGTGACCTCTACTGACTTCTC
VPS4A	NM_013245.2	1940-2040	CAAGCTCTGCCTCAAAGACCGAGTGACATAAGCCATTCCCACCCTCCTAGGTTCACATCCAGGGCTGTGTCTTCCTTGGGGGAGGAGATGGTGTCGTTTA
ZFP36	NM_003407.2	1430-1530	CTGGAACCTCTCCTGAGGGGGAATCCTGGTGCTCAAATTACCCTCCAAAAGCAAGTAGCCAAAGCCGTTGCCAAACCCCACCCATAAATCAATGGGCCCT
ZFP36L1	NM_004926.2	1238-1338	AGGCCCTACATTAACAAGGTTAAGCTCAACCCCTTTCCCCCAGCACCTCAGAATGTGCCCTCCCTCTCCCCCTCATAACCCCACCTAACATAAGGACAAG
ZFP36L2	NM_006887.4	270-370	GCCACTGCGGGATCCAGAAACATGTCGACCACACTTCTGTCCGCCTTCTACGATGTCGACTTCTTGTGCAAGACAGAGAAATCCCTGGCCAACCTCAACC
ZNF225	NM_013362.2	137-237	TCGAATTAGGGGAAAAGAAACCTCGTCGGAGAGCAGAGGCAGGATTCTGCTTTCCCTTGGACTGTATCACTCAGGACTCT

Table 2: Target sequences of the second NanoString code sets

Gene	Accession #	Region	Target Sequence
AGPAT9	NM_032717.3	145-245	GGAAGATCCTTTCCACCTGGCTGACGCTGGTTCTCGGCTTCATCCTTTTACCTTCGGTCTTCGGAGTGTCTCTGGGCATCTCCGAGATCTACATGAAGAT
AKAP12	NM_005100.3	640-740	TCACAGATGATGGGCAGGAGGAGACACCCGAAATAATCGAACAGATTCCTTCTTCAGAAAGCAATTTAGAAGAGCTAACACAACCCACTGAGTCCCAGGC
ATF3	NM_001040619.1	1005-1105	CGAGAAGCAGCATTTGATATACATGCTCAACCTTCATCGGCCCACGTGTATTGTCCGGGCTCAGAATGGGAGGACTCCAGAAGATGAGAGAAACCTCTTT
B3GNT5	NM_032047.4	130-230	GGAAGGAAAGCCGACCTCCGATTTGGACATTTAAAGAGCTGGGCTTGAACTTCGTGAGTTTCGCTCTAAACTGCCCTTGAAATGAAGCTGGACTTGGAGG
BHLHB2	NM_003670.1	560-660	AGAGTGGTTTACAAGCTGGTGAGCTGTCAGGGAGAAATGTCGAAACAGGTCAAGAGATGTTCTGCTCAGGTTTCCAGACATGTGCCCGGGAGGTGCTTCA
BIRC2	NM_001166.3	1760-1860	TGGGATCCACCTCTAAGAATACGTCTCCAATGAGAAACAGTTTTGCACATTCATTATCTCCCACCTTGGAACATAGTAGCTTGTTCAGTGGTTCTTACTC
BIRC3	NM_001165.3	950-1050	GTGATGTTTCTCCTGCCACCTGGAAACAAAGCATTGAAGTCTGCAGTTGAAAAGCCCAACGTCTGTGAGATCCAGGAAACCATGCTTGCAAACCACTGGT
BTG2	NM_006763.2	1700-1800	TGCTCTCCTTGGGATGATGGCTGGCTAGTCAGCCTTGCATGTATTCCTTGGCTGAATGGGAGAGTGCCCCATGTTCTGCAAGACTACTTGGTATTCTTGT
C3	NM_000064.2	4396-4496	CATCTACCTGGACAAGGTCTCACACTCTGAGGATGACTGTCTAGCTTTCAAAGTTCACCAATACTTTAATGTAGAGCTTATCCAGCCTGGAGCAGTCAAG
CBL-B	NM_170662.3	3195-3295	TAATGTCGAAGTTGCCCGGAGCATCCTCCGAGAATTTGCCTTCCCTCCTCCAGTATCCCCACGTCTAAATCTATAGCAGCCAGAACTGTAGACACCAAAA
c-CBL	NM_005188.2	7485-7585	GTTGTGGTAAGGATGCAGGGTATTTCGCAGAACCCAGGACGGGAAGTGCCTTTGGTTCTTGGGTGGAGCTGGAACTGCAGAGCTTTGCACCTAGTCCTTT
CCL2	NM_002982.3	0-100	GAGGAACCGAGAGGCTGAGACTAACCCAGAAACATCCAATTCTCAAACTGAAGCTCGCACTCTCGCCTCCAGCATGAAAGTCTCTGCCGCCCTTCTGTGC
CDKN1A	NM_078467.1	2065-2165	CCTTCCAGCTCCTGTAACATACTGGCCTGGACTGTTTTCTCTCGGCTCCCCATGTGTCCTGGTTCCCGTTTCTCCACCTAGACTGTAAACCTCTCGAGGG
CDKN2AIP	NM_017632.2	485-585	AGTGACAGATGCTCCAACCTATACAACAAGAGATGAACTGGTTGCCAAGGTGAAGAAAAGAGGGATATCGAGTAGCAATGAAGGGGTAGAAGAGCCATCC
CEBPB	NM_005194.2	1420-1520	CAACCGCACATGCAGATGGGGCTCCCGCCCGTGGTGTTATTTAAAGAAGAAACGTCTATGTGTACAGATGAATGATAAACTCTCTGCTTCTCCCTCTGCC
CGA	NM_000735.2	280-380	ATATCCCACTCCACTAAGGTCCAAGAAGACGATGTTGGTCCAAAAGAACGTCACCTCAGAGTCCACTTGCTGTGTAGCTAAATCATATAACAGGGTCACA
CHAC1	NM_024111.3	914-1014	GATATGGTGGGTGGCTGGAGGCTTCTCTTTCTCAGTCCCTGCCTGTCTGCCAGCCTGCAGCTCTCCTGCTTGACACTGACTTACTACTTGAAACTTTATT
CHC	NM_004859.2	290-390	GGGTATCAACCCAGCAAACATTGGCTTCAGTACCCTGACTATGGAGTCTGACAAATTCATCTGCATTAGAGAAAAAGTAGGAGAGCAGGCCCAGGTGGTA
CLDN1	NM_021101.3	410-510	GCAAAGTCTTTGACTCCTTGCTGAATCTGAGCAGCACATTGCAAGCAACCCGTGCCTTGATGGTGGTTGGCATCCTCCTGGGAGTGATAGCAATCTTTGT
CXCL1	NM_001511.1	445-545	AGGCCCTGCCCTTATAGGAACAGAAGAGGAAAGAGAGACACAGCTGCAGAGGCCACCTGGATTGTGCCTAATGTGTTTGAGCATCGCTTAGGAGAAGTCT
CXCL2	NM_002089.3	845-945	TGATGACATATCACATGTCAGCCACTGTGATAGAGGCTGAGGAATCCAAGAAAATGGCCAGTGAGATCAATGTGACGGCAGGGAAATGTATGTGTGTCTA
CYR61	NM_001554.3	1390-1490	AAGGGAGAAGAGTGTCAGAATCAGAATCATGGAGAAAATGGGCGGGGGTGGTGTGGGTGATGGGACTCATTGTAGAAAGGAAGCCTTGCTCATTCTTGAG
DDIT3	NM_004083.4	40-140	TTAAAGATGAGCGGGTGGCAGCGACAGAGCCAAAATCAGAGCTGGAACCTGAGGAGAGAGTGTTCAAGAAGGAAGTGTATCTTCATACATCACCACACCT
DKK1	NM_012242.2	75-175	CGGCACGGTTTCGTGGGGACCCAGGCTTGCAAAGTGACGGTCATTTTCTCTTTCTTTCTCCCTCTTGAGTCCTTCTGAGATGATGGCTCTGGGCGCAGCG
DNM1	NM_004408.2	2842-2942	AAAACTTGTGCCCCTTCTGTGGTATGCCCTTGCCCTGTTCTATAAATATCTATAAATACTCATATATATACACACCTACACATGGCCAACCGCCTCGCCT
DNM2	NM_001005360.1	362-462	CGGCCTCTCATTCTGCAGCTCATCTTCTCAAAAACAGAACATGCCGAGTTTTTGCACTGCAAGTCCAAAAAGTTTACAGACTTTGATGAAGTCCGGCAGG
DUSP1	NM_004417.2	987-1087	TCAAGAATGCTGGAGGAAGGGTGTTTGTCCACTGCCAGGCAGGCATTTCCCGGTCAGCCACCATCTGCCTTGCTTACCTTATGAGGACTAATCGAGTCAA
DUSP2	NM_004418.3	1235-1335	CTGGCCCTCATTCGGGGTCGGGAACCAAGGGTGTGTCTGCTCTTTCCCTCCCCATCCTCTGGCAGAAATCAGCTAGACGCTATACCGTGGACTCTCCCTG
DUSP4	NM_001394.5	45-145	GCGACAGGAGCCGCGCGACCGGCAAAAATACACGGGAGGCCGTCGCCGAAAAGAGTCCGCGGTCCTCTCTCGTAAACACACTCTCCTCCACCGGCGCCTC
DUSP5	NM_004419.3	675-775	GTGGATGTAAAACCCATTTCACAAGAGAAGATTGAGAGTGAGAGAGCCCTCATCAGCCAGTGTGGAAAACCAGTGGTAAATGTCAGCTACAGGCCAGCTT
DUSP6	NM_001946.2	1535-1635	ATGTGACAACAGGGTTCCAGCACAGCAGCTGTATTTTACCACCCCTTCCAACCAGAATGTATACCAGGTGGACTCTCTGCAATCTACGTGAAAGACCCCA
DUSP7	NM_001947.2	1065-1165	CTAAGCAGCCCGTGCGACAACCACGCGTCGAGTGAGCAGCTCTACTTTTCCACGCCCACCAACCACAACCTGTTCCCACTCAATACGCTGGAGTCCACGT
EGFR	NM_005228.3	2760-2860	GCAGCCAGGAACGTACTGGTGAAAACACCGCAGCATGTCAAGATCACAGATTTTGGGCTGGCCAAACTGCTGGGTGCGGAAGAGAAAGAATACCATGCAG
EGR1	NM_001964.2	1505-1605	GAGGCATACCAAGATCCACTTGCGGCAGAAGGACAAGAAAGCAGACAAAAGTGTTGTGGCCTCTTCGGCCACCTCCTCTCTCTCTTCCTACCCGTCCCCG
EGR2	NM_000399.3	1891-1991	GGTGGAGCTAGCACTGCCCCCTTTCCACCTAGAAGCAGGTTCTTCCTAAAACTTAGCCCATTCTAGTCTCTCTTAGGTGAGTTGACTATCAACCCAAGGC
EGR3	NM_004430.2	3170-3270	CGTACAGGGTGGCTCCTTTGAAGTGGAGTAATAGGGAAGGTTGCTCTCTGCCACAGCTTGCAGCATGGTCTTGACTGAATGTACTGTTCCTGTTAGCGTT
ELF3	NM_001114309.1	200-300	TCCAGAGGATTTGCAGTTCTGAACCTGCACACTCCAGTCTAGGATCTCCGAGCAAGAGCGTAGCCTCATGGCTGCAACCTGTGAGATTAGCAACATTTTT
EMP1	NM_001423.1	2000-2100	AGCAAAAACTCTTGTGGTACCTAGTCAGATGGTAGACGAGCTGTCTGCTGCCGCAGGAGCACCTCTATACAGGACTTAGAAGTAGTATGTTATTCCTGGT
EPHA2	NM_004431.2	1525-1625	GAGCCGAGTGTGGAAGTACGAGGTCACTTACCGCAAGAAGGGAGACTCCAACAGCTACAATGTGCGCCGCACCGAGGGTTTCTCCGTGACCCTGGACGAC
EREG	NM_001432.2	290-390	GAGAGTCCAGTGATAACTGCACAGCTTTAGTTCAGACAGAAGACAATCCACGTGTGGCTCAAGTGTCAATAACAAAGTGTAGCTCTGACATGAATGGCTA
ERRFI1	NM_018948.3	592-692	TTAAGAAACTCACAGTGAATGGGGTTTGTGCTTCCACCCCTCCACTGACACCCATAAAAAACTCCCCTTCCCTTTTCCCCTGTGCCCCTCTTTGTGAACG
FGF2	NM_002006.4	620-720	GTCCGGGAGAAGAGCGACCCTCACATCAAGCTACAACTTCAAGCAGAAGAGAGAGGAGTTGTGTCTATCAAAGGAGTGTGTGCTAACCGTTACCTGGCTA
FOS	NM_005252.2	1475-1575	ACTCAAGTCCTTACCTCTTCCGGAGATGTAGCAAAACGCATGGAGTGTGTATTGTTCCCAGTGACACTTCAGAGAGCTGGTAGTTAGTAGCATGTTGAGC
FOSB	NM_006732.1	3200-3300	ATATATGGATGTGTGTGTGTGCGTGCGCGTGAGTGTGTGAGCGCTTCTGCAGCCTCGGCCTAGGTCACGTTGGCCCTCAAAGCGAGCCGTTGAATTGGAA
FOSL1	NM_005438.2	280-380	CAGCAGAAGTTCCACCTGGTGCCAAGCATCAACACCATGAGTGGCAGTCAGGAGCTGCAGTGGATGGTACAGCCTCATTTCCTGGGGCCCAGCAGTTACC
GADD45B	NM_015675.2	365-465	TGTGGACCCAGACAGCGTGGTCCTCTGCCTCTTGGCCATTGACGAGGAGGAGGAGGATGACATCGCCCTGCAAATCCACTTCACGCTCATCCAGTCCTTC
GAPDH	NM_002046.3	245-345	ATATGATTCCACCCATGGCAAATTCCATGGCACCGTCAAGGCTGAGAACGGGAAGCTTGTCATCAATGGAAATCCCATCACCATCTTCCAGGAGCGAGAT
GEM	NM_005261.2	575-675	GGGAGAAGATACATATGAACGAACCCTGATGGTTGATGGGGAAAGTGCAACGATTATACTCCTGGATATGTGGGAAAATAAGGGGGAAAATGAATGGCTC
HBEGF	NM_001945.1	1995-2095	AGACATTTCTCTAACTCCTGCCATTCTTCTGGTGCTACTCCATGCAGGGGTCAGTGCAGCAGAGGACAGTCTGGAGAAGGTATTAGCAAAGCAAAAGGCT
HRAS	NM_176795.3	712-812	CTCGCGCTGGAGTGGAGGATGCCTTCTACACGTTGGTGCGTGAGATCCGGCAGCACAAGCTGCGGAAGCTGAACCCTCCTGATGAGAGTGGCCCCGGCTG
IER2	NM_004907.2	1-101	GTCCGAGTTCGGAATTTCGGTTCAAGGCCCAGTTCCTCGGATTGTTCCTGCGCAACTTCAGTTTCCCTTCCAGGCACGGGCAATGAGTGTTTGGCCGCGA

IER3	NM_003897.3	1042-1142	CTCAACTCCGTCTGTCTACTGTGTGAGACTTCGGCGGACCATTAGGAATGAGATCCGTGAGATCCTTCCATCTTCTTGAAGTCGCCTTTAGGGTGGCTGC
IL11	NM_000641.2	1145-1245	TGAGACAGAGAACAGGGAATTAAATGTGTCATACATATCCACTTGAGGGCGATTTGTCTGAGAGCTGGGGCTGGATGCTTGGGTAACTGGGGCAGGGCAG
IL1A	NM_000575.3	1085-1185	ACTCCATGAAGGCTGCATGGATCAATCTGTGTCTCTGAGTATCTCTGAAACCTCTAAAACATCCAAGCTTACCTTCAAGGAGAGCATGGTGGTAGTAGCA
IL1R1	NM_000877.2	4295-4395	CCAGAGAGTGGGGGTGATGATGACCAAGAATTACAAGTAGAATGGCAGCTGGAATTTAAGGAGGGACAAGAATCAATGGATAAGCGTGGGTGGAGGAAGA
IL6	NM_000600.1	220-320	TGACAAACAAATTCGGTACATCCTCGACGGCATCTCAGCCCTGAGAAAGGAGACATGTAACAAGAGTAACATGTGTGAAAGCAGCAAAGAGGCACTGGCA
IL7R	NM_002185.2	1610-1710	TTGCTTTGACCACTCTTCCTGAGTTCAGTGGCACTCAACATGAGTCAAGAGCATCCTGCTTCTACCATGTGGATTTGGTCACAAGGTTTAAGGTGACCCA
IL8	NM_000584.2	25-125	ACAGCAGAGCACACAAGCTTCTAGGACAAGAGCCAGGAAGAAACCACCGGAAGGAACCATCTCACTGTGTGTAAACATGACTTCCAAGCTGGCCGTGGCT
INPP1	NM_001128928.1	1515-1615	CAAAGCTGCATTGTCACGTGTGTGTGGAGATCGCATATTTGGGGCAGCTGGGGCTGGTTATAAGAGCCTATGTGTTGTCCAAGGCCTCGTTGACATTTAC
IRF1	NM_002198.1	510-610	CTGTGCGAGTGTACCGGATGCTTCCACCTCTCACCAAGAACCAGAGAAAAGAAAGAAAGTCGAAGTCCAGCCGAGATGCTAAGAGCAAGGCCAAGAGGAA
ITGA2	NM_002203.2	475-575	CAACGGGTGTGTGTTCTGACATCAGTCCTGATTTTCAGCTCTCAGCCAGCTTCTCACCTGCAACTCAGCCCTGCCCTTCCCTCATAGATGTTGTGGTTGT
JUN	NM_002228.3	140-240	ACACAGCCAGCCAGCCAGGTCGGCAGTATAGTCCGAACTGCAAATCTTATTTTCTTTTCACCTTCTCTCTAACTGCCCAGAGCTAGCGCCTGTGGCTCCC
JUNB	NM_002229.2	1155-1255	GCGCGCCTGGAGGACAAGGTGAAGACGCTCAAGGCCGAGAACGCGGGGCTGTCGAGTACCGCCGGCCTCCTCCGGGAGCAGGTGGCCCAGCTCAAACAGA
KLF10	NM_005655.1	570-670	GCTCAGGCAACAAGTGTGATTCGTCATACAGCTGATGCCCAGCTATGTAACCACCAGACCTGCCCAATGAAAGCAGCCAGCATCCTCAACTATCAGAACA
KLF2	NM_016270.2	1015-1115	GGAAGTTTGCGCGCTCAGACGAGCTCACGCGCCACTACCGAAAGCACACGGGCCACCGGCCATTCCAGTGCCATCTGTGCGATCGTGCCTTCTCGCGCTC
KLF6	NM_001300.4	1339-1439	CGGCGCCTAAGCCTTTGCCGTGAGCATGCACACTGAGAATGCTAATGGTTGGGTTGATTGTATGTTGAGGATCTATTACTGACCGTATGATGAGGCCAAC
LDLR	NM_000527.2	4625-4725	TTTCTGAAATCGCCGTGTTACTGTTGCACTGATGTCCGGAGAGACAGTGACAGCCTCCGTCAGACTCCCGCGTGAAGATGTCACAAGGGATTGGCAATTG
LIF	NM_002309.2	180-280	ATGTCACAACAACCTCATGAACCAGATCAGGAGCCAACTGGCACAGCTCAATGGCAGTGCCAATGCCCTCTTTATTCTCTATTACACAGCCCAGGGGGAG
Luciferase	DES_00001.1	139-239	TCGAGGTGAACATCACGTACGCGGAATACTTCGAAATGTCCGTTCGGTTGGCAGAAGCTATGAAACGATATGGGCTGAATACAAATCACAGAATCGTCGT
MAFF	NM_012323.2	210-310	GCCCAGAAGCGGGTCTGCAGCCCAGAGGGCACCTTCTGCAAACATGTCTGTGGATCCCCTATCCAGCAAAGCTCTAAAGATCAAGCGAGAGCTGAGCGAG
NFKB1	NM_003998.2	1675-1775	AGGGTATAGCTTCCCACACTATGGATTTCCTACTTATGGTGGGATTACTTTCCATCCTGGAACTACTAAATCTAATGCTGGGATGAAGCATGGAACCATG
NFKB2	NM_002502.2	825-925	ATCTCCGGGGGCATCAAACCTGAAGATTTCTCGAATGGACAAGACAGCAGGCTCTGTGCGGGGTGGAGATGAAGTTTATCTGCTTTGTGACAAGGTGCAG
NFKBIA	NM_020529.1	945-1045	GGATGAGGAGAGCTATGACACAGAGTCAGAGTTCACGGAGTTCACAGAGGACGAGCTGCCCTATGATGACTGTGTGTTTGGAGGCCAGCGTCTGACGTTA
NFKBIZ	NM_031419.2	2075-2175	ATGTTGCTGCCAGCTTGCAGTATCGGTTGACACAATTAGATGCTGTCCGCCTGTTGATGAGGAAGGGAGCAGACCCAAGTACTCGGAACTTGGAGAACGA
NR4A1	NM_002135.3	155-255	CGGCCGGGTAGGGTGCAGCCTGAGGCTTGTTCAGCAGAACAGGTGCAAGCCACATTGTTGCCAAGACCTGCCTGAAGCCGGATTCTCCCCACTGCCTCCT
NR4A2	NM_006186.3	1380-1480	TTCAGAAGTGCCTGGCTGTTGGGATGGTCAAAGAAGTGGTTCGCACAGACAGTTTAAAAGGCCGGAGAGGTCGTTTGCCCTCGAAACCGAAGAGCCCACA
NR4A3	NM_173198.1	2590-2690	GTCGTCTGCCTTCCAAACCAAAGAGCCCATTACAACAGGAACCTTCTCAGCCCTCTCCACCTTCTCCTCCAATCTGCATGATGAATGCCCTTGTCCGAGC
PDCD6IP	NM_013374.3	1350-1450	ACAGTGTCAATACAAAGATACTCTCCCCAAGGAGGTGTTCCCTGTCTTGGCTGCAAAGCACTGTATCATGCAGGCCAATGCTGAGTACCATCAGTCTATC
PHLDA1	NM_007350.3	800-900	ATGGCAGAGGGCAAGGAGATCGACTTTCGGTGCCCGCAAGACCAGGGCTGGAACGCCGAGATCACGCTGCAGATGGTGCAGTACAAGAATCGTCAGGCCA
PICALM	NM_007166.2	1865-1965	TTGCCAAACTCCCACCTAGCAAGTTAGTATCTGATGACTTGGATTCATCTTTAGCCAACCTTGTGGGCAATCTTGGCATCGGAAATGGAACCACTAAGAA
PMAIP1	NM_021127.2	7-107	AAAAGCGTGGTCTCTGGCGCGGGGATCTCAGAGTTTCCCGGGCACTCACCGTGTGTAGTTGGCATCTCCGCGCGTCCGGA
PTGS2	NM_000963.1	495-595	GCTACAAAAGCTGGGAAGCCTTCTCTAACCTCTCCTATTATACTAGAGCCCTTCCTCCTGTGCCTGATGATTGCCCGACTCCCTTGGGTGTCAAAGGTAA
RGS2	NM_002923.1	855-955	AACAGCTTCCCTCACTGTGTACAGAACGCAAGAAGGGAATAGGTGGTCTGAACGTGGTGTCTCACTCTGAAAAGCAGGAATGTAAGATGATGAAAGAGAC
RHOB	NM_004040.2	870-970	CTGCCAAGACCAAGGAAGGCGTGCGCGAGGTCTTCGAGACGGCCACGCGCGCCGCGCTGCAGAAGCGCTACGGCTCCCAGAACGGCTGCATCAACTGCTG
RUNX3	NM_001031680.2	3545-3645	CACACTGGCAGGTTAGGCAGTCCTTCTGGTGATCCTATTCCATTCCCTCCTGCTGCGGTTTCTCTTGGCCTGTCCTCACTGGAAAAACAGTCTCCATCTC
SDC4	NM_002999.2	1310-1410	ACTGTTCATTCCTTTGTGCAGAGTGTATATCTCTGCCTGGGCAAGAGTGTGGAGGTGCCGAGGTGTCTTCATTCTCTCGCACATTTCCACAGCACCTGCT
SERPINB8	NM_002640.3	1820-1920	ATCTTTCCATAAGCCTGAGATACAAGTTCAGGGACTCAGCAATGCACTTTAGGACTGAGCTAGGAGGCAAATATCTGAAGCTTGCTATGCTGTTCTTTCC
SHC4	NM_203349.2	1570-1670	AGCAGCCACCAGTAGGTGGTGTTTCAGATATGCGGATCAAAGTTCAAGCCACGGAACAAATGGCTTACTGCCCCATACAGTGTGAAAAGTTGTGCTATTT
SLC7A11	NM_014331.3	8904-9004	CCAGAATTTCAGGGGCATCGTGGGTTTGGTCTAGTGATTGAAAACACAAGAACAGAGAGATCCAGCTGAAAAAGAGTGATCCTCAATATCCTAACTAACT
SNX12	NM_013346.2	310-410	AAAATGAGCTGGAGAGAGATAGCAAGATTGTAGTACCACCACTGCCTGGGAAAGCCTTGAAGCGGCAGCTCCCTTTCCGAGGAGATGAAGGGATCTTTGA
SNX3	NM_003795.3	412-512	CAGCAACTTCCTCGAGATCGATGTGAGCAACCCGCAAACGGTGGGGGTCGGCCGGGGCCGCTTCACCACTTACGAAATCAGGGTCAAGACAAATCTTCCT
SOCS2	NM_003877.3	1020-1120	GGAACGGCACTGTTCACCTTTATCTGACCAAACCGCTCTACACGTCAGCACCATCTCTGCAGCATCTCTGTAGGCTCACCATTAACAAATGTACCGGTGC
SOCS3	NM_003955.3	1870-1970	GGAGGATGGAGGAGACGGGACATCTTTCACCTCAGGCTCCTGGTAGAGAAGACAGGGGATTCTACTCTGTGCCTCCTGACTATGTCTGGCTAAGAGATTC
ST3GAL1	NM_003033.3	4720-4820	GGGAGAGGACAGCGATTGTTGACTCTAGTTCCTGATGTTTAATCAGAAAAACCACTTTTCCTGTAGAGCACATTTCCTAAAAGGCTGCTGCTGTGTAGGG
TFAP2C	NM_003222.3	1410-1510	TTGTCTCATTTCAGCCTGATTACCCACGGGTTTGGCAGCCAGGCCATCTGTGCCGCGGTGTCTGCCCTGCAGAACTACATCAAAGAAGCCCTGATTGTCA
TIPARP	NM_015508.3	835-935	CCAATACATTCTGGACACCAGTGATAAGCTGAGTACTGAGCTCTTTCAGGACAAAAGTGAAGAGGCTTCCCTTGACCTCGTGTTTGAGCTGGTGAACCAG
TNFAIP3	NM_006290.2	45-145	GGAGAGGTGTTGGAGAGCACAATGGCTGAACAAGTCCTTCCTCAGGCTTTGTATTTGAGCAATATGCGGAAAGCTGTGAAGATACGGGAGAGAACTCCAG
TSG101	NM_006292.2	1205-1305	GAAGCATGTACGTCTTCTGTCCCGTAAACAGTTCCAGCTGAGGGCACTAATGCAAAAAGCAAGAAAGACTGCCGGTCTCAGTGACCTCTACTGACTTCTC
VPS4A	NM_013245.2	1940-2040	CAAGCTCTGCCTCAAAGACCGAGTGACATAAGCCATTCCCACCCTCCTAGGTTCACATCCAGGGCTGTGTCTTCCTTGGGGGAGGAGATGGTGTCGTTTA
ZFP36	NM_003407.2	1430-1530	CTGGAACCTCTCCTGAGGGGGAATCCTGGTGCTCAAATTACCCTCCAAAAGCAAGTAGCCAAAGCCGTTGCCAAACCCCACCCATAAATCAATGGGCCCT

4. Microarray analysis – EGF response genes

Table 3: Fold change in EGF-responsive genes (Fig. 4 A, see legend for details; bold: values for grouping and ranking)

condition	mock				HRS				TSG101				VPS4A				ALIX			
EGF [min]	0	30	120	360	0	30	120	360	0	30	120	360	0	30	120	360	0	30	120	360
EGR1	1	**20.53**	5.58	1.52	1.38	16.80	9.71	2.73	0.97	19.43	7.84	1.27	1.12	20.25	6.32	1.54	0.80	17.88	5.78	1.92
FOS	1	**8.06**	0.68	0.41	0.95	7.46	0.73	0.37	0.93	8.34	0.98	0.41	0.97	8.51	0.77	0.41	0.99	7.78	0.64	0.40
JUN	1	**7.78**	3.12	1.58	1.49	7.57	3.97	2.16	1.25	8.94	3.63	1.53	1.29	10.34	3.14	1.53	1.15	7.94	2.93	1.47
JUNB	1	**5.58**	3.89	2.55	1.04	4.50	5.70	3.01	1.08	5.50	4.92	2.46	1.04	5.78	3.66	2.20	1.07	5.50	3.34	2.45
ATF3	1	**5.35**	2.13	0.87	1.48	5.74	2.58	0.93	1.00	5.28	1.83	0.79	1.04	6.06	2.11	0.92	1.16	4.59	2.17	0.99
IL6	1	**5.13**	4.99	4.06	2.91	15.24	27.86	12.64	1.35	6.87	14.22	5.58	1.58	7.11	7.94	3.84	1.27	5.82	8.51	3.81
EGR2	1	**5.06**	1.64	1.02	1.14	3.92	2.23	1.21	0.86	4.29	2.07	1.01	0.95	5.86	1.52	0.95	0.86	3.76	1.59	1.24
FOSB	1	**4.96**	3.34	0.93	1.46	4.99	4.41	1.04	1.31	5.70	3.56	0.85	1.26	6.23	4.03	1.04	1.03	4.08	2.97	1.06
BTG2	1	**4.86**	1.59	0.98	1.22	4.76	1.95	0.90	1.24	6.11	1.80	0.97	1.26	6.28	2.23	1.13	1.22	4.59	1.66	1.00
DUSP1	1	**4.44**	2.75	1.61	1.20	3.84	3.14	1.87	0.88	4.41	3.46	1.71	1.02	4.47	2.83	1.62	0.88	4.17	2.89	1.65
PTGS2	1	**4.14**	2.89	1.35	1.37	4.35	5.98	2.11	0.97	3.66	4.20	1.65	0.97	4.08	3.23	1.46	0.99	3.89	3.34	1.65
IER2	1	**3.92**	2.27	1.72	1.21	3.76	3.01	2.14	1.09	4.14	3.01	1.78	1.09	4.11	2.38	1.73	1.09	3.76	2.39	1.88
NR4A2	1	**3.41**	2.39	1.15	0.69	2.91	3.01	0.98	1.01	3.97	2.79	1.20	0.90	3.56	2.53	1.34	1.01	3.07	2.85	1.39
ZFP36	1	**3.34**	1.48	1.42	1.30	2.83	2.01	1.66	1.02	3.61	1.85	1.38	1.00	3.51	1.71	1.39	1.01	3.18	1.39	1.55
CYR61	1	**3.25**	1.35	0.52	1.57	3.48	2.73	0.95	0.69	2.97	1.80	0.44	0.80	3.03	1.42	0.46	0.64	2.73	1.49	0.51
CTGF	1	**2.97**	2.58	1.02	1.11	2.85	2.66	0.86	0.64	2.75	2.79	0.86	0.91	2.97	2.73	0.86	0.66	2.36	1.87	0.82
ZC3H12A	1	**2.73**	1.69	1.77	1.18	2.22	2.08	1.97	1.02	2.73	1.93	1.77	1.06	2.69	1.65	1.75	1.04	2.46	1.58	1.74
NFKBIZ	1	**2.64**	1.00	0.69	1.26	2.93	1.30	0.98	1.25	3.01	1.25	0.78	1.08	3.05	1.01	0.76	1.15	2.33	1.11	0.74
EGR3	1	**2.64**	1.79	0.99	0.99	2.23	1.83	1.07	1.05	1.77	1.56	0.97	1.04	2.04	1.72	0.99	1.01	1.67	1.48	1.03
DUSP2	1	**2.58**	1.21	1.29	1.26	2.23	1.22	1.16	0.97	2.64	1.21	1.16	0.93	2.79	1.27	1.13	0.95	2.33	1.01	1.23
UGT2B7	1	**2.31**	1.82	1.87	1.78	2.85	1.21	1.64	1.29	2.08	1.47	2.14	1.77	1.97	1.85	1.62	1.54	1.09	1.71	1.57
SOCS3	1	**2.25**	1.23	1.13	0.78	1.39	1.48	1.16	1.04	2.35	1.62	1.26	1.01	2.25	1.42	1.25	1.10	2.55	1.46	1.32
ADAMTS1	1	**2.13**	1.21	0.92	0.82	1.48	1.32	0.84	0.91	2.03	1.49	1.03	1.12	2.27	1.31	1.09	0.90	1.79	1.21	1.01
KLF6	1	**1.99**	1.32	1.13	1.21	1.99	1.52	1.09	1.03	2.07	1.72	1.17	1.06	1.96	1.53	1.12	1.09	2.16	1.36	0.99
RHOB	1	**1.92**	1.43	1.04	0.90	1.60	1.68	1.03	1.07	2.03	1.62	1.07	1.14	1.99	1.60	1.05	0.93	1.84	1.24	0.97
SNORD51	1	**1.87**	0.90	1.30	1.27	2.83	1.27	1.28	1.25	2.53	1.33	1.18	1.23	2.71	1.21	1.71	1.34	1.93	1.23	1.31
CCNL1	1	**1.84**	1.30	1.13	1.25	2.62	2.01	1.21	1.23	2.27	1.80	1.16	1.19	2.23	1.37	1.19	1.10	1.89	1.59	1.23
MAP1LC3B	1	**1.83**	1.41	1.39	0.92	2.08	1.48	1.59	1.02	1.83	1.65	1.41	0.90	1.35	1.44	1.49	0.98	1.64	1.56	1.44
EDN1	1	**1.82**	1.51	1.25	1.08	2.06	2.48	1.43	0.93	1.58	1.66	0.91	1.04	1.96	1.62	1.19	1.04	1.74	1.84	1.15
TMEM229B	1	**0.51**	1.20	0.86	0.88	0.82	1.06	0.81	0.89	0.93	0.63	0.75	1.22	1.23	0.85	0.81	0.97	0.95	0.81	0.90
TMEM229A	1	**0.51**	0.68	0.65	0.91	0.95	0.59	0.54	0.69	0.68	0.45	0.61	0.72	0.71	0.68	0.63	0.75	0.52	0.71	0.81
AREG	1	3.48	**78.25**	20.25	1.24	2.36	68.59	27.10	1.52	3.97	106.15	34.30	1.59	4.23	85.63	28.44	1.15	3.25	99.73	26.91
ERRFI1	1	1.54	**10.27**	3.25	0.80	1.21	8.00	4.26	0.98	1.27	11.79	3.20	1.06	1.45	9.00	3.23	1.12	1.32	9.06	2.31
DKK1	1	1.06	**7.26**	3.61	0.81	0.71	5.17	4.03	0.81	0.88	7.94	3.53	0.99	1.09	8.69	5.21	0.96	0.96	10.70	4.06
GEM	1	1.23	**6.92**	2.16	0.75	0.84	3.68	1.78	0.96	1.14	9.45	2.43	0.90	1.23	7.89	2.19	1.07	1.26	7.41	2.23
CHAC1	1	0.97	**6.23**	2.89	1.20	1.33	5.06	2.97	0.87	1.01	7.73	2.53	1.18	1.16	5.21	2.30	0.90	1.09	5.74	2.08
NR4A1	1	4.56	**5.82**	0.85	0.94	3.68	6.54	0.89	1.12	4.92	6.06	0.88	1.09	4.53	5.94	0.88	1.08	3.63	4.76	0.93
HAS2	1	1.37	**5.78**	4.11	0.61	0.73	3.34	2.71	1.04	1.46	7.84	4.50	0.89	1.39	5.39	3.48	1.14	1.56	6.87	4.11
PHLDA1	1	1.47	**5.43**	3.25	1.32	1.65	6.28	4.17	1.09	1.57	6.50	3.23	1.05	1.61	5.90	3.32	1.06	1.64	6.63	3.56
STC2	1	1.06	**5.39**	4.72	1.19	1.35	7.26	7.62	1.10	1.13	5.58	4.79	0.88	1.14	4.99	4.41	1.13	1.14	5.82	4.41
CCL2	1	1.57	**5.28**	1.22	1.13	1.82	6.41	2.23	0.75	1.37	6.87	1.72	0.88	1.71	5.74	1.14	0.77	1.37	5.21	0.84
IL8	1	1.77	**5.06**	2.22	1.39	2.39	11.55	4.79	1.21	1.39	8.94	2.17	1.29	2.20	5.06	3.03	1.31	1.53	5.74	2.51
NR4A3	1	2.46	**4.76**	0.84	0.84	2.31	4.17	0.68	1.17	2.77	4.92	0.85	0.95	2.30	4.23	0.72	1.09	2.06	4.32	0.86
IL11	1	1.17	**4.66**	3.56	0.77	0.94	3.97	3.78	1.13	1.34	5.74	3.68	1.09	1.15	4.72	3.51	0.88	0.88	4.56	3.41
DUSP5	1	3.84	**4.47**	2.39	1.39	4.63	6.96	3.20	0.86	4.00	5.35	2.27	1.09	3.94	4.32	2.14	0.84	3.27	3.58	2.07
TFAP2C	1	1.34	**4.26**	1.46	0.86	1.27	4.76	1.74	0.84	1.06	5.66	1.46	0.80	1.13	3.89	1.36	0.85	1.23	4.63	1.41
CSRNP1	1	3.03	**4.26**	1.72	1.01	2.41	6.19	1.87	1.09	3.23	7.06	1.84	0.95	3.32	5.10	1.64	1.04	2.79	4.86	1.61
TIPARP	1	1.52	**4.14**	1.55	1.88	2.20	6.28	2.35	1.01	1.34	4.23	1.38	1.06	1.56	3.84	1.60	1.31	1.75	5.13	2.20
CYP1B1	1	1.11	**4.06**	2.53	2.00	1.65	5.70	4.11	0.95	1.06	3.03	2.13	0.96	1.10	2.73	2.16	1.09	1.26	4.89	3.29
B3GNT5	1	1.00	**4.03**	3.41	0.93	0.99	5.78	5.06	1.13	1.38	6.36	4.44	1.00	1.07	4.41	4.20	0.91	1.23	6.28	3.71
CXCL2	1	3.86	**3.97**	1.85	1.52	6.19	7.46	3.12	0.89	4.41	5.78	2.20	1.18	4.82	3.94	1.83	0.58	3.66	4.41	1.41
LIF	1	1.28	**3.86**	2.28	1.16	1.53	5.74	3.81	1.12	1.57	4.26	2.23	1.31	1.46	3.78	2.58	1.25	1.52	4.53	2.89
ZNF331	1	1.23	**3.73**	1.37	0.91	1.07	4.32	1.25	1.06	1.27	4.72	1.58	0.97	1.26	3.58	1.35	1.07	1.16	4.26	1.57
RGS2	1	1.62	**3.71**	1.88	1.08	1.31	2.79	1.64	1.14	1.43	4.53	2.08	1.04	1.58	3.76	2.11	1.21	1.57	3.92	1.95
EMP1	1	1.06	**3.68**	3.20	0.76	0.90	2.89	3.53	0.82	0.85	4.14	3.29	0.78	0.85	3.27	2.87	0.86	0.96	3.29	2.51
KLF10	1	1.88	**3.61**	1.54	1.23	2.25	4.53	1.75	1.16	1.97	4.14	1.54	1.10	2.03	3.51	1.61	1.15	2.07	3.03	1.42
DDIT3	1	1.37	**3.56**	1.56	1.39	1.68	3.51	2.41	1.20	1.27	4.56	1.56	1.25	1.38	2.79	1.53	1.19	1.41	3.23	1.62
MCL1	1	1.88	**3.36**	2.30	0.93	1.84	3.41	2.60	1.03	1.99	3.68	2.45	1.02	2.04	3.66	2.62	0.93	1.79	3.68	2.38
C8orf4	1	1.93	**3.36**	1.67	2.08	2.93	4.56	2.53	1.09	2.17	4.20	1.78	1.06	2.17	3.12	1.53	0.95	1.61	3.39	1.42
PMAIP1	1	1.39	**3.34**	2.01	1.62	1.82	3.92	2.93	1.18	1.35	3.78	2.19	1.06	1.46	2.99	1.93	1.06	1.38	2.89	1.66
ITK	1	1.21	**3.14**	1.64	0.86	0.94	2.28	1.53	0.83	1.01	4.23	2.35	0.98	0.95	2.75	1.61	0.86	0.83	2.64	1.54
SOCS2	1	1.09	**3.14**	2.30	1.11	1.13	3.94	3.48	1.07	1.24	4.99	3.34	1.04	1.17	3.34	2.36	1.29	1.21	3.34	2.25

condition	mock				HRS				TSG101				VPS4A				ALIX			
EGF [min]	0	30	120	360	0	30	120	360	0	30	120	360	0	30	120	360	0	30	120	360
SLC16A6	1	1.21	**3.12**	2.68	1.67	2.08	5.35	3.78	1.28	1.44	3.92	3.12	1.47	1.73	3.89	3.48	1.85	2.22	5.24	4.41
ANKRD57	1	1.68	**3.10**	1.85	1.13	1.77	3.43	2.14	0.99	1.61	3.56	1.89	0.76	1.51	2.28	1.36	1.13	1.60	3.41	2.03
FST	1	1.13	**3.03**	2.69	0.85	0.91	1.93	2.38	1.11	1.10	3.29	2.77	1.15	1.30	3.29	3.29	1.04	1.10	3.36	2.39
ARRDC3	1	1.79	**2.99**	2.28	0.92	1.87	2.79	2.39	1.29	2.03	3.48	2.62	1.32	2.17	2.97	2.55	1.33	2.10	3.27	2.57
KLF4	1	1.24	**2.95**	1.85	1.04	1.14	2.58	1.77	0.96	1.21	3.23	1.92	1.01	1.29	2.68	1.87	1.06	1.39	2.87	1.75
THBS1	1	1.52	**2.95**	1.53	0.93	1.48	3.41	2.48	0.68	1.24	2.71	1.33	0.75	1.37	2.60	1.38	0.55	0.86	2.25	1.04
IER3	1	2.50	**2.95**	1.95	1.78	3.84	4.72	2.71	0.82	2.57	3.76	1.93	0.88	2.71	2.73	1.97	0.88	2.43	2.68	2.07
STEAP4	1	1.03	**2.85**	2.46	0.67	0.78	2.43	2.25	0.78	1.00	3.66	2.93	1.08	1.37	3.63	3.46	1.49	1.60	4.03	2.79
HBEGF	1	1.31	**2.85**	1.89	1.11	1.18	2.62	2.35	1.15	1.29	3.63	1.80	1.13	1.27	2.97	1.91	0.82	1.02	2.46	1.38
EPHA2	1	1.13	**2.81**	2.07	0.93	1.05	3.14	2.23	0.93	1.06	3.10	1.85	0.99	1.12	2.66	1.85	0.88	0.93	2.93	1.84
HOMER1	1	1.23	**2.77**	1.36	0.66	0.79	1.85	1.36	1.25	1.22	3.10	1.43	0.97	1.20	2.17	1.60	1.16	1.40	2.99	1.22
C3orf59	1	0.97	**2.73**	1.52	1.01	0.94	4.11	2.25	0.99	1.02	4.08	2.16	0.85	0.88	3.05	1.58	0.97	1.06	3.94	1.79
CDKN2AIP	1	1.72	**2.73**	1.59	1.41	1.97	3.25	1.82	0.93	1.51	2.95	1.45	0.97	1.79	2.87	1.60	0.97	1.73	3.48	1.77
DUSP4	1	1.27	**2.73**	2.01	0.80	1.23	2.93	2.08	0.99	1.36	2.99	2.11	0.93	1.23	2.62	1.88	0.97	1.37	3.03	2.04
F3	1	1.15	**2.66**	2.10	0.78	1.04	2.41	2.10	0.78	0.99	3.25	1.84	0.77	0.99	2.30	1.79	0.82	0.94	2.81	1.85
TNS4	1	1.09	**2.64**	2.48	0.80	0.93	2.93	2.51	0.98	1.12	2.93	2.55	1.04	1.23	2.58	2.75	1.02	1.05	3.29	2.91
DUSP10	1	1.30	**2.64**	1.59	0.83	0.92	2.68	1.64	1.04	1.28	2.97	1.43	1.13	1.51	2.89	1.80	0.93	1.19	2.51	1.18
CREM	1	1.29	**2.64**	2.16	1.03	1.16	2.20	1.96	1.31	1.56	3.48	2.48	1.17	1.49	2.60	2.35	1.35	1.58	3.16	2.27
NCEH1	1	1.11	**2.62**	1.99	1.11	1.25	2.50	2.35	1.17	1.30	3.05	2.27	1.24	1.34	2.68	2.19	1.19	1.30	2.87	2.17
GDF15	1	1.39	**2.60**	2.06	1.55	1.89	3.20	2.46	1.21	1.53	2.87	1.64	1.42	1.64	2.51	1.84	1.14	1.38	2.35	1.83
IRF1	1	2.11	**2.60**	1.52	1.30	2.51	5.31	1.83	1.09	1.87	3.61	1.58	1.11	1.95	2.58	1.55	0.97	1.59	2.07	1.29
RIMKLB	1	1.09	**2.58**	1.45	0.87	0.96	2.16	1.04	1.25	1.28	3.18	1.33	1.25	1.20	2.55	1.48	1.13	1.04	3.01	1.16
TBX3	1	1.21	**2.57**	1.80	0.96	1.06	2.36	1.85	0.97	1.29	2.99	1.92	1.05	1.20	2.64	1.84	1.24	1.21	2.87	2.03
GPRC5A	1	1.05	**2.53**	1.96	0.86	0.97	2.46	1.99	0.83	0.93	2.30	1.83	0.93	0.95	2.14	1.97	0.83	0.97	2.53	1.95
GADD45A	1	1.08	**2.51**	1.35	1.33	1.51	2.85	2.00	1.00	1.06	2.93	1.49	1.06	1.20	2.31	1.32	0.96	0.94	2.10	1.20
ITPRIP	1	1.37	**2.46**	1.85	0.80	1.01	2.66	1.95	1.12	1.46	2.71	1.85	1.09	1.41	2.55	1.88	1.24	1.57	2.66	1.75
CASP9	1	1.09	**2.45**	1.69	0.90	0.93	2.06	1.36	1.28	1.22	3.25	2.16	1.01	1.19	2.71	1.62	1.21	1.27	3.10	1.78
SERPINE1	1	1.12	**2.43**	2.07	1.00	1.07	1.87	2.13	0.98	1.18	2.36	1.74	0.90	1.04	2.16	1.88	0.95	1.10	2.31	1.95
SERTAD1	1	1.30	**2.39**	1.27	1.01	1.38	2.22	1.29	0.97	1.12	2.48	1.27	1.09	1.20	2.23	1.27	0.97	0.99	1.93	1.32
TNFRSF12A	1	1.06	**2.39**	2.33	1.22	1.38	2.43	2.53	0.94	1.16	2.62	2.48	1.02	1.13	2.60	2.30	0.79	0.95	2.01	1.78
ELL2	1	1.14	**2.39**	1.82	0.84	0.89	2.23	1.71	1.33	1.09	2.30	1.88	1.03	0.99	1.88	1.58	1.08	1.16	2.33	1.59
NFIL3	1	1.71	**2.39**	0.95	0.98	1.67	2.58	0.98	1.21	1.84	2.83	1.14	1.10	1.77	2.25	1.09	1.10	1.69	2.27	1.03
BHLHE40	1	1.89	**2.38**	1.65	0.81	1.69	3.18	1.59	0.98	2.10	2.89	1.62	0.88	1.89	2.06	1.51	1.07	2.03	2.16	1.79
NAB2	1	1.04	**2.31**	1.44	0.99	0.95	1.95	1.66	0.95	0.89	2.04	1.55	0.99	0.99	1.95	1.48	0.88	0.95	2.16	1.41
ENC1	1	1.14	**2.30**	1.96	1.06	1.03	1.97	2.53	0.88	1.18	2.50	1.92	0.80	0.94	1.68	1.68	0.90	0.86	2.30	1.67
OTUD1	1	1.40	**2.28**	1.60	1.14	1.31	2.64	1.85	1.01	1.42	2.68	1.64	0.88	1.28	1.87	1.45	1.15	1.51	2.35	1.57
NEDD9	1	1.20	**2.28**	1.24	0.97	0.81	2.25	1.23	0.95	0.95	2.48	1.21	0.94	1.04	2.58	1.15	0.91	0.93	2.25	1.06
CLK1	1	1.33	**2.25**	1.72	1.08	1.33	2.31	2.14	1.32	1.37	2.64	1.60	1.17	1.39	2.17	1.85	1.23	1.19	2.48	1.69
SNAI2	1	1.69	**2.25**	0.91	1.24	1.91	2.55	1.01	0.96	1.87	2.38	0.90	0.99	1.83	2.01	0.89	1.02	1.74	1.95	0.85
SLC2A3	1	1.32	**2.23**	1.03	1.27	1.79	2.85	1.13	0.68	1.13	2.03	0.81	0.86	1.29	2.13	0.88	0.89	1.24	2.57	1.03
CEBPB	1	1.55	**2.22**	1.85	1.14	1.42	2.53	2.16	1.11	1.55	2.57	2.03	1.19	1.54	2.11	1.92	1.15	1.45	1.88	1.88
TMEM2	1	1.14	**2.22**	1.91	0.93	1.04	2.51	1.80	0.98	1.01	2.16	1.96	0.84	0.99	2.04	1.75	1.17	1.21	2.73	2.13
AMOTL2	1	1.16	**2.20**	1.48	0.80	0.82	2.83	1.96	0.70	0.84	2.27	1.23	0.80	0.91	2.45	1.41	0.77	0.85	2.00	1.18
ZNF699	1	1.32	**2.19**	1.34	1.13	1.16	2.35	1.49	1.06	1.21	2.89	1.31	1.16	1.33	1.91	1.28	1.10	1.16	2.16	1.33
MAFK	1	1.41	**2.17**	1.99	0.81	1.13	2.57	2.08	1.33	1.75	2.69	2.20	1.10	1.43	2.25	1.93	1.14	1.35	2.36	2.08
MAP3K14	1	1.04	**2.16**	1.05	0.78	0.75	2.31	1.21	0.87	0.91	2.17	1.04	0.94	0.92	1.99	1.09	0.93	0.96	2.13	1.06
TNFAIP1	1	1.22	**2.14**	1.96	0.97	1.09	2.14	2.08	1.17	1.29	2.48	2.23	1.14	1.26	2.06	1.89	1.27	1.40	2.25	1.97
DCUN1D3	1	1.06	**2.13**	1.05	0.76	0.96	2.58	1.20	0.68	0.84	2.48	1.12	0.93	1.09	2.64	1.26	0.93	0.98	2.69	1.15
ZC3H12C	1	1.09	**2.11**	1.31	1.01	1.11	2.89	1.52	1.09	1.18	2.89	1.18	0.84	1.09	2.11	1.19	0.98	1.23	2.48	1.12
USP53	1	1.35	**2.11**	1.49	0.93	1.12	1.77	1.66	1.52	1.48	2.50	1.66	1.28	1.40	1.84	1.77	1.53	1.75	2.55	1.68
DUSP6	1	1.06	**2.08**	1.78	0.90	0.79	1.55	1.69	1.06	1.04	2.64	1.78	1.04	1.17	1.97	2.01	1.04	1.10	2.03	1.77
EPCAM	1	1.39	**2.06**	1.40	1.05	1.66	1.97	1.43	1.40	1.33	2.50	1.60	1.54	1.36	1.21	1.87	2.10	2.11	1.72	1.35
FOSL2	1	1.15	**2.04**	1.04	0.81	1.09	2.45	1.10	0.95	1.19	2.19	1.02	0.91	1.10	2.07	0.96	0.84	1.00	1.91	0.89
ARL5B	1	1.23	**2.04**	1.01	1.05	1.25	2.28	1.07	1.12	1.39	2.31	1.02	1.02	1.40	2.17	1.07	1.17	1.37	2.39	1.16
DGKD	1	1.06	**2.01**	1.40	0.91	0.95	2.20	1.66	1.06	1.15	2.28	1.48	1.04	1.11	2.23	1.49	1.06	1.09	2.41	1.39
CDKL5	1	1.20	**2.01**	1.26	0.91	1.16	1.79	1.33	1.35	1.30	2.23	1.42	1.24	1.35	1.85	1.47	1.39	1.47	2.69	1.40
PPAP2B	1	0.94	**2.01**	1.75	0.96	0.86	1.39	1.66	0.98	1.00	2.07	2.13	0.95	1.04	2.08	2.00	1.01	0.99	1.79	1.95
CDKN1A	1	1.10	**2.00**	1.58	0.78	0.90	2.00	1.64	1.04	1.32	2.36	1.67	1.12	1.33	2.28	1.68	1.07	1.21	2.28	1.68
EREG	1	1.01	**1.97**	1.57	0.97	0.95	2.03	1.78	0.76	0.97	2.45	1.60	0.88	0.88	1.87	1.64	0.78	0.80	2.04	1.60
STK40	1	1.13	**1.96**	1.84	1.20	1.13	1.80	1.95	1.07	1.15	1.96	1.84	1.12	1.13	1.91	1.72	1.13	1.35	2.22	1.78
ZSWIM6	1	1.05	**1.96**	1.01	0.85	0.95	2.11	1.02	0.85	0.99	1.87	0.93	0.93	1.00	1.96	1.09	0.86	0.91	1.89	0.97
BCAR3	1	1.15	**1.93**	1.73	0.86	1.12	1.85	2.06	0.86	0.93	1.96	1.75	0.97	1.07	1.95	1.92	0.90	0.89	2.03	1.71
SLC25A25	1	1.39	**1.93**	1.58	0.91	1.15	2.11	1.78	1.09	1.52	2.27	1.59	1.10	1.45	2.14	1.57	1.21	1.44	2.08	1.58
SESN2	1	1.03	**1.93**	1.52	1.06	0.78	1.71	1.53	0.95	1.04	2.07	1.58	1.13	1.04	1.74	1.40	0.93	1.01	1.82	1.21
BDNF	1	1.16	**1.92**	1.36	0.90	1.01	1.91	1.21	0.95	1.00	2.66	1.46	0.95	1.14	2.03	1.27	0.92	1.11	2.17	1.35
DDIT4	1	0.91	**1.92**	1.35	1.21	1.06	1.44	1.36	0.93	0.92	1.74	1.25	1.09	1.13	1.69	1.25	0.95	0.99	1.39	0.97
GRAMD3	1	1.20	**1.92**	1.28	0.82	0.99	2.17	1.28	0.94	1.00	1.97	1.19	0.99	1.10	1.80	1.21	1.01	1.12	1.99	1.12

condition	mock				HRS				TSG101				VPS4A				ALIX			
EGF [min]	0	30	120	360	0	30	120	360	0	30	120	360	0	30	120	360	0	30	120	360
PPP1R15B	1	1.27	**1.91**	1.17	0.79	1.19	2.03	1.13	0.88	1.26	2.06	1.21	0.85	1.18	1.78	1.16	0.90	1.17	1.87	0.98
MAFF	1	1.24	**1.89**	1.27	1.23	1.43	1.91	1.47	0.88	1.16	1.75	1.46	0.97	1.34	1.69	1.47	0.87	1.10	1.47	1.37
IL1RAP	1	1.02	**1.88**	1.43	0.91	1.03	2.08	1.96	0.90	0.93	1.95	1.51	0.71	0.75	1.85	1.21	0.91	1.04	2.16	1.33
EED	1	1.10	**1.87**	1.32	1.21	1.37	1.92	1.37	1.16	1.29	2.13	1.49	1.15	1.29	1.78	1.36	1.14	1.15	1.79	1.24
TRIB1	1	1.48	**1.85**	1.31	1.13	1.52	2.58	1.47	0.93	1.34	2.22	1.26	0.94	1.42	1.95	1.38	1.01	1.29	1.77	1.23
DNMBP	1	1.01	**1.85**	1.56	0.75	0.77	1.74	1.52	1.07	1.01	1.96	1.54	1.03	1.02	1.89	1.57	1.09	1.06	2.03	1.41
HES1	1	1.29	**1.84**	1.48	1.21	1.58	2.31	1.68	0.98	1.37	1.97	1.49	1.01	1.27	1.57	1.42	0.95	1.31	1.67	1.47
SPRY2	1	1.27	**1.84**	1.59	1.16	1.23	2.19	1.66	0.90	1.16	2.31	1.55	1.06	1.25	1.97	1.82	0.95	1.24	1.88	1.51
SPRY4	1	1.11	**1.84**	1.58	1.08	1.16	1.74	1.93	0.85	1.05	1.89	1.58	1.06	1.01	1.88	1.64	1.02	0.91	1.74	1.91
RNF19A	1	1.01	**1.83**	1.08	0.97	1.14	2.03	1.26	1.05	1.16	2.13	1.12	1.02	1.16	1.87	1.16	1.13	1.13	2.13	1.08
EID3	1	0.90	**1.83**	1.53	1.09	1.21	1.71	2.04	1.11	0.97	1.68	1.44	0.86	0.89	1.46	1.26	0.86	0.81	1.33	1.20
BACH1	1	1.12	**1.83**	1.36	0.99	0.92	1.85	1.60	0.97	1.03	1.75	1.41	0.82	0.99	1.79	1.48	0.99	1.05	1.71	1.18
ATG12	1	1.10	**1.83**	1.56	1.06	1.33	1.83	1.67	1.15	1.15	2.31	1.68	1.16	1.15	1.93	1.62	1.10	1.26	2.27	1.59
SCHIP1	1	1.08	**1.82**	1.00	0.94	0.95	1.88	1.16	1.00	1.01	2.14	1.15	1.06	1.16	2.06	1.05	1.09	1.18	2.22	1.21
BCL10	1	1.31	**1.80**	1.27	1.01	1.21	2.00	1.34	1.14	1.26	2.10	1.49	1.22	1.25	1.88	1.42	1.09	1.39	2.06	1.52
ADAMTS5	1	1.26	**1.80**	1.68	1.21	1.18	1.91	1.56	1.06	1.23	1.74	1.67	1.11	1.29	1.80	1.78	1.21	1.35	2.08	1.64
ALX1	1	1.18	**0.54**	0.78	1.00	1.12	0.63	0.93	1.13	1.15	0.71	0.86	1.07	1.16	0.49	0.88	1.18	1.37	0.65	0.90
SHC4	1	1.24	3.86	**4.92**	1.10	1.04	3.68	7.46	1.05	1.20	5.43	7.26	1.22	1.27	4.38	5.66	1.23	0.95	6.19	5.82
AGPAT9	1	1.03	2.23	**4.47**	0.97	0.97	1.66	4.44	1.06	1.16	2.60	5.21	0.86	0.99	2.03	4.79	1.13	1.26	2.99	4.76
SLC7A11	1	1.07	2.04	**4.38**	1.35	1.59	2.23	5.03	1.18	1.16	2.13	4.59	0.97	0.94	1.83	4.03	0.85	0.90	1.85	3.66
TFPI2	1	1.14	2.83	**4.38**	1.09	1.18	3.51	6.41	0.97	1.01	3.07	4.47	1.32	1.35	2.85	4.66	0.84	0.90	2.53	3.68
IL7R	1	1.11	3.78	**4.23**	0.68	0.78	2.62	4.89	0.62	0.72	3.94	5.21	1.01	1.16	4.66	5.58	0.61	0.67	3.61	3.32
CGA	1	1.21	3.07	**3.68**	1.72	1.47	2.16	2.39	1.69	2.03	4.26	5.31	1.17	1.55	3.25	3.66	1.75	2.10	4.00	3.92
ITGA2	1	1.07	2.06	**3.63**	0.88	1.15	1.99	4.06	1.34	1.33	2.97	5.86	1.20	1.38	2.58	5.43	1.34	1.41	2.79	4.69
IL1R1	1	1.01	2.73	**3.20**	0.86	0.90	2.89	3.29	0.97	1.14	3.43	4.47	0.95	1.09	3.23	4.38	0.87	1.02	3.43	3.05
DCLK1	1	1.04	1.40	**3.12**	0.85	0.85	1.12	2.08	0.99	0.97	1.51	2.95	1.06	1.13	1.46	3.86	1.04	1.20	1.65	2.85
SMOX	1	1.04	1.67	**3.01**	1.01	0.80	1.61	3.01	0.98	1.06	2.00	3.43	0.96	0.94	1.85	3.29	0.95	0.99	2.11	2.77
SDC4	1	1.02	2.79	**2.99**	1.06	1.15	4.20	5.39	0.86	0.97	3.53	3.29	0.83	0.96	3.18	3.01	0.78	0.91	3.53	2.91
NAMPT	1	1.20	2.33	**2.87**	0.98	1.29	2.77	3.89	1.39	1.35	2.99	3.78	1.14	1.36	2.62	3.36	1.27	1.46	2.62	2.71
NT5E	1	1.09	1.53	**2.87**	0.62	0.75	1.16	2.58	0.91	0.95	1.49	2.93	0.88	0.94	1.44	3.03	1.10	1.18	1.75	3.25
ST3GAL1	1	1.28	2.25	**2.83**	1.00	0.97	1.95	2.77	1.14	1.27	2.39	3.12	1.06	1.13	2.00	2.71	1.31	1.42	2.62	2.95
CLDN1	1	1.04	2.03	**2.64**	1.23	1.24	3.03	5.90	1.01	1.08	3.03	4.26	1.20	1.27	2.50	3.23	0.60	0.74	1.80	1.96
SERPINB8	1	1.15	2.35	**2.60**	1.03	1.17	2.35	2.97	1.13	1.07	2.79	2.77	1.06	1.17	2.16	3.07	1.11	1.06	2.27	2.60
AMIGO2	1	0.95	1.95	**2.60**	0.94	0.98	2.07	3.46	0.87	1.07	2.27	2.43	0.73	0.91	1.62	2.03	0.83	0.90	2.00	1.97
RAET1E	1	0.95	1.47	**2.55**	0.75	0.89	1.32	2.27	1.06	1.01	1.79	2.68	1.10	1.14	1.78	2.71	1.08	1.13	1.87	2.68
INPP1	1	1.32	1.82	**2.53**	1.27	1.28	1.87	2.73	1.47	1.22	2.01	2.57	1.23	1.39	1.89	2.53	1.29	1.48	2.08	2.36
GCLC	1	1.09	1.11	**2.53**	0.90	0.94	1.01	2.60	1.03	1.01	1.18	2.85	0.90	0.97	0.99	2.22	0.90	1.01	1.01	2.07
PTPRE	1	1.04	1.35	**2.43**	1.22	1.21	1.45	2.66	1.25	1.13	1.45	2.89	1.10	1.14	1.30	2.77	1.19	1.24	1.67	2.87
AKAP12	1	1.06	2.35	**2.43**	1.27	1.42	3.14	3.58	1.04	1.06	2.58	2.71	1.07	1.09	2.79	2.93	1.07	1.13	3.25	3.18
PSPH	1	0.97	1.30	**2.43**	0.95	0.94	1.26	2.46	0.97	0.92	1.36	2.69	1.03	1.12	1.39	2.46	0.94	0.99	1.38	2.03
CYP24A1	1	0.89	1.28	**2.43**	0.75	0.95	1.03	1.68	0.93	1.14	1.36	2.99	0.84	0.87	1.05	2.11	1.10	1.13	1.80	3.34
SLFN5	1	1.22	1.54	**2.41**	1.16	1.34	1.62	2.64	0.95	0.97	1.60	2.60	1.02	1.09	1.51	2.41	0.81	0.91	1.46	2.08
CREB5	1	1.06	1.16	**2.41**	1.25	1.37	1.51	3.25	1.35	1.27	1.40	3.32	1.21	1.36	1.24	2.81	1.17	1.27	1.27	2.69
CCNA1	1	1.05	1.55	**2.39**	1.07	1.40	1.74	2.27	0.93	0.92	1.84	2.39	0.90	0.85	1.15	1.71	1.03	1.09	1.67	1.85
STAMBPL1	1	1.11	1.78	**2.39**	0.90	0.91	1.39	2.48	0.99	1.13	1.88	2.45	1.01	1.16	1.59	2.81	0.95	1.06	1.97	2.50
GCLM	1	1.16	1.57	**2.36**	0.99	1.09	1.61	2.62	1.26	1.20	1.71	2.93	0.98	1.03	1.16	1.99	1.16	1.29	1.40	1.99
CASP4	1	1.11	1.60	**2.35**	0.97	1.09	1.41	2.60	0.96	0.98	1.71	2.77	1.10	1.20	1.64	2.99	1.01	1.05	1.40	2.14
GPT2	1	0.99	1.53	**2.33**	0.86	0.88	1.27	2.30	1.06	0.98	1.61	2.38	1.13	1.26	1.39	2.25	1.03	1.13	1.49	1.91
CARS	1	1.01	1.55	**2.30**	0.84	0.83	1.48	2.45	0.99	1.06	1.61	2.30	1.12	1.13	1.62	2.41	0.97	0.98	1.59	1.89
ETV5	1	0.90	1.07	**2.27**	0.78	0.62	0.97	2.08	1.21	0.93	1.18	2.17	0.97	1.03	1.07	2.41	0.98	1.03	0.97	1.87
TM4SF19	1	0.78	1.10	**2.22**	0.90	1.27	1.30	2.30	0.77	1.01	1.36	2.33	1.03	0.96	1.54	2.66	1.00	1.01	1.55	2.64
MICAL2	1	0.91	1.19	**2.19**	1.01	1.00	1.35	2.83	0.95	0.85	1.23	2.20	0.96	0.99	1.03	2.39	0.77	0.86	1.19	1.89
OSMR	1	1.05	1.51	**2.17**	0.71	0.69	1.41	2.17	1.13	1.06	1.69	2.53	0.97	1.11	1.66	2.35	1.01	1.05	1.57	1.89
MTHFD2	1	1.15	1.57	**2.17**	0.88	0.98	1.36	2.06	1.09	1.06	1.69	2.20	1.11	1.02	1.25	1.79	1.14	1.20	1.52	1.96
CD58	1	1.25	1.41	**2.17**	0.99	1.19	1.33	2.22	1.40	1.32	1.71	2.60	1.23	1.32	1.42	2.71	1.25	1.29	1.46	1.80
ETV4	1	1.06	1.24	**2.17**	0.96	0.96	1.51	2.50	1.10	1.11	1.43	2.31	0.98	1.04	1.20	2.31	1.31	1.34	1.60	2.62
SRXN1	1	1.04	1.39	**2.17**	1.09	1.04	1.34	2.20	0.98	1.01	1.32	2.48	0.89	0.93	1.13	1.71	1.04	1.16	1.20	1.66
SERPINE2	1	1.05	1.27	**2.16**	0.64	0.67	0.92	2.08	1.16	1.04	1.39	2.23	0.94	0.90	1.11	1.99	1.01	1.09	1.39	2.08
SNORA56	1	1.09	1.28	**2.16**	1.31	1.25	1.43	2.00	1.29	1.41	1.66	1.64	1.25	1.38	1.39	2.14	1.40	1.06	1.67	2.20
CTH	1	0.96	1.43	**2.16**	0.72	0.90	0.93	1.41	1.14	1.15	1.67	2.27	1.04	1.27	1.56	2.07	1.05	1.23	1.58	1.72
SLC25A37	1	1.06	1.41	**2.14**	0.98	1.27	1.78	2.62	1.21	1.23	1.57	1.99	1.16	1.21	1.48	2.14	1.19	1.13	1.48	1.68
TNFRSF11B	1	1.11	1.42	**2.14**	0.71	0.81	1.15	1.80	1.16	1.13	1.91	3.23	1.07	1.21	1.42	2.58	1.00	1.16	1.68	2.28
PMEPA1	1	1.04	1.77	**2.13**	0.78	0.83	1.62	1.83	1.03	1.12	2.01	2.41	0.99	1.03	1.89	2.28	1.00	1.04	1.99	1.91
TRIB3	1	0.97	1.45	**2.13**	0.93	0.84	1.29	2.25	0.99	0.96	1.64	2.43	0.95	0.98	1.49	2.10	0.99	1.08	1.53	1.88
NDRG1	1	0.99	1.31	**2.11**	0.81	0.90	1.23	1.72	0.81	0.87	1.24	1.96	0.69	0.76	1.15	1.67	0.84	0.91	1.36	2.03
SPHK1	1	1.16	1.95	**2.11**	1.04	1.08	2.22	2.33	0.92	1.26	2.14	2.27	1.05	1.22	2.01	2.04	0.94	1.19	1.89	1.68
SERPINB9	1	0.97	1.68	**2.11**	0.75	0.80	1.61	2.48	0.94	1.05	1.77	2.11	0.74	0.87	1.58	2.33	0.84	0.97	1.96	1.88

condition	mock				HRS				TSG101				VPS4A				ALIX			
EGF [min]	0	30	120	360	0	30	120	360	0	30	120	360	0	30	120	360	0	30	120	360
EPAS1	1	0.97	2.06	**2.10**	0.64	0.61	1.88	2.41	0.79	0.82	2.00	2.41	0.95	0.99	2.08	2.43	0.73	0.76	1.73	1.79
SAT1	1	1.44	2.08	**2.10**	1.16	1.57	2.36	2.83	1.24	1.58	3.10	2.69	1.16	1.71	2.17	2.50	1.05	1.38	2.39	1.95
MYPN	1	0.89	1.58	**2.10**	0.57	0.70	0.97	1.57	0.61	0.68	1.16	1.52	0.78	0.80	1.61	2.17	0.64	0.72	1.53	1.77
CTSL1	1	1.03	1.51	**2.08**	1.01	1.17	1.54	2.50	1.00	1.07	1.66	2.58	0.94	1.04	1.48	2.13	0.97	1.04	1.52	1.96
WARS	1	1.01	1.17	**2.08**	0.76	0.85	1.15	2.10	0.95	0.95	1.21	2.27	1.03	1.02	1.21	2.06	0.92	1.03	1.25	1.80
ARNTL	1	1.21	1.52	**2.07**	0.80	0.77	1.10	1.99	1.23	1.24	1.62	2.20	1.27	1.33	1.35	2.19	1.04	1.21	1.46	1.82
TGM2	1	1.01	1.46	**2.06**	0.64	0.58	1.36	1.73	0.90	0.89	1.43	2.16	0.94	1.02	1.58	2.10	0.98	1.02	1.57	2.01
KCNK2	1	1.11	0.92	**2.06**	0.82	0.84	0.77	1.77	0.93	0.96	0.90	1.84	0.95	1.16	1.09	2.27	0.97	1.09	0.92	1.84
OSGIN2	1	1.40	1.61	**2.06**	1.62	1.79	1.53	1.40	1.32	1.04	1.47	0.71	1.17	0.83	1.34	1.61	1.72	1.19	1.79	1.17
TPBG	1	0.94	1.27	**2.04**	1.01	1.06	1.11	1.74	0.85	0.96	1.37	2.08	0.98	0.91	1.43	1.88	0.83	0.87	1.14	1.83
C16orf45	1	0.99	1.13	**2.04**	0.97	0.88	1.19	2.11	0.97	0.99	1.35	2.10	0.89	0.94	1.16	2.04	1.17	1.21	1.48	2.39
GRAMD1B	1	0.89	1.89	**2.03**	0.76	0.78	1.45	1.88	1.13	1.16	2.17	2.64	1.07	1.13	2.01	2.50	1.09	1.08	2.22	2.20
F2RL2	1	1.12	1.03	**2.03**	0.87	0.70	0.97	1.73	0.93	1.00	1.38	2.75	1.06	1.12	1.27	2.11	0.91	0.93	1.07	1.32
TMEM154	1	1.28	1.13	**2.01**	1.25	1.27	1.13	1.99	1.22	1.27	1.17	2.11	1.11	1.07	1.09	2.06	1.09	0.94	1.11	1.99
CHRNA9	1	1.15	1.48	**2.00**	0.99	1.07	1.00	1.49	1.10	0.91	1.38	1.73	0.99	1.19	1.38	2.22	1.05	1.03	1.39	1.66
MT2A	1	1.01	1.46	**2.00**	1.95	2.10	1.88	2.53	0.93	0.97	1.26	1.73	1.04	1.04	1.44	1.77	0.88	0.95	1.40	1.88
SLC30A1	1	0.93	1.80	**1.99**	1.64	1.31	2.87	2.97	1.08	1.01	1.57	1.97	1.09	1.09	1.72	1.85	1.14	1.12	3.18	2.10
PSAT1	1	0.98	1.18	**1.97**	0.71	0.76	0.97	1.87	0.95	0.94	1.21	2.00	0.97	0.93	1.08	1.91	1.01	1.06	1.18	1.68
TNFRSF21	1	1.06	1.55	**1.96**	1.01	1.11	1.67	2.19	0.96	0.95	1.48	1.88	0.96	1.09	1.49	1.97	0.96	1.06	1.69	1.93
MID1	1	1.00	1.06	**1.95**	0.96	1.05	1.03	2.03	1.10	1.04	1.14	2.04	1.02	1.01	0.98	1.99	1.03	1.09	1.22	2.06
CDCP1	1	0.93	1.20	**1.95**	0.77	0.78	1.33	2.45	0.97	0.98	1.39	2.22	0.84	0.90	1.24	2.06	0.80	0.77	1.31	1.60
IRAK2	1	1.02	1.27	**1.95**	1.10	0.81	1.45	2.50	0.96	0.98	1.39	2.30	0.98	1.10	1.23	1.99	1.10	0.99	1.39	1.91
MAFG	1	0.91	1.49	**1.93**	0.84	1.07	1.79	2.27	1.05	1.15	1.61	1.85	0.91	1.01	1.36	1.84	0.90	1.06	1.41	1.54
C17orf91	1	1.38	1.53	**1.93**	1.26	1.47	1.67	1.85	0.96	1.46	1.69	1.49	1.13	1.33	1.60	1.64	1.01	1.13	1.44	1.43
CEBPG	1	1.07	1.84	**1.93**	1.09	1.12	1.65	2.06	1.08	1.06	2.07	2.00	1.01	1.18	1.80	1.77	0.97	1.05	1.87	1.56
PLCL2	1	1.01	1.09	**1.92**	1.00	0.98	1.19	2.00	1.15	1.19	1.25	2.11	1.09	1.13	1.06	2.17	1.26	1.45	1.44	2.16
SLC1A5	1	0.98	1.30	**1.91**	0.66	0.70	1.17	1.75	0.97	0.94	1.26	1.88	0.88	0.92	1.21	1.67	0.98	0.97	1.22	1.65
LRRC8C	1	1.09	1.28	**1.91**	0.97	0.93	1.29	1.80	1.01	1.10	1.30	1.88	1.02	1.04	1.53	1.97	1.03	1.06	1.25	1.67
PDZD2	1	0.80	0.97	**1.91**	0.82	0.90	0.85	1.92	0.84	0.95	0.82	1.87	0.97	0.93	1.04	2.07	0.91	0.88	0.82	1.82
NEDD4	1	1.15	1.32	**1.91**	0.70	0.75	0.98	1.85	1.14	1.09	1.45	2.10	1.20	1.33	1.36	2.35	1.03	1.22	1.26	1.57
RHEBL1	1	1.21	1.41	**1.91**	2.01	1.69	1.56	2.50	1.41	1.48	1.39	2.27	1.43	1.49	1.44	2.07	1.16	1.30	1.21	1.74
ASNS	1	0.95	1.37	**1.89**	0.60	0.57	1.02	1.93	0.84	0.88	1.35	1.97	0.80	0.76	1.06	1.77	0.94	1.01	1.27	1.62
DMBT1	1	1.10	1.87	**1.89**	0.85	0.90	1.68	1.58	1.51	1.59	2.41	1.99	1.22	1.41	2.03	1.91	1.27	1.39	1.99	1.69
MAP1LC3B2	1	1.28	1.71	**1.87**	0.84	1.17	1.68	1.88	1.06	1.29	1.85	2.00	0.97	1.22	1.41	1.79	1.17	1.31	1.64	1.66
PRKAA2	1	1.09	1.27	**1.87**	1.01	1.27	1.37	1.71	1.32	1.31	1.59	1.95	1.27	1.29	1.39	2.19	1.16	1.28	1.69	2.20
AIM1	1	0.97	1.10	**1.85**	0.68	0.74	0.78	1.46	0.82	0.84	0.95	1.69	0.82	0.76	0.90	1.62	0.71	0.68	0.79	1.28
CXorf61	1	1.75	1.72	**1.85**	1.29	1.83	1.84	1.80	1.07	1.71	1.95	1.80	1.26	1.82	1.87	1.91	1.20	1.69	1.88	1.58
FGFBP1	1	1.06	1.16	**1.83**	0.47	0.49	0.56	0.67	1.01	1.00	1.19	1.66	1.13	1.13	1.25	1.97	0.97	1.04	1.09	1.52
TRIML2	1	1.16	1.39	**1.83**	1.01	1.06	1.19	1.39	0.91	0.99	1.59	1.45	1.13	1.00	1.46	1.85	0.94	0.89	1.58	1.79
SPRED2	1	1.09	1.62	**1.83**	0.97	1.06	2.00	2.07	1.07	1.15	1.77	1.79	1.13	1.11	1.67	2.01	1.13	1.16	2.08	1.80
DRAM1	1	1.01	1.39	**1.83**	0.90	1.01	1.58	2.48	1.08	1.06	1.58	2.30	0.87	0.95	1.26	1.78	0.93	1.03	1.31	1.51
IL4R	1	0.93	1.41	**1.82**	0.99	0.95	1.67	2.25	0.96	0.90	1.69	2.64	1.05	1.00	1.61	2.62	0.99	0.97	1.99	2.13
NRP1	1	1.02	1.06	**1.82**	0.69	0.84	0.90	1.52	1.02	1.03	1.01	1.73	0.97	1.01	0.94	1.88	0.93	1.04	1.04	1.41
GLIPR1	1	1.14	1.54	**1.82**	0.86	1.07	1.51	1.85	1.23	1.25	1.96	2.14	1.16	1.30	1.61	2.08	0.86	1.01	1.37	1.43
PICALM	1	0.99	1.49	**1.82**	0.77	0.88	1.41	1.88	1.04	0.95	1.60	2.07	0.99	1.04	1.39	1.87	1.04	1.15	1.60	1.83
CA13	1	1.01	1.39	**1.80**	0.91	0.86	1.45	1.67	1.06	1.11	1.77	2.01	1.16	1.21	1.59	1.99	1.16	1.35	1.88	1.97
CPEB4	1	1.13	1.78	**1.80**	0.86	1.02	1.92	1.79	1.24	1.49	1.71	1.95	1.03	1.16	1.71	1.97	1.37	1.43	2.22	2.06
NPAS2	1	1.01	1.10	**1.80**	0.71	0.76	1.04	1.62	0.92	0.96	0.99	1.44	0.97	0.98	1.09	1.77	1.06	1.05	1.43	1.99
RNFT1	1	1.25	1.39	**1.80**	1.00	0.96	1.21	1.54	1.64	1.43	1.75	2.13	1.25	1.39	1.54	2.04	1.45	1.48	1.83	1.96
GATSL1	1	0.91	0.81	**0.54**	0.56	0.62	0.73	0.45	0.88	0.89	0.78	0.53	0.85	0.90	0.76	0.53	0.96	0.95	0.74	0.50
FOXP2	1	0.90	0.90	**0.53**	0.55	0.56	0.74	0.43	0.90	0.90	1.12	0.55	0.88	0.96	0.93	0.68	0.95	1.03	1.07	0.47
GPR141	1	1.01	0.94	**0.53**	1.35	1.32	1.31	0.69	1.09	1.15	1.13	0.54	1.21	1.39	1.20	0.65	1.61	1.83	1.43	0.82
PRAME	1	1.04	0.73	**0.53**	0.83	0.86	0.72	0.49	0.91	0.97	0.81	0.50	1.06	1.16	0.85	0.65	0.92	0.95	0.80	0.62
PDE8B	1	1.08	0.93	**0.52**	0.99	1.01	0.94	0.48	1.00	1.01	0.94	0.45	0.99	1.10	0.92	0.57	1.06	1.13	0.98	0.49
IGSF10	1	1.01	0.86	**0.51**	0.62	0.75	0.66	0.38	1.05	0.99	0.78	0.51	1.05	1.04	0.86	0.62	1.12	1.06	0.90	0.50
ARID5B	1	1.08	0.84	**0.51**	0.86	0.91	0.93	0.56	0.90	0.98	0.81	0.57	0.90	1.03	0.90	0.57	1.03	1.10	0.88	0.56
ZMYM3	1	0.99	0.77	**0.51**	0.84	0.77	0.78	0.51	0.98	0.94	0.79	0.43	1.01	1.04	0.78	0.57	0.96	1.01	0.76	0.46
TGFB3	1	0.93	0.84	**0.51**	0.87	1.06	0.90	0.59	0.91	0.90	0.83	0.51	0.85	0.95	0.86	0.54	0.98	1.06	0.73	0.57
BTN3A3	1	1.09	0.65	**0.48**	0.65	0.72	0.61	0.50	1.11	0.94	0.93	0.62	1.01	1.11	0.86	0.68	1.04	1.10	0.77	0.46
FAM13C	1	1.24	0.88	**0.48**	1.09	1.17	0.81	0.49	1.17	1.26	0.99	0.55	1.13	1.37	0.88	0.46	1.39	1.35	0.94	0.49
CTTNBP2	1	1.04	0.66	**0.48**	0.69	0.81	0.65	0.39	1.04	0.94	0.71	0.41	0.89	1.01	0.65	0.45	0.88	0.91	0.60	0.46
EPB41L4A	1	0.95	0.82	**0.48**	0.68	0.64	0.68	0.34	0.95	0.91	0.86	0.43	0.88	0.93	0.76	0.46	0.84	0.87	0.78	0.37
ELF3	1	1.39	0.82	**0.47**	1.04	1.55	1.21	0.49	0.85	1.39	0.74	0.54	0.86	1.40	0.82	0.47	0.82	1.21	0.73	0.58
SEMA6D	1	1.06	0.58	**0.46**	0.72	0.72	0.47	0.39	0.98	1.01	0.56	0.39	1.01	1.14	0.69	0.53	0.90	0.91	0.49	0.40
KIT	1	1.07	0.81	**0.43**	1.03	1.16	0.89	0.50	1.28	1.26	1.04	0.68	1.36	1.32	1.05	0.65	1.38	1.53	1.04	0.73
MPPED2	1	1.03	0.91	**0.43**	0.74	0.79	0.94	0.40	0.93	0.97	0.96	0.38	0.88	0.91	0.86	0.37	0.94	0.95	0.84	0.34
METTL7A	1	1.04	0.82	**0.40**	0.73	0.75	0.71	0.38	1.01	0.92	0.97	0.48	1.23	1.36	0.95	0.52	1.13	1.22	0.90	0.43

5. Microarray analysis – knockdown effects

Table 4: Knockdown effects in unstimulated, starved cells (top 40 genes, values in % above or below mock)

HRS		TSG101		VPS4A		ALIX	
0 min up							
IL6	191.26	SNORD25	136.64	LCN1L1	137.42	HEY1	115.77
MT1E	153.32	SCARNA9	95.13	HIST1H2AJ	65.75	SLC16A6	85.54
LCN1L1	148.48	PAR5	95.10	C1orf63	63.22	SCML1	78.04
GAGE13	131.87	SNORD1B	94.45	SCML1	59.60	LCN1L1	76.36
CTSS	108.92	SNORD38B	93.86	AREG	59.55	CGA	75.12
C8orf4	108.18	SNORD27	93.56	CST11	58.66	SNORD59B	74.41
MT1F	106.48	SCML1	90.81	IL6	57.94	DLEU2	73.08
TESC	103.56	ZNF675	81.32	DOC2BL	56.91	UNC13A	72.70
RHEBL1	101.82	SNORD49A	78.61	SPRYD5	55.08	SNORD38B	72.14
CYP1B1	100.15	SNORD58A	78.03	PLEKHH1	53.55	LYAR	67.27
MT1X	97.63	SNORA4	76.93	RRP7B	52.24	SNORD25	66.96
MT2A	94.88	SNORD56B	72.86	GOLGA6	51.35	ZNF675	64.73
GAGE12B	92.11	SNORD47	72.48	SIRPD	51.24	SLC1A3	63.68
TIPARP	87.34	CHORDC1	70.28	SNORD38B	51.12	ARID4A	63.31
ISG15	87.08	SNORD63	70.18	ZNF799	50.66	GPR141	61.36
CXorf40B	84.75	OCLN	69.96	RPL7A	50.22	HIST1H2AJ	61.09
DDTL	84.60	CGA	69.27	RFESD	49.99	SNORD7	60.77
COX7A2	82.80	SNORA40	68.44	C20orf69	48.87	MSL3L2	59.56
MT2A	82.58	RPL7A	68.33	SLC16A6	47.64	TNFRSF1B	58.72
KIAA0125	81.51	SNORD50B	68.07	EML6	47.59	ZNF594	58.18
DOC2BL	80.10	SNORD5	67.91	ATRX	46.30	CEP170	58.17
MT1L	80.04	ZNF248	64.37	WDR19	46.27	ADAP2	57.47
IER3	77.61	SNORD28	64.37	NBEAL1	45.68	ZNF343	57.33
C21orf119	76.89	SNORD75	63.98	C21orf119	44.92	SCARNA9	56.97
C7orf59	74.59	SCARNA9	63.85	C3	44.87	ATRX	56.88
RPL39L	72.99	RNFT1	63.70	C9orf53	44.70	ZNF14	56.80
IFRD1	71.84	SNORD42B	62.93	ZNF675	43.78	ZNF615	54.14
CGA	71.59	SEPSECS	62.72	RHEBL1	43.71	SNORD77	53.98
ATP5G1	71.41	PIGF	62.37	TOM1L1	43.63	SNORD58A	53.79
ZNF778	71.33	RNU13P1	62.14	CRHR1	43.57	HSD3B1	53.75
ACAA1	71.24	ARID4A	62.06	SEPSECS	42.73	PDK4	53.27
NDUFA13	69.74	ZNF616	61.83	GDF15	42.08	POLR3G	53.18
CKMT2	69.18	SNORD59A	61.49	CHORDC1	41.49	ZNF721	53.06
C3	69.17	RRP7B	61.30	SNORA1	41.33	SEPSECS	52.85
DYNLL1	69.15	PDP2	60.90	FCGR2B	41.24	USP53	52.62
HSD3B1	68.54	ALG6	60.88	SNORA27	41.04	GOLGA4	52.60
TCL1A	67.40	KIAA1009	60.65	DBF4	40.78	CCDC41	51.22
KCTD12	66.51	TAS2R14	60.32	C5orf44	40.73	TESC	50.67
SLC16A6	66.49	SNORD80	60.08	PIGF	40.64	CHORDC1	50.57
PI3	65.67	SNRPN	59.85	C13orf27	40.47	DNM3	50.34
0 min down							
FAM29A	-45.07	TECTA	-33.52	CLDN12	-29.34	SYTL5	-32.51
MPP7	-45.08	HAS3	-33.53	GPR1	-29.37	MMP13	-33.24
SNORD45B	-45.09	ACBD7	-33.63	FBXW10	-29.39	PCDHB6	-33.30
SLC25A44	-45.54	C3orf15	-33.92	C15orf43	-29.60	PSG5	-33.46
SETD7	-45.55	FIBIN	-34.04	EXDL1	-29.61	CTGF	-33.59
MAP2	-46.00	LCE2C	-34.50	PDGFRB	-29.66	GYG2	-33.67
TAPBP	-46.04	CPA4	-34.53	LYPD6B	-29.76	EYS	-33.82
RAB23	-46.17	DND1	-34.56	IFITM5	-30.02	CTSK	-33.87
CNDP2	-46.27	OR6B2	-34.59	EIF5A	-30.09	PDGFRB	-33.92
NDST1	-46.28	PDGFRB	-34.69	AKAP4	-30.12	KCNJ1	-33.98
CP110	-46.36	EXDL1	-34.76	SLC22A24	-30.22	IGFBP3	-34.31
PCSK9	-46.53	CD28	-34.99	ZNF443	-30.25	C3orf15	-34.40
ATP1B1	-46.61	CHI3L1	-35.22	CLEC6A	-30.43	TAAR6	-34.67
WIPF1	-46.96	H19	-35.63	MGC26718	-30.44	NDN	-34.84
SEC24D	-47.58	CTGF	-35.64	OR13C9	-30.54	C8orf73	-35.28
AXL	-47.74	KRTAP24-1	-35.81	CD1E	-30.87	SNRPN	-35.68
TAGLN	-47.83	CD1E	-35.92	RAB25	-30.92	OR6C3	-35.75
GALNT2	-48.17	SH2D7	-36.10	CYP2B6	-31.12	GPR148	-35.80
GPR64	-48.34	AMAC1	-36.13	NDRG1	-31.35	LY6G6D	-35.89
HGS	-49.64	SLC22A24	-36.19	MYO1C	-31.55	CYR61	-36.40
PRUNE2	-49.81	OLFML3	-36.25	PSG4	-32.32	MYPN	-36.46
MYBL1	-50.01	OR4B1	-36.44	ACBD7	-32.49	PSG4	-37.43
RAB1C	-50.33	PSG4	-36.56	PCDHB6	-32.61	C6orf99	-37.51
CTDSP2	-50.38	PSG5	-36.64	PSG5	-33.02	ZNF154	-37.59
AAK1	-50.64	OR52K3P	-36.68	APOBEC3F	-33.07	EFCAB4B	-37.83
NPNT	-50.95	SCGN	-36.73	PLA2R1	-33.10	OR4B1	-37.88
SC4MOL	-51.05	CYP4A11	-36.83	IGSF9B	-33.47	USP18	-37.98
RALGPS2	-51.93	KCNJ1	-36.89	TLR1	-33.51	PIGZ	-38.10
FREQ	-51.95	IL7R	-37.86	PIGZ	-33.70	GPR1	-38.29
ITGA5	-52.21	ASPHD2	-38.08	LCE2C	-35.37	CD82	-38.60
NPR1	-53.36	PRLR	-38.13	C2orf19	-35.55	IL7R	-39.30
FGFBP1	-53.38	MORN5	-38.52	ADAM21	-36.50	CLDN1	-39.92
LOX	-53.62	MYPN	-38.89	SEMA4D	-37.35	OR1F2P	-39.93
GTPBP1	-53.79	AK5	-39.29	UGT3A2	-37.46	PLSCR4	-40.36
EFNB2	-54.31	CYP2B6	-41.60	OR3A3	-39.03	OR52K3P	-41.94
GALNT7	-54.78	SNRPN	-42.61	NDN	-44.13	CXCL2	-42.06
YWHAH	-54.81	OR1F2P	-42.79	LOXL2	-45.87	AOX1	-43.73
MFAP5	-59.79	STELLAR	-43.45	FAM183B	-52.48	CPA4	-44.34
ACSS2	-60.74	C6orf99	-46.06	CDRT1	-62.71	THBS1	-44.48
DNER	-64.15	TSG101	-74.91	VPS4A	-74.50	PDCD6IP	-78.52

Table 5: Knockdown effects at 30 min EGF (top 40 genes, values in % above or below mock)

HRS		TSG101		VPS4A		ALIX	
30 min up							
IL6	196.46	TMEM229B	79.19	TMEM229B	139.45	HEY1	101.87
CTSS	129.66	CGA	67.57	SNORA69	84.12	SLC16A6	83.91
DYNLL1	112.20	EYS	61.86	SNRPN	67.17	TMEM229B	82.92
MT2A	108.81	SCARNA9	59.48	MME	58.33	UNC13A	82.14
MT1E	103.64	SNORD102	58.55	SNORD77	56.60	GPR141	80.79
IFI27L1	96.72	HLA-DQA1	57.39	SNRPG	55.38	SLC1A3	80.71
DDT	91.70	DNAH14	56.75	LGALS13	54.95	CGA	73.02
COX7A2	89.62	AADACL3	55.90	IFI44	54.94	SNRPN	69.75
NDUFA1	87.65	LRRC37B	50.79	PRSS2	54.39	ARID4A	65.51
MT1X	86.66	SCARNA9	50.66	PIN4	52.65	LGR5	62.89
TMEM229A	85.99	CDRT1	49.91	MLANA	52.37	FABP3	60.61
TESC	85.05	SNORA46	49.68	SERPINI1	52.20	ZNF852	60.56
LRRFIP1	84.35	TRA2A	48.89	EYS	51.32	LRRC37A2	59.83
MYCNOS	83.06	LYZL2	46.90	LYZL2	48.92	SCARNA9L	58.39
SNORD95	81.12	LGALS13	46.33	LIPK	48.79	ZNF860	57.73
LDB2	80.44	MPEG1	46.16	DEFB114	48.37	ZNF846	57.30
C3orf47	79.33	IFI44	45.68	TBC1D8B	47.29	STEAP4	56.81
C7orf59	78.91	DMBT1	45.03	HSPA1L	47.01	C14orf19	56.53
ZNF487	78.89	SNORD21	44.91	C7orf58	46.84	HSPA1L	55.99
GAGE12B	78.67	SLC16A14	43.72	SNORA13	46.15	VAV3	55.55
C3	78.12	TESC	43.56	ZNF847P	46.03	LIPK	55.48
RPL39L	78.04	CFHR1	43.33	SNORD51	45.41	FIGF	54.32
MT2A	77.26	SNORA69	43.26	SNORA65	44.85	LYZL2	53.01
LRRFIP1	76.70	ANKRD55	43.24	SCARNA4	44.73	KRT10	52.37
BLVRA	76.26	OR10K2	43.08	PCDHB2	44.65	KLRA1	52.00
ZNF720	76.15	PSG3	42.30	MMP8	44.32	MCF2	51.49
ATP5G1	75.43	UQCRB	42.29	FCGR2A	44.32	TBC1D30	51.34
MIR21	75.24	SMPD3	42.18	SLC16A6	44.00	CHORDC1	50.46
MT2A	74.50	RBM14	41.92	ZNF654	43.25	CFHR1	50.33
SEPP1	74.35	TUBB8	41.85	C2orf76	43.04	RFESD	50.24
C17orf61	73.67	LHB	41.82	LRRC37A2	41.32	OR6B2	49.15
SLC16A6	73.04	HSPA1L	41.22	C3	41.31	ACSL1	48.40
COX8A	72.24	DPPA5	41.22	ZNF222	41.05	ZNF208	48.09
GAGE13	72.17	OR12D3	41.01	GPC2	40.90	SNORD13	47.01
LCN8	70.90	NFKB2	40.84	CFHR1	40.34	TRIM22	46.16
SNORD21	70.90	SNORA65	40.79	SNORA14B	40.17	SLC44A2	45.87
FCGR2B	70.44	OR10A2	40.54	STELLAR	40.03	PDE1C	45.65
OR10S1	70.27	IGLON5	40.44	GDEP	39.82	EVI5	45.55
SNORD6	70.25	C4orf12	40.42	TMEM229A	39.76	C5orf25	45.34
CRIPAK	70.23	LCE2D	40.33	TUBD1	39.72	ZNF235	45.27
30 min down							
RAB5B	-43.12	GOT1L1	-26.47	PSG4	-27.20	C8orf73	-29.28
P4HB	-43.17	NUAK1	-26.52	RUNDC2C	-27.22	AOX1	-29.37
ITGA3	-43.21	FAM129A	-26.63	IGSF9B	-27.32	OR2AJ1	-29.49
ATP1B1	-44.17	FAM81B	-26.89	PEX5L	-27.37	DGCR6	-29.50
ESYT1	-44.20	CST4	-27.02	MYH9	-27.47	C1QTNF9	-29.55
AXL	-44.26	LCT	-27.03	CYP3A4	-27.47	LHX8	-29.71
MVD	-44.29	MSL3L2	-27.16	TRPC4	-27.70	STH	-29.74
ELK3	-44.53	SPINK5	-27.30	PPP1R14B	-27.92	GPR1	-29.91
SCD5	-44.98	ZNF154	-27.56	C5orf17	-27.93	AIM1	-30.10
PLBD2	-45.33	C14orf37	-27.74	AKR1CL1	-27.95	OR10H5	-30.64
C1orf128	-45.36	CPA3	-27.75	RUNDC2B	-28.39	EFCAB4B	-30.89
MAPK3	-45.37	CCL4	-27.79	KLRK1	-28.54	FCN2	-31.12
SEC23A	-45.38	CES4	-28.11	LHX8	-28.77	GK2	-31.22
GALNT2	-45.50	SMCR5	-28.22	C8orf73	-28.78	OR2D3	-31.33
KCNG1	-46.11	AMOTL2	-28.33	DIO2	-28.96	ITK	-31.37
FSCN1	-46.21	KLRK1	-28.54	KRTAP5-6	-29.09	SIGLEC9	-31.50
DIO2	-46.25	WNT5A	-28.73	PSG1	-29.11	NPNT	-31.70
C1orf144	-46.27	GLDC	-28.97	CRCT1	-29.26	C1orf46	-31.76
CNDP2	-46.34	SAA2	-29.00	GPR82	-29.33	GOLGA6	-32.27
HAS2	-46.62	LY86-AS	-29.16	KCNG1	-29.41	CLDN24	-32.39
RALGPS2	-46.80	TUBA3E	-29.18	FETUB	-29.44	CDRT1	-32.45
MPP7	-47.97	OR6Q1	-29.36	OR2T4	-29.54	TAGLN	-32.55
PDGFRL	-48.08	DNAJC28	-29.62	GRIN1	-29.68	SNCB	-32.82
FREQ	-48.21	PSG1	-30.64	LOH3CR2A	-29.73	LSP1	-34.41
EFNB2	-48.76	TAS2R46	-30.70	CPN1	-30.10	PLSCR4	-34.57
CTDSP2	-49.36	TNNC1	-30.88	OR5M3	-30.11	AKR1CL1	-35.76
PCSK9	-51.46	PMCHL1	-31.11	PCDHB8	-30.33	CD82	-35.96
GALNT7	-52.00	MC4R	-31.34	RASGRP3	-30.41	HSD3B1	-35.97
FGFBP1	-53.93	RNU4-2	-31.66	PRAMEF2	-31.38	EGR3	-36.79
IFI44L	-54.25	EFCAB4B	-32.36	RNU4-2	-32.45	CARD16	-37.23
PRUNE2	-55.05	EGR3	-32.81	LRRFIP1	-32.66	CPA4	-37.28
ITGA5	-55.28	PSG4	-32.84	C1QTNF9	-35.67	OR6Q1	-38.02
YWHAH	-55.47	TPRX1	-33.96	IRAK3	-35.86	RSHL3	-39.22
HGS	-55.65	IL7R	-34.99	DEFB109	-36.14	DAPK1	-39.38
NPNT	-56.41	AK5	-34.99	HIST1H2AJ	-36.18	IL7R	-39.55
NPR1	-57.36	TMEM63C	-36.14	PRM1	-36.73	OR5M3	-42.90
LOX	-57.63	SNRPN	-37.71	TAS2R46	-36.89	THBS1	-43.36
MFAP5	-58.37	FAM99A	-42.42	LOXL2	-39.86	KLRK1	-47.39
ACSS2	-61.16	OLR1	-44.80	HSD3B1	-44.64	UIMC1	-49.66
DNER	-66.18	TSG101	-77.81	VPS4A	-72.45	PDCD6IP	-78.06

Table 6: Knockdown effects at 120 min EGF (top 40 genes, values in % above or below mock)

HRS		TSG101		VPS4A		ALIX	
120 min up							
IL6	456.57	IL6	184.48	PNMA6A	65.79	SLC30A1	75.38
CTSS	180.46	BIRC3	93.29	PTPN20B	65.37	C21orf94	73.46
TNFAIP3	160.95	IL8	76.00	C21orf94	62.55	SNORA62	69.98
IL1A	152.46	SNORD1B	72.04	SNRPN	61.47	IL6	69.74
C3	140.27	AXUD1	65.84	IL6	58.43	UNC13A	68.38
IL8	126.87	PLEKHM1	65.39	PLEKHM1	55.09	SLC16A6	67.71
NFKBIA	123.31	ANKRD49	63.66	DEFB105A	54.34	USH1C	67.65
PTGS2	108.01	AGXT2L1	60.00	LBA1	54.26	GOLGA9P	65.50
BIRC3	105.27	PNMA6A	59.52	OR12D3	52.18	PSG8	64.96
IRF1	105.14	SOCS2	59.24	FAM99B	51.00	SHC4	59.85
CYR61	102.66	C1orf201	58.56	OR12D3	50.97	CCDC76	58.55
C21orf94	100.16	SERPINI1	58.25	ADAM21	48.92	LYZL1	55.84
UGCG	91.30	B3GNT5	57.40	CFHR2	48.47	B3GNT5	55.61
CXCL2	88.40	EFCAB7	57.31	ROPN1L	48.39	SNORD77	55.61
TESC	85.92	SNORA28	56.16	OR2T6	47.90	SNORD44	55.45
NFKB2	82.03	SNRPA1	55.98	C10orf41	47.33	PNMA6A	54.95
EFNA1	82.02	OR5M3	55.49	SERPINI1	46.19	SNORD58A	54.67
SNORD1B	76.68	SNORA62	54.68	DSC2	45.49	ALKBH8	53.04
NUAK2	74.87	LRRFIP1	54.67	CC2D2B	45.42	GPR141	52.92
EGR1	73.15	SNORD117	54.06	TSPAN18	45.01	TCN1	52.89
KIR2DL3	72.22	GCNT2	54.01	ZNF627	44.68	USPL1	51.25
SNORD44	72.10	SCARNA9	53.95	OR4C46	44.58	EIF2C4	50.98
SLC16A6	71.90	FAM83B	52.80	DGKZ	44.45	SLC1A3	50.92
NFKB1	68.75	TSPAN8	52.45	PPP1R1C	43.91	SNORA33	50.78
SNORA62	68.01	FAM72A	51.89	C3	43.67	SNORD1B	50.78
CCL20	66.97	TLR6	51.04	PSMAL	42.78	PDE1C	50.37
MIR21	66.73	SNORA4	50.68	OR8K1	42.59	SNORA13	50.36
SNORD45B	65.38	SENP7	50.49	OR6F1	42.33	P4HA1	50.04
EDN1	64.89	IL15	50.07	OR56A4	42.01	TMEM135	49.95
PTBP2	64.83	CLDN1	49.73	C21orf94	41.77	SST	49.67
SNORD78	63.04	NFKBIA	49.71	CHL1	41.67	CRLF3	49.39
HTR1D	62.20	SNORA69	49.37	TRIM75	41.64	SNORD78	49.18
PI3	61.92	CCDC132	49.29	B3GNT1	41.57	DNM3	48.95
DNAH14	61.52	SNORD77	49.18	WDR63	41.40	TSGA14	48.07
SNORA33	61.47	C3orf59	49.00	HLA-DPA1	41.38	ZNF620	47.94
MAP3K8	61.30	PAPPAS	48.90	ZBTB37	41.12	TAS2R40	47.89
LPA	60.59	SAT1	48.87	DUOX2	40.82	FAM169A	47.28
IER3	60.26	TSHZ2	48.71	TRPC2	40.79	DKK1	47.21
SNORD47	59.85	MCF2	48.57	ZP4	40.54	CNOT6L	47.14
CCDC88C	59.68	RAB7A	48.31	MMAA	40.48	TESC	46.95
120 min down							
SEC23A	-37.23	RAB3B	-29.19	OR2T10	-29.51	RMRP	-31.96
RALGPS2	-37.26	RNF186	-29.40	ARMETL1	-29.52	DMRTA2	-31.97
HSD17B7	-37.41	ESPNP	-29.52	LCE2C	-29.59	NPNT	-31.98
HGS	-37.77	LHB	-29.66	NCRNA00116	-29.63	TMOD4	-32.30
DIO2	-37.82	ZNF487	-29.69	TMSB4X	-29.91	IGLON5	-32.35
SLC25A30	-38.20	PSG9	-29.84	NDUFB2	-30.16	AGTRAP	-32.56
SCD	-38.20	FAM99A	-30.15	CCDC15	-30.61	TMEM229B	-32.62
SOD1	-38.29	H19	-30.36	ZFP92	-30.91	NDUFA1	-32.66
CTDSPL	-38.37	DMRTA2	-30.62	ORM2	-31.57	TSP50	-32.76
DAPK1	-38.41	POU3F1	-30.82	C9orf3	-31.63	OR2T10	-33.01
MYPN	-38.54	FCGR1A	-30.83	SNRPN	-31.82	FBXO32	-33.31
SLC39A10	-39.12	MRGPRX4	-30.88	PLCXD3	-32.45	CITED4	-33.34
PRUNE2	-39.16	FAM83E	-30.93	CYP1B1	-32.56	COX8A	-33.41
CYBRD1	-39.18	TSP50	-30.98	IL18	-32.62	LBH	-33.59
PRUNE2	-39.18	AKR1B10	-31.39	RAB1C	-32.63	GAGE13	-33.81
PRKACA	-39.20	FUT5	-31.47	HIST1H2BC	-32.65	OR2B6	-34.09
NPNT	-39.28	CR1	-31.62	C3orf10	-32.72	RPL26L1	-34.45
PIK3R3	-39.34	C7orf52	-31.65	GRAP	-32.82	FTMT	-34.48
ZMAT3	-39.57	KLK12	-31.94	PLAC8	-33.35	DDT	-34.59
MVD	-40.39	SYN2	-32.08	FAM131C	-33.39	DHRS3	-34.65
SCD5	-41.11	OTUD6A	-32.11	FAM92A2	-33.76	S100A7	-34.66
GPR64	-41.73	SLC7A3	-32.48	OR7D4	-33.86	AKR1B10	-35.01
CP110	-42.11	OR1D2	-32.53	PLA2R1	-33.94	FAM128B	-35.04
MAPK3	-42.17	C9orf106	-32.80	PCDHB8	-34.17	ORM2	-35.51
HAS2	-42.41	OR51M1	-32.82	C20orf69	-34.31	C3AR1	-35.59
SC4MOL	-42.82	OR2T10	-33.11	RNU5F	-34.41	SCARNA6	-35.87
LOX	-43.02	TRGV9	-33.16	FAM99A	-34.77	PSG3	-35.93
HSD17B7P2	-44.26	CST9	-33.36	CDRT1	-34.87	ANKRD42	-36.12
YWHAH	-44.53	MRGPRD	-33.95	EIF4B	-35.56	C6orf52	-36.16
C1orf128	-45.89	TMEM229A	-33.96	LOXL2	-35.92	DAPK1	-36.18
GALNT7	-46.69	MYO1G	-34.02	OR2B6	-36.06	GRAP	-36.44
GEM	-46.85	HSPA6	-34.42	TMSB4X	-36.51	FAM131C	-37.18
LPIN1	-47.03	HCG4	-34.86	DHFR	-36.58	AOX1	-37.67
SESN3	-48.82	SPRR2D	-35.41	TXNIP	-37.57	CD82	-38.29
OR1F2P	-50.94	CCL4	-36.10	TMSB4X	-37.83	IFNA10	-38.62
FGFBP1	-51.78	PCDHB8	-37.86	OR1F2P	-39.81	PLSCR4	-40.55
DNER	-52.16	PLAC8	-38.46	COX7B	-40.94	CPA4	-43.85
ACSS2	-56.93	TMEM229B	-47.50	MSL3L2	-42.00	FAM183B	-44.87
CCL4	-58.72	FAM183B	-50.68	DLEU2	-45.45	SNRPN	-45.16
MFAP5	-60.13	TSG101	-79.05	VPS4A	-77.46	PDCD6IP	-79.21

Table 7: Knockdown effects at 360 min EGF (top 40 genes, values in % above or below mock)

HRS		TSG101		VPS4A		ALIX	
360 min up							
IL6	209.79	SERPINB3	115.05	CCL4	89.89	IGLON5	90.63
CTSS	206.65	BIRC3	81.91	ZNF487	71.90	SERPINB3	77.63
BIRC3	168.07	ACAA1	78.36	CHL1	70.32	KIT	72.40
C3	130.65	CTSS	72.70	CASP1	65.18	LCN1L1	69.85
CLDN1	122.93	AREG	69.26	TTC39B	57.29	SNORD3A	65.96
IL1A	121.52	OPN1LW	68.50	SCARNA9	56.57	FCGR3A	65.81
IL8	115.03	SERPINB4	67.27	OR14I1	54.10	LCN8	65.77
PI3	108.25	LCN1L1	65.26	KIT	53.23	GNG4	65.50
NFKB1	93.24	IFIT2	64.53	TYW1B	51.30	SLC16A6	64.11
RELB	92.86	HSD3B1	63.86	BTBD11	50.58	RP4-621O15.2	63.88
NFKB2	84.89	CLDN1	61.52	FAM27A	50.25	HSD3B1	63.69
MT1E	84.71	ITGA2	61.38	ITGA2	49.15	SLC1A1	61.09
CCL2	82.77	KIT	60.46	C2orf76	49.07	PRSS1	57.72
CYR61	82.68	VN1R4	60.17	CCR2	47.91	OR10G2	56.79
SDC4	80.74	ZNF285B	57.77	HSD3B1	47.85	RASGRP4	55.66
EGR1	79.89	DDX58	55.65	NOX4	46.86	IL24	54.11
TNFAIP3	77.35	NFKB2	54.92	FAM133A	46.74	GPR141	53.70
ETS1	77.29	OR1F2P	54.32	ACAA1	46.73	RUNDC2C	53.26
LCN1L1	73.85	TNFRSF9	53.93	C3	46.62	SCUBE1	51.31
ICAM1	73.38	IDO1	53.82	NBEAL1	46.40	OR5M3	50.98
MIR21	73.15	ARNTL2	51.88	DNAJB14	46.17	C6orf138	50.29
SOD2	71.45	TNFRSF11B	51.42	STELLAR	45.95	ADAP2	50.03
SNORD25	70.97	IFIT3	50.08	CD40LG	45.44	TMEM191A	49.99
IL32	70.42	CCDC146	49.75	DKK1	44.78	IGHE	48.68
STELLAR	69.60	SDR16C5	48.25	SNORD13	44.55	CCL3	47.72
CXCL2	67.10	SHC4	47.52	OR5B2	44.55	SNORA62	47.21
LIF	67.02	SLIT2	47.35	IL4R	44.09	OR5D16	47.19
TMEM136	64.71	AREG	46.66	ACRC	43.17	ZNF487	45.93
PRO2012	64.40	WDR72	46.26	SNORA1	42.74	DEFB109	45.89
SNORD3A	64.40	GBP3	45.36	AREG	42.59	SPINK5	45.46
MT1X	63.46	GALNT3	45.27	CC2D2B	41.83	CLIC5	45.34
IL1B	63.41	SOCS2	45.25	ACBD7	41.78	HEY1	45.27
BIRC2	62.97	IL4R	45.03	SKAP2	41.78	C21orf94	44.20
CYP1B1	62.80	GK3P	44.95	LRRFIP1	41.62	FAM186A	44.02
IKBKE	62.75	CGA	44.57	BTN3A3	41.14	RGS5	44.02
THBS1	61.93	RAD51L1	44.36	MMP10	40.72	CCDC140	43.50
OLR1	61.92	FBXO9	44.32	STEAP4	40.20	TTC39B	43.35
STC2	60.44	ANKRD20B	43.92	AREG	39.75	KLK11	42.36
IFIT2	60.34	CCL8	43.57	OR5H14	39.68	SNORD59B	42.20
RP4-621O15.2	60.30	ITK	43.48	CCDC68	39.58	TIPARP	41.95
360 min down							
PDGFRB	-37.02	S100A2	-26.88	PROZ	-27.27	F2RL2	-35.33
SCD5	-37.14	EDN1	-27.02	RAPGEF5	-27.36	POLR2G	-35.50
FAM105A	-37.20	AK5	-27.07	CEACAM1	-27.53	S100A2	-35.75
CNDP2	-37.31	PSG4	-27.13	GZMH	-27.53	C8orf40	-35.78
VASH2	-37.40	S100A1	-27.13	SORCS3	-27.56	HERC3	-36.01
NEU1	-37.43	KCNIP2	-27.13	C4BPB	-27.57	USMG5	-36.04
C14orf1	-37.66	FFAR3	-27.25	FOXR2	-27.69	RHEB	-36.09
MAP2	-38.03	TRIM75	-27.27	C20orf106	-27.71	SNRPE	-36.47
LPIN1	-38.17	CAV1	-27.32	AMAC1	-28.19	COX7B	-36.47
FAM127A	-38.49	EYS	-27.35	OR11H6	-28.30	RPS27A	-37.24
HPD	-38.59	C9orf3	-27.46	OR6J1	-28.37	GPR64	-37.45
HGS	-39.74	TIMP2	-27.64	C11orf44	-28.43	RPL27	-37.69
ZMAT3	-40.36	OR7C1	-27.66	CDRT1	-28.49	RPS19	-37.98
INPP4B	-40.39	MYPN	-27.79	UNC13C	-28.57	RAB7A	-38.22
SMARCA2	-40.60	OR56A5	-27.90	NAG18	-28.79	CD82	-38.37
LOX	-40.65	GAGE13	-28.06	CCNA1	-28.81	LIFR	-38.72
SERPINI1	-41.03	PPP2R2B	-28.08	CYP8B1	-28.88	PLSCR4	-39.49
SNRPN	-41.70	EGFL6	-28.10	GSTA1	-29.06	C4orf27	-39.79
SLC39A10	-41.96	SNORD37	-28.59	BIN2	-29.08	ATL3	-40.27
CPM	-41.96	GPX5	-28.68	NCRNA00116	-29.08	NPNT	-40.28
MVD	-42.06	FKBP1A	-28.94	GABRA4	-29.24	COX7A2	-40.57
LSS	-42.11	RAB7A	-29.18	OSGIN1	-29.60	RPS29	-41.80
CP110	-42.21	GPR111	-29.25	OR1L8	-29.81	SESN3	-41.83
SOD1	-42.87	GPX2	-29.68	RAB7A	-29.89	AOX1	-41.96
PCSK9	-43.19	TDGF3	-30.11	PSG4	-30.75	RPL39L	-42.61
DIO2	-43.39	C14orf65	-30.44	EGFL6	-31.22	SNRPG	-43.14
YWHAH	-44.05	CAPNS2	-30.79	CYP2F1	-31.90	UBL5	-43.51
MAPK3	-44.63	RNU5F	-30.94	OR10H1	-32.15	EIF4B	-44.12
IFI44L	-44.92	OR3A3	-31.19	PATE1	-32.79	COX8A	-44.46
GALNT7	-45.54	LY86-AS	-31.61	IGSF9B	-33.56	NDUFB6	-44.48
NPNT	-45.76	TNS3	-32.02	GAGE13	-33.64	C6orf173	-45.07
CYBRD1	-45.82	RNU5B-1	-33.01	RNU5F	-34.80	RPS27A	-45.52
C1orf128	-46.67	LGALS9	-34.48	C14orf19	-36.20	FAM99A	-45.97
PRUNE2	-52.94	ZNF578	-34.60	LOXL2	-36.39	IL18	-46.67
SESN3	-55.15	ZNF208	-36.10	CXorf27	-36.41	CPA4	-47.96
GPR64	-55.73	SNRPN	-36.16	RBMY1E	-39.21	FBXO32	-49.35
DNER	-57.94	SPRYD5	-36.74	KRTAP10-5	-39.58	NDUFA1	-49.60
MFAP5	-59.25	RFT1	-39.88	LGALS9	-40.19	DDT	-50.98
ACSS2	-62.57	GABRE	-40.34	MST1	-50.14	GAGE13	-58.94
FGFBP1	-63.15	TSG101	-73.73	VPS4A	-72.05	PDCD6IP	-80.22

The phosphoinositide-binding protein SNX16 controls the formation of tubulo-cisternal membrane domains in late endosomes

Ben Brankatschk (1), Véronique Pons(1,2), Rob Parton (3) and Jean Gruenberg (1,4)

1) Department of Biochemistry, University of Geneva, 30 quai E. Ansermet, 1211 Geneva-4, Switzerland
2) VP new address is INSERM, U563, Toulouse, F-31300 France, and Université Toulouse III Paul-Sabatier, Centre de Physiopathologie de Toulouse Purpan, Toulouse, F-31300 France.
3) Institute for Molecular Bioscience and Center for Microscopy and Microanalysis, University of Queensland, Brisbane 4072, Australia.
4) To whom correspondence should be addressed; tel: +41-22-379-6464; fax: +41-22-379-6470; email: jean.gruenberg@unige.ch

ABSTRACT

In this paper, we report that the PX domain-containing protein SNX16, a member of the sorting nexin family, is associated to late endosome membranes and that membrane association depends on an intact PX domain. We found that SNX16 is selectively enriched on tubulo-cisternal elements of the late endosomal membrane system, whose highly dynamic properties and formation depend on intact microtubules. By contrast, SNX16 was not found on vacuolar elements that typically contain LBPA, presumably corresponding to multivesicular endosomes. We conclude that SNX16, together with its partner phosphoinositide, define a highly dynamic subset of late endosomal membranes, supporting the notion that late endosomes are organized in distinct morphological and functional regions. Our data also suggest that SNX16 plays a direct role in the regulation of late endosome membrane dynamics, and thereby transport through this compartment.

INTRODUCTION

It is now generally accepted that some long-lived lipids are not stochastically distributed in cellular membranes but are differentially distributed in subcellular compartments. The cholesterol content of the endoplasmic reticulum (ER) is low – sensing cholesterol levels in the ER regulates the expression of cholesterol-dependent gene expression – and increases from the Golgi apparatus to the plasma membrane (Brown and Goldstein, 2009). Together with glycosphingolipids, cholesterol forms raft-like microdomains, which are believed to play a role in numerous cellular processes in the plasma membrane and other cellular membranes, including protein and lipid sorting, signaling, infection and immunity (Lingwood and Simons, 2010). Other lipids also show restricted distributions, in particular the unconventional phospholipid lysobisphosphatidic acid (LBPA), also called bis-monoacylglycerophosphate (BMP), which is abundant in late endosomes and not detected elsewhere in the cell (Kobayashi et al., 1999). In addition, phosphoinositides, signaling lipids that are typically very short-lived, are distributed in different cellular territories, through the concerted action of lipid kinases and phosphatases (Di Paolo and De Camilli, 2006; Lindmo and Stenmark, 2006; Nicot and Laporte, 2008). Typically, PtdIns(4,5)P_2 and PtdIns(3,4,5)P_3 are present in the plasma membrane, PtdIns(4)P in the Golgi, while PtdIns(3)P and presumably PtdIns(3,5)P_2 are both present in endosomes.

The human genome encodes more than 60 proteins that contain either one of two conserved motives, FYVE or PX, binding phosphoinositides that are phosphorylated at the 3 position of the inositol ring (Hurley, 2006). To the best of our knowledge, all PtdIns(3)P-

binding proteins that have been characterized are present on early endosomal membranes, whether they contained a FYVE or a PX domain, leading to the notion that PtdIns(3)P is restricted to early endosomes. Consistently, endosomal PtdIns(3)P is mostly synthesized by the PtdIns 3-kinase VPS34, which is itself an effector of the small GTPase RAB5 that controls early endosome dynamics (Shin et al., 2005). Conversely, FYVE- or PX-containing proteins are expected to be restricted to early endosomes, where some may exhibit differential distributions in specialized domains or vesicle subpopulation depending on their protein partners (Miaczynska et al., 2004; Schnatwinkel et al., 2004; Zoncu et al., 2009).

In this paper, we studied the PX domain-containing protein SNX16, which is a member of the so-called sorting nexin family (Teasdale et al., 2001). We were intrigued by the observations that SNX16 is not present on early endosomes, yet membrane association depends on an intact PX domain, and is reversed by the PtdIns 3-kinase inhibitor wortmannin. We found that SNX16 is selectively enriched on tubulo-cisternal membranes of the late endosomal system, which exhibit highly dynamic properties, depending on an intact microtubule network. However, upon ectopic expression at low levels, SNX16 was hardly found on LBPA-containing vacuolar elements, presumably corresponding to multivesicular endosomes. We conclude that SNX16, together with its partner phosphoinositide, define a highly dynamic subset of late endosome membranes, underscoring that late endosomes are organized in highly distinct morphological and functional regions. Our data also indicate that SNX16 is involved in the regulation of late endosome membrane dynamics, and that this process in turn, may control late endosomal cholesterol homeostasis and tetraspanin transport through the compartment.

RESULTS

SNX16 is not present on early endosomes

To analyze the subcellular distribution of SNX16, cells were transfected with constructs encoding for fluorescent SNX16 fusion proteins and analyzed by light microscopy. The ectopically expressed protein showed a punctate pattern reminiscent of endosomes (Fig 1A and 1B, left) and a cytosolic pattern after treatment with the PtdIns 3-kinase inhibitor wortmannin (Fig 1B, right), consistent with the notion that SNX16 becomes membrane-associated via interactions with PtdIns(3)P. Indeed, mutation of SNX16 Arg144 to Ala – a conserved residue of the PX domain necessary for PtdIns(3)P binding in $p40^{phox}$ (Bravo et al., 2001) – abolished membrane association (Fig 1B, middle). These observations suggested that SNX16 might be present on early endosomes that contain the bulk of PtdIns(3)P.

However, to our surprise, mRFP-SNX16 did not colocalize to any significant extent with GFP-RAB5 (Fig 1A). This small GTPase, which controls early endosome dynamics (Zerial and McBride, 2001), is the best-accepted marker of early endosomal membranes and distributes to the different early endosome sub-populations that have been studied, including APPL-containing endosomes (Miaczynska et al., 2004). We also failed to observe significant colocalization of SNX16 fused to Venus, an improved YFP variant that allows detection of very low protein amounts (Nagai et al., 2002), with any other early endosome marker tested, including TFR (Fig 1C) and EEA1 (Fig 1D). GFP-SNX16 has been previously reported to distribute to early endosomes (Choi et al., 2004; Hanson and Hong, 2003). Although the reason for this discrepancy is not clear, early endosomal localization may be due to overexpression (see also below).

SNX16 distributes to late endosomal membrane domains

We investigated whether SNX16 was present on other subcellular organelles, but did not observe colocalization with markers of biosynthetic membranes (not show). By contrast, Venus-SNX16 showed significant colocalization with LAMP1 (Fig 2A), an abundant glycoprotein of late endosomes and lysosomes. Quantification of colocalization after 3D image reconstruction of confocal sections with Imaris software revealed that approximately half of the Venus-SNX16 structures also contained LAMP1, while LAMP1 showed a broader distribution with ≈20% present in SNX16-containing membranes (Fig 3). Surprisingly, we observed little colocalization of Venus-SNX16 with the late endosome phospholipid LBPA (Fig 2B, quantification in Fig 3A), while LBPA itself showed extensive colocalization with LAMP1 (Fig 3A), as expected (Kobayashi et al., 1998). LBPA is abundant in the multivesicular regions of late endosomes and is not detected elsewhere in the cell (Kobayashi et al., 1998), raising the possibility that multivesicular late endosomes do not contain significant amounts of SNX16. Consistent with this notion, the tetraspanin CD63, which is also abundant in multivesicular late endosomes containing LBPA (Escola et al., 1998; Kobayashi et al., 2002), showed only modest colocalization with SNX16 (Fig 2C, quantification in Fig 3B), much like with LBPA. CD63, however, showed extensive colocalization with LAMP1 (Fig 3B). We conclude that, while LBPA, CD63 and SNX16 are all present in LAMP1-containing late endosomes, SNX16 distributes to membrane regions or elements that are largely distinct from those containing LBPA and CD63.

The notion that SNX16 and LBPA distribute to different membrane domains was strengthened considerably by observations that membranes containing either marker exhibited different physical properties in sucrose gradients. After subcellular fractionation, the small GTPase RAB5 and LBPA were enriched, as expected (Aniento et al., 1993), in early

and late endosome fractions, respectively (Fig 3C). Strikingly, SNX16 co-purified with early endosomes containing RAB5 and not with LBPA-containing late endosomes. Presumably, LBPA-containing endosomes exhibit higher buoyancy on gradients (Fig 3) because of the higher lipid to protein ratio of this multivesicular compartment (Kobayashi et al., 2002). While LAMP1 did not co-purify with RAB5, a very significant fraction of the total LAMP1 amounts (≈ 50%) was found in early endosomal fractions together with SNX16 (Fig 3D), presumably corresponding to the membranes that contained both LAMP1 and SNX16 but not LBPA (total amounts of LBPA are much lower in early endosomal fractions than total LAMP1; Fig 3D).

Late endosome tubulo-cisternal regions

Live cell microscopy, shown in Fig. 2C and Fig. 6, already suggested that a part of SNX16 is present on late endosomal tubules. To gain more insight into the structures that contain SNX16, cells expressing the Venus-tagged protein were analyzed after fixation in glutaraldehyde as in sample preparation for electron microscopy to better preserve the ultrastructure. Indeed, the ultrastructure of organelles, in particular membrane tubules that are notoriously fragile, is not well preserved after fixation in paraformaldehyde. After fixation in glutaraldehyde, SNX16 and LAMP1 overlapped significantly although some LAMP1-positive structures were devoid of SNX16 (Fig 4B), much like in paraformaldehyde-fixed cells (Fig 4A). Strikingly, however, SNX16 was also found within long tubulo-cisternal elements that often extended over 1-2 µm (Fig 4B and C). Moreover, it appeared that, while SNX16-positive tubules frequently contained LAMP1 (Fig 4B, white arrows), some were devoid of LAMP1 (Fig 4B, green arrows, and inset), suggesting that SNX16-containing tubules can be heterogeneous in composition. Confocal microscopy analysis and 3D reconstruction with Imaris software revealed that tubules decorated by Venus-SNX16 often contain LAMP1 (Fig 4C, right) and sometimes CD63 (not shown) at discrete sites (arrows in Fig 4C), and not all along the tubules. Since recycling endosomes also exhibit a tubular morphology (Gruenberg and Maxfield, 1995; Tooze and Hollinshead, 1991), we investigated whether the SNX16-positive tubules that were devoid of LAMP1 originated from recycling endosomes. Even in the absence of glutaraldehyde fixation, brefeldin A causes a dramatic tubularization of early/recycling endosomes containing the transferrin receptor (Tooze and Hollinshead, 1992) (TFR in Fig 4D). Yet, the drug did not have any effect on SNX16 distribution, demonstrating that SNX16 tubules without detectable levels of LAMP1 are not part of the early/recycling endosome system. The effect of brefeldin A was confirmed by labeling for p23, which re-distributes from its characteristic *cis*-Golgi pattern (Fig 4D, inset) to discrete punctate structures (Fig 4D), reminiscent of the ER-Golgi intermediate compartment (Rojo et al., 1997).

These observations indicate that SNX16 tubules themselves may be somewhat heterogeneous in composition. To analyze the distribution of SNX16 in more detail, cells were co-transfected with LAMP1-HRP (Hopkins et al., 2000) and Venus-SNX16. After fixation, LAMP1-HRP is easily revealed cytochemically using DAB as a substrate (Hopkins et al., 2000; Stoorvogel et al., 1996) (Fig 5A). As expected from our immunofluorescence data (Fig 2-4), we found that a significant portion of SNX16 colocalized with LAMP1 (Fig 5). In addition, this analysis also revealed that SNX16-positive structures that did not contain detectable levels of LAMP1 were frequently observed in close apposition to – and often in continuity with – LAMP1-containaing structures (high magnification in Fig 5D). Moreover, SNX16 and HRP-LAMP1 were often found together on tubular profiles (Fig 5E and F).

Dynamics of late endosome tubules containing SNX16

The nature of SNX16-contanining tubular elements became apparent when Venus-SNX16 was analyzed by time-lapse video microscopy (Fig 6A and supplementary movie Venus-SNX16.avi). The protein was primarily found in distinct elements with a characteristic tubulo-cisternal morphology similar to those observed in glutaraldehyde-fixed cells (Fig 4), which distributed across the entire cell cytoplasm (arrows in Fig 6A) – a distribution that differs from the characteristic centripetal motion of endosomal vesicles containing internalized tracers. These elements aligned on microtubule tracks (not shown) and exhibited high bidirectional motility (Fig 6 and supplementary movie Venus-SNX16.avi) that required the presence of polymerized microtubules (Fig 6C). Indeed, in the absence of a polymerized microtubule network, SNX16-positive structures only exhibited Brownian-like motion. Moreover, tubules disappeared after nocodazole treatment and SNX16 collapsed onto vesicles, which were immobile (Fig 6C) and apparent even after glutaraldehyde fixation (Fig 7A). In addition, microtubule depolymerization increased SNX16 colocalization with LAMP1 by light microscopy (Fig 7A), as well as SNX16 co-purification with late endosomes after subcellular fractionation, without affecting early and late endosomal markers (Fig 7B). Presumably, tubule formation no longer occurred after drug treatment, leading to SNX16 accumulation on vesicular late endosomes.

Altogether, these observations further support the notion that SNX16 distributes to specialized regions of late endosomal membranes and indicate that microtubules not only support the motility of SNX16-containing tubules but also their biogenesis, as expected (Lebrand et al., 2002). We conclude that late endosomes contain elements with different composition, dynamic characteristics and physical properties on gradients, and that SNX16 colocalizes with LAMP1 in highly dynamic tubulo-cisternal regions of the late endosome, which typically lack the markers of multivesicular late endosomes LBPA and CD63.

SNX16 overexpression interferes with the dynamics of late endosomal tubules and trafficking through the compartment.

Bio-computing analysis does not predict the presence of a BAR domain that senses or induces membrane curvature in SNX16, in contrast to other members of the SNX family (Habermann, 2004). But SNX16 contains a predicted coiled-coil domain reminiscent of a BAR domain. A hallmark of BAR-containing proteins is their capacity to induce membrane tubulation upon overexpression (Frost et al., 2008; Peter et al., 2004). However, SNX16 overexpression did not increase membrane tubulation (Fig 8), in marked contrast to SNX1 and other BAR-proteins, but caused the opposite effects. SNX16-positive structures appeared clustered upon overexpression in the perinuclear region and SNX16 was no longer observed in tubules across the cell cytosplasm (Fig 8). Moreover, while SNX16 expressed at low amounts did not colocalize with LBPA to any significant extent (Fig 2 and 3), overexpression redistributed a significant portion of SNX16 to LBPA-positive perinuclear endosomes (Fig 8A), and increased SNX16 co-purification with late endosomes after fractionation (Fig 8B). Strikingly, overexpressed GFP-SNX16 is found associated with multivesicular profiles in electron micrographs (Fig 8C). In addition, late endosome motility was reduced by SNX16 overexpression (not shown). We thus conclude that, much like after microtubule depolymerization, SNX16 overexpression inhibits the biogenesis of late endosomal tubules, leading to an accumulation of SNX16 on the vesicular portions of late endosomes, which contain LBPA and are abundant in the perinuclear region.

We and others have shown that late endosomes play a crucial role in the transport of LDL-derived cholesterol (Ikonen and Holtta-Vuori, 2004; Storch and Xu, 2009; van der Goot and Gruenberg, 2006) and, conversely, that cholesterol accumulation in late endosomes inhibits late endosomal motility and membrane dynamics (Ko et al., 2001; Lebrand et al., 2002; Zhang et al., 2001). Strikingly, we observed that SNX16 overexpression caused the accumulation of cholesterol in late endosome membranes containing SNX16 (Fig 8D) and other late endosomal markers (not shown), in a process reminiscent of the cholesterol storage disorder Niemann-Pick type C (Kobayashi et al., 1999). We were not able to investigate in a conclusive manner the effects of SNX16 depletion with the siRNAs that we have tested. However, it seems fair to conclude that SNX16, which distributes to a highly dynamic subset of tubulo-cisternal late endosome membranes, plays a role in late endosomal dynamics and thereby regulates the trafficking of LDL-derived cholesterol in the endosomal system. Moreover, SNX16 overexpression leads to a re-distribution of the cell surface tetraspanin CD81 (Levy et al., 1998; Vaickus and Levy, 1985), which has been shown to traffic through multivesicular endosomes (Escola et al., 1998), from the plasma membrane to the perinuclear compartment containing cholesterol and LBPA (Fig 8E). Thus, trafficking of

several cargo molecules through late endosomes is affected by SNX16 overexpression, as has been shown for the inhibition of endosome-to-cytosol transport of viral nucleocapsids by high amounts of SNX16 (Le Blanc et al., 2005).

DISCUSSION

In this paper, we studied the PX domain-containing protein SNX16, which is a member of the so-called sorting nexin family. We were intrigued by the observations that SNX16 is not present on early endosomes, yet membrane association depends on an intact PX domain, and is reversed by the PtdIns 3-kinase inhibitor wortmannin. We found that SNX16 labels tubulo-cisternal elements that are part of the late endosomal membrane system. By contrast, SNX16 was not found on multivesicular endosomes that typically contain LBPA. The highly dynamic properties of SNX16-containing membranes are microtubule-dependent. SNX16 overexpression inhibits tubule formation and dynamics, and leads to a re-distribution of several markers and cargo molecules to the perinuclear, LBPA-containing compartment. We conclude that SNX16 together with its partner phosphoinositide define a highly dynamic sub-set of late membranes, and that interference with the organization of late endosomes in distinct morphological and functional regions affects trafficking for example of cholesterol and CD81 through the compartment.

SNX16 localization is surprising, since it contains a PX domain that binds 3-phosphorylated inositides necessary for SNX16 membrane association. Yet, SNX16 distributes to late endosomal membranes. In addition to PtdIns(3,4,5)P_3 at the plasma membrane, mammalian cells contain two other 3-phosphorylated inositides in the endocytic pathway. PtdIns(3)P has only been found on early endosome membranes, where the bulk of PtdIns(3)P is synthesized (Shin et al., 2005), and all proteins that bind PtdIns(3)P that have been characterized to date are present on early endosomal membranes. Mammalian cells also contain PtdIns(3,5)P_2, a phosphoinositide that accumulates under hypertonic stress (Shisheva, 2008) and may be involved in autophagy (Ferguson et al., 2010). The steady state amounts of this lipid in the absence of stress are very low, and its precise localization is debated. PtdIns(3,5)P_2 is synthesized from PtdIns(3)P via the PtdIns(3)P 5-kinase PIKFYVE/Fab1, which is itself a PtdIns(3)P-binding protein containing a FYVE domain (Shisheva, 2008) perhaps present on early endosomes (Cabezas et al., 2006; Rutherford et al., 2006). However, knockdown of PIKFYVE had no effect on SNX16 distribution (not shown), indicating that SNX16 binds a specific late endosomal pool of PtdIns(3)P via its PX domain.

One possible explanation of our findings is that SNX16 becomes associated to early endosomes via PtdIns(3)P and then remains endosome-associated during transport to late endosomes, where SNX16 accumulates via protein-protein interactions. This, however, seems rather unlikely, since SNX16 was never observed on early endosomes, including under conditions that interfere with early-to-late endosome transport, e.g. after microtubule depolymerization. An alternative explanation is that SNX16 interacts on late endosomes with unknown protein partners. Indeed, deletion of the coiled-coil domain leads to loss of late endosomal localization and increased association with early endosomes (Hanson and Hong, 2003) (and our observations; not shown), indicating coincidence detection of PtdIns(3)P and another factor on specific late endosomal membranes. The PtdIns(3)P may be synthesized on late endosomes by PtdIns 3-kinase effectors of the late endosome small GTPase RAB7 (Stein et al., 2003). One may also envision that late endosome PtdIns(3)P is derived from a pool originally synthesized on early endosomes and incorporated into intralumenal vesicles (Gillooly et al., 2000), which may eventually be released on the late endosome limiting membrane via back-fusion of intralumenal vesicles (van der Goot and Gruenberg, 2006). In any case, whether PtdIns(3)P is synthesized on early or late endosomes or whether it is released by back-fusion, it is attractive to propose that PtdIns(3)P-containing sites give rise to nascent tubules upon SNX16 recruitment and further stabilization by protein-protein interactions. Overexpression of SNX16 may interfere with the process by titrating out components that are necessary for tubule biogenesis, including perhaps PtdIns(3)P itself. In turn, this situation may inhibit the transport of cholesterol and of the tetraspanin CD81 by reducing the dynamic properties of endosomal membranes, leading to CD81 re-distribution from the cell surface to LBPA-containing multivesicular late endosomes and NPC-like cholesterol accumulation. This agrees well with our previous observations that, during vesicular stomatitis virus infection, excess SNX16 inhibits the delivery of viral RNA to the cytoplasm, presumably by preventing the back-fusion of intra-endosomal vesicles containing the viral RNA with the limiting membrane (Le Blanc et al., 2005). Similarly, viral infection is inhibited by the NPC-like accumulation of cholesterol in late endosomes (Sobo et al., 2007).

This scenario is attractive, since it provides a simple framework for the regulation of late endosome membrane dynamics. Indeed, late endosomal membranes at steady state undergo concomitant deformation in two opposite directions, towards the endosome lumen during intralumenal vesicle biogenesis and towards the cytoplasm during the formation of SNX16-containing tubules. Both processes must be controlled and integrated to ensure that membrane homeostasis is maintained. Given the key role of phosphoinositides in endosome dynamics, it is attractive to believe that such homeostatic process is under the control of PtdIns(3)P signaling via specific effectors, including SNX16 in late endosomes.

MATERIALS AND METHODS

Cells, antibodies, reagents and constructs. HeLa and BHK cell maintenance was described (Gruenberg et al., 1989), as was the mouse monoclonal anti-LBPA antibody (Kobayashi et al., 1998). We are very grateful to Reinhard Jahn (Göttingen, Germany) for the mouse monoclonal antibody against RAB5, and to Wanjin Hong (Singapore, Singapore) for rabbit polyclonal antibodies against SNX16. Mouse monoclonal anti-CD63 (1B5) was a kind gift of Mark Marsh (London, UK), and mouse monoclonal anti-CD81 was kindly provided by Jean-Michel Escola (Geneva, Switzerland). Rabbit polyclonal anti-p23 was described previously (Rojo et al., 1997). We also used mouse monoclonal antibodies against transferrin receptor (TFR) (Zymed Laboratories, South San Francisco, CA); rabbit polyclonal anti-EEA1 (Enzo Life Sciences, Plymouth Meeting, PA); mouse monoclonal anti-EEA1 (BD Biosciences, Franklin Lakes, NJ); mouse monoclonal anti-human LAMP1 (CD107a; BD Biosciences) and rabbit polyclonal anti-human LAMP1 (Thermo Fisher Scientific, Waltham, MA). HRP-labeled secondary antibodies were from Amersham (UK) or Sigma-Aldrich (St Louis, MO) and fluorescently labeled secondary antibodies from Jackson Immunoresearch Laboratories (West Grove, PA). Wortmannin, nocodazole, brefeldin A, paraformaldehyde, glutaraldehyde, filipin, diaminobenzidine (DAB) and *o*-dianisidine were from Sigma-Aldrich (St Louis, MO).

We obtained pGFP-RAB5 from Marino Zerial (Dresden, Germany), HRP-LAMP1 from Matt Russell (Boulder, Colorado), and pDMYC-SNX16 from Wanjin Hong (Singapore, Singapore). SNX16 was introduced into pEGFP-C2 or fused with monomeric RFP or Venus, kindly provided by Atsushi Miyawaki (Wako City, Saitama, Japan). CD63-expressing constructs were a kind gift from Cynthia Leifer (Ithaca, NY).

Microscopy. Immunofluorescence microscopy has been described (Gu et al., 1997). When indicated, cells analyzed by immunofluorescence microscopy were fixed with glutaraldehyde (Parton et al., 1992). Pictures were captured using a Zeiss Axiophot microscope equipped with a Zeiss 63x Plan-NEOFLUAR objective, a Leica AS MDW widefield microscope with a Leica 63x Plan-APOCHROMAT oil immersion objective, or a Leica TCS SP2 AOBS confocal microscope equipped with a Leica 100x Plan-APOCHROMAT oil immersion objective. For quantification, 3D image reconstruction and analysis was carried out with Imaris software. Time-lapse video microscopy was as described (Lebrand et al., 2002). The distribution of HRP-LAMP1 was revealed cytochemically with DAB as a substrate and visualized by phase contrast light microscopy, according to (Hopkins et al., 2000; Stoorvogel et al., 1996). Sample preparation for electron microscopy was as described previously (Griffiths et al., 1984; Pons et al., 2008).

Other methods. Cells were transfected with FuGene (Roche Diagnostics, Basel, Switzerland) according to the manufacturer's instructions. Microtubules were depolymerized with 10 µM nocodazole for 2 h (Aniento et al., 1993; Gruenberg et al., 1989). Early and late endosome fractionation by flotation in a sucrose step gradient was described (Aniento et al., 1993). Cholesterol was revealed using filipin as described (Kobayashi et al., 1999), treatment with brefeldin A was described in (Rojo et al., 1997), and LBPA measurement by ELISA was reported in (Kobayashi et al., 1998).

ACKNOWLEDGEMENTS

We are grateful to Brigitte Bernadets and Marie-Claire Velluz for technical assistance. Support was from the Swiss National Science Foundation, PRISM from the EU Sixth Framework Programme, LipidX from the Swiss SystemsX initiative, evaluated by the Swiss National Science Foundation and NCCR in Chemical Biology (to J.G.), and the Human Frontier Science Foundation (R.G.P.).

LIST OF REFERENCES

Aniento, F., Emans, N., Griffiths, G., and Gruenberg, J. (1993). Cytoplasmic dynein-dependent vesicular transport from early to late endosomes. J Cell Biol *123*, 1373-1387.

Bravo, J., Karathanassis, D., Pacold, C.M., Pacold, M.E., Ellson, C.D., Anderson, K.E., Butler, P.J., Lavenir, I., Perisic, O., Hawkins, P.T.*, et al.* (2001). The crystal structure of the PX domain from p40(phox) bound to phosphatidylinositol 3-phosphate. Mol Cell *8*, 829-839.

Brown, M.S., and Goldstein, J.L. (2009). Cholesterol feedback: from Schoenheimer's bottle to Scap's MELADL. J Lipid Res *50 Suppl*, S15-27.

Cabezas, A., Pattni, K., and Stenmark, H. (2006). Cloning and subcellular localization of a human phosphatidylinositol 3-phosphate 5-kinase, PIKfyve/Fab1. Gene *371*, 34-41.

Choi, J.H., Hong, W.P., Kim, M.J., Kim, J.H., Ryu, S.H., and Suh, P.G. (2004). Sorting nexin 16 regulates EGF receptor trafficking by phosphatidylinositol-3-phosphate interaction with the Phox domain. J Cell Sci *117*, 4209-4218.

Di Paolo, G., and De Camilli, P. (2006). Phosphoinositides in cell regulation and membrane dynamics. Nature *443*, 651-657.

Escola, J.M., Kleijmeer, M.J., Stoorvogel, W., Griffith, J.M., Yoshie, O., and Geuze, H.J. (1998). Selective enrichment of tetraspan proteins on the internal vesicles of multivesicular endosomes and on exosomes secreted by human B-lymphocytes. J Biol Chem *273*, 20121-20127.

Ferguson, C.J., Lenk, G.M., and Meisler, M.H. (2010). PtdIns(3,5)P2 and autophagy in mouse models of neurodegeneration. Autophagy *6*, 170-171.

Frost, A., Perera, R., Roux, A., Spasov, K., Destaing, O., Egelman, E.H., De Camilli, P., and Unger, V.M. (2008). Structural basis of membrane invagination by F-BAR domains. Cell *132*, 807-817.

Gillooly, D.J., Morrow, I.C., Lindsay, M., Gould, R., Bryant, N.J., Gaullier, J.M., Parton, R.G., and Stenmark, H. (2000). Localization of phosphatidylinositol 3-phosphate in yeast and mammalian cells. Embo J *19*, 4577-4588.

Griffiths, G., McDowall, A., Back, R., and Dubochet, J. (1984). On the preparation of cryosections for immunocytochemistry. J Ultrastruct Res *89*, 65-78.

Gruenberg, J., Griffiths, G., and Howell, K.E. (1989). Characterization of the early endosome and putative endocytic carrier vesicles in vivo and with an assay of vesicle fusion in vitro. J Cell Biol *108*, 1301-1316.

Gruenberg, J., and Maxfield, F.R. (1995). Membrane transport in the endocytic pathway. Curr Opin Cell Biol *7*, 552-563.

Gu, F., Aniento, F., Parton, R.G., and Gruenberg, J. (1997). Functional dissection of COP-I subunits in the biogenesis of multivesicular endosomes. J Cell Biol *139*, 1183-1195.

Habermann, B. (2004). The BAR-domain family of proteins: a case of bending and binding? EMBO Rep *5*, 250-255.

Hanson, B.J., and Hong, W. (2003). Evidence for a role of SNX16 in regulating traffic between the early and later endosomal compartments. J Biol Chem *278*, 34617-34630.

Hopkins, C., Gibson, A., Stinchcombe, J., and Futter, C. (2000). Chimeric molecules employing horseradish peroxidase as reporter enzyme for protein localization in the electron microscope. Methods Enzymol *327*, 35-45.

Hurley, J.H. (2006). Membrane binding domains. Biochim Biophys Acta *1761*, 805-811.

Ikonen, E., and Holtta-Vuori, M. (2004). Cellular pathology of Niemann-Pick type C disease. Semin Cell Dev Biol *15*, 445-454.

Ko, D.C., Gordon, M.D., Jin, J.Y., and Scott, M.P. (2001). Dynamic movements of organelles containing niemann-pick c1 protein: npc1 involvement in late endocytic events. Mol Biol Cell *12*, 601-614.

Kobayashi, T., Beuchat, M.H., Chevallier, J., Makino, A., Mayran, N., Escola, J.M., Lebrand, C., Cosson, P., and Gruenberg, J. (2002). Separation and characterization of late endosomal membrane domains. J Biol Chem *277*, 32157-32164.

Kobayashi, T., Beuchat, M.H., Lindsay, M., Frias, S., Palmiter, R.D., Sakuraba, H., Parton, R.G., and Gruenberg, J. (1999). Late endosomal membranes rich in lysobisphosphatidic acid regulate cholesterol transport. Nat Cell Biol *1*, 113-118.

Kobayashi, T., Stang, E., Fang, K.S., de Moerloose, P., Parton, R.G., and Gruenberg, J. (1998). A lipid associated with the antiphospholipid syndrome regulates endosome structure and function. Nature *392*, 193-197.

Le Blanc, I., Luyet, P.P., Pons, V., Ferguson, C., Emans, N., Petiot, A., Mayran, N., Demaurex, N., Faure, J., Sadoul, R.*, et al.* (2005). Endosome-to-cytosol transport of viral nucleocapsids. Nat Cell Biol *7*, 653-664.

Lebrand, C., Corti, M., Goodson, H., Cosson, P., Cavalli, V., Mayran, N., Faure, J., and Gruenberg, J. (2002). Late endosome motility depends on lipids via the small GTPase Rab7. Embo J *21*, 1289-1300.

Levy, S., Todd, S.C., and Maecker, H.T. (1998). CD81 (TAPA-1): a molecule involved in signal transduction and cell adhesion in the immune system. Annu Rev Immunol *16*, 89-109.

Lindmo, K., and Stenmark, H. (2006). Regulation of membrane traffic by phosphoinositide 3-kinases. J Cell Sci *119*, 605-614.

Lingwood, D., and Simons, K. (2010). Lipid rafts as a membrane-organizing principle. Science *327*, 46-50.

Miaczynska, M., Christoforidis, S., Giner, A., Shevchenko, A., Uttenweiler-Joseph, S., Habermann, B., Wilm, M., Parton, R.G., and Zerial, M. (2004). APPL proteins link Rab5 to nuclear signal transduction via an endosomal compartment. Cell *116*, 445-456.

Nagai, T., Ibata, K., Park, E.S., Kubota, M., Mikoshiba, K., and Miyawaki, A. (2002). A variant of yellow fluorescent protein with fast and efficient maturation for cell-biological applications. Nat Biotechnol *20*, 87-90.

Nicot, A.S., and Laporte, J. (2008). Endosomal phosphoinositides and human diseases. Traffic *9*, 1240-1249.

Parton, R.G., Schrotz, P., Bucci, C., and Gruenberg, J. (1992). Plasticity of early endosomes. J Cell Sci *103 (Pt 2)*, 335-348.

Peter, B.J., Kent, H.M., Mills, I.G., Vallis, Y., Butler, P.J., Evans, P.R., and McMahon, H.T. (2004). BAR domains as sensors of membrane curvature: the amphiphysin BAR structure. Science *303*, 495-499.

Pons, V., Luyet, P.P., Morel, E., Abrami, L., van der Goot, F.G., Parton, R.G., and Gruenberg, J. (2008). Hrs and SNX3 functions in sorting and membrane invagination within multivesicular bodies. PLoS Biol *6*, e214.

Rojo, M., Pepperkok, R., Emery, G., Kellner, R., Stang, E., Parton, R.G., and Gruenberg, J. (1997). Involvement of the transmembrane protein p23 in biosynthetic protein transport. J Cell Biol *139*, 1119-1135.

Rutherford, A.C., Traer, C., Wassmer, T., Pattni, K., Bujny, M.V., Carlton, J.G., Stenmark, H., and Cullen, P.J. (2006). The mammalian phosphatidylinositol 3-phosphate 5-kinase (PIKfyve) regulates endosome-to-TGN retrograde transport. J Cell Sci *119*, 3944-3957.

Schnatwinkel, C., Christoforidis, S., Lindsay, M.R., Uttenweiler-Joseph, S., Wilm, M., Parton, R.G., and Zerial, M. (2004). The Rab5 effector Rabankyrin-5 regulates and coordinates different endocytic mechanisms. PLoS Biol *2*, E261.

Shin, H.W., Hayashi, M., Christoforidis, S., Lacas-Gervais, S., Hoepfner, S., Wenk, M.R., Modregger, J., Uttenweiler-Joseph, S., Wilm, M., Nystuen, A.*, et al.* (2005). An enzymatic cascade of Rab5 effectors regulates phosphoinositide turnover in the endocytic pathway. J Cell Biol *170*, 607-618.

Shisheva, A. (2008). PIKfyve: Partners, significance, debates and paradoxes. Cell Biol Int *32*, 591-604.

Sobo, K., Le Blanc, I., Luyet, P.P., Fivaz, M., Ferguson, C., Parton, R.G., Gruenberg, J., and van der Goot, F.G. (2007). Late endosomal cholesterol accumulation leads to impaired intra-endosomal trafficking. PLoS One *2*, e851.

Stein, M.P., Feng, Y., Cooper, K.L., Welford, A.M., and Wandinger-Ness, A. (2003). Human VPS34 and p150 are Rab7 interacting partners. Traffic *4*, 754-771.

Stoorvogel, W., Oorschot, V., and Geuze, H.J. (1996). A novel class of clathrin-coated vesicles budding from endosomes. J Cell Biol *132*, 21-33.

Storch, J., and Xu, Z. (2009). Niemann-Pick C2 (NPC2) and intracellular cholesterol trafficking. Biochim Biophys Acta.

Teasdale, R.D., Loci, D., Houghton, F., Karlsson, L., and Gleeson, P.A. (2001). A large family of endosome-localized proteins related to sorting nexin 1. Biochem J *358*, 7-16.

Tooze, J., and Hollinshead, M. (1991). Tubular early endosomal networks in AtT20 and other cells. J Cell Biol *115*, 635-653.

Tooze, J., and Hollinshead, M. (1992). In AtT20 and HeLa cells brefeldin A induces the fusion of tubular endosomes and changes their distribution and some of their endocytic properties. J Cell Biol *118*, 813-830.

Vaickus, L., and Levy, R. (1985). Antiproliferative monoclonal antibodies: detection and initial characterization. J Immunol *135*, 1987-1997.

van der Goot, F.G., and Gruenberg, J. (2006). Intra-endosomal membrane traffic. Trends Cell Biol *16*, 514-521.

Zerial, M., and McBride, H. (2001). Rab proteins as membrane organizers. Nature Reviews Molecular Cell Biology *2*, 107-117.

Zhang, M., Dwyer, N.K., Love, D.C., Cooney, A., Comly, M., Neufeld, E., Pentchev, P.G., Blanchette-Mackie, E.J., and Hanover, J.A. (2001). Cessation of rapid late endosomal tubulovesicular trafficking in Niemann-Pick type C1 disease. Proc Natl Acad Sci U S A *98*, 4466-4471.

Zoncu, R., Perera, R.M., Balkin, D.M., Pirruccello, M., Toomre, D., and De Camilli, P. (2009). A phosphoinositide switch controls the maturation and signaling properties of APPL endosomes. Cell *136*, 1110-1121.

LEGENDS OF THE FIGURES

Figure 1: SNX16 is not present on early endosomal membranes.

A) HeLa cells co-expressing GFP-RAB5 and mRFP-SNX16 were analyzed by fluorescence microscopy. **B**) HeLa cells were transfected with GFP-SNX16 or GFP-SNX16^{R144A} and then treated or not with 100 nM wortmannin for 30 min at 37°C, as indicated, and analyzed by fluorescence microscopy. **C**) HeLa cells were transfected with Venus-SNX16, fixed, labeled with antibodies against TFR, and analyzed by fluorescence microscopy. **D**) HeLa cells were transfected with Venus-SNX16, fixed, labeled with antibodies against EEA1, and analyzed by fluorescence microscopy.

Figure 2: SNX16 is associated to late endosomes.

A-B) HeLa cells were transfected with Venus-SNX16 and analyzed by immunofluorescence microscopy using antibodies against LAMP1 (A) and LBPA (B). **C**) HeLa cells were co-transfected with Venus-SNX16 and CD63-RFP and analyzed by fluorescence video microscopy.

Figure 3: Analysis of SNX16 distribution by fluorescence microscopy and fractionation.

A-B) HeLa cells transfected with Venus-SNX16 were labeled with antibodies against LAMP1 and LBPA (A) or LAMP1 and CD63 (B), and analyzed by confocal microscopy. The distribution of Venus-SNX16 under low expression conditions, LAMP1, and LBPA (A) or Venus-SNX16, LAMP1, and CD63 (B) was analyzed and quantified after 3D image reconstruction using Imaris software. The data are expressed as the percentage of LAMP1, which co-distributes with the indicated marker. **C-D)** Untransfected BHK cells were homogenized and a post-nuclear supernatant (PNS) was prepared. The PNS was fractionated by floatation using a well-established step sucrose gradient, and early (EE) and late (LE) endosome fractions were collected (Aniento et al., 1993). Fractions were analyzed by SDS gel electrophoresis and western blotting with antibodies against LAMP1, SNX16 or RAB5, or by ELISA with antibodies against LBPA. In (A), the gels were loaded with equal amounts of protein (2.5 µg), as were the wells in the ELISA analysis (5 µg), to visualize enrichment of the corresponding markers in the fractions. In (B), the gels were loaded with equal volume (1/3 of the total fraction) to visualize the yields of the corresponding markers in the fractions. In the LBPA analysis, yields were calculated from the quantification of the ELISA data.

Figure 4: SNX16 distribution after glutaraldehyde fixation, and after brefeldin A treatment.

A-B) HeLa cells transfected with Venus-SNX16 were fixed with paraformaldehyde (A) or glutaraldehyde (0.3%) and paraformaldehyde (3%) for 50 min (B) and analyzed by

immunofluorescence microscopy using antibodies against LAMP1. Green arrows point to Venus-SNX16-positive tubules without detectable LAMP1; white arrows point to LAMP1- and SNX16-containing tubules. **C**) The left panel shows a confocal section through a cell expressing Venus-SNX16 and labeled for LAMP1 (fixation as in B). The middle panel shows a 3D reconstruction of the corresponding confocal stack with Imaris software, and the right panel shows a magnification of the boxed region, displaying only Venus-SNX16 and its colocalization with LAMP1. **D**) HeLa cells transfected with Venus-SNX16 were treated with brefeldin A (5 µg/ml for 30 min) prior to fixation with paraformaldehyde and analyzed by immunofluorescence microscopy using antibodies against TFR and the *cis*-Golgi protein p23. The insert in the p23 panel shows the characteristic ribbon-like distribution of p23 in control cells without brefeldin A.

Figure 5: HRP-LAMP1 and SNX16 distribution on tubular and vesicular late endosomes.
A-F) HeLa cells co-transfected with Venus-SNX16 and HRP-LAMP1 were processed as described in (Hopkins et al., 2000; Stoorvogel et al., 1996). Briefly, cells were chased with 1 mM DDT for 30 min, to ensure proper HRP-LAMP1 localization (Hopkins et al., 2000). DAB reaction to reveal HRP-LAMP1 cytochemically and permeabilization were done on living cells (in each case for 30 min at 4°C under physiological osmolarity conditions (Stoorvogel et al., 1996) prior to fixation. Samples were analyzed by phase contrast microscopy to reveal HRP-LAMP1 (A) and by fluorescence microscopy to reveal Venus-SNX16 (B). Panel C shows the merged image of A) and B), and panel D a high magnification view of the region boxed in C). In E), an example of a cell is shown where Venus-SNX16 and HRP-LAMP1 colocalize on numerous tubules (magnification in F).

Figure 6: Motility of Venus-SNX16-containing endosomes depends on microtubules.
A) HeLa cells transfected with Venus-SNX16 were analyzed by video microscopy. Panel (A) shows a frame of the supplementary movie Venus-SNX16.avi, which illustrates the dynamic tubulo-cisternal elements containing SNX16. **B-C**) HeLa cells co-transfected with Venus-SNX16 were pretreated (C) or not (B) with 10 µM nocodazole for 2 h, and analyzed by time-lapse video microscopy in the presence (C) or absence (B) of nocodazole. In the left panels, the first (green) and last (red) frames were color-coded and superimposed. The presence of the red and green colors indicates that the labeled vesicles moved, while the yellow color shows that they remained immobile. The right panels show the trace of the vesicles after superimposition of all frames acquired over time.

Figure 7: SNX16 and LAMP1 distribution in the absence of polymerized microtubules.
A) HeLa cells transfected with Venus-SNX16 were treated or not with 10 µM nocodazole to depolymerize the microtubules as in Fig 5, fixed in 0.3% glutaraldehyde and 3%

paraformaldehyde, and analyzed by immunofluorescence microscopy using antibodies against LAMP1. **B**) BHK cells treated or not with nocodazole as above were fractionated as in Fig 3. Early (EE) and late (LE) endosome fractions were analyzed by SDS gel electrophoresis and western blotting using the indicated antibodies. Gels were loaded with equal amounts of protein.

Figure 8: Overexpressed SNX16 localizes to LBPA-containing multivesicular late endosomes and interferes with cholesterol and CD81 trafficking through the compartment

A) After Venus-SNX16 overexpression, HeLa cells were analyzed by immunofluorescence microscopy using antibodies against LBPA. **B**) BHK cells overexpressing myc-SNX16 were fractionated as in Fig 3. Early (EE) and late (LE) endosome fractions were analyzed by SDS gel electrophoresis and western blotting using the indicated antibodies. Gels were loaded with equal amounts of protein. **C**) GFP-SNX16-overexpressing cells were processed for cryosectioning and labeled with anti-GFP antibodies, as described (Griffiths et al., 1984; Pons et al., 2008). **D**) After Venus-SNX16 overexpression, HeLa cells were analyzed by fluorescence microscopy using filipin to reveal the distribution of cholesterol. **E**) CD81 distribution was analyzed by fluorescence microscopy in cells with low Venus-SNX16 (upper panels) or high Venus-SNX16 (lower panels) expression levels.

Brankatschk Fig 1

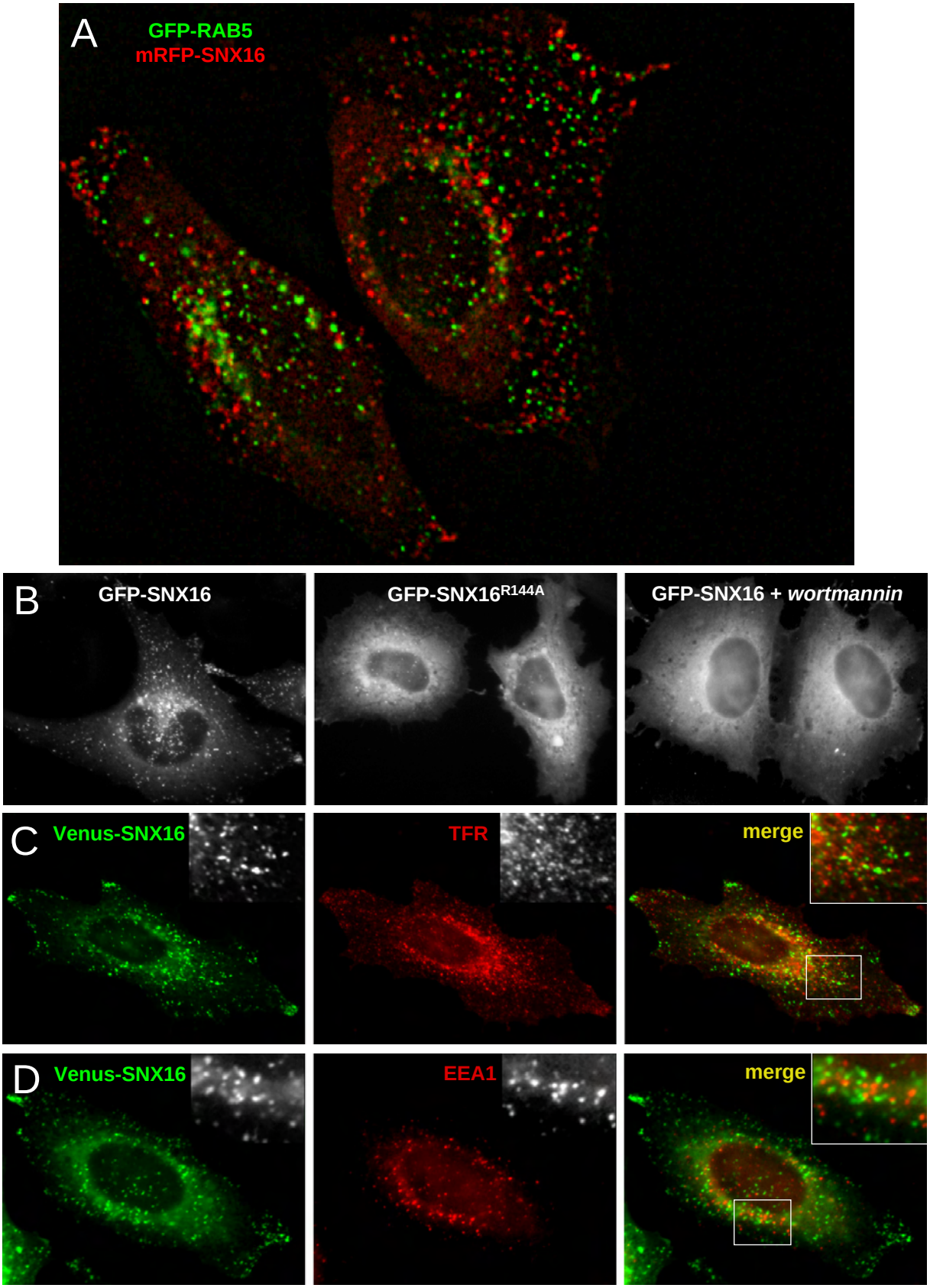

Brankatschk Fig 2

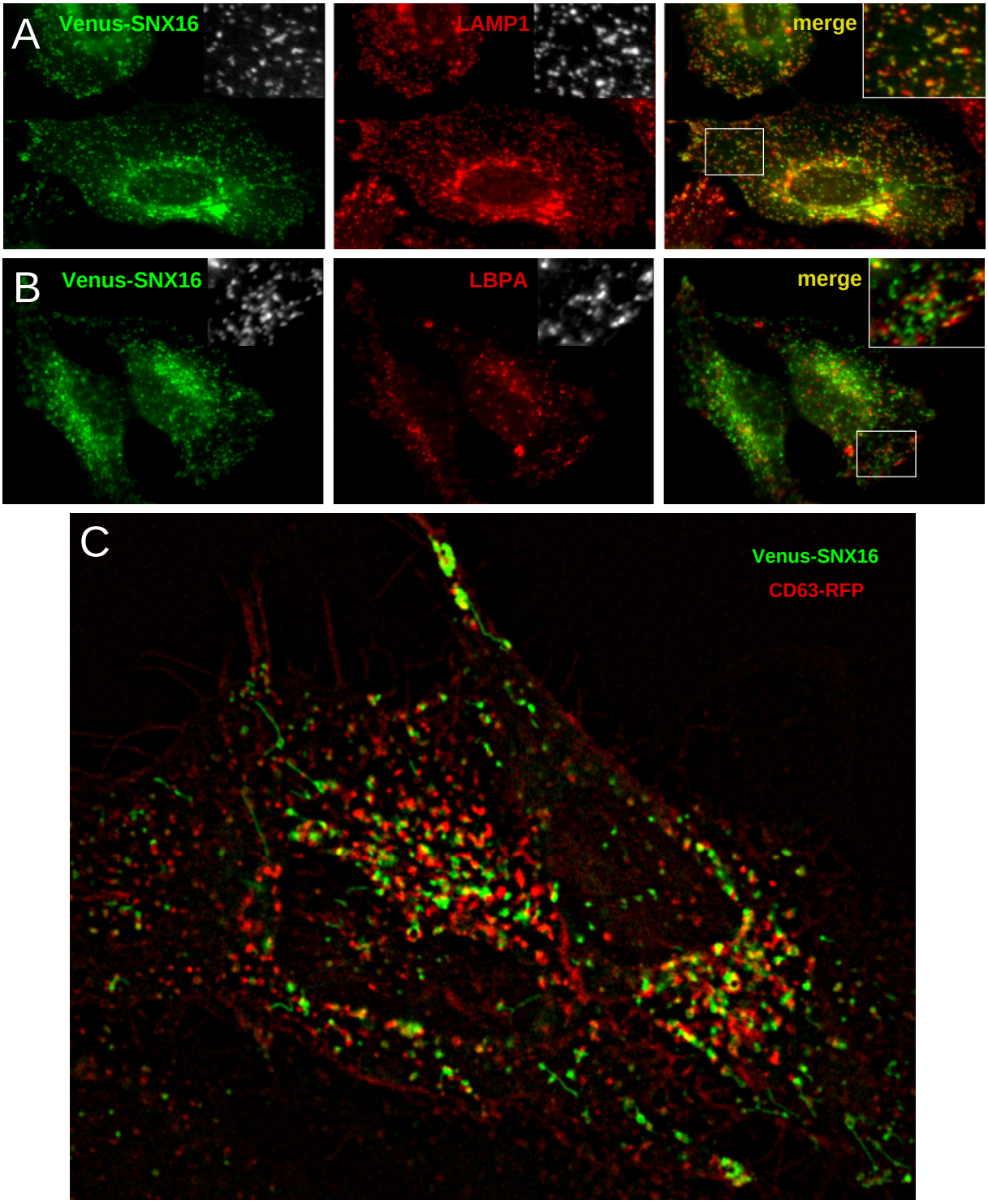

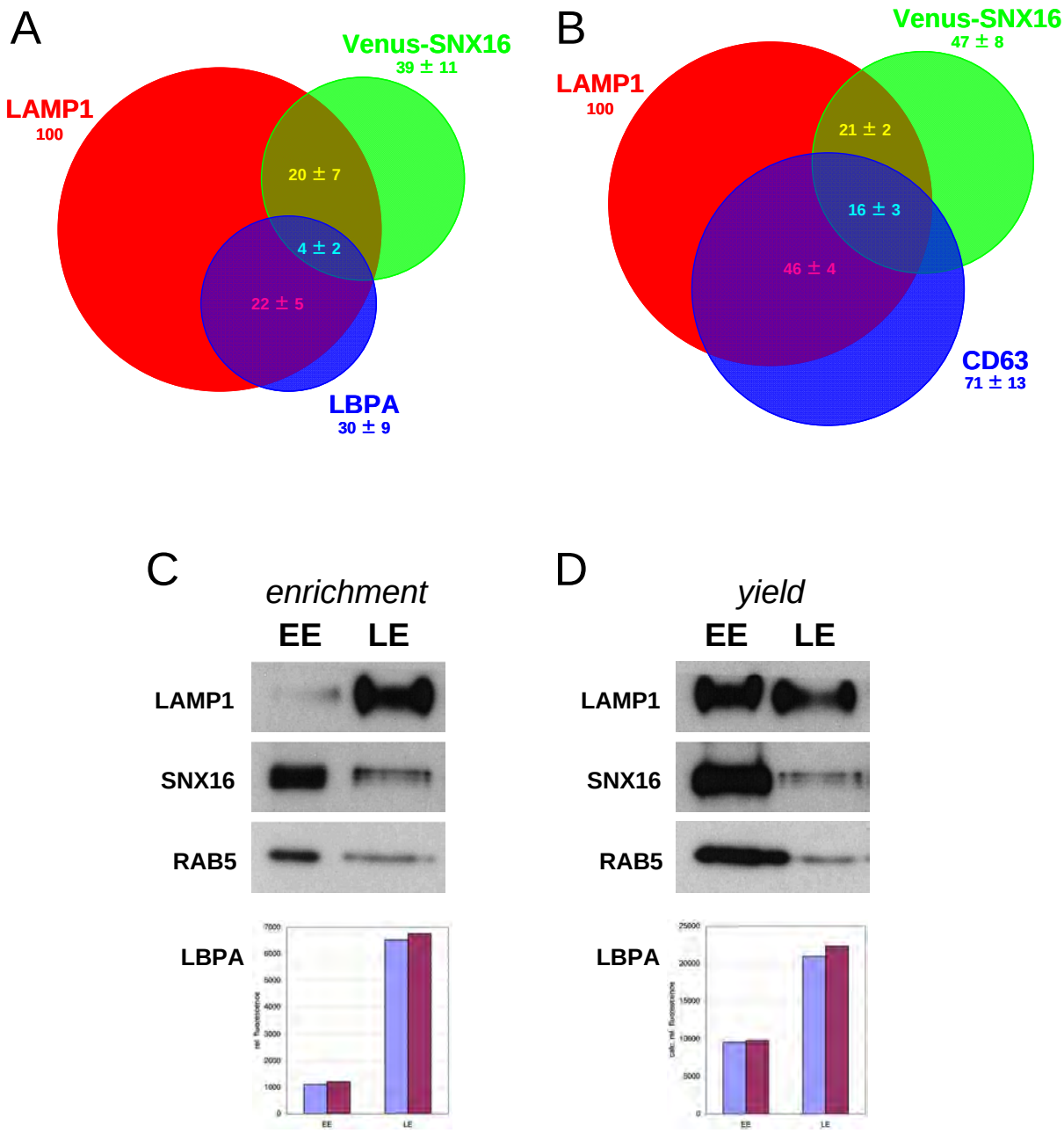
A
Venus-SNX16
39 ± 11
LAMP1
100
20 ± 7
4 ± 2
22 ± 5
LBPA
30 ± 9
B
Venus-SNX16
47 ± 8
LAMP1
100
21 ± 2
16 ± 3
46 ± 4
CD63
71 ± 13
C
enrichment
EE
LE
LAMP1
SNX16
RAB5
LBPA
D
yield
EE
LE
LAMP1
SNX16
RAB5
LBPA

Brankatschk Fig 4

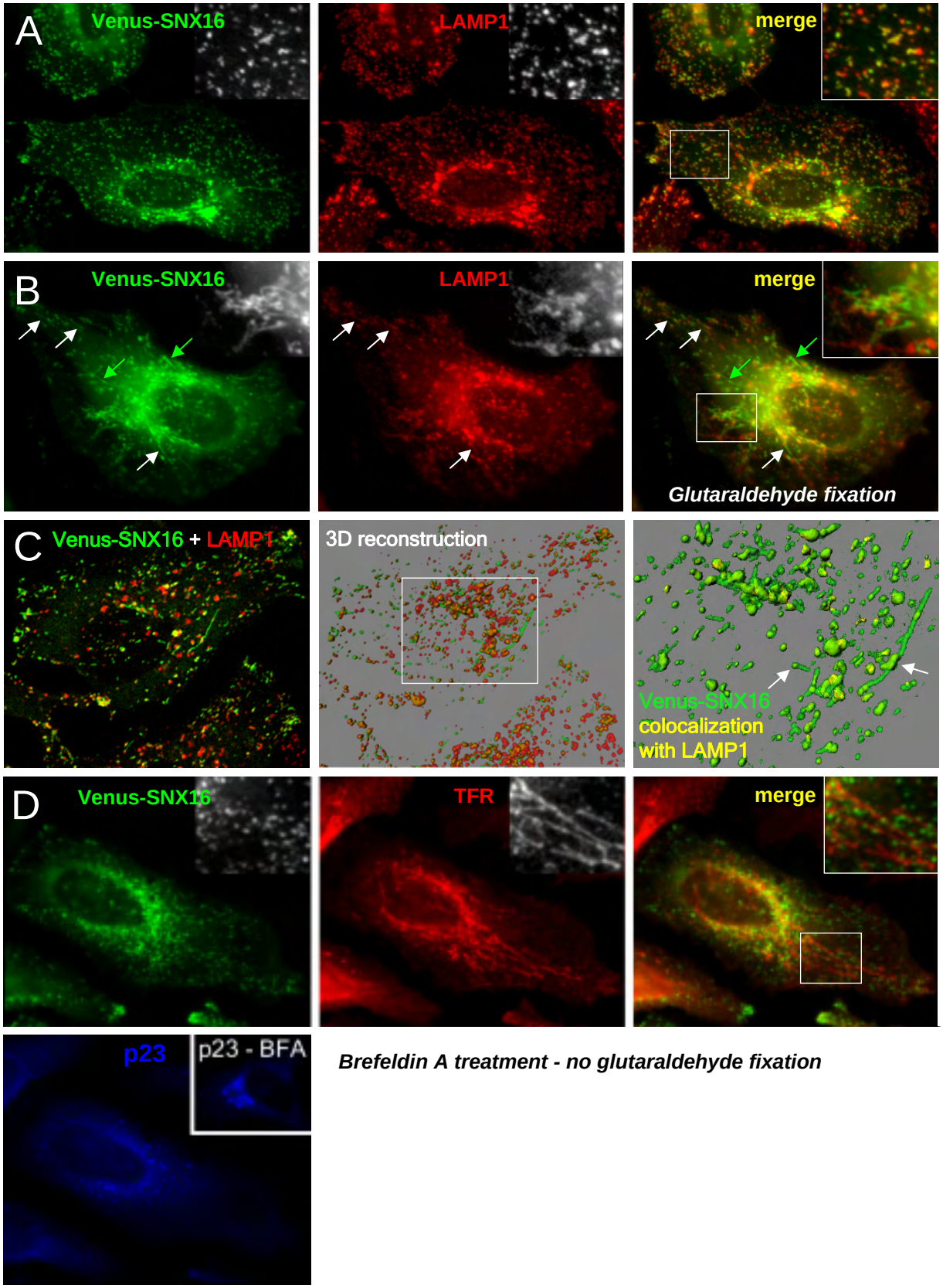

Brefeldin A treatment - no glutaraldehyde fixation

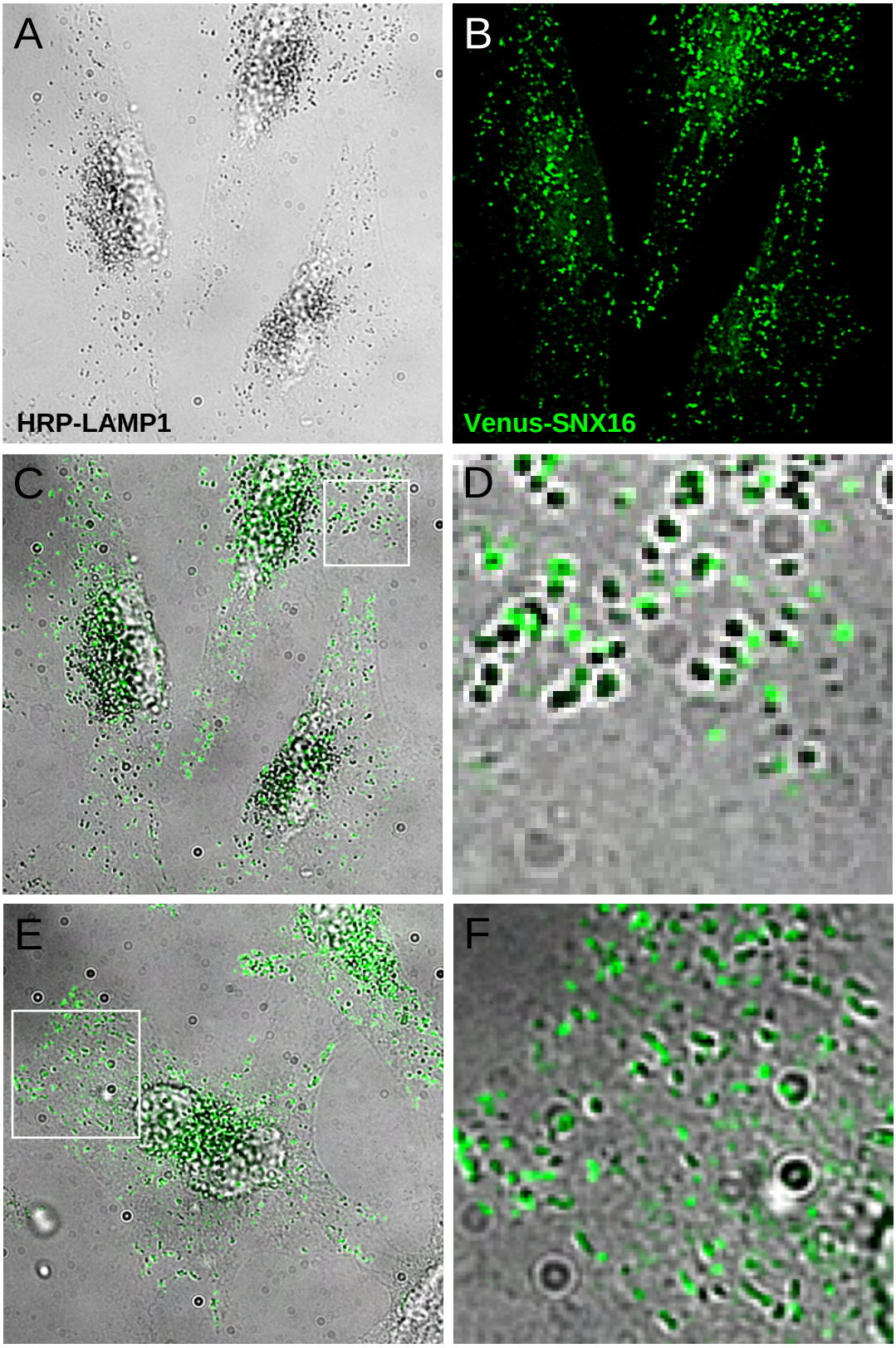
A
HRP-LAMP1
B
Venus-SNX16
C
D
E
F

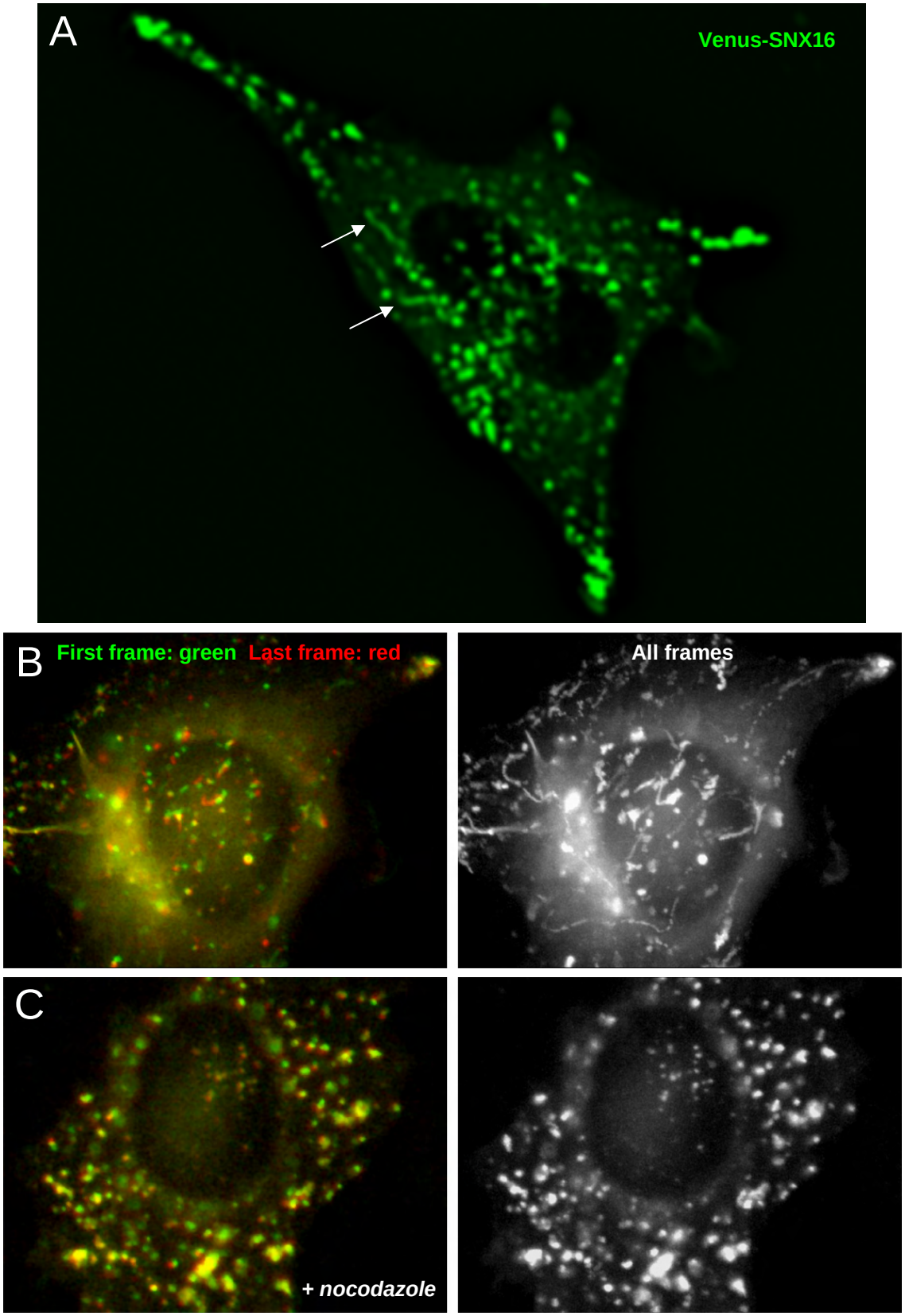
A
Venus-SNX16
B
First frame: green
Last frame: red
All frames
C
+ nocodazole

A

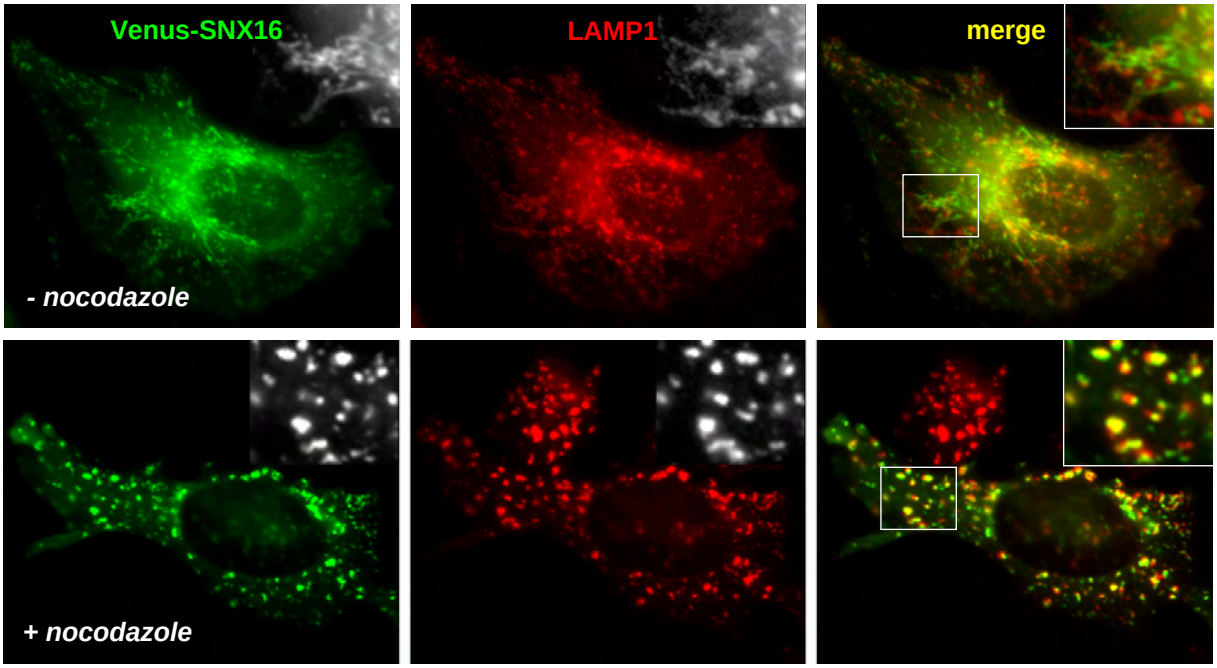
Venus-SNX16
LAMP1
merge
- nocodazole
+ nocodazole

B

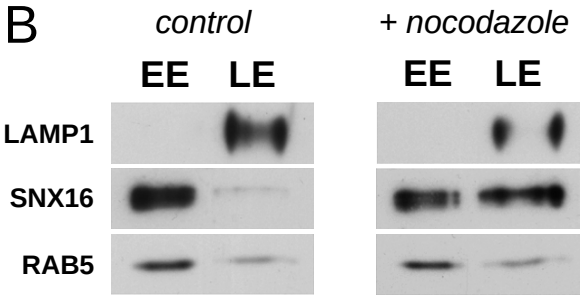
control
+ nocodazole
EE
LE
EE
LE
LAMP1
SNX16
RAB5

Brankatschk Fig 8